Characterising Gene Regulation during Epileptogenesis in Different Models of Epilepsy

Bao-Luen Chang

A thesis submitted for the degree of

Doctor of Philosophy

University College London

Department of Clinical and Experimental Epilepsy

Institute of Neurology

Queen Square

2018

Declaration

I, Bao-Luen Chang, confirm that the work presented in this thesis is my original research work. Where information has been derived from other sources, I confirm that this has been indicated in the thesis.

Acknowledgements

I would like to express my deepest appreciation to my supervisor Professor Stephanie Schorge for providing me the opportunity to study in the Institute of Neurology, Queen Square. Sincere thanks for her guidance, encouragement and fully support on my research. I am fortunate to meet such a scholar as my role model of a genuine scientist in the research field. I am especially grateful to Professor Matthew Walker and Professor Dimitri Michael Kullmann for their academical expertise, scientific guidance and suggestions on my study.

I specially thank Dr. Marife Cano-Jaimez, Dr. Elodie Chabrol, Dr. Gabriele Lignani, and Dr. Pishan Chang for teaching me scientific methods and providing necessary expertise and advice. I am very appreciative to the senior clinical scientist, Dr. James Polke, for his kindly assistance in showing me how to use the gradient PCR and qRT-PCR machines and sharing his experience of experiments using qRT-PCR. I am thankful to all my colleagues in the department of clinical and experimental epilepsy, especially Andrianos Liavas, Albert Snowball, Janosch Heller, Kotaro Sugao, Gareth Morris, Andreas Lieb and Jenna Carpenter, for all their help and friendship. Thank you also to my dear friends in London, in particular to Qiang Gang, Chiawei Wu, and Yenwen Cheng with whom I have shared the ups and downs of our PhD life, and made it an unforgettable period in my life. Specific thanks to Mr. David Blundred at ION Education unit for always providing very helpful support and information. I also thank the IT officer Mr. Mat Shaffi for the professional IT support.

An immense gratitude to my dear family, in particular to my parents for tolerating me to be unable to accompany them during these years, and giving me endless love, bravery and support; also to my brother, Chih-Jung, and sister, Pao-Ting, for their excellent care to all my family members that allows me to complete and concentrate on my PhD study abroad.

Finally, I would like extend my thanks to Chang Gung Memorial Hospital, Taiwan for funding me this Doctor of Philosophy programme.

Abstract

As epilepsy develops an enormous range of changes occurs in neurons. This process, epileptogenesis, involves complex spatiotemporal alterations of neuronal homeostasis and neural networks. The molecular mechanism of epileptogenesis remains obscure and gene regulation during the epileptogenic process dynamically controls various signalling and functional pathways which play an important role in defining the mechanisms of epilepsy. This thesis explores gene regulation in different *in vitro* models of seizure like activity, and further focuses on the temporal profiles of molecular changes during an *in vivo* model of epilepsy. We seek to identify important regulators of epileptogenesis which may be the targets for further study of the mechanism of epilepsy in human.

The High-K^+, Low-Mg^{2+}, Kainic acid, and Pentylenetetrazole models were used to elicit seizure like activity in cortical neuronal cultures. The tetanus toxin (TeNT) model of focal neocortical epilepsy in rats was utilised to characterise gene regulation in different time points: acute, subacute and chronic stages (48-72 hours, 2 weeks, and 30 days after first spontaneous seizure, respectively). A set of candidate genes relevant to epilepsy was selected to analyse changes in mRNA expression during these *in vitro* and *in vivo* models. The mRNA expression of the different candidate genes reveals diverse regulatory behaviours in different models, as well as at different time points during the process of epileptogenesis. The cell culture model treated with Low-Mg^{2+} for 72 hours displayed the most similar mRNA expression profile to the *in vivo* model of TeNT neocortical epilepsy during subacute to chronic stages. Furthermore, in the *in vivo* model, GFAP, mTOR, REST, and SNAP-25 are all temporarily apparently up-regulated during epileptogenesis, while CCL2 is strongly up-regulated later when epilepsy is established. Transient down-regulation of BDNF in the acute stage, and the distinctly lower expression of GABRA5 in late stage suggest that this GABAergic signalling pathway may be down-regulated in the late phase of epileptogenesis. Our work highlights how different candidate genes are differentially regulated during epileptogenesis, and how the regulation of individual genes changes as epileptogenesis progresses.

Table of Contents

List of Figures

List of Tables

Abbreviations

ActB	Beta actin
ADK	Adenosine kinase
AED(s)	Anti-epileptic drug(s)
AMPA	α-amino-3-hydroxy-5-methyl-4-isoxazolepropionic acid
AMPAR	α-amino-3-hydroxy-5-methyl-4-isoxazolepropionic acid receptor
ARBP	Acidic ribosomal phosphoprotein P0
BBB	Blood-brain barrier
BDNF	Brain-derived neurotrophic factor
CA	*Cornu Ammonis*
CCL2	Chemokine C-C motif ligand 2
CCR2	Chemokine C-C motif receptor 2
CREM	cAMP-responsive element modulator
EAAT	Excitatory amino acid transporters
ECoG	Electrocorticography
EEG	Electroencephalopathy
EPSP	Excitatory post-synaptic potential
Erg3	Early growth response factor 3
FC	Fold change
GABRA5	Y-aminobutyric acid A receptor, alpha 5
GFAP	Glial fibrillary acidic protein
GOI	Genes of interest

HCN1	Hyperpolarization-activated cyclic nucleotide-gated channel 1
HCN2	Hyperpolarization-activated cyclic nucleotide-gated channel 2
ICER	inducible cAMP early repressor II
IPSP	Inhibitory post-synaptic potential
K.A.	Kainic acid
KCNA1	Potassium voltage-gated channel subfamily A number 1 (Kv1.1)
LED	Light-emitting diode
LFP	Local field potential
LTD	Long-term depression
MCP-1	Monocyte chemotactic protein-1, also known as CCL2
mTLE	Mesial temporal lobe epilepsy
mTOR	mammalian Target of rapamycin
NPY	Neuropeptide Y
NRGN	Neurogranin
Nrf2	Nuclear factor erythroid 2-related factor
NMDA	N-methyl-D-aspartate
NMDAR	N-methyl-D-aspartate receptor
NRSE(s)	Neuron-restrictive silencer element(s)
NRSF	Neuron-restrictive silencer factor
Pgk1	Phosphoglucerate kinase 1
PTEN	Phosphatase and tensin homolog
PTZ	Pentylenetetrazole
RE-1	Repressor element 1

REST	Repressor element 1-silencing transcription factor
SDHA	Succinate dehydrogenase complex, subunit A
SE	Status epilepticus
SNAP-25	Synaptosomal-associated protein 25
SNARE	SNAP receptor (soluble N-ethylmaleimide-sensitive factor attachment protein receptor)
RPM	Revolution per minute
TeNT	Tetanus toxin
TSC	Tuberous sclerosis complex

Chapter 1 Introduction

1.1 Seizures, Epilepsy, Refractory Epilepsy and Status Epilepticus

1.1.1 Introduction

Epilepsy is one of the world's oldest recognized conditions (WHO, 2017) and the first description of an epileptic seizure can be traced back to 2000 B.C. from a written record in the Akkadian language (Magiorkinis et al., 2010). Historically, the physiologist Fritsch (1838-1927) and psychiatrist Hitzig (1838-1907) were the first to delineate and demonstrate that epilepsy originates from the hyper-excitability of brain; they published their experiments entitled "On the Electric Excitability of the Cerebrum" in which they provoked seizure convulsion in dogs by applying electric stimulation on the animals' cortex (G. Fritsch and Hitzig, 1870; Magiorkinis et al., 2014).

In the contemporary era, epilepsy is still one of the most prevalent neurological disorders affecting approximately 0.8%-1% (50-60 million) people world-wide and an incidence of 2.4 million people per year (according to the World Health Organization). Epilepsy is a spectrum disorder and comprises a group of heterogeneous syndromes affecting individuals of all ages and both genders but it is more common in people under 20 or over 60 years old (Hauser et al., 1996). Many possible aetiologies can lead to epilepsy and these can be divided into three major categories: idiopathic (genetic), symptomatic (acquired) including structural, infectious, metabolic and immune aetiologies, as well as unknown/cryptogenic (presumed symptomatic) (Engel and International League Against, 2001; ILAE, 1989; Scheffer et al., 2017). In total, approximately 40% patients are classified as having acquired epilepsy and these have an identified aetiology (Banerjee et al., 2009). In the past decades, many new antiepileptic drugs and novel therapeutic strategies have been introduced for epilepsy treatment, but the prevalence of refractory

epilepsy still has not significantly improved and approximately 20-30% epilepsy patients continue to experience uncontrolled seizures (Kwan and Brodie, 2000, 2004; Leppik, 1992) which can have devastating burdens on their health and welfare. Focal seizures are a major type of epilepsy, approximately 75% of pharmacoresistant epilepsies are focal, and neocortical focal epilepsy is one of the most pharmacoresistant forms of epilepsy (Loscher et al., 2008). Although some possible mechanisms of epileptogenesis have been proposed, there is still no consensus, consequently the mechanism of epileptogenesis remains obscure, even though understanding the underlying mechanism of epileptogenesis is likely to be crucial for developing effective approaches for epilepsy treatment.

1.1.2 Definitions

According to the International League against Epilepsy (ILAE) definition, an *epileptic seizure* is a transient occurrence of signs and/or symptoms due to paroxysmal abnormal and excessive hypersynchronous electrical discharge of a set of neurons in the brain (Fisher et al., 2005b). The clinical manifestations are stereotyped and are the results of abnormal neuronal activities, either convulsive or non-convulsive.

Epilepsy is defined as a chronic pathological brain disorder characterized by enduring predisposition to generate recurrent unprovoked, and usually unpredictable, epileptic seizures. Conceptually, the definition of epilepsy requires the occurrence of at least two unprovoked seizures on separate days, at least 24 hours apart. Furthermore, in 2014, the ILAE committee revised a practical clinical definition of epilepsy as any of following conditions: (1) at least two unprovoked (or reflex) seizures occurring >24 hrs apart; (2) one unprovoked (or reflex) seizure and a probability of further seizures similar to the general recurrence risk (at least 60%) after two unprovoked seizures occurring over the next 10 years; (3) diagnosis of an epilepsy syndrome (Fisher et al., 2014a). However, the ILAE also emphasizes that this revised practical definition is for the purpose of clinical practice and is probably not

suitable for research. Therefore, it is appropriate to compare and use the core definition of "two-unprovoked seizures". In essence, epilepsy should be viewed as a disorder arising from a variety of underlying neurological diseases and conditions that are caused by many different aetiologies rather than as a single disease entity (Fisher et al., 2005b).

Medically *refractory epilepsy* (where the term 'refractory' can be used interchangeably with intractable, drug resistant or pharmacoresistant) implies seizures persist and that seizure freedom is very unlikely to be achieved with further application of anti-epileptic drug (AED) therapy. Currently, *refractory epilepsy* is defined as "failure of adequate trials of two tolerated and appropriately chosen and used AED schedules (whether as monotherapies or in combination) to achieve sustained seizure freedom" (Kwan et al., 2010).

Traditionally, generalized convulsive *status epilepticus* refers to a single seizure lasting more than 30 minutes or to two or more repeated generalized seizures without full recovery of consciousness (DeLorenzo, 2006; Hauser et al., 1991; ILAE, 1989). However, generalized convulsive *status epilepticus* is recognized as an emergency situation with high mortality and morbidity, and animal studies have shown that prolonged or repetitive seizures are highly risky and can lead to self-sustaining and pharmacoresistant seizures within 15-30 minutes (Chen and Wasterlain, 2006; Mazarati et al., 1998; Wasterlain, 1974), as well as resulting in permanent neuronal damage and neuronal death (Fujikawa, 1996; Lowenstein and Alldredge, 1998; Meldrum et al., 1973). In order to meet the clinical necessity for treating status epilepticus rapidly, an operational definition of *status epilepticus* has been established. For this, *status epilepticus* has been re-defined as a seizure persisting longer than 5 minutes (Lowenstein et al., 1999; Meldrum, 1999; Trinka et al., 2015). Practically, the more precise definitions are: (1) early or impending status epilepticus, defined as continuous or intermittent seizures lasting more than 5 minutes, without fully conscious recovery between seizures; (2) established status epilepticus reverting to clinical or electrographic seizures persisting more than 30 minutes without fully conscious recovery between seizures; (3) refractory status

epilepticus is indicated by status epilepticus that fails to respond to optimal 1st line and 2nd line therapy after 2 hours; finally, (4) super-refractory status epilepticus is defined as status epilepticus which has continued or recurred despite therapy with general anaesthesia for 24 hours or more. Moreover, the length of 5 minutes is the time when the patient needs to be treated as for status epilepticus even though not all such patients are in established status epilepticus (Chen and Wasterlain, 2006; Millikan et al., 2009; Shorvon and Ferlisi, 2011).

1.1.3 Classification of Seizures and Epilepsies

Understanding the classification of epilepsies and a correct classification of epileptic syndromes is important to diagnosis, epilepsy management, and prognostic predictions. As different epilepsy types and syndromes often have different responses to medical or surgical treatment, as well as different prognoses. Also, some specific seizure types and epileptic syndromes have known suitable medications and treatment approaches. Traditionally, the classification system most frequently used and accepted world-wide for seizures and epilepsies is the classification and Terminology system of the ILAE Commission. Although the ILAE classification of seizures and epilepsies has been revised and updated several times in the past decades, the current revision is still based on the ILAE reports of seizure classification in 1981 and epilepsy classification in 1989. This classification system includes several items such as seizure semiology, aetiology, anatomy (location of the ictogenic zone), precipitating factors, age of onset, severity, chronicity, diurnal and circadian cycling, and some prognosis. The latest revisions of classification of seizure types and epilepsies were published in 2017 (Figure 1.1) and these can be classified to three major categories: focal, generalized and unknown. However, the division between focal epilepsy and generalized epilepsy is still the most useful classification for basic neuroscience investigations in animal model systems. The concept of focal or partial epilepsy is of seizures with onset limited to a part of one hemisphere, and they may be discretely localized or more widely distributed. On the other hand,

generalized epilepsy means seizures apparently originate and involve simultaneously in both hemispheres from the beginning. In addition, since the 2010 revision, the term of “secondarily generalized seizure” have been replaced by “focal to bilateral tonic-clonic seizure” indicating focal seizures propagating to bilateral hemispheres (Berg et al., 2010; Fisher et al., 2017a; Fisher et al., 2017b).

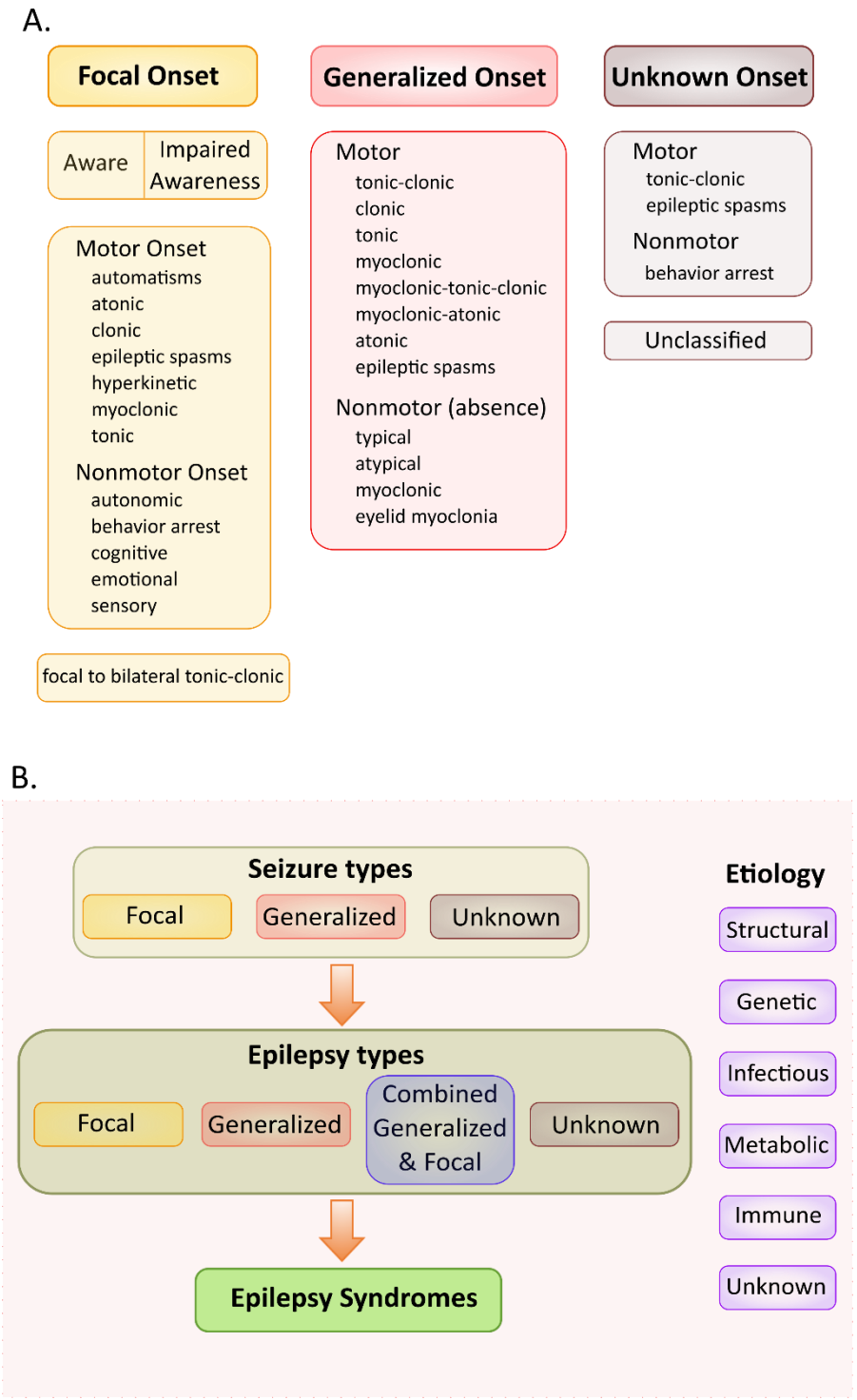

Figure 1.1 The ILAE 2017 Classification of Seizure types & Epilepsies

(A) The ILAE 2017 Classification of Seizure types

The preservation of awareness indicates the individual is aware of self and environment during the seizure regardless of immobility. The focal aware seizure corresponds to the prior term of “simple partial seizure”, while the focal impaired awareness seizure conforms to the

prior term “complex partial seizure”. Moreover, focal seizures can be described without mention of awareness if the awareness is not applicable or available. Seizures can be further characterised by motor or nonmotor symptoms in all the focal, generalised, or unknown onset seizures. In addition, the motor or nonmotor-onset symptoms of focal seizures refer to the first and earliest prominent sign or symptom in the focal seizures. Further classification of motor or nonmotor seizures in generalized or unknown seizures reflects the dominant and major feature throughout the seizure.

(B) The 2017 ILAE Classification of Epilepsies

The framework for the new classification of the epilepsies is a multilevel classification which is designed for making the clinical diagnosis depending on the resources available in different clinical environments. Importantly, the aetiology of the epilepsy should be always sought at all levels if possible.

The figure is based on (Fisher et al., 2017b; Scheffer et al., 2017)

1.1.4 Current treatment strategies for epilepsy

With the advances in the management of epilepsy, many new antiepileptic drugs and innovative therapies have been proposed for epilepsy treatment over the past decades. Generally, current available therapy strategies can be grossly divided into four categories, these are (1) pharmacological treatment, (2) ketogenic diet, (3) surgical resection, and (4) neuromodulation therapy (Karceski et al., 2005; Wheless et al., 2007). Currently, pharmacological therapy is still the major and first line treatment for epilepsy and many modern antiepileptic drugs (AEDs) have been developed in the past 15 years. Even though many new antiepileptic drugs are available, and these do reduce the adverse effects and improve tolerance for epilepsy patients, the proportion of medically refractory epilepsy still has not significantly decreased (Perucca and Tomson, 2011). Furthermore, current existing AEDs act as a symptomatic treatment (i.e. antiseizure treatment) to suppress or reduce the frequency and severity of seizures instead of antiepileptogenesis or disease modification (Galanopoulou et al., 2012a; Loscher et al., 2013). Also, epilepsy is not a static disorder and these medications do not prevent the development of epilepsy or alter its course and progression. At present, there are about 20 marketed AEDs worldwide and their actions can mainly be categorised into: (1) modulation of voltage-gated ion channels (e.g. targeting the α subunits of voltage-gated Na^+ channels or T-type voltage-gated Ca^{2+} channels, and A- or M-type voltage-gated K^+ channels); (2) enhancement of synaptic inhibition mediated by $GABA_A$ receptors or through the glycine or adenosine systems; (3) inhibition of synaptic excitation via blocking the glutamate receptors (NMDA, AMPA, kainate, metabotropic mGluR1 & mGluR5) or modulation of excitatory neurotransmitter release by presynaptic mechanisms (α2δ subunit of L-type Ca^{2+} channels or SV2A: synaptic vesicle protein) (Bialer and White, 2010; Meldrum and Rogawski, 2007; Rogawski and Loscher, 2004).

The Ketogenic diet is an adjunctive management for epilepsy which seizures are difficult to control by AEDs alone. It is particularly effective in some epilepsy syndromes, such as Lennox-Gastaut syndrome, myoclonic astatic epilepsy, Dravet syndrome, West syndrome, mitochondrial disorders, glucose transporter type 1

(GLUT1) deficiency syndrome, pyruvate dehydrogenase deficiency, and tuberous sclerosis complex. Ketogenic diet is a high-fat, low-carbohydrate, and moderate protein diet that results in fats becoming the primary fuel of body rather than carbohydrates. Hence, the primary source of energy for neurons is switched from glucose to ketone bodies (Lutas and Yellen, 2013). However, the mechanism of the ketogenic diet for the seizure remission is not yet completely understood. In addition to the classical ketogenic diet, some modified formulas (such as medium chain triglyceride diet, modified Atkins diet, and low-glycemic-index treatment) have been designed to improve the availability and convenience, as well as to reduce the side effects (Kossoff and Hartman, 2012; Lee and Kossoff, 2011).

The conventional invasive treatment for medical refractory epilepsy is surgical resection of the ictogenic or epileptogenic zones, or disrupting the connections of abnormal brain circuits to prevent seizure propagation from the seizure onset zone to other brain regions. Resective surgery including lesionectomy and non-lesional resection is a therapeutic option for some drug-resistant epilepsy patients for either palliative or curative purposes. However, surgical resection is only appropriate in the minority of cases where the epileptogenic zone is not in the eloquent cortex. In addition, many novel interventions have been proposed in recent years, multiple modalities of neuromodulation therapy, such as vagal nerve stimulation, deep brain stimulation, mesial temporal lobe stimulation, cortical stimulation, as well as transcranial magnetic brain stimulation have been applied in clinical management of epilepsy (Cox et al., 2014; Elger and Schmidt, 2008; Fisher, 2012). Although it is still unclear that how these neuromodulations work, a possible hypothesis is applying a certain frequency of current or magnetic field to a focal neuronal network will elicit local inhibition sufficient to inhibit the overexcitable neuronal tissue or its projections between hyperconnected networks.

1.2 Mechanisms of Epileptogenesis

1.2.1 Introduction

A seizure is composed of both electrical and behavioural characteristics involving chemical, molecular, cellular and anatomic features (Kandratavicius et al., 2014) and is characterized by hypersynchronized neural activity owing to the excitatory and inhibitory imbalance in brain (Prince et al., 1997). In fact, chronic epilepsies are more complicated than acute seizures and different epileptogenic mechanisms may be involved in different epileptic seizures and epilepsy syndromes (Engel and Pedley, 1997; Vreugdenhil et al., 2002). On the other hand, because different initiating events may lead to a similar consequence, it is also likely that different epileptic syndromes with diverse epileptogenic mechanisms, both genetic and acquired, may share some mechanisms of epileptogenesis. Current understanding of the pathophysiological basis for epileptogenesis is the increasing propensity for transient loss of inhibition and increased excitation of neural networks. Although the mechanisms of epileptogenesis are still not well understood, several functional pathways and postulated mechanisms have been suggested, including dysfunctional or defective ion channels and receptors (Graves, 2006), transcriptional signalling pathways, neurotransmission signalling pathways, as well as immunological and inflammatory pathways (Loscher et al., 2013). Also, much current evidence suggests that epileptogenesis is a multifactorial process involving complex changes in neural plasticity and circuitry affecting multiple facets and numerous levels, such as gene regulation, neurobiological, physiological, blood-barrier dysfunction and morphological changes which ultimately result in spontaneous recurrent discharges (Goldberg and Coulter, 2013; Pitkanen and Lukasiuk, 2009; Stables et al., 2002). The long-term alterations in structure and network excitability are primarily attributed to the complex gene expression changes that lead to a series of downstream molecular and protein modifications. Some of these changes are pro-epileptic effects, whereas others are the compensatory phenomena tending to suppress over-excitation. Epileptogenesis may result from a genetic basis or acquired

insults (e.g. stroke, brain trauma, infection, anoxia, tumors, status epilepticus and others) (Engel, 2011; Garcia Garcia et al., 2010; Pitkanen et al., 2007) and is a continuous and slow process which could take several months to years to develop into chronic epilepsy.

1.2.2 Definitions

Epileptogenesis is defined as the developing and progressive process from a normal neuronal network to a hyperexcitable condition that enables the brain to generate spontaneous recurrent seizures. The latent period of epileptogenesis presents from the time of the occurrence of the insult to the first spontaneous recurrent seizure in acquired epilepsies or to the time that the developmental programming of gene expression leads to the maturation of abnormal circuitry in genetic epilepsies (Pitkanen and Lukasiuk, 2011). Epileptogenesis is a continuously dynamic process that extends much beyond the first spontaneous recurrent seizure. Therefore, there is an emerging concept of using epileptogenesis to refer to a stage which encompasses both the latent period and the period while initial seizure frequency and severity progressively increases over time (Kadam et al., 2010; Williams et al., 2009). A cascade of complex molecular and cellular events occurs during the process of epileptogenesis that alters neuronal excitability and networks to eventually cause epilepsy. Three major stages are usually described in the epileptogenic cascade: early acute changes, subacute changes and the late phase (chronic stage) (Rakhade and Jensen, 2009). The early acute changes occur within minutes to days following the initial insult and this stage involves the activation of immediate early genes and post-translational modification of receptor and ion-channel related proteins. Next, the subacute changes happen within hours to days and can include alterations of gene regulation, neuronal death, and inflammation. Finally, the late phase, lasting weeks to months or even years, and involving morphological alterations (such as mossy fibre sprouting), synaptogenesis, as well as network reorganization (Figure 1.2).

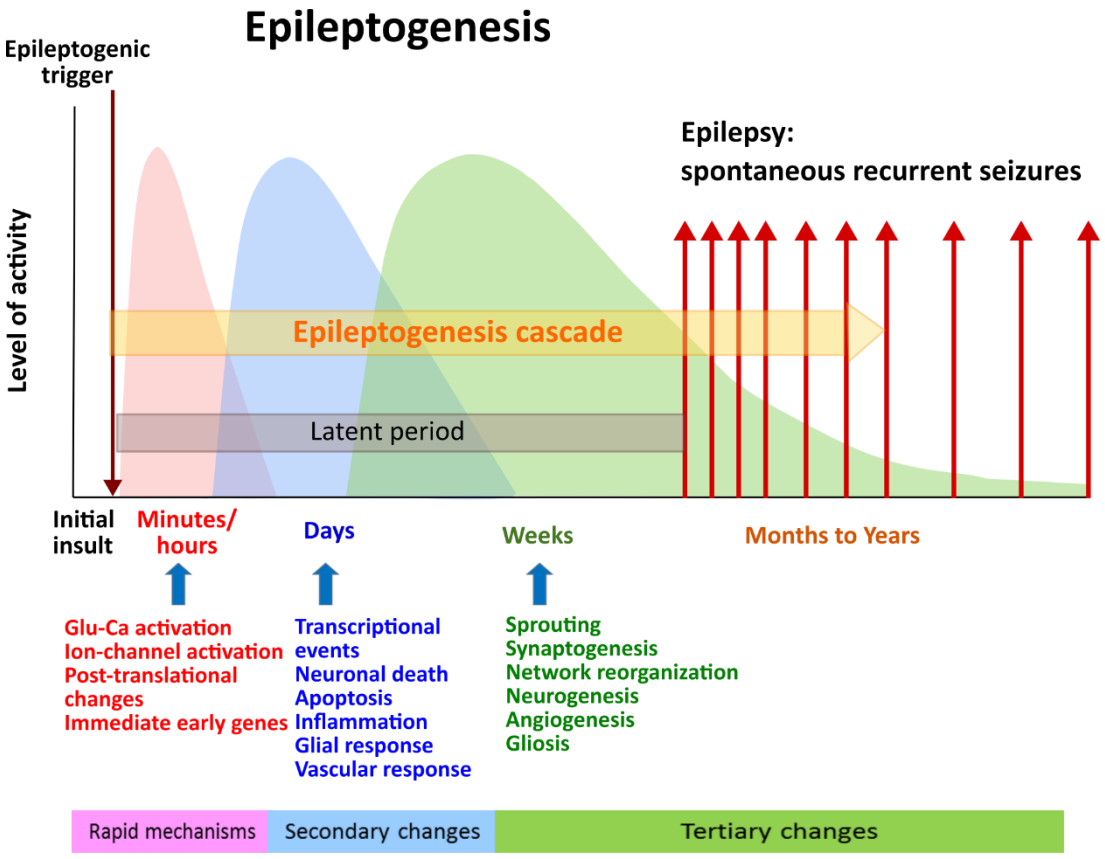

Figure 1.2 Time course and the process of Epileptogenesis

Epileptogenesis is a continuous temporal process involving complex cascades at many different levels and can be described as three sequential changes: rapid mechanisms, secondary changes, and tertiary changes. Alteration of the cascade of these events during the epileptogenic process has been demonstrated by experimental evidence. The figure is based on (Rakhade and Jensen, 2009).

1.2.3 Circuit dysfunction in epileptogenesis

Epileptic seizures and epilepsies are network-level phenomena resulting from neural circuit dysfunction. In current understanding, whatever the aetiologies (gene mutations or acquired), underlying various dysfunctions of molecular signalling pathways or specific cell types, the alteration of neural circuitry is the cornerstone to developing epilepsy. Rearrangement of circuits causes the formation of aberrant connections and the re-entrant activation of neuronal populations within aberrant circuits results in epilepsy (Goldberg and Coulter, 2013). Neural networks are composed of various microcircuit motifs including feed-forward inhibition, feed-back inhibition, counter-inhibition, and recurrent excitation (Figure 1.3). Epilepsies result from disturbance and imbalance of these diverse microcircuit motifs and the hyper-excitability of a neural network can be derived from gains or losses of some circuit components (Paz and Huguenard, 2015). Epileptic seizures originate from dysfunction of local microcircuits in the epileptogenic zone then engage other microcircuits and propagate through the cerebral networks. Also, these network microcircuits and their relevant circuits outside of the microcircuits, such as long-range excitatory, inhibitory and neuromodulatory connections project to distal brain areas, which can further organize and modulate the dynamic seizure activity and diffuse effects of the epileptic networks (Caputi et al., 2013).

Among these microcircuit motifs, feed-forward inhibition has been broadly implicated in epilepsies. Feed-forward inhibition exists extensively in several regions of brain including neocortical, hippocampal, thalamic and even basal ganglia networks and adequate feed-forward inhibition is a key microcircuit in normal function of neural networks. The feed-forward inhibition is predominantly mediated by fast-spiking parvalbumin basket cells (PV cells) (Figure 1.3a). The incoming excitatory inputs from the extrinsic cortex strongly activate inhibitory interneurons (PV cells), thereby recruiting a robust and powerful feed-forward inhibition of relay excitatory neurons (Gabernet et al., 2005). Many studies have shown that failure or the loss of feed-forward inhibition plays a major role in epileptic seizures (Paz et al., 2011; Rossignol et al., 2013; Sah and Sikdar, 2013; Sasaki et al., 2006).

In contrast to feed-forward inhibition, somatostatin-positive (SOM) interneurons primarily participate in feed-back inhibition (Figure 1.3b). Feed-back inhibition is also a common microcircuit in neural networks but unlike feed-forward inhibition which is excited by extrinsic excitatory sources, feed-back inhibition arises from excitation in local microcircuit elements. In the cortex and hippocampus, feed-back inhibition can prevent over-excitation of pyramidal neurons thus providing a potent seizure-suppression role (Cossart et al., 2001). However, the TC-RT-TC feed-back inhibition (TC: thalamocortical neuron; RT: reticular thalamic neuron) in the thalamus engages a powerful seizure-promoting role (Sohal et al., 2006).

In addition to excitatory neurons, inhibitory interneurons also can target other interneurons via the chemical or electrical synaptic connections and may even form potent autaptic connections (they synapse to themselves) which shapes counter-inhibition (Bacci et al., 2003) (Figure 1.3c). The gamma oscillations and related higher frequency oscillations which have been implicated in epilepsies are produced by counter-inhibition microcircuits. Enhancing counter-inhibition in neocortex and hippocampus promotes network synchrony, hyperexcitation and seizure activity (Paz and Huguenard, 2015). However, RT-RT counter-inhibition in thalamus has an anti-oscillatory effect and can desynchronize epileptiform oscillatory responses in TC-RT connections (Sohal et al., 2003).

Enhancement of recurrent excitation microcircuits has been demonstrated in many experimental epilepsies and this is the major mode of connectivity in cortical networks (Figure 1.3d). These microcircuit activities can be dynamically modulated by many synaptic and cellular components of the circuits that alter the balance among different forms of inhibition or excitation. In addition, the activities within microcircuits can propagate to distal brain regions through long-range efferent projections to connect circuit elements outside of the microcircuits that influence local and global neural networks. For instance, the intra-hemispheric cerebrocortical networks, and corticothalamocortical networks are composed of long-range, reciprocal excitatory projections. Finally, extrinsic influences can also selectively or

specifically affect individual microcircuit components via long-range neuromodulatory connections (Gradinaru et al., 2009; Paz et al., 2007).

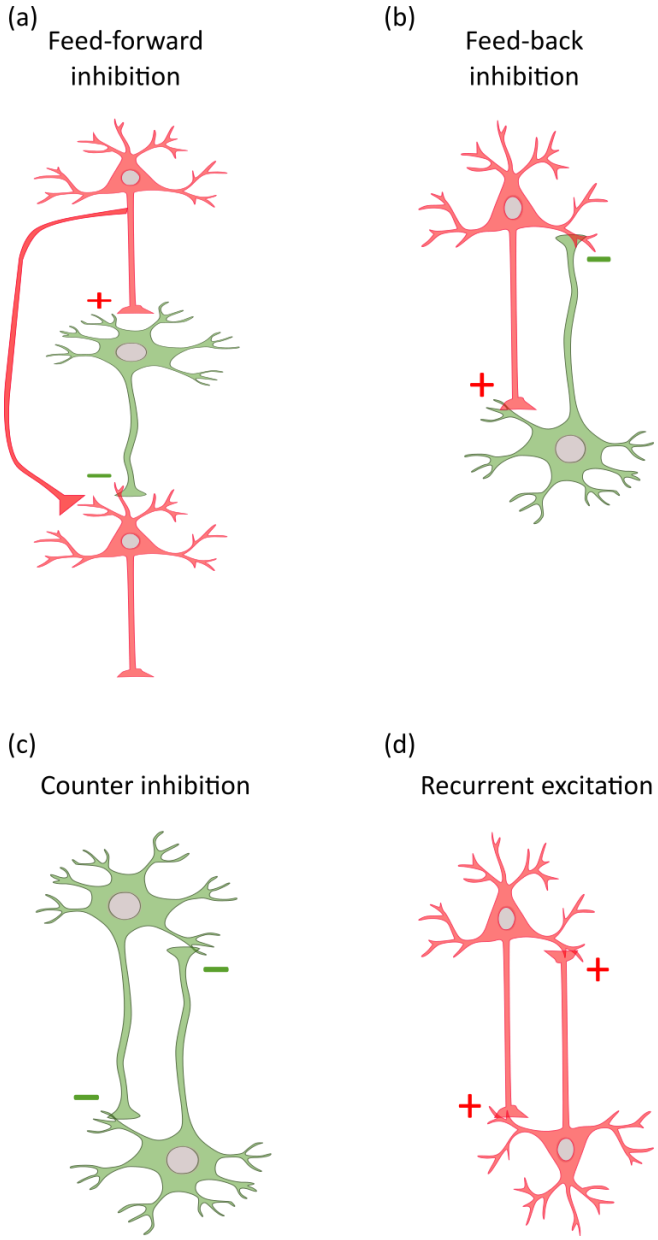

Figure 1.3 Microcircuit motifs in neural network

It has been suggested that epilepsy can be attributed to the dysfunction of different microcircuit motifs. (a) Feed-forward inhibition: local inhibitory cells receive excitatory inputs from remote brain regions which can control the strength of the efferent signal of the local inhibitory networks. (b) Feed-back inhibition: recurrent activation and inhibitory contacts between local excitatory and inhibitory neurons. (c) Counter-inhibition: autaptic connections formed by interactions between inhibitory interneurons. (d) Recurrent excitation: recurrent local connections between excitatory neurons enhance local excitation. Red and green represent excitatory glutamatergic and inhibitory GABAergic interneurons, respectively. Figure is based on (Paz and Huguenard, 2015).

1.2.4 Cellular biology of epileptogenesis

Epileptogenesis involves diverse molecular and cellular changes resulting in structural and functional alterations in neurons and neural circuits that eventually lead to epilepsies. Neural circuits undergo continuing remodelling during the process of epileptogenesis and the progression of epilepsy. A variety of cellular alterations in epileptogenic process or epileptic seizures have been shown from either animal studies or pathological tissue from epileptic patients receiving surgical resection. These alterations include neurodegeneration, axonal sprouting, axonal injury, dendritic plasticity, neurogenesis, synaptic reorganisation, altered glial function and gliosis, angiogenesis, blood-brain barrier (BBB) dysfunction, activated inflammatory cells, and changes in the extracellular matrix (Pitkanen and Lukasiuk, 2009).

1.2.4.1 Neurodegeneration and Cell death

The association between neurodegeneration and cell death with epilepsy mainly comes from observations of experimental models and hippocampal sclerosis in epileptic patients (Pitkanen and Sutula, 2002). Such neuronal death is caused by two major mechanisms: excitotoxic and apoptotic cell death. The excitotoxicity after seizures is due to prolonged over-activation of ionotropic glutamate receptors (NMDA) gating intracellular calcium overload via excessive calcium influx and calcium release from intracellular stores. This activates downstream proteolytic enzymes and induces oxidative stress, organelle swelling and rupture resulting in neuronal death (Fujikawa, 2005). Apoptosis is a programmed cell death mechanism which can be triggered by prolonged or repeated seizures. The programmed cell death involves complex highly ordered molecular cascades and regulatory signalling pathways. Among the apoptosis-associated signalling pathways, the Bcl-2 family genes play a particularly crucial role in the intrinsic pathway (mitochondrial pathway) and regulate apoptosis through the effects on mitochondria (Henshall and Murphy, 2008). The second major apoptosis signalling pathway is the extrinsic pathway (TNF pathway)

via the surface-expressed death receptors of the tumor necrosis factor (TNF) superfamily (Bozzi et al., 2011).

However, whether neurodegeneration or cell death is essential in the epileptogenic process has been challenged. Neurodegeneration and cell loss are primarily described in the animal models of SE-induced epilepsy or in human epileptic tissue with hippocampal atrophy from pharmacoresistant mesial temporal lobe epilepsy, but may not be evident in other experimental models and epilepsy patients. In addition, evidence has shown that epileptogenesis is not stopped or prevented by substantially protecting and rescuing hippocampal neurons after SE (Brandt et al., 2003). Also, studies have revealed that neurodegeneration is not necessary for epileptogenesis (Dube et al., 2006). Moreover, while it has been recognized that SE can cause neuronal death, whether single or brief recurrent seizures contribute to neurodegeneration and neuronal death is still controversial. Although there is no compelling evidence suggesting that spontaneous recurrent seizures can cause neurodegeneration and neuronal loss, seizure-induced subtle neuronal damage may cumulate slowly to become significant (Henshall and Meldrum, 2012; Pitkanen and Sutula, 2002).

1.2.4.2 Neurogenesis and Neural reorganisation

Neurogenesis refers to the process of generating functional neurons from neural stem cells and progenitor cells. The majority of developmental neurogenesis occurs in embryonic and perinatal stages in mammals (Ming and Song, 2011). However, new neurons can also be generated from adult neural precursors throughout adulthood in restricted brain regions in mammals, by adult neurogenesis. In humans, adult neurogenesis is sustained in two regions of adult brain: the subgranular zone (SGZ) of the dentate gyrus in the hippocampus, as well as the subventricular zone (SVZ) of the lateral ventricles in forebrain (Zhao et al., 2008). Adult-born neurons in both SGZ and SVZ functionally integrate into the existing circuitry and obtain electrophysiological characteristics of mature cells.

Seizure activity promotes adult neurogenesis in both the SGZ of hippocampus and the SVZ of lateral ventricles. Hippocampal neurogenesis concomitant with the formation of aberrant connections via immature and adult-born neurons has been shown in many animal models of limbic epilepsy and studies of human tissue taken from epilepsy surgery (Jessberger et al., 2007; Takei et al., 2007). Aberrant hippocampal neurogenesis which can occur in the acute and chronic phases has been proposed as an important role in the epileptogenic process in mesial temporal lobe epilepsy (mTLE). Multiple morphological and cellular abnormalities in aberrant hippocampal neurogenesis have been well characterised, including mossy fibre sprouting, granule cell layer dispersion, ectopic hilar migration of granule cells, and prominent hilar basal dendrite formation in granular cells. Further, the synaptic reorganization attributed to mossy fibre sprouting which leads to numerous axons of dentate granule cells forming excitatory synaptic projections to the abnormal locations including in the dentate inner molecular layer, or to the hilar basal dendrites (Parent and Kron, 2012). This aberrant axonal sprouting and synaptogenesis consequently contributes to recurrent excitatory circuitry and abnormal connectivity (Hui Yin et al., 2013).

Neuronal circuit reorganisation is activity-dependent consequently recurrent seizures can contribute to continue neuronal reorganization and potentially lead to the progression of epilepsies and other cognitive consequences (Pitkanen and Sutula, 2002). In addition, lesion-specific neural reorganization in epilepsies has been suggested in many experimental epilepsy models (Brill and Huguenard, 2010; Jin et al., 2006; Morgan and Soltesz, 2008).

1.2.4.3 Gliosis

Glial proliferation accompanying selective reactive astrocytosis and altered protein expression in astrocytes is a pronounced phenomenon in the sclerotic hippocampus of human mTLE and in animal models of epilepsy (Borges et al., 2003; Cohen-Gadol et al., 2004; Shapiro et al., 2008). Several studies have suggested that

the gliosis related molecular markers such as glial fibrillary acidic protein (GFAP), and glia producing cytokines, chemokines as well as extracellular matrix proteins robustly increase in expression following epileptogenic insults (Lukasiuk et al., 2006). There are four major types of glial cells in brain: astrocytes, microglia, oligodendrocytes and NG2 cells (polydendrocytes). Astrocytes and microglia are most relevant to the epileptogenic process and they involve epileptogenesis through structural support, altered water and ionic hemeostasis, regulation of neurotransmission, inflammatory responses, regulation of vascular permeability, and neurogenic potential (Pitkanen and Lukasiuk, 2009). Further, accumulating evidence is emerging that glial cells play a critical role in modulation of synaptic transmission, reorganization and plasticity (Friedman et al., 2009; Wetherington et al., 2008). Astrocytic transformation and dysfunction during epileptogenesis contributes to neuronal hyper-synchronicity, excitability, as well as network reorganization. Astrocytes have dynamic and activity-dependent functional changes to the extracellular environment in epilepsy which mainly involve: (1) diminished expression of potassium inward-rectifying channels (Kir4.1) and water channels (aquaporin 4, AQP4) leading to impaired $[K^+]_0$ buffering; (2) reduced glutamine synthetase (GS), a astrocyte-specific enzyme, resulting in impaired glutamate uptake and metabolism; (3) upregulated adenosine kinase (ADK) which promotes metabolism of the inhibitory molecules, adenosine; (4) increased release of inflammatory mediators (Boison, 2008; Clasadonte and Haydon, 2012; Friedman et al., 2009; Jabs et al., 2008).

Microglia are extremely sensitive and respond quickly to homeostatic disturbances in brain. Microgliosis with activated microglial cells can secrete a variety of compounds into the extracellular space. Some of these secretory substances may have harmful effects on neurons such as pro-inflammatory cytokines (IL-1, IL-6, TNF-α), whereas some may have neuroprotective effects, like neurotrophin-3 and brain-derived neurotrophic factor (BDNF). However, the net balance of the harmful and protective effects and their actions on the epileptogenesis remains controversial and inconclusive (Pitkanen and Lukasiuk, 2009).

1.2.4.4 Angiogenesis and BBB dysfunction

Increasing evidence from human studies and animal models of epilepsy demonstrates that blood-brain barrier (BBB) disruption along with pathologic angiogenesis are common features of various epileptogenic processes and chronic epileptic foci regardless of the aetiologies (Pitkanen and Lukasiuk, 2009; Rigau et al., 2007; van Vliet et al., 2015). Extensive BBB impairment with vascular endothelial growth factor (VEGF)-mediated angiogenesis observed in latent period indicates that vascular remodelling serves a crucial role in epileptogenesis (Benini et al., 2016). BBB leakage extends into chronic phase after the establishment of epilepsy and the degree of vascularization is positively correlated with seizure activity, severity and frequency in chronic epileptic brain (Rigau et al., 2007; van Vliet et al., 2007). Upregulation of VEGF in neurons and astrocytes, as well as its receptor, vascular endothelial growth factors-2 (VEGF-R2 or flk 1) on endothelial cells further aggravates BBB breakdown with increasing vascular permeability followed by ions (such as K+) and neurotransmitters (such as glutamate) diffusing to the brain parenchyma which results in neuronal hyperexcitability (Lange et al., 2016; Morin-Brureau et al., 2012). In addition, serum albumin also leaks to the extravascular microenvironment of brain and can bind to transforming growth factor-β receptor 2 (TGFβR2) in astrocytes then trigger TGFβR2-mediated signalling cascade inducing rapid transcriptional modifications, local inflammation (cytokines), and astrocytic transformation which includes down-regulation of potassium channels (Kir4.1) and water channels (aquaporin 4) leading to impaired clearance of extracellular K^+ and facilitating NMDA receptor mediated neuronal hyperexcitability (Ivens et al., 2007), and consequently lowering seizure threshold in the affected area and eventually resulting in epileptogenesis leading to epilepsy.

1.2.5 Molecular mechanisms of epileptogenesis

Epileptogenesis is a complex multifactorial process involving different facets. The alterations in neuronal homeostasis, circuit dysfunction and cellular changes in epileptogenic mechanisms are attributed to diverse large-scale molecular changes. The genetic background and regulated genetic programmes predominantly influence these alterations and the epigenetic factors may also play a role (Pitkanen and Lukasiuk, 2009).

1.2.5.1 Dysfunctional ion channels and receptors

A number of ions such as Na^+, K^+, Ca^{2+}, Cl^-, H^+ flow cross the cell membrane via ion pumps, ligand-gated ion channels, or voltage-gated ion channels driving the changes in ionic currents which lead to alterations in the neuronal excitation state. Ion channel dysfunction, also known as channelopathy, has been proven in various epilepsy syndromes to play a central role in epilepsy. Increasing evidence suggests that neurons can adapt and modify the expression, property and functionality of their ion channels to maintain or alter their homeostasis and excitability. Inherited or acquired changes of ion channels and receptors such as acetylcholine, glutamate, and γ-aminobutryic acid receptors can alter neuronal function affecting seizure threshold, neuronal plasticity and efficacy of treatment (Avanzini and Franceschetti, 2003; Pitkanen and Lukasiuk, 2009).

An acquired channelopathy is distinguished from a genetic channelopathy by the development of ion channel dysfunction following acquired insults and independent of genetic background (Wolfart and Laker, 2015). Accumulating evidence from animal models of epilepsy and human epileptic tissue have demonstrated that dysregulation of ion channels plays a critical role during epileptogenesis and an acquired channelopathy is likely the final common pathway of induction and maintenance of epilepsy (Lerche et al., 2013; Poolos and Johnston, 2012). Acquired channelopathies involve transcriptional, translational, and post-

translational alterations of ion channel expression contributing to functional changes during epileptogenesis and even during the progression of epilepsy, and these changes possibly are the cause of pharmacoresistance of epilepsy (Poolos and Johnston, 2012).

Acquired alterations of ion channel properties can occur in both ligand-gated and voltage-gated channels. Also, unlike inherited or genetic epilepsies which can be caused by single ion channel dysfunction, acquired epilepsies probably comprise dysfunction of multiple ion channel species. (Poolos and Johnston, 2012). Numerous acquired channelopathies in epilepsy have been described and particularly focus has been made on hyperpolarization-activated cyclic nucleotide gated (HCN) channels, transiently upregulated T-type Ca^{2+} (Cav3.2 channel), potassium channels (Kv4.2, Kir2…etc), as well as sodium channels (Lerche et al., 2013; Richichi et al., 2008; Wierschke et al., 2010; Wolfart and Laker, 2015). GABA receptors associated with inhibitory postsynaptic potential (IPSP) encompass two major types: (1) the ionotropic $GABA_A$ receptor which is a ligand-gated Cl^- channel; and (2) metabotrophic (G-protein coupled) $GABA_B$ receptor rectify the opening of K^+ channel and closure of N and P/Q type Ca^{2+} channels (Badawy et al., 2009a). Altered $GABA_A$ receptor subunit composition (and reduction of GABAergic neurons) has been shown in some animal and human studies (Brooks-Kayal et al., 1998; Goodkin et al., 2007).

On the other hand, non-ion channel gene mutations such as in the APP/Aβ (Amyliod precursor protein/Amyliod β) gene pathway in Alzheimer's disease may also alter ion channel properties and expression in hippocampus and neocortex contributing to epileptogenesis and epileptic phenotypes in this animal model (Lerche et al., 2013; Noebels, 2011; Palop et al., 2007).

1.2.5.2 Molecular signalling pathways and related genes

Transcriptional signalling pathways which alter cellular gene expression and the intracellular signalling cascades further contribute to modification of cellular properties, synaptic plasticity and network functions. Morphological changes,

altered cellular functions, cell degeneration, cell death, synaptogenesis, as well as the formation of aberrant neuronal circuitry are driven by complex molecular signalling processes. Hence, the development of epilepsy may be through the maladaptive activity of some large-scale molecular signalling pathways and consequently associated with changes in expression of numerous genes. Also, these signalling pathways may not only have a role in epilepsy development but may also be relevant to the disease progress.

Understanding gene regulation during epileptogenesis, which might be controlled by disrupted transcription factors, has an important role in exploring the mechanisms of epilepsy. Many genes, either by over-expression or down-regulation, have been suggested to be involved in modulating the epileptogenic process in experimental and human studies. Further, as epileptogenesis is a dynamic process, different stages may involve different genes and molecular signalling pathways, as well as different expression levels of a gene across the time course of epileptogenic process. For example, Fos, Jun, Egr1, Egr4, Homer1, Nurr77 and Arc which have all been implicated as immediate early genes activated by phosphorylated transcription factors, such as cyclic-AMP response element binding protein (CREB) and CREB binding protein (CBP) in early changes of epileptogensis (Rakhade and Jensen, 2009). In addition to acute and early changes, long-term alterations in transcription and expression of neurotransmitter receptors may occur in the subacute and late phase of epileptogenesis. For instance, activation of transcriptional repressor, repressor element 1-silencing transcription factor (REST) reduces expression of the $GABA_A$ receptor β3-subunit, and inducible cAMP early repressor (ICER) decreases the $GABA_A$ receptor α1-subunit both changes which would diminish inhibition (Brooks-Kayal et al., 2009; Goldberg and Coulter, 2013).

Neuron-restrictive silencer factor (NRSF), also known as REST, is a transcriptional zinc-finger protein which can repress the expression of numerous neuron-specific genes in non-neuronal cells and neuronal precursor cells via binding to the DNA silencer motifs/sequences named neuron-restrictive silencer elements (NRSEs or RE1 element). In addition to supressing ectopic expression of neuronal

genes outside the nervous system, evidence has demonstrated that REST/NRSF also play a crucial role on negatively regulating the neuronal expression of NRSE-containing genes in mature neurons. The REST/NRSF signalling pathway can dynamically modulate various neuronal gene expression in adult brain, and the NRSF-NRSE system itself is also regulated by neuronal activity (Roopra et al., 2001). More than 2,000 genes have been reported to contain the REST-binding motifs (DNA silencer sequences) and approximately 10% of them are neuronally expressed genes (Otto et al., 2007). Accumulating evidence reveals that the REST/NRSF signalling pathway contributes to epileptogenesis by regulating the expression of many key genes such as: $GABA_A$ receptor β3 subunit, $GABA_A$ receptor δ subunit, glutamate receptors, HCN channel subunit 1-4 (HCN1-4), as well as BDNF, which are all implicated in the mechanisms of epilepsy (Goldberg and Coulter, 2013; Roopra et al., 2001).

The mammalian target of rapamycin (mTOR) is a serine/threonine protein kinase with the functions of integrating numerous extra- and intracellular signals to regulate gene expression and protein translation then modulate cell growth, differentiation, proliferation, survival and metabolism in the brain (Inoki et al., 2005). Furthermore, the mTOR signalling pathway also contributes to the regulation of long-term synaptic plasticity (Tang et al., 2002). Two functionally and structurally distinct mTOR complexes (mTORC) were discovered, mTORC1 and mTORC2. mTOR protein kinase is the core component of these two multi-protein complexes (Lipton and Sahin, 2014). mTORC1 acts as a pivotal switch on activation of multiple downstream pathways to modulate protein synthesis and functional effects (Laplante and Sabatini, 2009). In addition, tuberous sclerosis complex 1 (TSC1) and TSC2 are tumour suppressor genes which encode harmatin and tuberin, respectively and the TSC1/TSC2 (harmatin/tuberin) complex is the upstream of mTOR signalling pathway and negatively regulates the mTOR pathway by inhibiting mTORC1 activation (Ryther and Wong, 2012). Tuberous sclerosis complex and related focal cortical dysplasias which are common genetic causes of intractable epilepsy result from loss-of-function mutations in TSC1 and TSC2 (Loscher et al., 2013; Wong and Crino, 2012). Many experimental models of epilepsy and human studies have implicated that

dysregulation of mTOR pathway critically involved in the epileptogenic process and the pathogenesis of epilepsy is not only in TSC, but also in other common types of epilepsies (Galanopoulou et al., 2012b; Goldberg and Coulter, 2013; Meng et al., 2013; Vezzani, 2012).

The expression of neurotrophin genes contributes to diverse forms of neuronal plasticity. There are four types of mammalian neurotrophins: brain-derived neurotrophic factor (BDNF), nerve growth factor (NGF), neurotrophin 3 (NT-3) and NT4. BDNF has been demonstrated to regulate dendritic growth and the expression of GABAergic receptor components, to decrease GABAergic transmission and K^+-Cl^- cotransporter KCC2 expression (Scharfman, 2005). For example, upregulation of BDNF transcriptionally reduces $GABA_A$ α1 subunit levels via induction of ICER, but increases the extrasynaptic $GABA_A$ α4 subunit via the expression of early growth response factor 3 (Erg3) which consequently results in reduction of synaptic inhibition (Brooks-Kayal et al., 2009; Tanaka et al., 1997). In addition, the BDNF receptor, tropomycin-related kinase B (TrkB) receptor, is a tyrosine kinase receptor and the BDNF-TrkB signalling pathway has frequently been linked to epileptogenesis (Binder et al., 2001; Liang et al., 1998; McNamara et al., 2006).

The dopaminergic signalling pathway also has been shown to play a specific role in epileptogenesis and seizure modulation in animal and human studies. Dopamine D1 receptor signalling is considered to have a pro-epileptogentic effect, whereas dopamine D2 receptor signalling serves an anti-epileptogenic effect. In addition, the pathophysiology of autosomal dominant nocturnal frontal lobe epilepsy (ADNFLE) and juvenile myoclonic epilepsy (JME) has been shown to be associated with the dopaminergic pathway (Hui Yin et al., 2013). Further, some evidence has suggested that the alteration of the dopaminergic signalling pathway with increasing D1 receptor and decreasing D2 receptor functions and contributes to epileptogenesis might be through the activation of mTOR pathway (Bozzi and Borrelli, 2013).

Other notable molecular regulators include: Nrf2 (nuclear factor erythroid 2-related factor) defence pathway (Mazzuferi et al., 2013), Neuropeptide Y (NPY) (Noe

et al., 2008; Vezzani et al., 1999), Galanin (Mazarati et al., 2006; Mazarati, 2004), NRGN (Zhong and Gerges, 2012), Adenosine (Brooks-Kayal et al., 2009).

1.2.5.3 Inflammatory and Immune pathways

Rasmussen encephalitis, the refractory focal seizures caused by chronic localized encephalitis that involve activation of astrocytes, microglia, and disruption of BBB endothelial cells with triggering peripheral immune cells and production of inflammatory mediators, was the first demonstration of an epilepsy associated with chronic brain inflammation (Rasmussen et al., 1958). At present, growing evidence is emerging that inflammatory and immune pathways probably play a key role in both the origin of individual seizures and in the development of epilepsies with various aetiologies (Loscher et al., 2013; Vezzani et al., 2011). Two major inflammatory mechanisms have been linked to epilepsies: (1) chronic neuroinflammation which can directly affects neuronal, glial and neurovascular functions; (2) systemic inflammation mediated and facilitated by BBB breakdown can contribute to neuronal hyperexcitability through alterations of ion channel functions and dysregulation of neurotransmitter homeostasis (Marchi et al., 2014). Furthermore, there is a closely linked and reciprocal influence between the chronic neuroinflammation and systemic inflammation.

The inflammatory mediators which are mainly released by glia (astrocytes and microglia), BBB endothelial cells, leukocytes, and which also can be produced by neurons, contribute to neuronal hyperexcitability, neurodegeneration, as well as BBB dysfunction during epileptogenic process (Vezzani et al., 2011). Upregulation of cytokines such as interleukin-1β (IL-1β) and chemokines such as C-C motif ligand 2 (CCL2) have been displayed in both animal models of epilepsy and in the brain tissue of epileptic patients (Bozzi and Caleo, 2016; de Vries et al., 2016). Some proinflammatory and inflammatory pathways such as CCL2/CCR2 signalling, IL-1 receptor/Toll-like receptor signalling, cyclooxygenase-2/prostaglandin (COX-2) and transforming growth factor-β (TGF-β) signalling cascades has been proposed in the

mechanisms of epileptogenesis (Bozzi and Caleo, 2016; Hui Yin et al., 2013; Vezzani et al., 2013; Xu et al., 2013).

In addition, the leukocyte-endothelial adhesion interactions which govern the mechanisms of transmigration of circulating immune cells across BBB into the brain parenchyma have been suggested to have a role during epileptogenesis (Fabene et al., 2013). For instance, the vascular expression of leukocyte adhesion molecules, such as intracellular adhesion molecule-1 (ICAM-1) and vascular cell adhesion molecule-1 (VCAM-1), have been shown markedly increase in experimental animal models of epilepsy (Fabene et al., 2008). Moreover, the extracellular neuronal matrix (ECM) integrity, which is associated with the modulation of AMPA receptor mobility, paired-pulse depression, L-type voltage-dependent Ca^{2+} channel activity and long-term potentiation (LTP) processes, also can be altered by the inflammatory and immune processes in brain (Di Maio, 2014).

1.2.5.4 Synapse regulation

Two fundamental mechanisms contribute to the homeostatic regulation of neuronal excitability and seizure dynamics: (1) modulation of synaptic strength (also named synaptic plasticity) via synaptic modification mechanisms; (2) non-synaptic regulation of ion channels including changes of membrane potential (Da Silva et al., 2012).

A synapse consists of three major compartments: presynaptic terminal, postsynaptic site and glial cell processes surrounding them. Neurotransmitters such as GABA or glutamate are released from the presynaptic terminal and transmitted toward their postsynaptic receptors which enables signal communication between neurons. For example, presynaptic glutamate release can activate postsynaptic receptors such as NMDA, AMPA, kainate or metabotrophic receptors and neuronal depolarization followed by calcium influx leading to activation of kinase cascades and phosphatases that change the phosphorylation of transcriptional factors which ultimately trigger a variety of signalling pathways. Subsequently, these molecular

signals can modulate synaptic properties and functions through expansion of the postsynaptic density, enlargement of the postsynaptic dendritic spines and clustering of the postsynaptic excitatory neurotransmitter receptors (Bourne and Harris, 2008; Rakhade and Jensen, 2009). Astrocytes can respond to many neurotransmitters and hormones and release various factors to influence synaptic properties. Perisynaptic astrocytes importantly modulate the environment of the synapses, as well as affect synaptic function through regulation of extracellular K^+ concentration, neurotransmitter uptake (e.g. glutamate), energy supply (e.g. ATP) to neurons, dendritic spine formation and synaptic maturation etc. (Bernard, 2012).

Synaptic transmission is operated through the synaptic vesicle formation, release and endocytosis which requires many proteins including dynamin, syndapin, synapin, synaptic vesicle protein 2A (SV2A), synaptotagmins, and SNARE proteins such as syntaxin, synaptosomal-associated protein 25 (SNAP-25), vesicle-associated membrane protein (VAMP). Continuous synaptic vesicle recycling and the synaptic vesicle cycle maintain synaptic transmission. Synaptic transmission and plasticity can be regulated by many different neuropeptides such as BDNF, NPY, galanin, ghrelin and somatostatin (Casillas-Espinosa et al., 2012; Leal et al., 2014).

Modification of synaptic strength can occur in several ways: (1) reduce or increase the synapse number formed by a given presynaptic neuron on its target postsynaptic neuron can be attained via pruning/death of the presynaptic neuron or sprouting/neurosynaptogenesis, respectively; (2) modulate the properties of presynaptic terminal such as by changing the release probability, concentration of neurotransmitters in vesicles, or modifying presynaptic receptors; (3) alter the postsynaptic receptor subunit composition, number and function by phosphorylation or anchoring; (4) tune the milieu of synapse through glia to modulate neurotransmitter uptake, neuronal energy supply… and so on. Synaptic modifications of GABAergic and glutamatergic synapse strength during epileptogenesis are time-dependent and can modify network information processing and eventually enable seizure occurrence (Bernard, 2012).

1.3 Experimental Models of Seizure and Epilepsy

1.3.1 Introduction

The first issue is “why” do we need experimental model systems in seizure and epilepsy research? Epileptogenesis and ictogenesis (seizure generation) in epilepsies involve complex mechanisms and pathophysiologic disturbances. Due to ethical concerns, it is difficult to acquire comprehensive studies of basic mechanisms underlying epilepsy, antiepileptic drugs (AEDs), or to screen for discovery of new AEDs in human patients. As a result, different model systems, either *in vitro* preparations or *in vivo* animal models, have been developed and extensively used in epilepsy research.

The second issue is “what” we are modelling? A seizure is composed of both electrical and behavioural characteristics which comprise chemical, molecular and anatomical features. Hence, it is necessary to recognize that *in vitro* and *ex vivo* preparations are models of “seizure-like” phenomena which are called spontaneous recurrent epileptiform discharges (SREDs). In contrast, the *in vivo* animal models are able to mimic acute epileptic seizures, status epilepticus and/or epilepsy disorders.

Finally, the last issue is “how” to model? Overall, there are two categories of modelling systems: *in vitro* (including *ex vivo*) models and *in vivo* whole-animal models. The selection of models depends on the questions of interests, the need to be addressed, the technical expertise of the investigators, as well as available facilities (Kandratavicius et al., 2014; Pitkanen et al., 2006; Sarkisian, 2001).

1.3.2 *In Vitro* Models for Studying Seizure and Epilepsy

1.3.2.1 Introduction

Due to the complexity of brain function and neuronal connectivity, some aspects of epilepsy are difficult to study under *in vivo* conditions. Therefore, *in vitro*

preparations of seizure-like models provide a simplified method for investigating the mechanisms of epileptic seizures and epilepsies at different levels, such as electrophysiological properties, roles of ion channels in action potential generation, synaptic plasticity, molecular biology profiles, high-resolution molecular imaging analysis, and pharmacological studies. Some of these studies are enabled because *in vitro* preparations allow better control of various parameters: pH, temperature, and neuronal environment. However, clinical seizures consist of abnormal hypersynchronization of neuronal discharges associated with behaviours or motor components. Thus, while *in vitro* models of epilepsy are fundamentally based on the equivalents of characteristic bursts of electrical activity in seizures they cannot be properly called seizures as they cannot recapitulate the behavioural components.

A variety of *in vitro* experimental techniques that have been applied to model the hypersynchronized neuronal activity of seizures are summarized in Table 1.1 (Pitkanen et al., 2006). There are many different *in vitro* models which are widely used in seizure and epilepsy research, including acutely dissociated nerve cells from animal or human brain tissue, dissociated cell cultures, organotypic slice cultures, and acute *ex vivo* slices (Dichter, 1978; Pitkanen et al., 2006; Potter and DeMarse, 2001; Reddy and Kuruba, 2013). Dissociated cell cultures from neocortex or hippocampus have been extensively utilized for studying synapses, basic physiology, molecular biology and mechanisms of action of AEDs in epileptiform activity, and seizure-like activity.

Table 1.1 *In Vitro* Models for the study of Seizure and Epilepsy

Preparation Methods	Models	Mechanisms of Action	References
Acutely Dissociated Single Nerve Cells	Epilepsy human brain tissue (surgical biopsy or resection)		(Pitkanen et al., 2006)
	Tissue from Epileptic Animal models		
Dissociated Cell Cultures; Organotypic Slice Cultures; Acute Slices	Low Calcium	Inhibition of evoked synaptic neurotransmission causes spontaneous paroxysmal discharges	(Jefferys and Haas, 1982) (Taylor and Dudek, 1982)
	Low Magnesium (or Mg^{2+}-free)	Activated NMDA receptors, Ca^{2+} influx	(Anderson et al., 1986) (Mody et al., 1987)
	High Potassium	Induced spontaneous hyperexcitability and the elevated the general excitability of neuronal network	(Jensen and Yaari, 1988) (Traynelis and Dingledine, 1988)
	4-Aminopyridine	A K^+ channel blocker abolishes transient potassium currents and depolarises by reducing K^+ efflux from cells	(Galvan et al., 1982) (Perreault and Avoli, 1989)
	Kainic Acid	An excitotoxic glutamate analogue depolarizes neurons that express KA receptors	(Zaczek et al., 1981) (Robinson and Deadwyler, 1981) (Ben-Ari and Cossart, 2000)
	Glutamate	Enhances activity of excitatory glutamate receptors	(Sun et al., 2001) (DeLorenzo et al., 2007)
	Pentylenetetrazole (PTZ)	Block $GABA_A$ receptors leading to loss of inhibition and depolarization of neurons	(Qu et al., 2005)
	Bicuculline		(Debanne et al., 1995) (Jimbo and Robinson, 2000)
	Penicillin		(Schwartzkroin and Prince, 1978) (Swann and Brady, 1984)
	Picrotoxin		(Miles and Wong, 1986)
	Electrical Stimulation	Tetanic stimulation provokes a long term potentiation-like effects (Ictal-like after discharges)	(Stasheff et al., 1985) (Rafiq et al., 1993)
Chronic Brain Slice	Slices from Chronic Animal Models of Epilepsy		(Pitkanen et al., 2006)

1.3.2.2 High potassium model

Potassium plays a principle role in setting membrane potential, and the transmembrane potassium gradient mainly determines resting potential in neurons (Poolos et al., 1987). When the extracellular potassium concentration raises more than 3 mM above its baseline level (standard baseline level: 3-3.5 mM) and up to or beyond 7.5 mM $〔K^+〕_0$ ACSF, spontaneous hypersynchronous epileptiform activity can be induced *in vitro* (Balestrino et al., 1986; Jensen and Yaari, 1988; Poolos et al., 1987; Traynelis and Dingledine, 1988). The equilibrium potential for K^+ elevates to a more positive value while the extracellular potassium concentration increases, following the Nernst and Goldmann equations, and the neuronal resting membrane potential raises towards the threshold of action potential. As a result, neurons become hyperexcitable and eventually elicit bursts of epileptiform activity. This model increases the general excitability of all neuronal networks, and it may be particularly relevant to investigate changes in astrocytes because extracellular K^+, which affects neuronal excitability, is primarily buffered by astrocytes (Reddy and Kuruba, 2013).

1.3.2.3 Low magnesium model

Low or zero-magnesium model is also a widely used *in vitro* model for studying mechanisms of seizure like activity. Spontaneous epileptiform bursting can be evoked when extracellular Mg^{2+} concentration is lower than 1 mM or is completely removed from ACSF. Magnesium plays an important role in regulation of glutamate signalling in brain through following mechanisms: (1) the Mg^{2+} cation can block ionotropic NMDA (N-methyl-D-aspartate) receptors in a voltage-dependent manner (Figure 1.4) (Burnashev et al., 1992; Mori et al., 1992; Pitkanen et al., 2006); (2) High extracellular Mg^{2+} can inhibit presynapyic glutamate release by antagonizing calcium influx in presynaptic neurons (de Baaij et al., 2015).

Extracellular Mg^{2+} blocks NMDA channels under physiological conditions and inhibits NMDA-dependent currents while the membrane potential is close to resting potential (Decollogne et al., 1997). NMDA receptors are highly permeable to Ca^{2+} and are one of the receptors for the excitatory amino acid (EAA) neurotransmitter, glutamate. Therefore, reduction or omission of Mg^{2+} enhances activation of NMDA receptors and results in robust glutamate-dependent excitation and continuous hypersynchronous firing of neurons (DeLorenzo et al., 1998; Gibbs et al., 1997; Pal et al., 2001; Sombati and Delorenzo, 1995). Extracellular Mg^{2+} also has action in inhibition because it can stimulate $GABA_A$ receptors which contribute to neuronal hyperpolarization. Thus low Mg^{2+} conditions lead to less activation of $GABA_A$ receptors and consequent depolarisation of the membrane potential with subsequently releases Mg^{2+} from NMDA receptors resulting in increasing neuronal excitability (de Baaij et al., 2015). In addition, a possibly alternative mechanism has been reported is that low or free of magnesium concentration via activation of transient receptor potential melastanin 7 (TRPM 7) channels, ubiquitous and stress-activated nonselective cation channels, that lead to neuronal depolarization, because these channels may regulate the Mg^{2+} homeostasis and are important for setting the magnesium concentration in cells (Bates-Withers et al., 2011; Trzeciakiewicz et al., 2005; Wykes et al., 2007).

In the low-Mg^{2+} model, hyperexcitability can persist for the life of the cultured cells (typically more than 2 weeks) even if the cells are only treated with Low-Mg^{2+} or Free-Mg^{2+} condition for longer than 3 hours, and normal Mg^{2+} concentration has been restored after this (Pitkanen et al., 2006). There are two stages of epileptiform activity in this model: Initially, the seizure-like activity is sensitive to the clinical concentrations of phenytoin, carbamazepine, valproate, barbiturate, and/or benzodiazepine. However, the activity transitions to the late recurrent discharges around 1 hour (30 to 90 minutes) after the onset of epileptiform discharges. The late stage is characterized by a pharmacoresistant situation with these drugs losing their efficacy and this property lets low-Mg^{2+} model serve as a common approach for studying drug resistant epilepsy (Dreier et al., 1998; Reddy and Kuruba, 2013; Zhang et al., 1995).

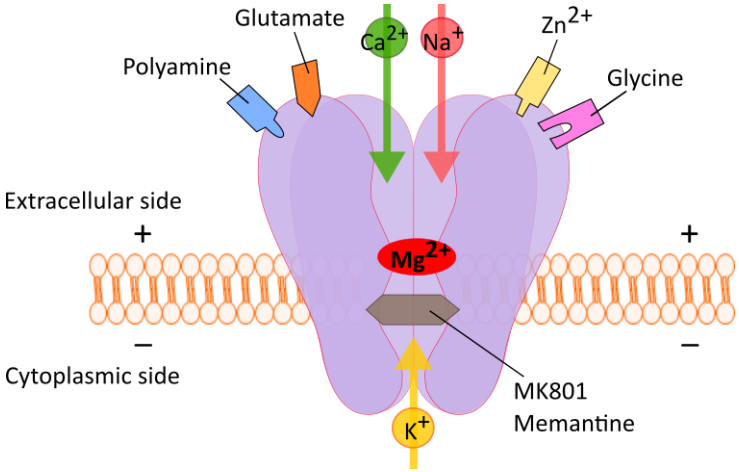

Figure 1.4 Structure of NMDA Receptor Complex and its binding sites

NMDA receptors are blocked by Mg^{2+} at normal resting membrane potential (-70 mV), but the Mg^{2+} block is relieved when the membrane potential rises above -60 mV and NMDA receptors are activated and opened upon glutamate binding and permit the influx of Na^{+}, Ca^{2+} and efflux of K^{+} then lead to cell depolarization.

1.3.2.4 Kainic acid model

Kainic acid (K.A.) is an analogue of L-glutamate and the prototype agonist of the kainate class of glutamate receptors with powerful convulsant activity (De Deyn et al., 1992; Levesque and Avoli, 2013). The excitatory effects of K.A. were initially described in rat neocortical cells (Shinozaki and Konishi, 1970). It is a potent convulsant with multiple presynaptic and postsynaptic effects and can generate excessive depolarization in neurons which express kainate receptors abundantly, such as hippocampal pyramidal cells and interneurons (Ben-Ari and Cossart, 2000; Cossart et al., 1998; Frerking et al., 1998b; Huettner, 2003; Olney et al., 1974). Experimental bath manipulation of K.A. can elicit spontaneous epileptiform activity in neuronal cells and long-lasting potentiation of synaptic excitation can be observed after brief application of K.A. to rat hippocampal slices or cultures (Collingridge and McLennan, 1981; Fisher and Alger, 1984; Qi et al., 2006a).

1.3.2.5 Pentylenetetrazole (PTZ) model

Pentylenetetrazole (PTZ) is an antagonist of $GABA_A$ receptors which possesses powerful convulsant effects in rodents, cats, and primates (De Deyn et al., 1992; Vernadakis and Woodbury, 1969). Y-Aminobutyric acid (GABA) is the major inhibitory neurotransmitter in central nervous system and its inhibitory function is primary through chloride-permeant ion channels. GABA serves as one of the most important neurotransmitters in maintaining the overall electrical activity of brain at a level below that of epilepsy (Olsen, 1981). Therefore, the mechanisms of many anticonvulsants involve enhancing GABA action at different levels including GABA uptake, synthesis, release from nerve endings, or promoting the action of postsynaptic GABA receptors, whereas chemicals which interfere with GABA inhibitory synaptic release, transmission or receptors are pro-convulsant agents (Meldrum and Rogawski, 2007; Olsen, 1981; Pfeiffer et al., 1996; Pitkanen et al., 2006). The action of GABA is mainly via $GABA_A$ receptors which are ligand-gated ion

channels (also known as ionotropic receptors), and $GABA_B$ receptors which are G protein-coupled receptors (also known as metabotrophic receptors).

Fast GABAergic responses are principally mediated by $GABA_A$ receptors (Duggan and Stephenson, 1990; Macdonald et al., 1996; McKernan et al., 1991). $GABA_A$ receptors are heteropentameric chloride permeable channels assembled by five subunits: two α-sunubits, two β-sububits and one Y- or δ-subunit (Barnard, 2001; Ma et al., 2006). The pharmacological $GABA_A$ receptor blockers have been commonly applied in studies of epilepsy and seizure like activity, both *in vivo* and *in vitro*. The major convulsant potency of PTZ is mediated by the blockade of $GABA_A$ receptors by closing their Cl^- pores, mostly interacting with the TBPS (t-butyl-bicyclo-phosphorothionate) binding site (Figure 1.5). However, the mechanisms of PTZ still are not fully understood and other mechanisms such as nonspecific membrane effects (Pitkanen et al., 2006) and effects on potassium channels (Brima et al., 2013; Louvel and Heinemann, 1981; Madeja et al., 1994) also have been proposed.

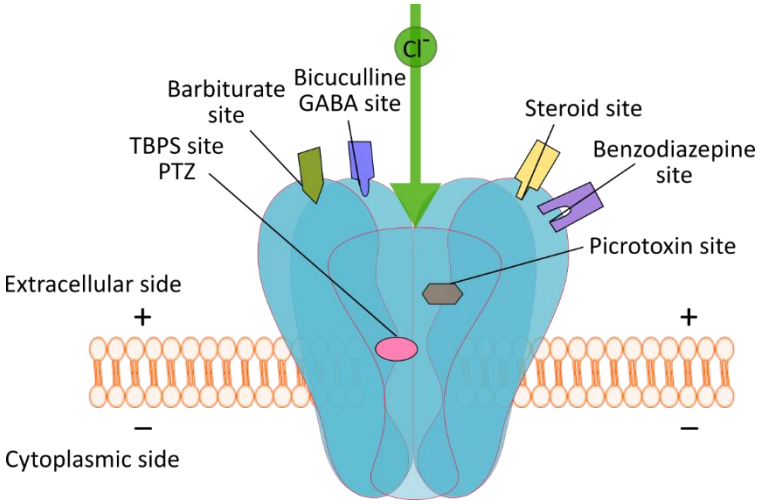

Figure 1.5 Schematic illustration of $GABA_A$ receptor and its binding sites

$GABA_A$ receptor is a ligand-gated ionotropic receptor which permits the influx of Cl^- through its pore upon activation resulting in neuronal hyperpolarization with decreasing membrane potential then inhibits the occurrence of action potential. However, when $GABA_A$ antagonists such as PTZ, Picrotoxin or Bicuculline binding to the receptors will block Cl^- influx by closing the ionophore of $GABA_A$ receptor. Reducing the $GABA_A$-mediated currents diminishes the inhibitory effects in neural networks.

1.3.3 *In vivo* epilepsy models

1.3.3.1 Introduction

Understanding the underlying mechanisms of epilepsy and epilepsy related phenomena is crucial for the development of new diagnostic approaches, novel therapeutic interventions, as well as preventive treatments. Animal models of epilepsies or seizures are the most often exploited tool and play an essential role in investigating the fundamental mechanisms of epilepsy, preclinical development and screening of novel AEDs, and assessment of the efficacy, and mechanisms of AEDs (Loscher, 2011). Many animal species have been developed for the study of epilepsy, from Drosophilia (Neobels, 1999; Timpe and Jan, 1987) to nonhuman primates (Jurgen Wenzel et al., 2000). However, rodents are the most commonly used species for model systems of epilepsies and acute seizures (Sarkisian, 2001) for several reasons: (1) they are mammals with genetic, biological, many behaviour characteristics and disease phenotypes closely resembling those of human beings; (2) they are convenient to handle, easily housed and maintained, as well as adapting well to new surroundings; (3) they have a relatively short lifespan of two to three years and can reproduce quickly; (4) they are less expensive and can be inbred for large quantities with almost identical genetically; (5) the use of rodents presents fewer ethical concerns than use of larger animals, including non-human primates.

Although a variety of animal models are available to demonstrate different types of epileptic seizures and epilepsies which are relevant to human diseases, it is difficult to perfectly reflect human conditions and fully reproduce known human epilepsy syndromes (Bagdy et al., 2007; Fisher, 1989; Hui Yin et al., 2013; Stables et al., 2003). However, animal models still provide an invaluable methodology to obtain information about basic electrophysiological, cellular and molecular mechanisms of epilepsy disorders. Moreover, the definition of epilepsy indicates the pathological conditions of spontaneous recurrent epileptic seizures (Fisher et al., 2005b), thus, it is necessary to discriminate between "models of seizures induced by experimental manipulations without chronic epileptic condition", and "models of epilepsy present

recurrent seizures associated with chronic epileptogenic disturbances" (Engel, 1992; Sarkisian, 2001).

Different epilepsy syndromes may encompass different clinical features, such as the manifestation of seizures, EEG features, response to antiepileptic drugs, trigger factors, interictal disturbances, onset age, family history, pathophysiological process, and structural anomaly (Engel and Pedley, 1997; Pitkanen et al., 2006). Consequently, it is important to select an appropriate animal model for a specific study purpose (Loscher and Brandt, 2010) and this can be achieved by considering whether the model we use satisfies the following criteria: (1) the model displays similar electrophysiological patterns /features observed in human as the EEG features represent an important hallmark of human epilepsy disorders; (2) having similar aetiologies with human epilepsies or acute seizures such as genetic predisposition, brain injury, neuronal migration disorders and so on; (3) animals exhibit pathological changes resembling those which characterise specific human conditions; (4) the model is able to reflect an equivalent age of onset for some specific epilepsy syndromes in human; (5) the model has similar response to AED as the human syndrome; (6) the seizure manifestations and associated behaviour characteristics are akin to human conditions (Sarkisian, 2001). Numerous frequently used animal models of epilepsies and acute seizures induced by chemical convulsants, metals, electrical stimulation, traumatic brain injury, metabolic dearrangements, and genetic models of seizures and epilepsies, as well as in utero chemical exposures and early irradiation are listed in Table 1.2.

Table 1.2 Summary of Animal models of epilepsy and acute seizure

Classification	Models	Mode of induction	Manifestations	Imitation of Human relevance
Chemically induced models	***Glutamate agonists:***			
	Kainic acid	Systemic (i.p.) Systemic chemical kindling ICV Intra-hippocampal Intra-amygdala Intra-substantia nigra	GTCs in systemic application; Focal seizures w & w/o generalization in limbic application	MTLE
	Others: NMDA; Homocysteine; Homocysteic acid; Domoic acid	Systemic (i.p.)	Generalized seizures	Acute GTCs
	Quisquialic acid	Systemic (i.p.) ICV	Generalized seizures	Acute GTCs
	Acetylcholine (Ach) -related substances:			
	Pilocarpine	Systemic (i.p.) Intra-hippocampal	GTCs in systemic application; Focal seizure w & w/o generalization in limbic application	MTLE
	Organophosphorous compound; Soman	Systemic (s.c.)	Generalized seizures	Acute GTCs

Table 1.2 (continued)

Classification	Models	Mode of induction	Manifestations	Imitation of Human relevance
Chemically induced models	***GABA antagonists:***			
	Pentylenetetrazole (PTZ)	Systemic (s.c., i.p. or i.v.) Neocortex	GTCs Focal seizure w & w/o generalization	Acute GTCs Acute cortical seizures
	Bicuculline	Systemic (i.p. or i.v.) Neocortex Area tempestas	Generalized seizures in systemic application; Focal seizures w & w/o generalization in cortical application	Acute GTCs; Acute cortical seizures
	Picrotoxin	Systemic (s.c., i.p. or i.v.) Intra-hippocampal	Generalized seizure in systemic application; Focal seizures w or w/o generalization in limbic application	Acute GTCs; Acute temporal lobe seizures
	Glutamic acid decarboxylase (GAD) inhibitors:			
	Allylglycine; 3-Mercaptopropionic acid(3-MPA); Thiosemicarbazide; Isonicotinehydrazide; β-carbolines; Ro 5-3663	Systemic (i.p.)	Generalized seizures	Acute GTCs

Table 1.2 (continued)

Classification	Models	Mode of induction	Manifestations	Imitation of Human relevance
Chemically induced models	***Other agents:*** Strychnine; Aminophylline/ Theophylline; Ricinine 4-Deoxypyridoxine	Systemic (i.p.)	Generalized seizures	Acute GTCs
	Opioids; Flurothyl	ICV; Systemic (inhalation)	Generalized seizures	Acute GTCs
	Potassium channel blocker: 4-Aminopyridine (4-AP)	Systemic (i.p. or s.c.) ICV Intra-hippocampal neocortex	Generalized seizures in systemic and ICV applications Focal seizures w & w/o generalization in focal cerebral applications	Acute GTCs Acute cortical or limbic seizures
	Sodium channel blocker: Tetrodotoxin (TTX)	Chronically infused into the developing neocortex or hippocampus of infant rats	Symmetric or asymmetric spasms	Infantile spasms
	Na+/K+ ATPase inhibitors: Ouabain	Systemic (i.p.)	Generalized seizures	Acute GTCs
	Tetanus toxin	Intra-hippocampal Neocortex	Focal seizures w & w/o generalization	MTLE Focal neocortical epilepsy

Table 1.2 (continued)

Classification	Models	Mode of induction	Manifestations	Imitation of Human relevance
Chemically induced models	***Antibiotics:*** Penicillin; Oxacillin; Methicillin; Ampicillin; 1st generation of Cephalosporins	Neocortex	Focal seizures w & w/o generalization	Acute cortical seizures
	Metals: Cobalt; Nickel; Antimony; Iron (Ferric chloride); Zinc; Tungsten; Aluminium (alumina gel)	ICV Neocortex	Focal seizures w & w/o generalization	Focal neocortical epilepsy Post traumatic epilepsy
Electrical stimulation models	Maximal electroshock (MES)	whole brain (via corneal or auricular)	GTCs	Acute GTCs
	Focal electrical stimulation	Neocortex	Focal seizures w & w/o generalization	Acute cortical seizures
	Subcortical electrical stimulation	Subcortcal	Focal seizures w & w/o generalization	Acute focal seizures
	Perforant pathway stimulation	Focal electrical stimulation in MTL	Focal seizures w & w/o generalization	MTLE
	Kindling (repeat afterdischarge induction)	Limbic system Neocortex	Focal seizures w & w/o generalization	MTLE Focal neocortical Epilepsy

Table 1.2 (continued)

Classification	Models	Mode of induction	Manifestations	Imitation of Human relevance
Metabolic dearrangement	Hyperthemia	Systemic	Generalized seizures	Acute GTCs
	Hypoxia	Systemic	Generalized seizures	Acute GTCs
	Insulin-induced hypoglycemia; Hyperbaric oxygen; Hypercarbia; CO_2 withdrawal; Uremia; Drug/Alcohol withdrawal	Systemic	Generalized seizures	Acute GTCs
Brain injury models	Freeze/ cryogenic	Freeze lesion to skull surface	GTCs with focal origin	Post-traumatic epilepsy
	Fluid percussion	Rostal parasaggital fluid percussion	GTCs with focal origin	Post-traumatic epilepsy
	Partial cortical isolation	Partially isolated cortical slab	Focal seizures w & w/o generalization	Post-traumatic epilepsy
Cerebral infarction models	MCA; MCA/CCA	MCA occlusion; Transient MCA/CCA occlusion	Focal seizures w & w/o generalization	Post stroke neocortical epilepsy
	Photothrombosis	Rose bengal injection from femoral vein followed by focal laser stimulation in neocortex	Focal seizures w & w/o generalization	Post stroke neocortical epilepsy

Table 1.2 (continued)

Classification	Models	Mode of induction	Manifestations	Imitation of Human relevance
CNS Infection models	Taenia crassiceps granuloma	Intra-amygdala Intra-hippocampal Neocortex	Focal seizures w & w/o generalization	Infectious encephalitis epilepsy (minic neurocysticercosis)
	Herpes simplex virus, type-1 (HSV-1)	Infected through corneal scarification or transal inoculation	Focal seizures w & w/o generalization	Herpes encephalitis epilepsy (predominatly involved hippocampi)
Brain tumour models	Glioma cells	Transplant to Neocortex	Focal seizures w & w/o generalization	Glioblastoma induced epilepsy
Immunization models	Glutamate receptor subunit GluR3 protein	Repeated subcutaneous immunization	Focal seizures w & w/o generalization	Rasmussen's encephalitis
Antibody	Anti-monosialoganglioside antibodies (Anti-GM 1)	Neocortex	Focal seizures w & w/o generalization	Focal neocortical epilepsy
In utero irradiation; **Freeze;** **Chemical exposure**	Irradiation Freeze Methylazonymethanol (MAM)	whole brain	Focal seizures w & w/o generalization	Cortical dysplasia epilepsy (Freeze induced microgyria)

Table 1.2 (continued)

Classification	Models	Mode of induction	Manifestations	Imitation of Human relevance
Genetic models	Audiogenic models (LGI 1 transgenic or knocknout mice)	Acoustic stimulation	Focal seizures w & w/o generalization	Reflex epilepsy & lateral temporal epilepsy
	GAERS (Genetic absence epilepsy in rats from Strasbourg); WAR/Rij rat (Wistar Albino Glaxo/Rijwijk rat); Mouse models of absence seizures			Absence epilepsy
	Genetically epilepsy prone rat (GEPR); Spontaneous epileptic rat (SER); EL mouse; Stargazer mouse; Serotonin receptor and synapsin-deficient mouse; Tottering mouse; Lethargic mousel Slow-wave epilepsy mice; Mocha mouse; Ducky mouse			
	seizure prone gerbil; Photosensitive Papio papio baboon; Epileptic beagle dog			
	Transgenic and genetic knockout mice models: targeting on seizure phenotype associated ion channels, transporters, and neurotransmission pathways.			

(Abbreviations: s.c. subcutaneous; i.p. intraperitoneal; i.v. intravenous; ICV: intracerebroventricular; MTL: mesial temporal lobe; MTLE: mesial temporal lobe epilepsy; GTCs: generalized tonic-clonic seizures; w: with ; w/o: without; MCA: middle cerebral artery; CCA: common carotid artery)

Reference: (Avanzini, 1995; De Deyn et al., 1992; Engel, 1992; Engel, 2009; Fisher, 1989; Kandratavicius et al., 2014; Loscher, 2011; Pitkanen et al., 2006; Reddy and Kuruba, 2013; Sarkisian, 2001)

1.3.3.2 Tetanus toxin Model of Focal Epilepsy

1.3.3.2.1 Introduction

Tetanus neurotoxin (TeNT) is secreted the by strictly anaerobic bacteria Clostridium tetani and is a metalloprotease (zinc-dependent protease) that specifically targets neurons (Schiavo et al., 1992b). TeNT is a heat labile protein which consists of three domains. Two domains comprise a heavy chain and one domain makes a light chain with a disulphide bond linked between both chains. Intact toxin is necessary for uptake by neurons since the function of the heavy chain is for specific binding and internalisation into neurons, as well as transportation along the neuronal processes (Schiavo et al., 2000). The action of light chain is proteolysis and it is inactive when it is bound to the heavy chain. The light chain can be activated by cleavage of the interchain disulphide bond once the TeNT inside cells (Schiavo et al., 2000). Then the activated light chain can specifically cleave synaptobrevin which is a vesicle-associated membrane protein (VAMP) and a component of the SNARE (**SNA**P **RE**ceptor) complex that is critically responsible for presynaptic neurotransmitter release (Montecucco and Schiavo, 1993; Schiavo et al., 1992a). As a result, TeNT causes vesicles to fail to fuse to the presynaptic membrane disrupting exocytosis and the release of neurotransmitters. Furthermore, it has been demonstrated that the TeNT effect is largely limited to inhibitory neurotransmission in spinal cord and brainstem which causes spastic paralysis of “lockjaw” reflex spasms and autonomic instability (Farrar et al., 2000; Shin et al., 2012). In brain, TeNT has been shown to affect both excitatory and inhibitory transmission but it has much higher selectivity and impact on inhibitory neurotransmission (Albus and Habermann, 1983; Ferecsko et al., 2015). Therefore, epilepsy can be generated by local injection of TeNT into the desired brain region which can be taken by nerve endings and predominantly interfere presynaptic vesicle release of inhibitory neurotransmitters, particularly at GABA mediated synapse.

1.3.3.2.2 TeNT Models of Focal Neocortical Epilepsy or Temporal Lobe Epilepsy

Seizures induced by TeNT in rats, mice, guinea pigs and rabbits were first described in 1898 by Roux and Borrell (Roux E, 1898). After that, Brooks et al. reported local injection of TeNT into cat motor cortex elicited seizures (Brooks and Asanuma, 1962). In 1977, Mellanby et al. introduced the rat model of temporal lobe epilepsy by focal administration of TeNT into rat hippocampus which produced spontaneous recurrent seizures for several weeks (Jefferys et al., 1995; Mellanby et al., 1977). In addition to the hippocampal epilepsy model induced by TeNT in rats, focal neocortical epilepsy models (motor cortex, parietal and somatosensory cortex) caused by local injection of TeNT in rats (Brener et al., 1991; Empson et al., 1993; Hagemann et al., 1999; Nilsen et al., 2005), or in mice visual cortex also have been developed (Mainardi et al., 2012).

The occurrence of spontaneous seizures after TeNT injection depends on dose and usually begins from around one week post injection. The seizures are sustained for weeks or months then subside (Brener et al., 1991; Finnerty and Jefferys, 2000, 2002; Hawkins and Mellanby, 1987). The tetanus toxin models of intra-hippocampal and neocortical epilepsies have been shown to produce frequent and severe focal seizures and may evolve to secondary generalised seizures as well (Brener et al., 1991; Jefferys et al., 1995; Louis et al., 1990). The behavioural manifestations of the seizures and the underlying epileptic activity are similar to that seen in human epilepsies (Mellanby et al., 1977; Nilsen et al., 2005). Another feature of this model is resistance to AEDs which mimics refractory focal epilepsy in humans (Nilsen et al., 2005).

Although the focal application of TeNT into neocortex or hippocampus has been a commonly used model of focal epilepsy for a long period, the mechanism by which TeNT induces epilepsy still is not fully understood. Tetanus toxin is cleared from the brain within a few days after local injection, however the process of epileptogenesis still proceeds, resulting in recurrent spontaneous seizures over

several weeks (Fisher, 1989; Mellanby et al., 1977). It remains unclear how the seizures and epileptiform activity persist in the long term despite the clearance of tetanus toxin in the brain and without apparent component of histological tissue damage.

1.3.3.3 Kainic Acid Model of Chronic Epilepsy

1.3.3.3.1 Introduction

Kainic acid (K.A.) is one of the excitatory amino acid-related drugs and is a close analogue of glutamate (Hayashi, 1952). According to different mechanisms of the postsynaptic current, glutamate receptors can be categorized into two major groups: ionotropic glutamate receptors and metabotropic glutamate receptors (Table 1.3). The ionotropic glutamate receptors contain an ion channel pore and tend to be activated quicker when glutamate binds to the receptors, whereas the metabotropic glutamate receptors activate ion channels indirectly through G protein related signalling cascades which are associated with a more prolonged stimulation (Palmada and Centelles, 1998). The ionotropic glutamate receptors are a family of ligand-gated cation channels which have three subtypes of receptors including NMDA receptors, AMPA receptors, and Kainate receptors (Figure 1.6). K.A. is a potent neurotoxin with powerful neuronal excitatory effect and has high affinity to kainate receptors which have the highest expression in the hippocampus (Collingridge and Lester, 1989; Levesque and Avoli, 2013; Miller et al., 1990). The K.A.-induced epilepsy model has been extensively used as a model of mesial temporal lobe epilepsy (mTLE) since it shares many features of human mTLE. Furthermore, it is also a common experimental model in status epilepticus (SE) and for studying the mechanisms of epileptogenesis after status epilepticus (Ben-Ari, 1985; Cavalheiro et al., 1982). Overall, the K.A. induced epilepsy model is characterized by three major stages: Initially, hour-long status epilepticus occurs upon administration of kainic acid. After this resolves, it is followed by a latent period of variable duration (days to weeks), and then chronic recurrent spontaneous seizures gradually develop with

progressively increasing frequency and become refractory (Ben-Ari, 1985; Ben-Ari and Cossart, 2000; Levesque and Avoli, 2013; Nadler, 1981; Pitkanen et al., 2006).

Table 1.3 The family of Glutamate Receptors

	Ionotropic			Metabotropic		
Subtypes	AMPA receptor	NMDA receptor	Kainate receptor	Group I receptors	Group II receptors	Group III receptors
	Subunits: $GluR_1$ $GluR_2$ $GluR_3$ $GluR_4$	Subunits: NR_1 NR_{2A} NR_{2B} NR_{2C} NR_{2D} NR_{3A} NR_{3B}	Subunits: $GluR_5$ $GluR_6$ $GluR_7$ KA_1 KA_2	 $mGluR_1$ $mGluR_5$	 $mGluR_2$ $mGluR_3$	 $mGluR_4$ $mGluR_6$ $mGluR_7$ $mGluR_8$
Binding sites	AMPA	Glutamate Glycine ketamine Polyamines PCP, MK-801	Kainate			

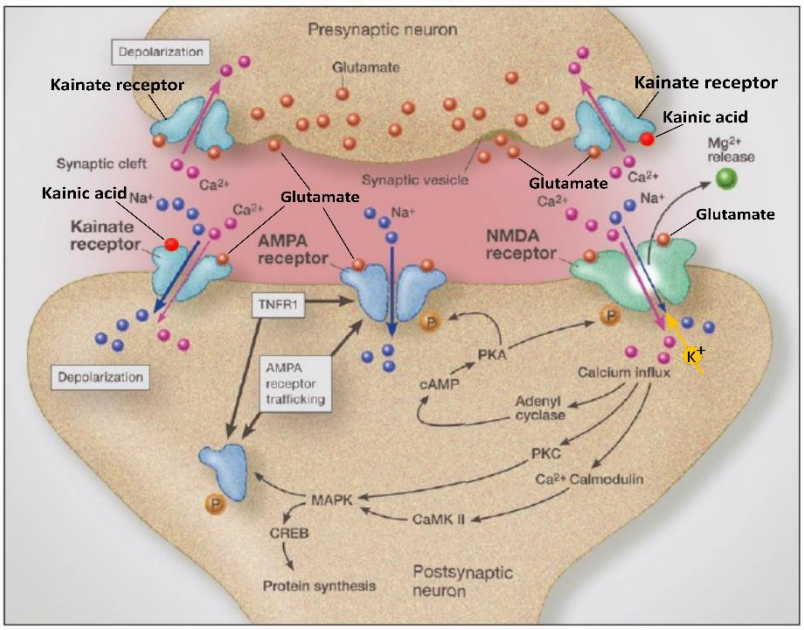

Figure 1.6 Illustration of Ligand-gated ionotropic glutamatergic receptors

Kainate receptors have both presynaptic and postsynaptic effects; NMDA receptors and AMPA receptors are mainly located in the postsynaptic membrane. (Adapted from Surgical Neurology International 2011, 2:107)

1.3.3.3.2 Systemic Application of Kainic Acid

Systemic administration of K.A. generates severe convulsions and wide-spread brain damage with neuronal necrosis and degeneration in several brain areas but the most profound neuronal lesions are observed in hippocampus, amygdala, and pyriform cortex (Ben-Ari et al., 1981; Schwob et al., 1980; Sperk et al., 1985). The hippocampus, especially CA3 pyramidal cells, is most vulnerable to the epileptogenic effects of K.A. because the highest density of kainate receptors is in the CA3 region (Ben-Ari et al., 1981; Zaczek et al., 1981). As a result, the ictogenic zone is initiated from the limbic structure, principally the hippocampus in the K.A. animal epilepsy model, and the seizure behavioural manifestations are classified as focal seizures with or without secondary generalisation (Levesque and Avoli, 2013; Lothman et al., 1981). Two strategies of systemic administration of K.A. have been applied: a single high dose injection and multiple low dose injections until the occurrence of status epilepticus. The later modality can reduce the mortality rate (Hellier and Dudek, 2005; Sharma et al., 2007). Generally, the severity of the seizure symptoms depends on the dose of K.A. and status epilepticus mostly takes place within 1 hour after K.A. injection, and can be terminated by benzodiazepines (e.g. diazepam) or a combination of diazepam and ketamine (Ben-Ari et al., 1984; Giorgi et al., 2005; Levesque and Avoli, 2013). However, a larger dosage of benzodiazepine is needed to cease SE in rats when the SE is sustained longer than 50 minutes, and this phenomenon is akin to the condition of decreasing or lacking therapeutic efficacy of benzodiazepines in humans with prolonged SE (Reddy and Kuruba, 2013).

1.3.3.3.3 Intra-amygdala Kainic Acid model

In addition to systemic administration of K.A., focal intracerebral manipulations of K.A. in hippocampus or amygdala provide an alternative approach to model mesial temporal lobe epilepsy in humans. This approach produces typical histopathological changes with a primarily unilateral hippocampal damage and limited extra-hippocampal lesions (Ben-Ari et al., 1979a; Ben-Ari et al., 1980a;

Cavalheiro et al., 1982; Henshall et al., 2000). Similar to systemic K.A. application, intra-amygdala K.A. administration is an effective trigger of generalised status epilepticus which starts approximately 5-60 minutes after injection. Subsequently, the animals enter an epileptogenic latent period which may last for 5-40 days, which is then eventually followed by chronic recurrent spontaneous seizures (Gurbanova et al., 2008; Mouri et al., 2008). The characterization of acute seizure behaviours after K.A. injection is similar in both the intrahippocampal and intra-amygdaloid K.A. model in rats which encompasses both non-convulsive and convulsive symptoms, but rats with intra-amygdaloid K.A. injection may exhibit additional symptoms such as salivation and exophthalmos (Levesque and Avoli, 2013). Furthermore, previous studies have suggested that epileptic activity initiates in amygdala then propagates to ipsilateral hippocampus, contralateral hippocampus and amygdala, as well as cortex (Ben-Ari et al., 1980a).

1.4 Selection of Candidate Genes

A vast number of genes are differently regulated in epileptogenesis, however, the aim of this project was not to comprehensively track all gene changes. We aimed to select a set of genes that could be pivotal molecules in the development of epilepsy and may be indicators of how similar or how different models are. Therefore, the candidate genes were chosen because (1) they have been linked to epileptogenesis; (2) are implicated in changes in crucial neuronal function, or (3) have repeatedly been shown to change in epilepsy. Totally, 13 candidate genes were selected from several different categories and these are: (1) important transcriptional factors involved in neuronal gene regulation: CREM/ICER II (cAMP-responsive element modulator/Inducible cAMP early repressor II), and REST/NRSF (repressor element 1-silencing transcription factor/Neuron-restrictive silencer factor); (2) translational regulators regulating protein synthesis (ex. synaptic proteins…etc.): mTOR (mammalian target of rapamycin) (Wong, 2008); (3) regulators of synaptic transmission and synaptic plasticity: BDNF (brain-derived neurotrophin

factor) (Leal et al., 2014); (4) key synaptic proteins contributing to synaptic vesicle fusion and ultimately impacting synaptic neurotransmitter release: SNAP-25 (synaptosomal-associated protein of 25 kDa) (Antonucci et al., 2016); (5) interaction with postsynaptic calmodulin (CaM), CaM-dependent protein kinase II (CaMKII) associated with regulation of long-term depression (LTD) or long-term potentiation (LTP): NRGN (Neurogranin) (Zhong and Gerges, 2012); (6) neuronal ion channel genes which play a key role in control of neuronal excitability and rhythmicity: HCN1 (hyperpolarization-activated cyclic nucleotide-gated channel 1), HCN2, and KCNA1 (potassium voltage-gated channel subfamily A number 1, also known as Kv1.1) (Baruscotti et al., 2010; Gautier and Glasscock, 2015; Shah, 2014); (7) genes supporting inhibitory neurotransmitter signalling: GABRA5 (Y-aminobutyric acid A receptor, alpha 5 subunit) (Glykys and Mody, 2006; Gonzalez et al., 2013); (8) astrocyte function related gene and astrocytic predominantly enzyme: GFAP (glial fibrillary acidic protein) and ADK (Adenosine kinase) (Clasadonte and Haydon, 2012; Devinsky et al., 2013); (9) critical chemokine mediated neuroinflammatory and immue pathways: CCL2 (C-C motif ligand 2) (Bozzi and Caleo, 2016).

Chapter 2 Thesis Aims

The overall aim of this thesis is to investigate the regulation of a subset of genes during epileptogenesis in multiple experimental models of epilepsy. We seek to identify common changes during epileptogenesis, which may highlight master regulators, clarify epileptogenic mechanisms and indicate pathways driving epileptogenesis. Ultimately this approach may broaden the range of targets for epilepsy treatment. This thesis is set out in the following aspects:

1. Determine the mRNA expression of candidate genes in different *in vitro* models of seizure like activity, and establish a molecular profile for further comparison between *in vitro* and *in vivo* models.

2. Characterize the temporal changes of gene regulation during the epileptogenic process using an *in vivo* model of epilepsy.

3. Optimise and validate an alternative rat model of epilepsy that can be applied for comparing this set of candidate genes at similar time points which may further provide how conserved (or not) gene regulation is during epileptogenesis, and could be suitable for further investigation of epilepsy gene therapy.

Chapter 3 Materials and Methods

3.1 *In vitro* experiments

3.1.1 Preparation and maintenance of cortical neuronal cultures

Postnatal day 0 (P0) or day 1 (P1) Sprague-Dawley rats collected from the University College London (UCL) Biological services were used. These animals were sacrificed according to the UK Home Office protocols as legislated by the Animals (Scientific Procedures) Act 1986.

The protocol we used for culturing and maintaining cortical neurons is modified from the method that was described by Deitch and Fischer in 1999 (Deitch J.S. and Fischer, 1999), and Kaech and Banker in 2006 (Kaech and Banker, 2006). This protocol encompasses three main components: (1) preparation and expansion of cortical astroglial feeder layers, (2) coverslip sterilisation and coating, and (3) cortical neuronal cultures.

3.1.1.1 Materials and media for neocortical neuronal cultures

The reagents and media used for preparing and maintaining cell cultures are shown in Table 3.1.

Glass coverslips (19 mm diameter; SLS, MIC 3284) placed in 12-well plates (polystyrene non pyrogenic sterile treated, 22.1 mm well diameter, 3.8 cm^2 growth area; from Corning) were used for plating cortical astroglial cells as feeding layer for further cortical neuronal cultures.

Other materials and equipment are listed in Table 3.2.

Table 3.1 Solutions and cell culture media for cortical neuronal culture preparation and maintenance

Media & Solution	Component	Amount	Source
Glial Medium	Minimum essential medium Eagle (MEM)	500 ml	Sigma, M2279
	D-glucose (45% solution)	7 ml	Sigma, G8769
	Penicillin-streptomycin (100x)	5.5 ml	Invitrogen, 15140-122
	Horse Serum	50 ml	Invitrogen, 16050-122
	L-Glutamine, 200 mM	5.5 ml	Sigma, G7513
Wash buffer	Hanks' balanced salt solution (HBSS)	500 ml	Sigma, H9394
	5 mM HEPES (1 M, pH 7.4)	2.5 ml	Invitrogen, 15630056
Digestion solution PH:7.2 with 10 N NaOH	137 mM NaCl (MW: 58.44)	1.6 g	Sigma, S9625
	5 mM KCL, 2 M Stock (MW: 74.55)	0.5 ml	Sigma, P5405
	7 mM Na_2HPO_4 (MW: 141.96)	0.2 g	Sigma, S5136
	25 mM HEPES (MW: 238.31)	1.19 g	Sigma, H4034
Dissociation solution	Wash solution	200 ml	
	12 mM $MgSO_4$ (MW: 120.37)	0.288 g	Sigma, M2643
DNAse stock solution	DNAse, 75 u/µl	150 KU/2 ml culture water	Sigma, D5025
Cystosine β-D-arabinofuranoside (araC)		Sigma, C6645	
Dissection solution	Wash solution	40 ml	
	Fetal Bovine Serum (FBS), 20%	10 ml	Invitrogen, 10082147
Complete Neurobasal A medium	Neurobasal A medium	500 ml	Invitrogen, 10888022
	B27 supplement (Final conc.: 2%)	10 ml	Invitrogen, 17504044
	Glutamax (Final 25 µM glutamine)	1.25 ml	Invitrogen, 35050038
Neurobasal A medium + araC	Complete Neurobasal A medium		
	1 µM araC	500 µl	Sigma
Digestion Mix	Trypsin XI	25-30 mg	Sigma, T1005
	Digestion solution	2.5 ml	
	DNase	10 µl	
Dissociation Mix	Dissociation solution	2.5 ml	
	DNase	12.5 µl	

Table 3.1 (continued)

Media & Solution	Component	Amount	Source
CMF-HBSS (Calcium-, Magnesium-, and Bicarbonate-free Hank's Balanced Salt Solution)	Tissue culture grade H_2O	900 ml	Sigma, W3500
	10x Hanks' balanced salt solution	100 ml	Invitrogen, 14185045
	1 M HEPES buffer, pH 7.3 (HEPES: 4-(2-hydroxyethyl)-1-piperazineethanesulfonic acid)	10 ml	Invitrogen, 15630056
2X Cell-Freezing Medium	Fetal Bovine Serum (FBS)	40 ml	Invitrogen, 10082147
	DMSO (Dimethyl Sulfoxide)	10 ml	Sigma, D2650
2.5% Trypsin		Invitrogen, 15090046	
0.05% Trypsin-EDTA (1x)		Invitrogen, 25300054	
H_2O	Tissue culture grade H_2O		Sigma, W3500
Trypan-blue		Sigma, T8154	
Boric acid		Sigma, B8768 – 500G	
Sodium tetraborate		Sigma, 221732	
Borate buffer, 0.1 M, pH 8.5	0.1 M Boric acid titrated by 0.1 M sodium tetraborate to pH 8.5		
PLL solution	Poly-L-lysinie (PLL) (MW: 30,000-70,000 kDa)	1 mg	Sigma, P2636
	Borate buffer, 0.1 M, pH 8.5	1 ml	
Sodium hydroxide (NaOH)		Sigma, S8045	

Table 3.2 Materials and Equipment for Neuronal Cultures

Materials or Equipment		Type ; Source
Laminar flow hood		Gelaire BSB4 ; Labcaire
Water bath (at 37 ^{o}C)		JB Series ; Grant
Oven		Autoclave oven ; Binder
Dissection microscope		Zeiss
Dissecting tools (sterilized)	Fine-tipped forceps	2x Dumont #5 ; WPI 500233
	Fine-tipped forceps	2x Dumont #55 ; WPI 500235
	Crooked forceps	WPI 500234
	Dissecting scissors	WPI 501749
	Sealed grip clamp	WPI 501324
	Micro-dissection scissors	WPI 500228
Hemacytometer (for counting cells)		Bright-line ; Sigma-Aldrich
Filters		70 µm, 0.2 µm ; VWR
Cell strainer with 70-mm mesh		BD Biosciences, 352350
Pipetters		Powerpette and Labmate pipetters ; Jencons Scientific
Serological pipettes		5-, 10- and 25- ml ; Sigma-Aldrich
Falcon Centrifuge tubes		15 ml & 50 ml ; Sigma-Aldrich
Disposable Petri dishes		30 mm, 60 mm & 90 mm ; Sigma-Aldrich
Freezing vials		Nunc CryoTubes (2 ml), 366656
Liquid nitrogen storage		
Ceramic coverslip-staining rack		Thomas Scientific, 8542E40
T75 tissue culture flasks		75 cm^2 EasyFlask angled neck radiation ; Fisher Scientific 10364131
Pasteur pipettes		Sigma, S6268

3.1.1.2 Coverslip Preparation

In order to improve the attachment and growth of cell cultures, an optimal environment of hydrophilic surface was prepared. Glass coverslips (19-mm diameter) were placed in ceramic coverslip-staining racks then soaked in concentrated nitric acid (65% wt/wt) for at least 18-24 hours (or over the weekend). After this, the coverslips were kept in the racks and rinsed with distilled water four times for 2 hours/rinse. Then coverslips in the racks were placed in a glass beaker covered with glass lids and baked overnight (12-16 hours) in an oven at 225^{o}C for sterilization. The following day, coverslips were placed into 12-well plates and 150 µl of PLL solution (Poly L-lysine in borate buffer; see Table 3.1) was applied to each coverslip and incubated at 37^{o}C overnight. The next day, PLL solution was removed from the coverslips and rinsed twice with 3 ml of sterile water, 2 hours each. After the last wash, 1 ml of Glial Medium was added into each well and plates were placed in 37^{o}C incubator until ready to use. Coverslips can be stored like this for up to a week.

3.1.1.3 Cortical Astroglial Cell Preparation

In order to provide trophic support and suitable physiological condition for neuronal cultures (Kaech and Banker, 2006), a monolayer astroglial feeder cultures were made on the PLL-treated coverslips prior to neocortical neuronal cultures. Cortices from three postnatal day 1 (P1) Sprague-Dawley rats were used for each preparation of the primary cultures of type I astroglia. The pups were decapitated with sharp scissors according to protocols on the licence. The heads were washed in 25 ml of ice-cold CMF-HBSS (see Table 3.1) two times then placed in a 60 mm Petri-dish and submerged in ice-cold CMF-HBSS completely. Under a dissecting microscope, the skull and all the meninges were removed and the cerebral hemispheres were dissected. The cerebral hemispheres were transferred to a new dish containing ice-cold CMF-HBSS and were chopped as finely as possible. The tissue was transferred to a 15 ml Falcon centrifuge tube with a freshly made ice-cold solution of 9.5 ml CMF-HBSS, 1.5 ml of 2.5% trypsin and 1.5 ml of DNase (10 mg/ml) then was incubated at

37°C water bath for 5 minutes with swirling occasionally. Then the tissue was triturated by passing the solution in a 10 ml pipette for 10-15 times and then incubated in 37°C water bath again for 10 minutes with swirling occasionally. Repeated trituration with a 5 ml pipette 10-15 times or until most chunks have been broken down. After this, the cells were passed through a cell strainer (70 µm) to remove chunks of un-dissociated tissue, and were collected in a 50 ml tube containing 15 ml of Glial Medium (see Table 3.1). The cells were centrifuged (2000 rpm, 5 minutes) to remove enzymes and lysed cells. Then the pellet was broken and resuspended in 15-20 ml of warmed Glial Medium and cells were counted using a hemacytometer.

Following above procedure, glial cells were plated in three of T75 flasks (the approximate density is 7-10 x 10^6 cells per flask) and Glial Medium was added to a final volume of 13 ml per flask then incubated at 37°C with a humidified, 5% CO_2/95% atmosphere incubator (Galaxy S; Wolf laboratories). One day after plating, loosely attached cells were removed by tapping and swirling the flask then aspirating off the medium and glial cells were fed with fresh, warmed Glial Medium. Following this, the glial cultures were fed by replacing Glial Medium every 2-3 days. Further expansion of glial cell cultures was done when they reached 90-95% confluence. One preparation can generate enough glial cells for several neuronal cultures. Glial cells were frozen in liquid nitrogen until needed.

3.1.1.4 Expansion and Freezing Glial Cells

Once the glial cells reached 90-95% confluence in a flask, splitting glial cells from 1 to 2 T75 flasks was performed. First, medium was removed from the flasks and the glial cultures were rinsed with 10 ml CMF-HBSS. After discarding the CMF-HBSS, 3 ml of 0.05% Trypsin-EDTA (1x) (see Table 3.1) was added into glial cells and cells were incubated for 3 minutes with tapping the side of flask intermittently to release the cells then 8 ml Glial Medium was added to stop the activity of trypsin. Cells released from several flasks were collected into a centrifuge tube and then

centrifuged at 2000 rpm for 5 minutes. The pellet was resuspended in warmed Glial Medium then the cell suspension was aliquoted to several new T75 flasks and Glial Medium was added to each flask with a final volume of 13 ml. Glial cells were incubated at 37^{o}C incubator for further expansion.

For freezing the glial cells, cells were resuspended with 0.5 ml Glial Medium + 0.5 ml of ice-cold 2X Cell-Freezing Medium (see Table 3.1) per cryotube (usually cells collected from one T75 flask were dispensed to one cryotube). These were frozen at -20^{o}C for 2 hours then -80^{o}C overnight, and then transferred to a liquid nitrogen device for long term storage.

3.1.1.5 Defrosting & Plating Glial Cells for Feeder layer

Before plating glial cells as the feeding layer for further neuronal cultures, the frozen glial cells were defrosted and cultured into T75 flasks for about 10 days. Frozen glial cells were thawed in 37^{o}C water bath for 3 minutes and transferred to a 15 ml centrifuge tube containing proper volume of Glial Medium (5 ml Glial Medium for one cryotube) then centrifuged (2000 rpm, 5 minutes). The cell pellet was resuspended in Glial Medium and then aliquoted into T75 flasks with a final volume of 10-13 ml Glial Medium in each flask then placed in 37^{o}C incubator. The next day, the dead cells were removed by tapping the flasks and the medium was discarded then replaced with fresh warm Glial Medium. The glial cells were cultured in T75 flasks and fed with fresh Glial Medium every 2-3 days.

When the glial cells were up to 90-95% confluent, the medium was removed and cells were rinsed with 10 ml CMF-HBSS. Then glial cells were incubated in 3 ml of 0.05% Trypsin-EDTA (1x) for 3 minutes and 8 ml Glial Medium was added to stop trypsin activity. Cells were released and transferred to a centrifuge tube and centrifuged at 2000 rpm for 5 minutes. The glial cell pellet was resuspended in Glial Medium and plated on sterilized coverslips pre-treated with PLL with an optimal density of glial cell (20-25K/well) and then Glial Medium was added in each well with a final volume of 1.5 ml. The following day, all the Glial Medium was removed from

the wells and replaced with fresh medium to remove debris. The Glial cells were fed every 2-3 days by exchanging 1/3 of Glial Medium.

3.1.1.6 Brain Dissection and Tissue Preparation

Postnatal (P0 or P1) Sprague-Dawley rats were decapitated and the heads were rinsed with 70% ethanol then placed in a tube and washed twice with ice-cold Wash buffer (see Table 1). The heads were transferred to a petri dish submerged in ice-cold Wash buffer then brains were extracted from the skull. Brains were transferred to a new petri-dish with clean ice-cold Wash buffer and cerebral cortices were dissected and isolated under dissecting microscope. First, the cerebellum and brain stem tissue attached to the cerebral hemispheres were removed, then all meninges were completely stripped away from the cerebral hemisphere in order to minimize fibroblast contamination. After that, the hippocampi, temporal cortices and part of anterior cortex were removed and the remaining cortices were chopped to several small pieces then were taken for further processing.

The cortical pieces were rinsed with 5 ml of Wash buffer five times then digested with 2.5 ml Digestion Mix (see Table 3.1) and incubated for 10 minutes in a 37^{o}C water bath to cleave extracellular protein. The Digestion Mix was removed gently, and the cortical tissue was rinsed with 5 ml of Dissection solution (see Table 3.1) for two times to stop trypsin activity, and then washed with 5 ml Wash buffer twice. The cortical tissue was treated with 2 ml of Dissociation solution (see Table 3.1) and triturated with fire-polished Pasteur pipettes roughly five strokes or until the solution was cloudy, in order to yield a homogenous dissociated cell solution. The suspension was transferred to a new tube and 4-5 ml Dissection solution was added then centrifuged (2000 rpm, 4^{o} C) for 5 minutes. The supernatant was carefully aspirated and the pellet was resuspended in 1ml of Complete Neurobasal A medium (see Table 3.1). To count the cells, 10 µl of the cell suspension was stained with 10 µl Trypan-Blue, and 10 µl of this stained cell suspension was placed on a hemacytometer to measure the viability of the culture.

3.1.1.7 Primary Culture of Neocortical Neurons

In the experiments involving cell culture models of seizure like activity, it was noticeable that a lot of neurons would die 72 hours after convulsant treatment (especially in High-Potassium and Low-Magnesium models). This resulted in difficulty in getting an adequate amount of RNA for further experiments. Thus, several different strategies were tested, such as testing different culture density from 100K, 200K, 300K,....to 700K per well (22.1 mm of well diameter in 12-well plates); or increasing the number of culture plates for each model; or using different RNA extraction methods. After testing several conditions for neocortical cultures with different manipulations, the optimized condition for neocortical culture models of seizure like activity was using high density of neuronal culture: 400-600 x 10^3/well in the 12-well plates. Neuronal cells were cultured in 6 wells in one 12-well plate (Figure 3.1) for one model to get sufficient amount and concentration of RNA extraction for seizure/epilepsy models in cell cultures.

Cortical neurons were plated in high density cultures (400-600 x 10^3 cells/well) onto glass coverslips (precoated with Poly-L-lysine solution) with the cortical astroglial cell feeding layer in a 12-well plate. The cells were plated in Complete Neurobasal A medium (2 ml) then kept at 37^o C in a humidified atmosphere containing 5% CO_2 and 95% air. One day after cortical neuron preparation, 1 ml of Neurobasal A medium with araC (see Table 3.1) was added in each culture well (final concentration of araC: 1 µM) to inhibit further glia cell proliferation. Cortical neuronal cultures were fed once per week by removing 1 ml of medium and replacing with 1 ml of fresh warmed Complete Neurobasal A medium. Neocortical cultures were maintained for up to 14-15 days *in vitro* (14-15 DIV) for further experimental procedures and to allow the maturation of synapses.

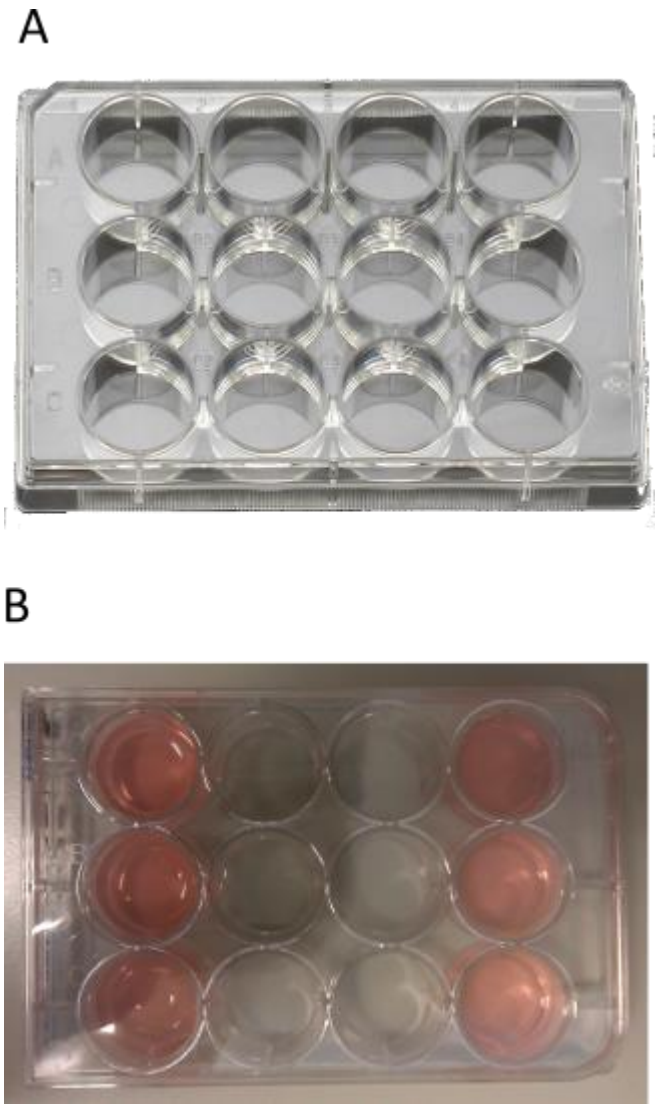

Figure 3.1 12-well Sterilized TC(Tissue Culture)-Treated Plates

(A) A 12-well sterilized TC-Treated plate, Diameter: 22.1 mm/well ; Cell Growth Area: 3.8 cm^2/well ; Well Volume: 6.9 ml. (B) Neuronal cells were cultured in 6 wells in one plate for one seizure/epilepsy model.

3.1.2 Solution Preparation

Four pharmacological agents for models of epilepsy in cell culture were prepared: stock high-concentration potassium solution (1 M) was made with KCl salt (Sigma-Aldrich) dissolved in distilled deionized water. Magnesium-free medium consisted of 145 mM NaCl, 2.5 mM KCl, 10 mM HEPES, 2 mM $CaCl_2$, 10 mM glucose, and 0.002 mM glycine in distilled deionized water then the solution was adjusted with NaOH to pH 7.4 and 325 mOsm with sucrose (Blair et al., 2004). Stock Kainic acid solution (5 mM) was prepared with Kainic acid (Tocris Bioscience, 0222/10) in cell culture grade water. Likewise, stock Pentylenetetrazole (PTZ) reagent was composed of PTZ (Sigma-Aldrich) dissolved in cell culture grade water.

All these solutions were filtered through 0.2 µm filters (VWR) in the Laminar flow hood (Gelaire BSB4; Labcaire) then immediately stored in aliquots at -20^{o} C and 4^{o} C as appropriate. The stimulants were diluted from the stock solutions on the day of the experiment.

3.1.3 Immunocytochemistry

Four different cell culture models for studying epilepsy (High-Potassium, Low-Magnesium, Kainic Acid, and PTZ models; see Section 5.3.1 – 5.3.4) with one control group were performed on cortical neurons grown on glass coverslips (see Section 3.1.1.7) up to 14-15 DIV. Following this, immunocytochemistry was carried out on neurons.

Cortical neurons grown on coverlips were transferred to new 12-well plates containing 1 ml of fresh warm Neurobasal-A Medium without phenol red (Invitrogen, 12349015) per well. For staining nonviable cells with red fluorescence, Propidium Iodide solution(PI) (Sigma, P4864) was added with a final concentration of 5 µg/mL per well and 12-well plates were wrapped with foil to avoid light then incubated in 37^{o} C incubator for 30 mins. Before fixation, neurons were rinsed briefly in 1X Phosphate-Buffered Saline (PBS) twice. Cells were fixed by using 4%

paraformaldehyde (PFA) in PBS pH 7.4 for 10 mins at room temperature followed by washing with ice-cold PBS three times (5 minutes, each wash). After fixation, cells were permeabilized by using PBS containing 0.1% Triton X-100 (Sigma) for 10 minutes then rinsed with ice-cold PBS three times. Following this, cells were incubated in 3% BSA (Albumin from Bovine Serum; Sigma) in PBS for 30 mins to block unspecific binding of the antibodies. After blocking, coverslips were incubated in the appropriate diluted primary antibody (anti-GABA antibody; see Table 3.5) in 3% BSA solution at 4^{o} C overnight. The next day, the primary antibody was washed off by three washes in ice-cold PBS (5 mins each wash). Then the cells were incubated in the secondary antibody (Alex Fluor 488 Donkey anti-rabbit IgG; see Table 3.5) diluted in 3% BSA solution for 1 hour at room temperature in the dark. Following three washes in ice-cold PBS (5 mins each wash) in the dark, coverslips were mounted on microscope slides with Antifade Mounting Medium with 4',6-diamidino-2-phenylindole (DAPI) (Vector Laboratories, VECTASHIELD HardSet, H-1500) then sealed with clear nail varnish to avoid drying.

3.1.4 Confocal Imaging and Cell count with Cell death measurements

A Zeiss LSM 710 confocal laser scanning microscope (Carl Zeiss AG, Germany) with Zen 2009 software was used for confocal imaging. Images for neuronal cultures were obtained using a 20X objective at 1024 x 1024 pixel resolution and laser intensity was adjusted for each image to obtain the best fluorescent signal and visibility of cells. Images were randomly collected from 4-5 areas (Figure 3.2) per coverslip and both imaging and the subsequent cell counting was performed while blinded to treatment.

Image J (FIJI version) software with a cell counter plugin was used for image processing and cell counting. In order to reveal all visible cells, the brightness and contrast were adjusted. The total number of cells in the field was counted using DAPI staining, and the number of dead cells was counted with PI staining confirmed with

DAPI staining, as well as the GABA stained cells (GABAergic neurons) that were also confirmed with DAPI staining were counted. In order to represent cell death ratio in a coverslip, sum of cell numbers for DAPI staining, PI staining and GABAergic neurons from 4-5 imaging areas in each coverslip were used to assess cell death.

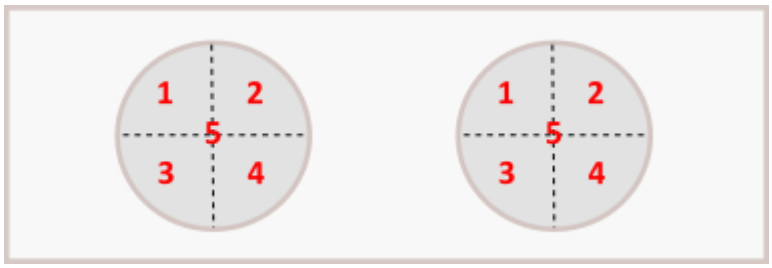

Figure 3.2 Schematic illustration of confocal images taken from a coverslip

Confocal images (20X objective) were randomly taken from 4 quadrants and the central area in each coverslip. The sum of the cell numbers from these 4 or 5 regions was used to represent the number of neurons for the different indicators in a coverslip.

3.2 In *Vivo* models of Chronic Epilepsies

All animal experiments were conducted in accordance with the UK Home Office Animal (Scientific Procedures) Act, 1986 and were subject to local ethical review.

3.2.1 Animals

Adult (~8-10 weeks old) male Sprague-Dawley rats weighing between 250-330 g (from Charles River, UK) were housed on a 12/12 hour light/dark cycle (light cycle 7 a.m./7 p.m.) with *ad libitum* access to food and water. Rats were maintained under controlled environmental conditions (ambient temperature 24-25^{o}C, humidity 50-60%). Before experiments, animals were group housed and left to acclimatise to the new environments for at least 1 week after arrival and then housed individually post-surgery, as animals with seizures can be aggressive if group housed.

3.2.2 Convulsant Agent Preparation

3.2.2.1 Tetanus Toxin (TeNT) preparation

Stock tetanus toxin was obtained as a gift from Dr. G. Schiavo. The toxin was diluted and aliquoted by the following procedures. First, a solution was prepared by mixing 10 mM HEPES and 150 mM NaOH and adjusting to pH 7.2, and then 0.1% BSA was added then filtered through 0.2 µm filters (VWR) in the Laminar flow hood (Gelaire BSB4; Labcaire). After this, stock tetanus toxin was added to the mixed solution to obtain a final concentration of 100 ng/µl or 50 ng/µl. All solutions and toxin were always kept on ice prior to aliquoting and stored at -80^{o}C freezer.

3.2.2.2 Kainic Acid preparation

Kainic acid (Tocris Bioscience, 0222/10) was dissolved in 1X PBS and adjusted to pH 7.4 with the final concentration of 10 mg/ml then filtered through 0.2 µm filters and stored in -20^{o} C freezer for further *in vivo* experiments.

3.2.3 Surgery and Implantation of wireless ECoG telemetry system

The rats were anaesthetised with isoflurane (3-4%) in 2 L/min O_2 in an anaesthetic chamber. Then the animals were placed in a stereotaxic frame (David Kopf Instruments, USA) were head-fixed and kept anaesthetised under 2-3% isoflurane in 2 L/min O2 throughout the whole surgical procedure. Eye gel (Viscot Tears) was given to protect the eyes. Analgesic medications, Metacam (1.3 mg/kg; Boehringer Ingelheim) was administered subcutaneously at the beginning of surgery and a total dose of 0.2 mg/kg Buprenorphine (40 minutes onset, 12 hour analgesia; Temgesic, Scherig-Plough, UK) was given subcutaneously during peri-operation. A Hamilton syringe with 33-gauge needle (Hamilton Company) mounted on a microinjector unit was prepared for stereotaxic injection of convulsant drugs.

Ear and toe pinch were used to confirm the animals had achieved sufficient anaesthesia before starting any surgical procedure. Skin was excised from the top of the head and subcutaneous tissue was cleared for better visible field, to provide a better surface for the tissue adhesive glue and to reduce infection. A stereotaxic drill (WPI) attached to the stereotaxic frame was used to drill burr holes through the skull for electrodes, cannula and anchor screws according to the coordinates in different models of epilepsy (see Sections 3.2.3.1 – 3.2.3.3). After surgery, 3 ml of normal saline was given subcutaneously and the animals were allowed to recover from anaesthesia under supervision.

3.2.3.1 Tetanus Toxin Model of Focal Neocortical Epilepsy

Three burr holes were drilled with the coordinates shown in Table 3.3 for tetanus toxin delivery, recording and reference electrodes, and an anchor screw. Tetanus toxin was stereotaxically injected into layer V of right primary visual cortex (coordinates: X= 3.0 mm and Y= -7.0 mm from Bregma at the depth of 1 mm below the pia) (Paxinos and Watson, 1998). 15 ng of tetanus toxin in a total volume of 1.0 µl with the injection rate of 200 nl/min was performed and the needle was left in place for further 10 minutes to minimize reflux and allow binding of the tetanus toxin. After tetanus toxin injection, an appropriate skin incision over the animal's right back was made then an ECoG transmitter (A3028E-AA, Open Source Instruments Inc., Watertown MA; see Figure 3.3) (Chang et al., 2011) was implanted subcutaneously. The wires of recording and reference electrodes (stainless steel helices insulated with silicone) were passed through the subcutaneous tunnel to the animal's head. About 1 mm of stainless steel tips of recording and reference electrodes (these had been gently straightened using forceps before transmitter implantation) were inserted into the burr holes and secured in place with stainless steel screws (Plastics One) (Figure 3.4). Thus, the subdural intracranial recording electrode was permanently placed at the TeNT injection site and the reference electrode was implanted in the contralateral frontoparietal cortex (coordinates see Table 3.3). An anchor screw (stainless steel screw; Plastics One) was secured in the right frontal region to stabilise the headset. Following this, a thin layer of Vetbond tissue adhesive (3M) was applied to the exposed skull surface then the wound was covered by a thick layer of dental cement (Simplex Rapid, Kemdent). The right flank incision wound was sutured with absorbable sutures (Ethicon, W9931). After surgery, animals were single housed in Faraday cages and continuous 24-hour/7 days telemetric video-ECoG (electrocorticography) recordings (see Section 3.2.4) were carried out until the end of the experiments.

For the rats in the control group, all the same surgical procedures were performed except 1 µl of 0.9% saline was injected in right visual cortex instead of tetanus toxin.

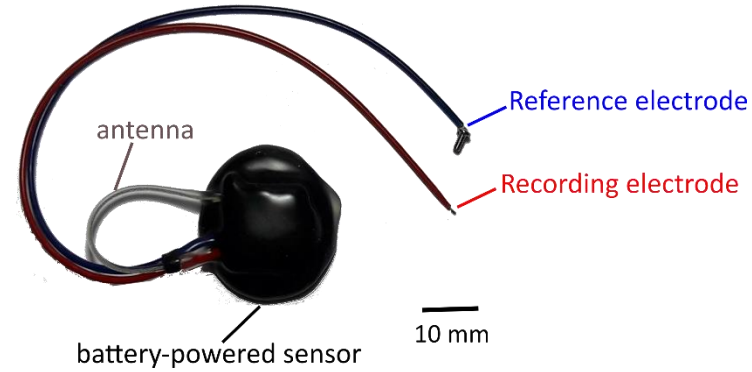

Figure 3.3 Subcutaneous ECoG transmitter (A3028E-AA) Opensource instruments

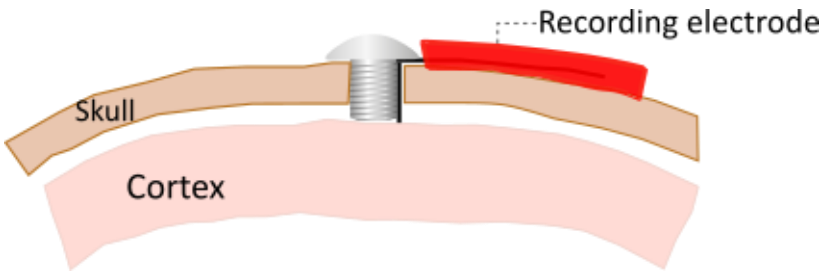

Figure 3.4 Schematic of ECoG electrode implantation

The recording or reference electrode (thick black line) was inserted into the burr hole along with a stainless steel screw and secured in place.

Table 3.3 Coordinates for electrodes and anchor screws in the visual cortex model of epilepsy (distance measured from bregma)

	medio-lateral; X (mm)	anterior-posterior; Y (mm)
Recording electrode	3	-7
Reference electrode	-1.8	-2.5
Anchor screw	0.6	-2.5

3.2.3.2 Kainic Acid Model of Visual Cortical Seizure

Adult male Lister black hooded rats weighing approximately 300g were used for surgeries. Three burr holes were drilled using the same coordinates as the TeNT model of visual cortical epilepsy (see Table 3.3) for the guide cannula, recording and reference electrodes, and an anchor screw. After making the burr holes, an ECoG transmitter (A3028E, OpenSource Instruments Inc.) was implanted into right flank subcutaneously then the reference electrode and anchor screw were secured in place (see Section 3.2.3.1). The recording electrode was inserted into right primary visual cortex and a guide cannula (Plastics One, C313G/20-49: C313G-SPG Guide 38177 22G cut 1.5 mm below pedestal) was placed along with the recording electrode then affixed with Vetbond tissue adhesive (3M) (Figure 3.5). Following this, another layer of Vetbond tissue then a thick layer of dental cement was applied to cover the head wound and secured the headset. Then a dummy cannula (a stainless steel stylet) (Plastics One, C313DC/50-99: C313DC-SPC Dummy LG 014-.36mm to fit 1.5mm C313G) was inserted into the guide cannula and well screwed on to prevent dried blood or any debris clogging the delivery tube of guide cannula. Animals were housed individually in Faraday cages and continuous ECoG recordings were commenced for recording the baseline ECoG before the application of kainic acid. All animals had a recovery period of one week prior to local K.A. administration.

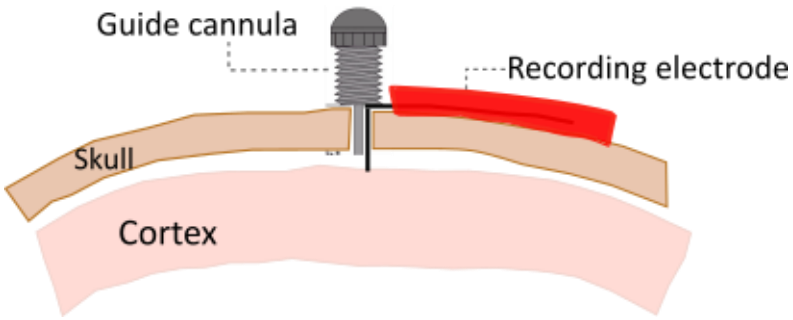

Figure 3.5 Schematic of the relative position of a guide cannula and the recording electrode. Note the guide cannula replaces the screw in holding the recording electrode in place.

3.2.3.3 Intra-amygdala Kainic Acid Model of Epilepsy

Surgeries were performed on adult male Sprague-Dawley rats (250-280g). Three burr holes were drilled for the guide cannula, depth recording electrode, and reference electrode and an additional three burr holes were made for anchor screws. These coordinates are shown in Table 3.4. An EEG transmitter (A3028E-HA, OpenSource Instruments Inc.; details see Section 3.2.4) soldered with a gold-plated D-pin at the tip of recording wire (Figure 3.6A) was implanted subcutaneously into the animal's right flank (see Section 3.2.3.1). The reference electrode was secured by stainless steel screw in left parietal cortex (coordinates see Table 3.4) and three anchoring screws were fixed in three places as the coordinates shown in Table 3.4 to stabilize the assembly. A depth electrode (Figure 3.6B) (OpenSource Instruments Inc.) made by 125 µm diameter full-hardened stainless steel with telflon insulation of diameter 200 µm was cut to an appropriate length (the length from socket to tip is skull thickness plus target depth) before implantation. Following this, the depth electrode was held by a stereotaxic holder (Kopf, 1766-AP) and the D-pin soldered in the recording electrode was plugged into the socket of the depth electrode (Figure 3.6C). Then this depth recording electrode was stereotaxically lowered slowly targeting to the pyramidal cell layer of right CA1 (Cornus Ammonis 1) region (coordinates see Table 3.4). After this, a guide cannula (Plastics One, C313G/20-49: C313G-SPG Guide 38177 22G cut 1.5 mm below pedestal) was positioned ipsilaterally to the depth recording electrode and above the dorsal hippocampus (coordinates see Table 3.4) for the following kainic acid injection. Vetbond tissue adhesive was coated around the socket of depth recording electrode, guide cannula and skull surface to affix these assemblies and the holding part of the depth electrode was removed. Dental cement was used to cover the socket and skull surface and to secure the whole assembly. A dummy cannula (a stainless steel stylet) (Plastics One, C313DC/50-99) was inserted into the guide cannula and screwed on followed by suturing the right flank wound. After surgery, animals were housed separately in Faraday cages and continuous 24-hour local field potential (LFP) recordings were commenced to acquire the baseline LFP data prior to the induction of kainic acid

induced status epilepticus and chronic epilepsy. All animals had a recovery period of one week prior to local kainic acid administration.

A

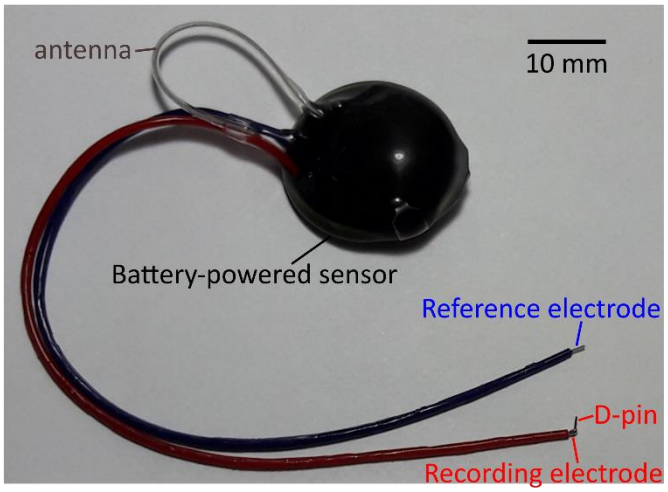

B

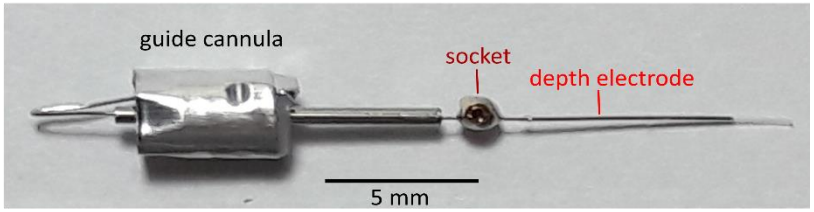

C

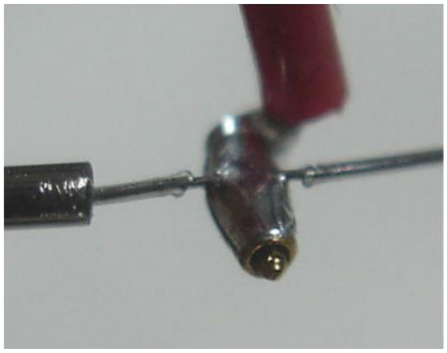

Figure 3.6 Apparatus for the Hippocampal EEG recording

(A) Subcutaneous EEG transmitter (A3028E-HA) designed for the use with depth electrode recording. (B) Full-hardened stainless steel depth electrode. (C) D-pin soldered in the recording electrode plugged into the socket of the depth electrode: this enables recording LFP from a deep region of the brain.

Table 3.4 Coordinates of electrodes, guide cannula and anchor screws for the Intra-amygdala Kainic Acid Model of Epilepsy (distance measured from Bregma)

	medio-lateral; X (mm)	anterior-posterior; Y (mm)	dorso-ventral; Z (mm)
Depth recording electrode	2.6	-4.3	-2.8
Reference electrode	-2.8	-2.8	-
Guide cannula	4.6	-2.8	-
Anchor screw #1	-2	-6	-
Anchor screw #2	1.8	-1.8	-
Anchor screw #3	4	-6.5	-

3.2.4 ECoG and Video monitoring

The setting of wirelesss ECoG telemetry system we used was designed and manufactured by Open Source Instruments Inc. (Watertown, MA, USA) and IP Cameras (Microseven, M7D12 POE or M7D12 HD) with iSpy video surveillance software were applied for continuous 24-hour/7 day video monitoring.

3.2.4.1 Wireless ECoG transmitters and ECoG telemetry system

Telemetry ECoG monitoring units were applied for long-term, continuous ECoG recordings to detect the emergence of spontaneous seizures. The circuit of the system consists of subcutaneous transmitter, Loop Antenna, Faraday Enclosures, Octal Data Receiver and Long-Wire Data Acquisition (LWDAQ) Driver (Figure 3.7). The Loop Antenna receives signals from the subcutaneous transmitters via radio-frequency (RF) (915 MHz) then conveys the signals to the Octal Data Receiver which is a RF detector. The Octal Data Receiver uploads data to the LWDAQ Driver, a TCPIP server on the internet, then signals were transferred to a data acquisition computer through internet. The Faraday Enclosures are applied to block ambient interference and to increase transmitter operating range, as the transmitter signals are broad-band and low-power and their transmissions are easily contaminated by interference.

The A3028E series transmitter is a subcutaneous, wireless and battery-powered telemetric sensor containing two electrodes (a reference and a recording electrodes) for signal-channel ECoG recording. The A3028E-AA subcutaneous transmitter (see Figure 3.3) with stainless steel helical wires on the tips of electrodes is made for ECoG recordings. The A3028E-HA subcutaneous transmitter (see Figure 3.6A) containing a D-pin on the tip of recording electrode is designed to use with depth recording electrode which enables us to target deep part of brain for LFP recordings. The sampling rate is 512 SPS (samples per second) which provides the frequency dynamic range (Bandwidth) of 0.3 - 160 Hz and the voltage dynamic range

is approximately 20 mV (-13 mV to +7 mV). The operating life of the transmitters is about 3200 hours and the transmitters can be turned on and off with a magnet.

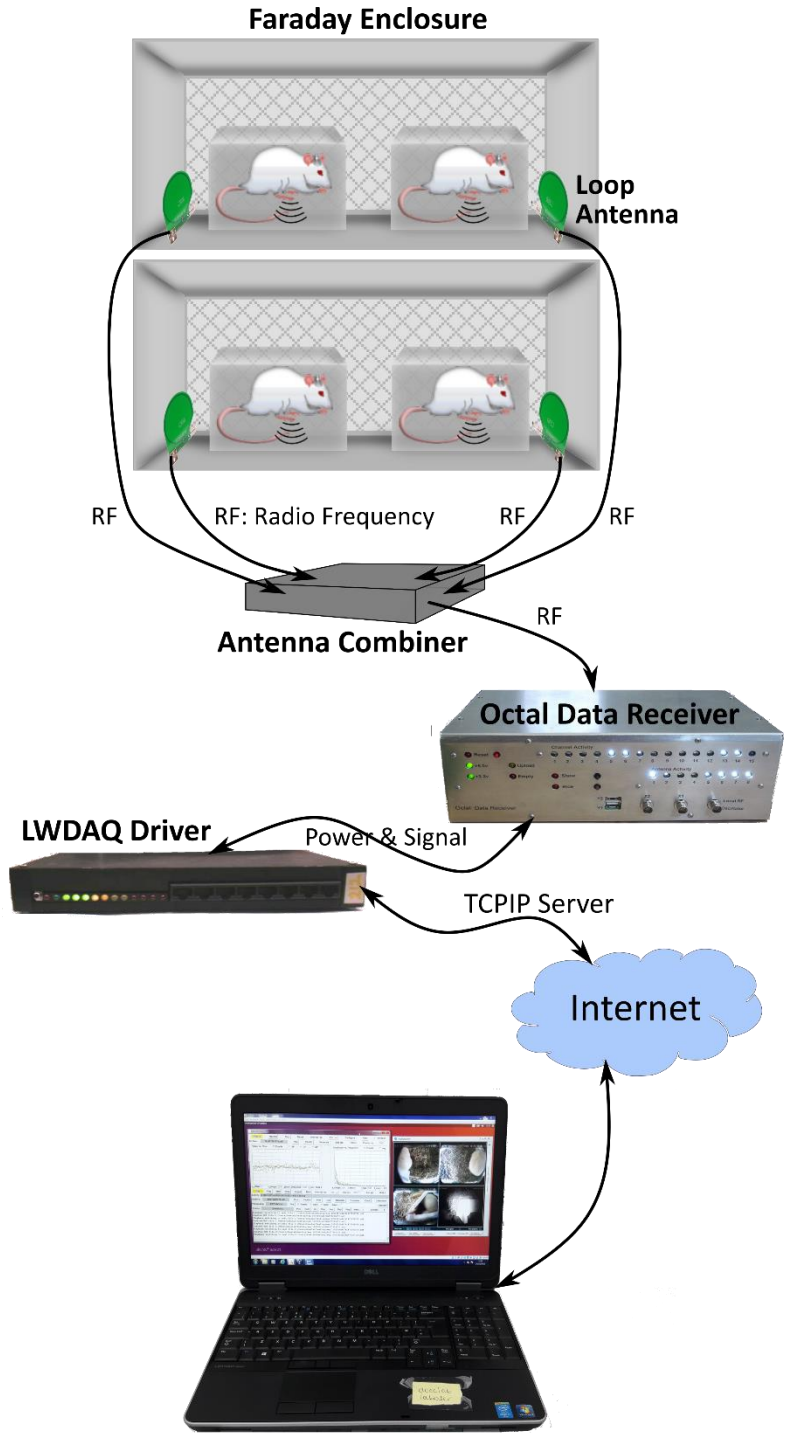

Figure 3.7 Schematic illustration of the main components of wireless ECoG telemetric system. The Loop antennas are connected via an antenna combiner and transmit signals to the octal data receiver. Data are then transferred to a computer via the LWDAQ driver and internet.

3.2.4.2 ECoG Data acquisition and analysis

The LWDAQ software with the Recorder Instrument and Neuroarchiver Tool plugin programmes running on a computer were used for ECoG data acquisition and analysis. The ECoG signals are downloaded to the Recorder Instrument from the Octal Data Receiver via a LWDAQ Driver through the internet and are divided into blocks of fixed time-duration. The Neuroarchiver downloads these data from Recording Instrument and the incoming signals are calculated, transformed and displayed by Fourier transformation and then stored to the disk. The ECoG dataset was analysed by the experimenter manually.

3.2.4.3 Video monitoring

In order to carry out observations of epileptic seizures to assess associated stereotyped behavioural changes, a continuous long-term 24-hour video surveillance system was applied. IP Cameras (Microseven, M7D12 POE or M7D12 HD) built-in with infrared were fixed on the top of the cage lids and focus had been adjusted which enabled the video to cover most of the field inside the cage. The iSpy video surveillance software was used to obtain the video.

3.2.5 Transcardial Perfusion and Brain Fixation

Animals were sedated with isoflurane (4-5%) in 2 L/min O_2 then lethal dose of sodium pentobarbital (500 mg/kg) was administered intraperitoneally (i.p.). Under the terminal anaesthesia, the animals were fixed on a dissecting table and after the rat was unresponsive to a harsh toe-pinch, the chest was opened to expose the thoracic cavity and heart. A needle connected to the perfusion pump was inserted into the base of the heart along its axis to access the left ventricle then a small cut over right atrium was made to allow blood flow drainage. The animals were transcardially perfused with approximately 150 ml of ice-cold heparinized PBS (80mg

of heparin sodium salt in 1 L PBS) and sequentially perfused with about 170 ml of 4% paraformaldehyde in PBS (4% PFA/PBS) (Affymetrix, 19943). After completing perfusion, carefully dissecting the rat brains from the skulls, the brains were immersed in 4% PFA/PBS at 4^{o} C fridge for over 24 hours. The next day, the brains were washed three times with PBS then submerged in PBS at 4^{o}C fridge until slicing for histology or immunohistochemistry stain.

3.2.6 Brain Slice preparation

The cerebellum and a small part of the rostral and caudal brain were removed prior to slicing. The caudal surface of the brain was glued on the centre of a rotating specimen holder with cyanoacrylic glue. Coronal brain slices were made in ice-cold PBS solution using a vibratome (Leica VT1000S, Leica Microsystems, Wetzlar, Germany). To minimize tissue tearing trauma, slow speed (0.12 ~ 0.16 mm/sec) and high frequency (60-90 Hz) of blade vibration were used.

For histology experiments, the brains were sectioned at 40 ~50 µm and placed by sequential order in 12-well plates filled with ice-cold PBS then transferred onto poly-L-Lysine-coated microscope slides (Polysine^{TM} VWR International, 631-0107) and dried in room temperature for one day before doing Nissl stain.

In immunohistochemistry experiments, animals received tetanus toxin or 0.9% saline coinjected with fluorescent beads (FluoSpheres, 10 µm, yellow/green fluorescent (505/515), Invitrogen, F8836) in a final volume of 1 µl into layer V of right visual cortex. One week after injection, brains were sliced at 70 µm and the slices were placed on microscope slides followed by quickly checking under an Axio Imager A1 fluorescence microscope (Carl Zeiss) to select the region of interest (6 adjacent slices of the peri-injection site). Then the slices were submerged in ice-cold PBS in 12-well plates in sequential order. In addition, 50 µm thick brain slices were sectioned for intra-amygdala kainic acid model of epilepsy.

3.2.7 Histology (Nissl Stain)

Nissl bodies (Nissl substances) are large granular bodies found in the cytoplasm of neurons and are composed of rough endoplasmic reticulum (RER) with rosettes of ribosomal RNA. Nissl staining which stains the Nissl substance is commonly used to identify the neuronal structure of brain and spinal cord. The Cresyl Violet method was used for Nissl staining. First, 6 jars were filled with the following solutions separately: ddH_2O, cresyl violet solution (Sigma, C5042), 70% Ethanol (ETOH; Merk), 95% Ethanol, 100% Ethanol, and Histo-clear (National diagnostics, HS-200). Then brain slices placed on microscope slides were dipped in these solutions through the following sequence: ddH_2O for 3 times to remove any residual salts and hydration, cresyl violet solution for 5-10 mins, and sequential dehydration by 70% ethanol (1 min), 95% ethanol (2-3 mins), 100% ethanol (1 min) then rinsed in Histo-clear for 5 mins. Finally, the slices were coverslipped and mounted in DPX mountant (Fluka BioChemika, Buchs, Switzerland).

3.2.8 Immunohistochemistry Stain of Floating Brain Slice

The floating brain slices were placed in 12-well plates with 2 floating slices in each well. 1 ml of ice-cold solution was applied in each well with gentle shaking on a rocker during immunofluorescent staining. Before immunohistochemistry staining, brain slices were rinsed in ice-cold PBS for three times (10 mins each rinse) to remove free PFA to reduce the interference of PFA in the quality of immunostaining.

Brain slices were immersed in PBS with 0.3% Triton X-100 for 15-20 mins to permit permeabilization. Following this, incubating brain slices in PBS containing 0.3% Triton X-100, 1% BSA and 4% goat serum (Invitrogen, 50062Z) for at least 1 hour to block nonspecific binding of the antibodies. After blocking, the brain slices were incubated in the appropriate diluted primary antibodies (anti-NeuN and anti-GFAP antibodies; see Table 3.5) in PBS with 0.3% Triton at 4^{o} C overnight (up to 20 hours). The next day, the primary antibodies were washed off with PBS three times (10 mins

each time) and the brain slices were incubated in the secondary antibodies (Alex Flour 488 Goat anti-rabbit IgG and Alex Flour 555 Goat anti-mouse IgG; see Table 3.5) diluted in PBS for 3 hours at room temperature in the dark. Thereafter, three washes with PBS (10 mins each time) were done and brain slices were transferred onto the microscope slides, coverslipped and mounted with Antifade Mounting Medium with DAPI (Vector Laboratories, VECTASHIELD HardSet, H-1500).

Table 3.5 Antibodies used for Confocal imaging

Antibody	Species	Concentration	Manufacturer
GABA antibody	Rabbit polyclonal	1: 400	Sigma-Aldrich; A2052
NeuN antibody [EPR 12763]	Rabbit monoclonal	1:500	Abcam; ab177487
GFAP antibody	Mouse monoclonal (clone GA5)	1:400	Merck Millipore; MAB3402
Alex Fluor 488 secondary antibody	Donkey anti-rabbit IgG (H+L)	1:400	Life Technologies; A-21206
Alex Fluor 488 secondary antibody	F(ab´)2-Goat anti-rabbit IgG (H+L)	1:500	Life Technologies; A-11070
Alex Fluor 555 secondary antibody	F(ab´)2-Goat anti-mouse IgG (H+L)	1:750	Life Technologies; A-21425

3.2.9 Confocal imaging and Cell counting

Confocal imaging was carried out by an inverted LSM 710 confocal laser scanning microscope (Carl Zeiss AG, Germany) with Zen 2009 software. Both imaging and the subsequent neuron counting were done while blinded to treatment. First, brain slices were scanned at x10 magnification to find the region of interest (ROI). Images were then taken for spatial extent of ROI using a 10X objective at 1024 x1024 pixel resolution with 4x2 tile scan configuration. Image acquisition for cell counting was performed by 40X oil-immersion objective at 512 x 512 resolution with 4x3 tile configuration and Z stack series projections of 12-16 images taken at depth intervals of 3 µm, and each averaged 2-4 times with 12 bit depth. Volocity 6.0 software was used for colocalization and manual cell counting. A three-dimensional ROI with X: 1000 µm (500 µm-length of left and right sides from the central injection track), Y: 1000 µm and Z: approximate 30 µm (10 layers of Z stack) (see Figure 3.8) was selected for cell counting. Manual cell counting was done under 100% zoom and only clearly visible NeuN stained cells confirmed with DAPI staining were assessed.

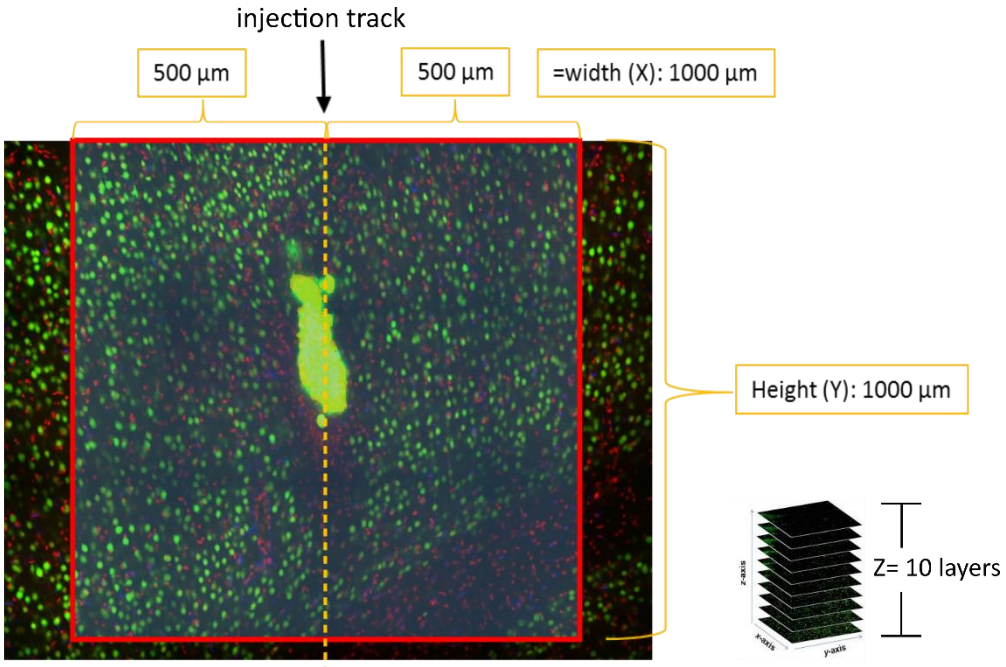

Figure 3.8 Three-dimensional collapse of the range of interest (ROI) for neuron counting

The yellow/green fluorescence (505/515) indicates the fluorescent beads along the injection track. The ROI determined for cell count is that the width(X) is within 500 µm-length of left and right sides from the centre of injection track, the height(Y) is 1000 µm from top of the image field, and the depth(Z) is counting 10 layers of Z stack (interval: 3 µm).

3.2.10 Intermittent Photic stimulation in Visual cortex TeNT Model of Epilepsy

Intermittent photic stimulation was performed on a subset of Lister black Hooded epileptic rats (approximate 300-350g) to determine whether the photoconvulsive (photoepileptiform) response could be triggered in the visual cortex TeNT model of epilepsy. Before starting intermittent photic stimulation, the lights in the telemetry room were switched off to enhance the photic effect of stimulation. A long LED strip with high intensity attached on a board was surrounded the cage and the range of stimulation frequency was from 1 Hz to 30 Hz. Different frequencies of photic stimulation were applied in the following sequence: 1Hz, 3Hz, 6Hz, 9Hz, 12Hz, 15Hz, 18Hz, 21Hz, 24Hz, 27Hz, 30Hz, and then a reverse sequence of stimulation frequencies (from 30 Hz to 1 Hz). The duration of stimulation in each frequency was 20 seconds and then rest for 20 secs before starting the next sequential frequency of stimulation.

3.3 Quantitative Reverse Transcription Polymerase Chain Reaction (qRT-PCR)

The performance of the quantitative reverse transcription polymerase chain reaction (qRT-PCR) was according to the MIQE guidelines (Bustin et al., 2009).

3.3.1 Primers

A total of 13 candidate genes and 4 endogenous reference genes were selected to investigate the gene regulation of seizures or epilepsies and most of the gene-specific oligonucleotide primers directed against flanking intronic sequence were designed using current genomic information available from the Ensemble Genome Browser (http://www.ensembl.org; National Centre for Biotechnology Information, NCBI) and the Primer 3 website resource (http://primer3.ut.ee/) (Rozen and Skaletsky, 2000). The primers were designed as a length of 15-25 bp resulting in a product size between 110-150 bp, and ~50% of G,C content in the primer with the melting temperature (Tm) between 55^{o} C ~ 62^{o} C (the ΔTm between forward and reverse primers was ≤ 4^{o} C). The primer sequences for BDNF, CREM, and CCL2 were used from the papers by Chavko et al, Storvik et al. and by Morioka et al. respectively (Chavko et al., 2002; Morioka et al., 2014; Storvik et al., 2000). Primer sequences of endogenous reference genes used for ARBP and Pgk1 were obtained from the papers by Zhang et al. and by Nelissen et al. (Nelissen et al., 2010; Zhang et al., 2014). The primer sequences are listed in Table 3.6 for: NRGN (Neurogranin), GFAP (Glial fribrillary acidic protein), ADK (Adenosine kinase), SNAP-25 (Synaptosomal-associated protein 25), KCNA1 (Potassium voltage-gated channel subfamily A number 1, also known as Kv1.1), HCN1 (Hyperpolarization-activated Cyclic Nucleotide-gated channel 1), HCN2 (Hyperpolarization-activated Cyclic Nucleotide-gated channel 2), REST/NRSF (RE1-Silencing Transcription factor/Neuron-restrictive silencer factor), mTOR (mammalian target of rapamycin), BDNF (Brain-derived neurotrophic factor), CREM/ICER II (cAMP responsive element modulator/Inducible

cAMP early repressor II), CCL2 (Chemokine C-C motif ligand 2), GABRA5 (Y-aminobutyric acid A receptor, alpha 5), ActB (Beta actin), SDHA (Succinate dehydrogenase complex, subunit A), ARBP (Acidic ribosomal phosphoprotein P0), and Pgk1 (Phosphoglucerate kinase 1). ActB, SDHA, ARBP, and Pgk1 are the internal control genes for qRT-PCR.

Table 3.6 Gene-specific primer sequences

Symbol	Primer Sequences	Amplicon length (bp)
NRGN	Forward 5'-CCTGAACTACCACCCAGCAT-3' Reverse 5'- TATCGTCGTCTGGCTTGGAG-3'	150
GFAP	Forward 5'- AATCTCACACAGGACCTCGG-3' Reverse 5'- TTCCTCTCCAGATCCACACG-3'	150
SNAP-25	Forward 5'- CCTCCGTCATATGGCCCTAG-3' Reverse 5'- CACGTTGGTTGGCTTCATCA-3'	150
KCNA1	Forward 5'- GAGATAGCTGAGCAGGAGGG-3' Reverse 5'- TGGCGGGAGAGTTTGAAGAT-3'	150
REST/NRSF	Forward 5'- CCGTGTCCCTCTGAAAGACT-3' Reverse 5'- ATTTCCTGAGACTCGGCCAA-3'	150
HCN 1	Forward 5'- AACCCTCAGCCATCCTTTCA-3' Reverse 5'- AATTGGGATGCAGTGGGAGA-3'	150
HCN 2	Forward 5'- GTCAACAAGTTCTCCCTGCG-3' Reverse 5'- CCCACCATGAACAACAGCAT-3'	150
ADK	Forward 5'- TTGGAAATGAGACGGAGGCT-3' Reverse 5'- TGCCTCTTCGAGTTCACCTT-3'	150
mTOR	Forward 5'- CCTGGCCAAAGAGAAGGGTA-3' Reverse 5'- TGCTGGGTGATTTCCTCCAT-3'	150
BDNF	Forward 5'- AGCCTCCTCTGCTCTTTCTGCTGG-3' Reverse 5'- CTTTTGTCTATGCCCCTGCAGCCTT-3'	298
CREM/ICER II	Forward 5'- ATGGCTGTAACTGGAGATGA-3' Reverse 5'- CTAATCTGTTTTGGGAGAGCAAATGTCTTTCAAAGT-3'	398
CCL2	Forward 5'- ACGCTTCTGGGCCTGTTGTT-3' Reverse 5'- CCTGCTGCTGGTGATTCTCT-3'	159
GABRA5	Forward 5'- CGCAGTGCCATCCCTTATTC-3' Reverse 5'- ACCGTCCTTTCCTCCAACTT-3'	150

Table 3.6 (continued)

Symbol	Primer Sequences	Amplicon length (bp)
ActB	Forward 5'- TCTTCCAGCCTTCCTTCCTG-3' Reverse 5'- CAATGCCTGGGTACATGGTG-3'	150
SDHA	Forward 5'- GAAGTCGATGCAGAGCCATG-3' Reverse 5'- TTCCAGACCATTCCCCTGTC-3'	150
ARBP	Forward 5'- TAGAGGGTGTCCGCAATGTG-3' Reverse 5'- CAGTGGGAAGGTGTAGTCAGTC-3'	137
Pgk1	Forward 5'- ATGCAAAGACTGGCCAAGCTAC-3' Reverse 5'- AGCCACAGCCTCAGCATATTTC-3'	104

3.3.2 RNA extraction

3.3.2.1 Prevention of RNase contamination

Ribonuclease (RNase) is ubiquitous presence in every cell type, and in tissues, bodily fluids, microorganisms and most environments which can degrade RNA rapidly (Peirson and Butler, 2007). Even minimal quantities of RNase can compromise the downstream experiments, therefore, minimizing RNase contamination and working in an RNase-free environment is very important. All equipment, pipettors, working benches and space were treated with an RNase decontamination solution, RNaseZAP (Sigma, R2020). RNase-free microfuge tubes and aerosol resistant tips (Axygen) were used and also gloves sprayed with RNaseZAP reagent and a lab coat were worn all the time during experiment.

3.3.2.2 Cell Harvesting, DNA decontamination & RNA extraction from Cortical Neuronal Culture

Total RNA was extracted from cortical neuronal cultures using the RNeasy Plus Micro Kit (Qiagen, 74034). The culture medium was completely removed from the cell culture plates and 350 µl Buffer RLT Plus was added to each well. Cells were detached and scraped off from the coverslips using cell scrapers (BD Bioscience, 734-0385), and the cell suspension pipetted into microcentrifuge tubes followed by pipetting up and down or vortexing to homogenize the lysate. Before RNA extraction, the sample was transferred to a gDNA Eliminator spin column placed in a 2 ml collection tube and centrifuged for 30 secs at ≥ 10,000 rpm (≥ 8000 g) for DNA decontamination. Then a volume of 350 µl of 70% ethanol was added to the flow-through and mixed well by pipetting. The sample was transferred to an RNeasy MinElute spin column placed in a 2 ml collection tube and centrifuged at ≥ 10,000 rpm for 15 secs. The subsequent steps of RNA extraction followed the manufacturer's instructions, and then the RNA was eluted and suspended in RNase-free water and stored at -80^{o}C freezer.

3.3.2.3 Brain tissue homogenization and RNA extraction from Visual Cortex TeNT Model of Epilepsy

At the end of ECoG recordings, animals were euthanized and a small piece (3 mm x 3 mm x thickness of cortex: approximate 1.2 mm) (Figure 3.9) of cortex was microdissected from the epileptogenic zone in epileptic rats or injection zone in control group animals using RNase-free tools. The brain was submerged in RNA*later* (Qiagen, 76106) during dissection for RNA stabilization and then transferred to liquid nitrogen immediately followed by storage at -80^{o}C until use.

Total RNA was extracted from the frozen brain tissue using miRNeasy Mini kit (Qiagen, 217004). The brain tissue was placed in a 2 ml tube containing Lysing Matrix D (MP Biomedicals, 116913050) and 800 µl of QIAzol (Qiagen) was added to the sample. Following this, the brain tissue was disrupted and homogenized using FastPrep-24 Homogenizer (MP Biomedicals, 116004500) and then the homogenized sample was incubated at room temperature for 5 mins. A volume of 160 µl (20% amount of the QIAzol) of chloroform (Sigma, C2432) was added to the homogenized sample, and then vortexed vigorously for 30 secs followed by incubating at room temperature for 10 mins. After incubation at room temperature, the sample was centrifuged at 12,000 xg at 4^{o} C for 30 mins and the aqueous phase (upper layer) of the sample was carefully transferred to a sterile 2 ml RNase-free collection tube. A 1.5x volumes (usually 525 µl) of 100% ethanol was added into the aqueous phase and mixed thoroughly by pipetting, and the sample was transferred into an RNeasy Mini column placed in a 2 ml collection tube and centrifuged at ≥ 8000 xg (≥ 10,000 rpm) for 1 min. The following steps were according to the manufacturer's protocol to complete the RNA extraction and the purified RNA eluate was stored at -80^{o} C.

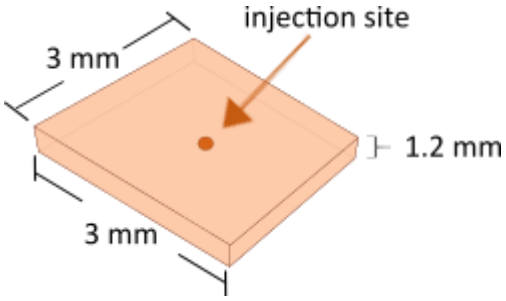

Figure 3.9 Schematic illustration of a microdissected brain sample for RNA extraction. A square (3 mm x 3 mm) around the centre of TeNT or 0.9% saline injection location with a thickness of whole cortical layer was microdissected from the animals for further RNA extraction.

3.3.3 RNA Concentration, Purity and Quality/Integrity

The purity, integrity and quality of RNA would strongly influence the downstream applications and the accuracy of gene expression evaluation, especially in qRT-PCR, micro-arrays, in situ hybridization, *in vitro* reverse transcription or translation (Fleige and Pfaffl, 2006). Before performing qRT-PCR, an assessment of RNA purity and quality/integrity for RNA samples was done. As obtaining the high purity and quality/integrity of RNA is a critical first step for meaningful gene expression data, RNA cleanup was carried out using the RNeasy MinElute Cleanup Kit (Qiagen, 74204) in a subset of RNA samples until they passed the RNA purity and quality measurement. RNA concentration and purity were measured by a NanoDrop ND-1000 spectrophotometer. The purity was measured by optical density (OD) ratio of absorbance at 260 nm and 280 nm (A260/A280), as well as A260/A230 absorbance ratio. The A260/A280 absorbance ratios were ≥ 2 and A260/A230 values were within the range of 2.0-2.2 for all the RNA samples, which indicated high purity of RNA samples (an A260/A280 ratio of ~2 is generally accepted as pure RNA).

The RNA quality/Integrity was analyzed for the RNA samples using Agilent 2100 Bioanalyzer (Agilent Technologies, USA) with Agilent RNA 6000 Nano Kit and following the manufacturer's instructions. The RNA integrity numbers (RIN) of the RNA samples were all ≥ 7 (range: 7-9.6) (Figure 3.10) which indicated high RNA quality and integrity.

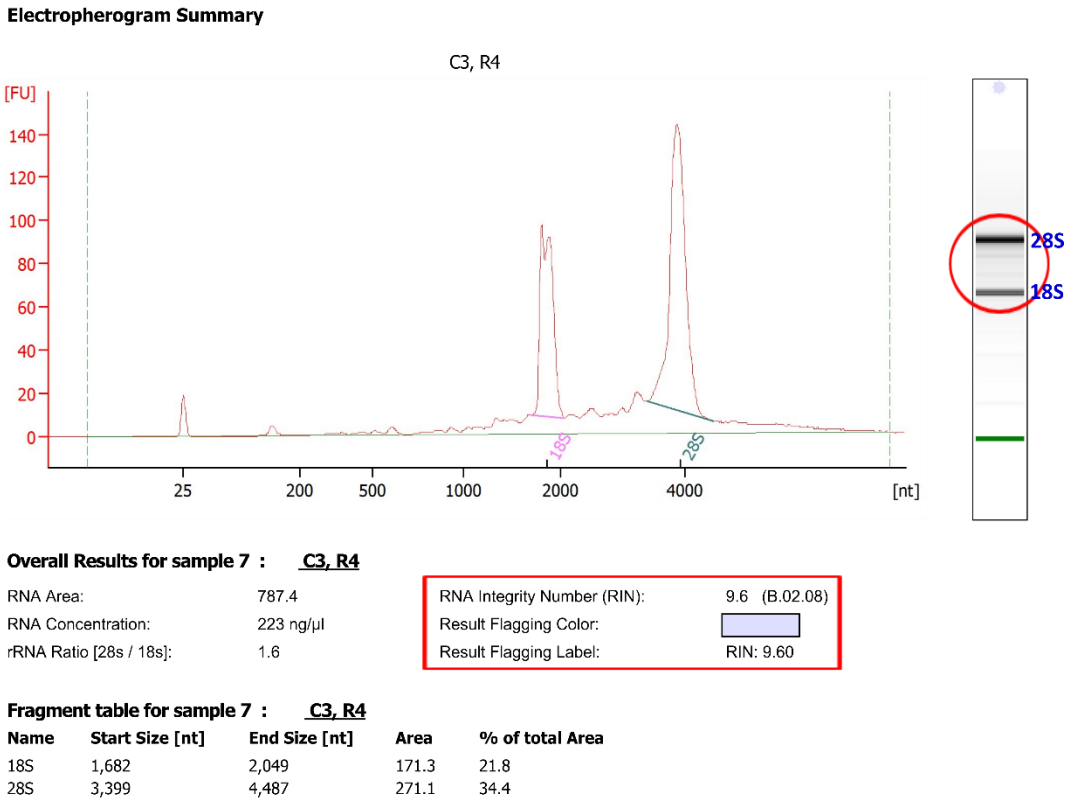

Figure 3.10 An example of RNA quality analysis result

Representative data for RNA quality/Integrity analysis: the 28S and 18S ribosomal RNA bands (Right) are separated by electrophoresis for micro-fluidic electrophoresis, which is used to assess the RNA integrity. The value of RIN is 9.6 that represents high RNA quality and integrity.

3.3.4 cDNA Preparation (RNA Reverse Transcription)

Two-step qRT-PCR was performed to evaluate the gene expression in epilepsy. The first step was to synthesize complementary deoxyribonucleic acid (cDNA) by using 1 µg of total RNA from each sample for reverse transcription. QuantiTect reverse transcription kit (Qiagen) was used according to manufacturer's instructions as follows: the genomic DNA elimination component was prepared on ice with 2 µl of gDNA Wipeout buffer(7x), 1 µg template RNA, and adjusted by RNase-free water to a total 14 µl reaction volume then incubated for 2 minutes at 42^{o} C to eliminate the genomic DNA. Following this, a volume of 6 µl reverse transcription master mix containing 1 µl of Quantiscript reverse transcriptase, 4 µl of Quantiscript RT buffer (5X), and 1 µl of RT primer mix was added into each template RNA (14 µl) from the previous step and incubated at 42^{o} C for 15 mins (synthesis) then at 95^{o} C for 3 minutes (to inactivate the reverse transcriptase) to obtain a final volume of 20 µl cDNA product. The resulting cDNA products were stored at -20^{o} C.

3.3.5 Quantitative Real-Time PCR (qPCR)

After acquiring cDNA, the quantitative PCR was carried out by using the SYBR green fluorescent staining method (QuantiTect SYBR Green PCR kit; Qiagen) on a Rotor Gene-6000 thermocycler system (Corbett Research Ltd). Each gene was assayed in triplicate with a final reaction volume of 25 µl in a single tube containing 2 µl cDNA samples, 2.5 µl primers (3 µM of forward and reverse primers respectively), 12.5 µl of QuantiTect SYBR Green PCR Master Mix (2x), and 8 µl H_2O. Triplicate of non-template control (NTC) containing sterilized dH_2O and reaction mix as the negative control of qRT-PCR were carried out for each qRT-PCR experiment. According to the manufacturer's protocol, the qPCR started with initial heat activation at 95^{o} C for 15 mins, and followed by 45 cycles of denaturation at 94^{o} C for 15 secs, primer annealing for 30 secs at an optimal annealing temperature (Tm) of each gene (see Section 4.2) and extension/elongation at 72^{o} C for 30 secs. Finally, the

values of the threshold cycle (Ct) were obtained (see Section 3.3.6) for the subsequent further calculation and analysis.

3.3.6 qRT-PCR Data Acquisition and Analysis

For the good quality control of qPCR data acquisition, the melting temperature of each gene in their triplicates was checked to exclude the possibility of primer-dimer formation or incomplete and non-specific amplicons (Figure 3.11). Replicates that had > 0.5 Ct of difference were avoided to acquire good reproducibility of each gene. In addition, the Ct values > 35 were excluded because of the implication of low qPCR efficiency which would result in poor precision. According to above specificity, reproducibility and efficiency principles of data acquisition, the threshold cycle (Ct) value was determined as the cycle number at which the fluorescent signal of the reaction significantly crosses the threshold of growth curve and was used to estimate the initial amount of cDNA. The Ct value is inversely related to the expression level of the gene, therefore, the lower Ct value means the fluorescence crosses the threshold earlier indicating that the amount of target in the sample is higher. After obtaining the Ct values, the gene expression levels for the genes of interest (GOI) were analyzed by comparative/relative quantification using the Delta delta Ct (ΔΔCt) method (Schmittgen and Livak, 2008; Winer et al., 1999), which was normalized with one or multiple endogenous reference genes (see Section 4.3). The ΔΔCt method is a comparison of experimental samples with an external control (calibrator; e.g. sample from saline-treated non-seizure control rats in my experiments) and internal control normalizers (reference genes). Consequently, the relative quantities of GOI were calculated by the ratio between the amount of target gene and the reference genes in experimental and calibrator samples and were presented as normalized fold changes.

Comparative quantification algorithm- the ΔΔCt method:

$\Delta Ct_{\text{calibrator}} = Ct_{\text{target gene}} - Ct_{\text{reference gene}}$

$\Delta Ct_{\text{sample}} = Ct_{\text{target gene}} - Ct_{\text{reference gene}}$

$\Delta\Delta Ct = \Delta Ct_{\text{sample}} - \Delta Ct_{\text{calibrator}}$

Fold Change (Fold Difference) = $2^{-\Delta\Delta Ct}$

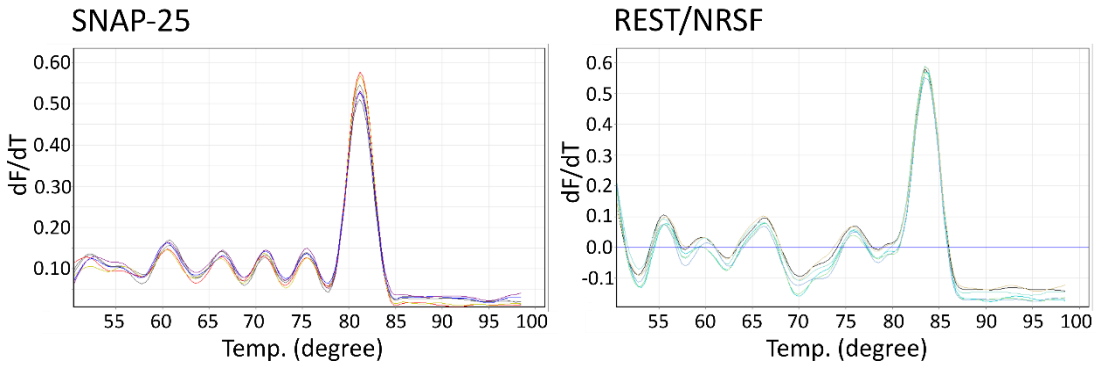

Figure 3.11 Representative results of melting curves in qRT-PCR

Melting curves with melting temperatures were used in each real-time PCR reaction to ensure the amplicon specificity of real-time PCR and to exclude non-specific products and primer-dimers. As the melting temperature is determined by the length and composition of the amplicon, thus non-specific products or primer-dimers which usually exhibit a lower melting temperature than the amplicon will show as additional peaks in the melting curve analysis. Consequently, a melting curve with a unique dissociation peak indicates a specific product and all the qRT-PCR data acquired in my experiments passed the melting curve analysis.

3.4 Statistical Analysis

Power calculations were conducted using Power Piface (version 1.70) (Lenth, 2007) or GPower for the sample size estimation based on data from published studies or pilot studies. The effect size was calculated with an alpha = 0.05 (two-tailed) and power > 0.8.

Statistical analysis was performed using Prism version 6.0 software (GraphPad Software, Inc., CA, USA). The D'Agostino-Pearson omnibus normality test was carried out for all data sets to determine whether they were normally distributed (fitted a Gaussian distribution) before further statistical analysis. If the data passed the normality test, paired or unpaired Student's t-test (two-tailed) were used for comparison of two groups. Analysis of variance (ANOVA) followed by correction for multiple comparisons was performed to compare > 2 groups. One-way ANOVA followed by Dunnett *post-hoc* test was used for comparing multiple treatments to a single control. Two way ANOVA followed by either Sidak or Tukey correction for multiple comparisons were carried out. If the data sets were non-normally distributed, Wilcoxon signed rank test was the non-parametric test for two paired datasets, whereas the Mann-Whitney non-parametric test was used for two unpaired data. For comparisons of more than two groups, the Friedman test was conducted for matched/paired data, whilst Kruskal-Wallis test was used for unpaired datasets and all followed by Dunn's multiple comparison test. Results were presented as mean ± the standard error of the mean (SEM) and the value of "n" represents the number of coverslips (cell viability experiments in neuronal cultures), brain slices (*In vivo* immunohistochemistry experiments), the number of different experiments/preparations (*in vitro* experiments) or animals (*in vivo* experiments). The statistical significance was presented as *p < 0.05, **p < 0.01, ***p < 0.001, ****p < 0.0001, and ns (not significant, p > 0.05).

For statistical analysis of qRT-PCR data, all qRT-PCR datasets have been transformed to the logarithmic transformation of fold change (Log_2 FC) (Ramon Goni et al., September 2009; Rieu and Powers, 2009).

Chapter 4 Primer Validation and Optimization of qRT-PCR

4.1 Introduction

Target specificity, dimerization and self-folding (secondary structure) in primers are critical factors which impact the accuracy of qPCR (Bustin et al., 2009). It is necessary to validate primers and determine the practical optimum annealing temperature of each primer experimentally prior to conducting qRT-PCR experiments. Therefore, all primers designed in my experiments were not only verified by bioinformatics tools (such as BLAST) but also validated by direct experimental evidence using PCR, gel electrophoresis and melting curve profile.

For obtaining a highly accurate, precise, sensitive, specific, efficient and reproducible qRT-PCR data, the parameters used in my experimental conditions were validated and optimized against a standard curve. The standard curve used a dilution series, which covered the complete range of expected expression, and was established for each gene to determine the optimal initial starting amount of the target templates, PCR efficiency, linear dynamic range, sensitivity, reproducibility and limit of detection (LOD: the lowest concentration at which 95% of positive samples are detected). The PCR efficiency represents the performance of a qPCR assay which is particularly important when using comparative quantification algorithm to analyse the levels of gene expression (Bustin et al., 2009). Poor PCR amplification efficiency can result in poor precision of qPCR assays and PCR efficiency within 90-110% is acceptable. The Correlation coefficient (R square, R^2) indicates the linearity of the PCR reaction over the dynamic range. Low R^2 value implies either no linear relation between the Ct value and the log of the DNA concentration, or pipetting inaccurately in the PCR reactions. To be acceptable, the R^2 value must be higher than 0.985.

4.2 Methods

An overview of primer validation and optimization of qRT-PCR is shown in Figure 4.1.

4.2.1 Polymerase Chain Reaction (PCR)

PCR reactions with different annealing temperatures ranging from 52° C to 66° C were performed in each target gene to ensure the optimal annealing temperature of each primer. A total volume of 25 µl PCR reaction mix was made of 2 µl DNA template (50 ng/µl), 2.5 µl of forward primer (3 µM) and reverse primer (3 µM), 12.5 µl of FastStart PCR MasterMix (Roche Applied Science) and 8 µl sterile deionised H_2O. The PCR was done on an Eppendorf MasterCycler thermal cycler with the following cycling conditions: initial activation at 96° C for 5 mins, 40 cycles of denaturation (96° C, 30 secs), annealing primers (annealing temperature, 30 secs) and elongation (72° C, 15 secs), followed by a final extension at 72° C for 5 mins. After the PCR amplification, further agarose gel electrophoresis was carried out on the PCR products.

4.2.2 Agarose Gel Electrophoresis

Agarose gel electrophoresis was performed to verify the size of PCR products. 1% (w/v) agarose gel was prepared by dissolving 1 g of agarose power (Roche) in 100 ml of 1x TAE buffer (40 mM Tris, 20 mM acetic acid and 1 mM EDTA) and heating up the mixture in the microwave for complete dissolution. After cooling down, 10 µl of GelRed Nucleic Acid Gel Stain (10,000X) (Biotium, 41003-BT) was added and well mixed to visualize DNA (via intercalation between the strands). This mixture was poured into a gel electrophoresis tray with a comb for gel polymerisation. Each DNA sample was mixed with one-fifth total volume of GelPilot DNA loading dye (5x) (Qiagen, 239901) and then 25 µl of each sample was loaded into each well. Also, 5 µl

of 100 bp DNA ladder (New England BioLabs, N0467S) was loaded in the first loading well as molecular weight markers. Electrophoresis was run on 60V for 90 mins then the bands were visualized under an Ultraviolet (UV-light) transilluminator.

4.2.3 Standard Curves of qRT-PCR

The cDNA templates prepared from the neocortical tissue of chronic epileptic rats were used to set up standard curves. A standard curve with at least 5 points of a cDNA dilution series (each of them in triplicate) was established for each gene. The qRT-PCR was carried out as the protocol described in section 3.3.5 and then the standard curve was plotted by using the Rotor-Gene 6000 Series software. The PCR efficiency was given by estimating the slope of the standard curve and the R^2 value was acquired. A standard curve slope of -3.32 indicates a 100% PCR efficiency and a more negative value means the amplification efficiency is less than 100%. The mid-point of the concentration in the standard curve was chosen as the initial starting amount of the target template.

4.2.4 Results

Figure 4.1 summarizes the process of the validation and optimization, as well as the results of optimal parameters of qRT-PCR for the genes of interest and the reference genes. All primers were validated and their optimal annealing temperatures were determined and verified by PCR and agarose gel electrophoresis (Figure 4.2). Briefly, the optimal annealing temperatures of these genes were categorized into three different temperatures: (1) 54^{o} C for NRGN, KCNA1, GFAP, SNAP-25, HCN1, HCN2, REST/NRSF, mTOR, ADK, and GABRA5; (2) 57^{o} C for BDNF; and (3) 58^{o} C for CREM/ICERII and CCL2. The reference genes also had good annealing at these three temperatures. The R^2 values of the standard curves for each gene (which reflects the linearity of PCR assay) were all higher than 0.985 and the PCR efficiency in each gene was between 90-110% (Figure 4.3). Two optimal initial starting amount

of target templates for qPCR were (1) 1:20 dilution of cDNA templates for NRGN, GFAP, SNAP-25, HCN1, HCN2, REST, mTOR, ADK, and BDNF; (2) 1/10 dilution of cDNA templates for GABRA5, CREM and CCL2.

PCR

Testing different annealing temperatures
(range from 52 °C ~ 66 °C)
for each primer

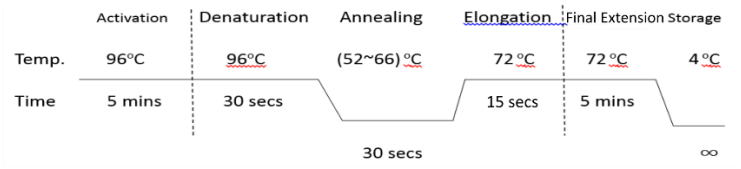

Agarose Gel Electrophoresis

Determine and validate the practical optinum temperature

Practical optimum annealing temperature		
54°C	**57°C**	**58°C**
NRGN, KCNA1, GFAP, SNAP25, HCN1, HCN2, REST/NRSF, mTOR, ADK, GABRA5	BDNF	CREM/ICERII, CCL2
ActB, SDHA, ARBP, Pgk1		

qRT-PCR for Standard Curves

Testing different cDNA dilution series (1:10, 1:5; 1:2...etc) for each gene

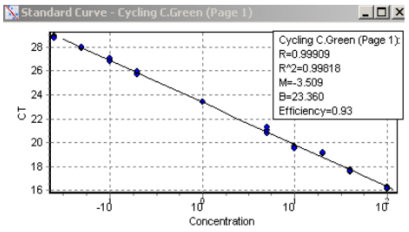

Determine and validate the optimal parameters for qRT-PCR

Results of optimal parameters for qRT-PCR				
Target template Starting amount	**1/20**		**1/10**	
Annealing temp.	**54°C**	**57°C**	**54°C**	**58°C**
Target Genes	NRGN, KCNA1, GFAP, SNAP25, HCN1, HCN2, REST/NRSF, mTOR, ADK	BDNF	GABRA5	CREM/ICERII CCL2

Figure 4.1 Flow chart and results of primer validation and optimized parameters for qRT-PCR.

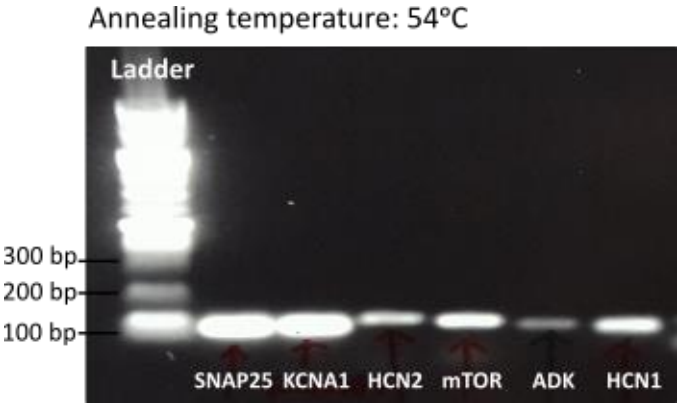

Figure 4.2 An example of the agarose gel electrophoresis results

Most of the primers were designed with the amplicon length between 100-150 bp and PCR followed by agarose gel electrophoresis was carried out for all genes to identify their optimal annealing temperatures and PCR products.

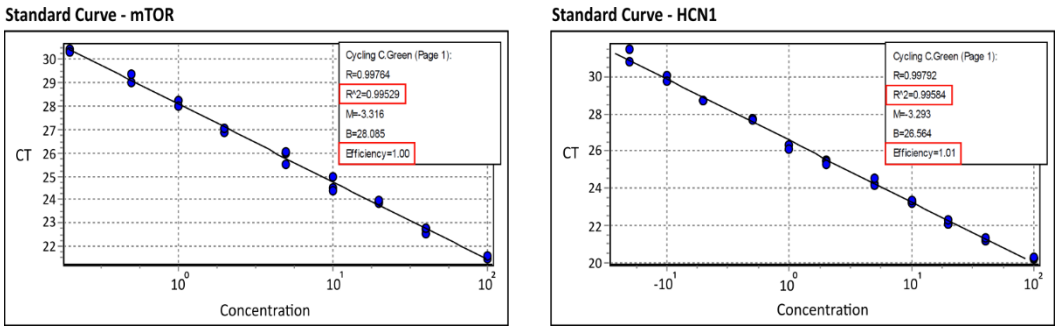

Figure 4.3 Examples of Standard curves of qRT-PCR for each gene

The standard curve for each gene covered the expected expression range of the selected genes in the experiments and was plotted by at least five points of dilution series. The correlation coefficient (R^2) value higher than 0.985 and the PCR efficiency within 90-110% (0.9-1.1) were acceptable.

4.3 Reference Genes Selection

4.3.1 Introduction

Normalization is an essential and the most important component for accurate and reliable analysis of gene expression profile, particularly in comparative quantification of qPCR assays (Bustin et al., 2009; Vandesompele et al., 2002). The most common strategy for normalizing the levels of mRNA expression is the use of endogenous reference genes as the internal controls. The endogenous reference genes often refer to as housekeeping genes which are ideally constitutively expressed genes required for the maintenance of basic cellular functions and exist in all cell types of an organism, regardless of normal or pathological conditions, development stages, or external signals. The reference genes used in qPCR experiments must be expressed at a consistent level in all study samples and should not vary in different experimental treatments or disease states and in tissues or cell types under investigation (Vandesompele et al., 2002). Consequently, proper endogenous reference genes specific to particular tissues and the experimental conditions must be selected and validated experimentally to ensure their stability of expression (Cook et al., 2009; Guenin et al., 2009). It is also necessary to perform further analysis for the experimental results of the candidate reference genes to determine how many reference genes are needed for optimal normalization and to select the most stably expressed reference genes in my experimental system. GeNorm housekeeping gene selection software (PrimerDesign Ltd) is a frequently used analysis software for this purpose. Two major parameters, gene-stability measure (M) and pairwise variation (V), are generated by GeNorm analysis from the experimental data of reference genes. The average expression stability value M of reference genes was ranked from the highest M value (which indicates the least stable gene) to the lowest M values which are the two most stable genes. The pairwise variation (V) can help to determine the optimal number of reference genes for the experiment and the V score < 0.15 is ideal for the system.

4.3.2 Methods

Four candidate reference genes, ActB, SDHA, ARBP and Pgk1, were selected from published studies (Benn et al., 2008; Cook et al., 2009; Nelissen et al., 2010; Vandesompele et al., 2002; Zhang et al., 2014) which were identified as potentially suitable for use and as having stable expression in rat cortex and my experimental conditions. To validate the stability of their expression in my experiments, these four candidate reference genes were tested in my study samples according to different experimental conditions to determine which were the most stable genes to use as the optimal reference genes in each specific experimental condition. After performing qRT-PCR for these four candidate reference genes in my study samples, the GeNorm algorithm was used to identify the optimal reference genes and to assess the ideal number of reference genes for the experimental samples and conditions.

4.3.3 Results

Overall, these four studied candidate reference genes all have high expression stability (low M value: < 0.7) in my experimental samples and conditions. According to the analysis and validation results, ActB was selected as the optimal reference gene for my *in vitro* epilepsy models of neocortical cultures. Different sets of the two most stable reference genes were applied to visual cortex TeNT model of epilepsy according to the different stages of epileptogenesis. The optimal set of reference genes are ARBP and Pgk1 for acute stage experiments (Figure 4.4A); ARBP and SDHA for subacute stage experiments (Figure 4.4B); and SDHA and Pgk1 for chronic stage experiments (Figure 4.4C).

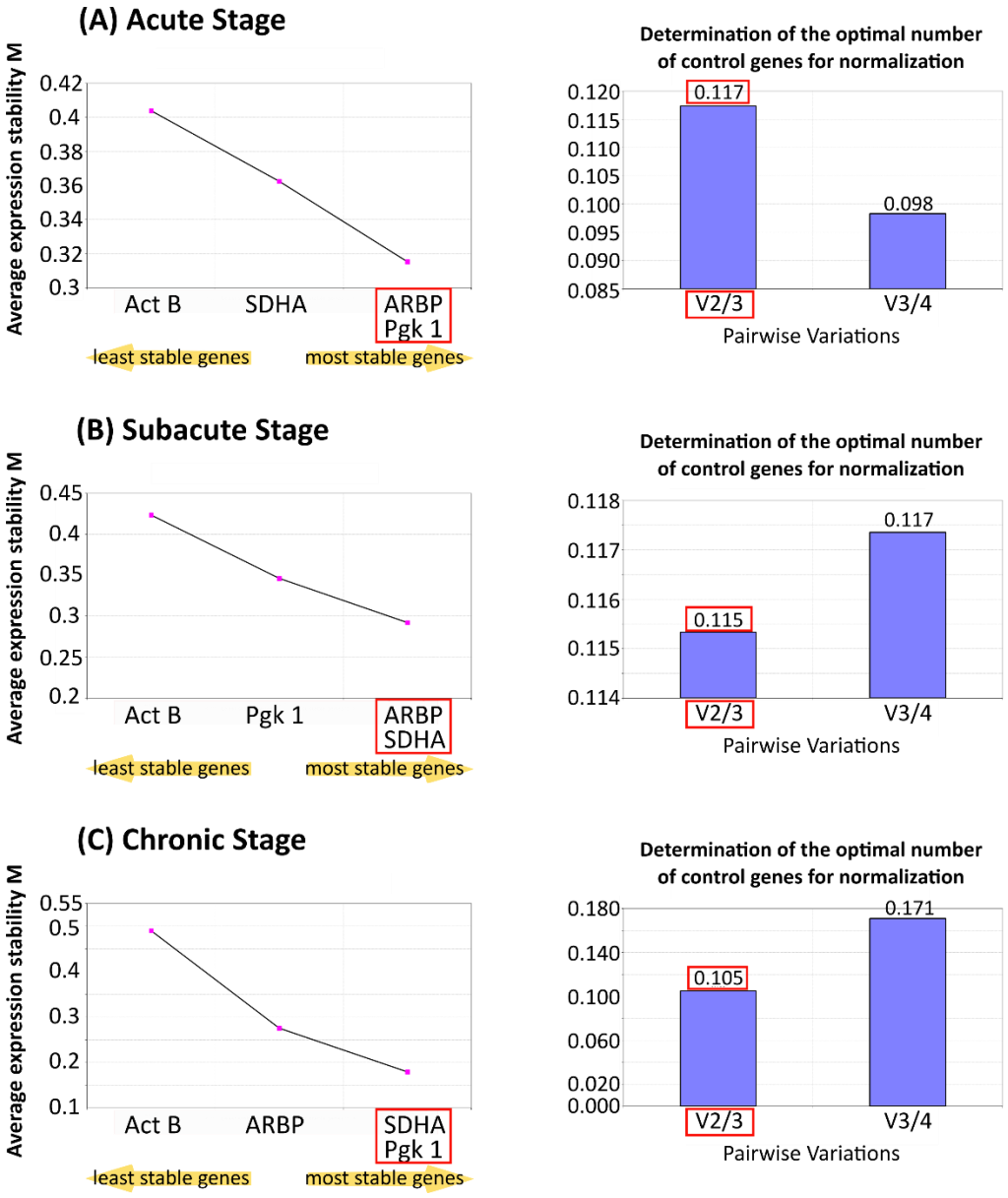

Figure 4.4 Gene expression stability (M) and Pairwise variation (V)

The charts on the left present the average expression stability value, M, of the candidate reference genes (ActB, SDHA, ARBP, Pgk1) in three different experimental conditions. The curve ranks the least stable gene at the left and ends with the two most stable genes on the right. The bar charts on the right show the score of pairwise variation measurement to evaluate how many reference genes were needed for optimal normalization. The V score < 0.15 is achieved with two reference genes in all of these three experimental conditions.

Chapter 5 Gene Regulation in Cell Culture Models for Epilepsy Study

5.1 Introduction

In vitro preparations of seizure-like models have been extensively employed for studying mechanisms of seizures, epilepsies and the pharmacological mechanisms and efficacy of AEDs, as well as for the screening of new AEDs. Among diverse methodologies of *in vitro* preparations, dissociated primary neuron cultures have been a common technique in epilepsy research (Potter and DeMarse, 2001). As the majority of epilepsies are focal epilepsies and most of these involve the hippocampus or neocortex, cultures produced from hippocampal or neocortical cells are the most popular tools exploited in epilepsy research (Garcia Garcia et al., 2010; Pitkanen et al., 2006). In addition, it is well known that different brain regions exhibit different molecular profiles and gene expression levels. Thus, in order to reproduce the molecular regulation of visual cortical epilepsy for comparison to the *in vivo* model of focal neocortical epilepsy that we used for gene therapy studies in the group (see chapter 6), neocortical cultures were prepared from the same animal strain with cells from the equivalent neocortical region (posterior neocortex).

There are contradictory findings regarding changes of mRNA or protein expression of some regulatory molecules, receptors and ion channels from different experimental models of epilepsy study. Downregulation of HCN has been demonstrated in K.A. and pilocarpine models of epilepsy (Jung et al., 2007; Shah et al., 2004). However, upregulation of the h-current has been described in a febrile seizure model (Chen et al., 2001; Dyhrfjeld-Johnsen et al., 2008). These contradictions are perhaps due to these epilepsy models being induced via different mechanisms.

High-potassium, Low-magnesium, Kainic acid and PTZ are commonly used *in vitro* models in epilepsy study and they elicit seizure-like activity through different

mechanisms, and consequently may indicate which changes in gene regulation are conserved in different models, and which changes depend on the model used. We compared gene regulation in these four cell culture models to explore the gene regulation in epilepsy.

5.2 Aims

The first aim of this chapter is to characterise and understand how similar or different the changes of gene expression are in cell culture models using different mechanisms to induce epileptiform activity.

The second aim is to establish a baseline for further comparison between *in vitro* models and *in vivo* models to have a better insight into which *in vitro* models might provide the most similar molecular profile to the *in vivo* model of epilepsy.

5.3 Methods

To give an overview of how the samples were processed, an outline of how to obtain the data from one experiment/preparation (n=1) for the gene expression of the 13 candidate genes in these four cell culture models of epilepsy study is shown in Figure 5.1. Briefly, the convulsant drugs for experimental groups or PBS for the control group were applied to the neocortical cell cultures on 14 DIV then incubated. The RNA was harvested 72 hours after drug applications, and followed by reverse transcription to yield cDNA. Subsequently, quantitative real-time PCR was carried out in control and experimental samples simultaneously. Afterwards, the data was analysed by delta-delta Ct method to acquire the relative quantification of mRNA expression.

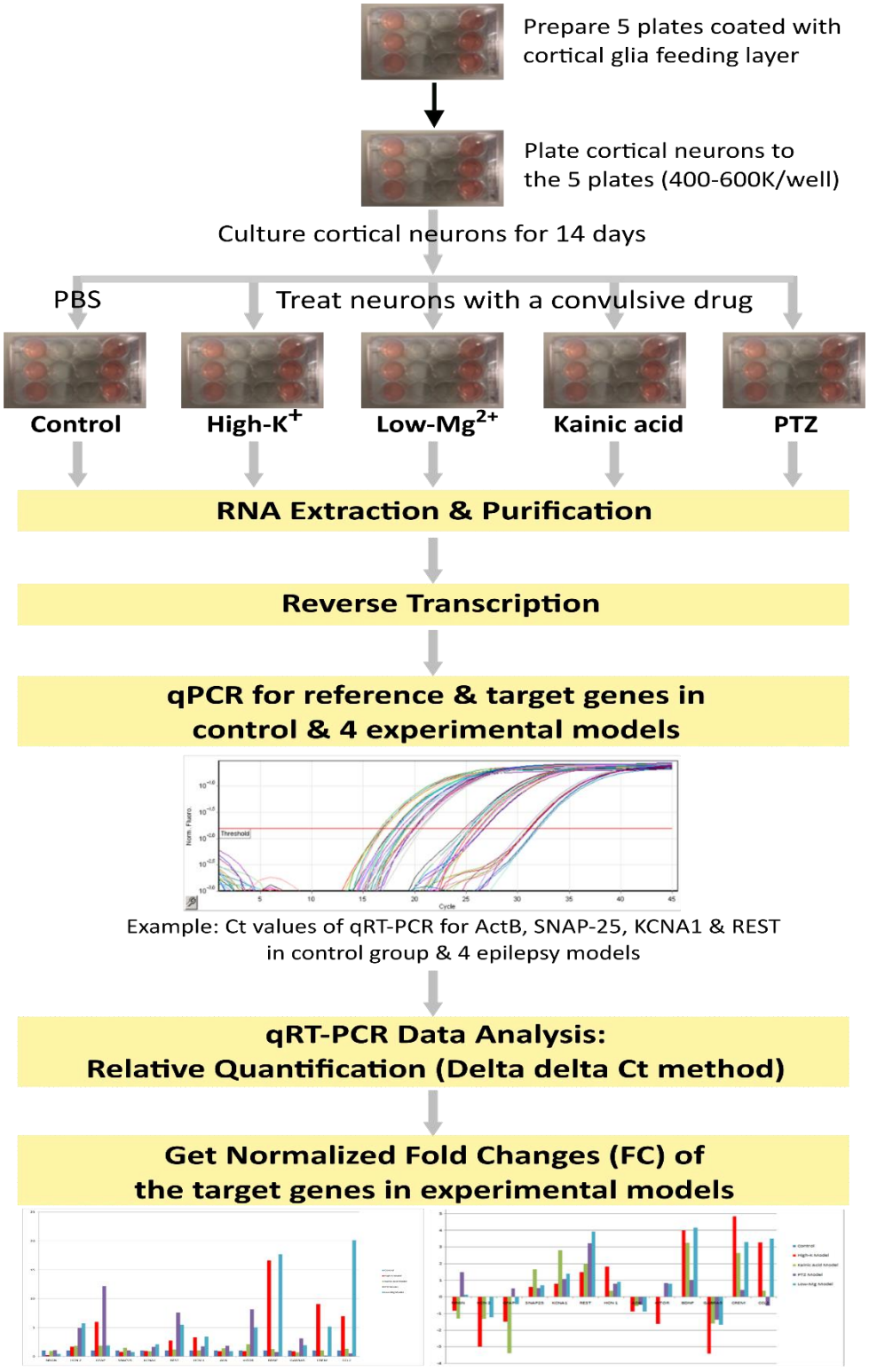

Figure 5.1 The outline of one experiment/preparation (n=1) for gene expression quantification in cell culture models of epilepsy study.

5.3.1 High Potassium model

Stock high-potassium solution (1M) was added to Complete Neurobasal A medium in neocortical cultures on 14 DIV with a final concentration of $〔K〕_0$ to 35 mM per culture well. Then cortical neurons were bathed in this high-potassium medium for 72 hours at 37^o C under a humidified 5% CO_2 and 95% air for the duration of the experiment (see Figure 5.1).

5.3.2 Low Magnesium model

The method used for Low-Mg^{2+} treatment was based on the protocol described by Robert E. Blair in 2004 (Blair et al., 2004). Cortical neurons cultured for 2 weeks (14 DIV) were utilized for this model. First, the culture medium was removed and stored in a sterilized tube for the later use. Cells were rinsed gently with 2.5 ml of Magnesium-free medium three times. The neuronal cultures were then incubated in 3 ml of Magnesium-free medium for 3 hours at 37^{o}C under a humidified atmosphere containing 5% CO_2 and 95%. At the end of this treatment, cells were washed gently with 2.5 ml of warmed Neurobasal medium 3 times then restored to the physiological concentration (0.8-1 mM) of $MgCl_2$ by returning to the maintenance medium and incubated at 37^o C with a humidified, 5% CO_2 / 95% atmosphere incubator. Three days after low-Mg^{2+} treatment, the cortical cells proceeded to the RNA extraction (as shown in Figure 5.1).

5.3.3 Kainic Acid model

Chronic kainic acid treatment was carried out with incubation of cells in 5 μM kainic acid for 72 hours. This protocol was modified from the method delineated by Qi and Yao in 2006 (Qi et al., 2006b). Briefly, 5 mM of stock kainic acid was added into the complete neurobasal A medium of 14 DIV neocortical cultures with the final

concentration of kainic acid at 5 µM. Cells were then incubated in 37° C, humidified, 5% CO2 and 95% air until RNA collection (see Figure 5.1).

5.3.4 Pentylenetetrazole (PTZ) model

Complete Neurobasal A medium was supplemented with 10 mM Pentylenetetrazole (PTZ) on the day of the experiment using 1M stock PTZ and warmed Complete Neurobasal A medium. Maintenance medium was removed from 14 DIV neocortical cultures and replaced by 3 ml of Complete Neurobasal A medium containing 10 mM PTZ then incubated at 37° C in a humidified atmosphere with 5% CO_2 and 95% air for 2 hours (Qu et al., 2005). After this treatment, the PTZ containing medium was removed and cells were rinsed gently with 2.5 ml of warmed neurobasal A medium three times followed by refeeding with maintenance medium and kept at 37° C until RNA harvesting 72 hours later (Figure 5.1).

5.4 Results

5.4.1 Cell Viability Assay in Different Cell Culture Models of Seizure like activity

To examine whether the mRNA expression changes were biased by convulsant-induced neuronal death, a cell viability assay was conducted for each model. The cell-death analysis compares the percentage of PI-positive cells (dead cells) to the number of DAPI-positive cells (all cells). Then the cell-death ratio in each experimental model was compared to control group. There was a small proportion of dead neurons in both control cultures (~11.4%) and convulsant-treated cultures (Figure 5.2). Compared to the control group, the Low-Mg^{2+} model had a slightly higher neuronal death ratio ($F(4, 25) = 1.0$, $p = 0.326$; one-way ANOVA with Dunnett *post-hoc* test) and followed by K.A.-treated group ($p = 0.456$), High-K^+ model ($P = 0.663$), and PTZ model ($p = 0.997$) (Figure 5.3). However, none of these were significantly different in neuronal death ratio compared with the control group. These data suggest that there is no significant convulsant-induced neuronal loss across these cell culture models, and changes in mRNA levels are not likely due to disproportionate cell death.

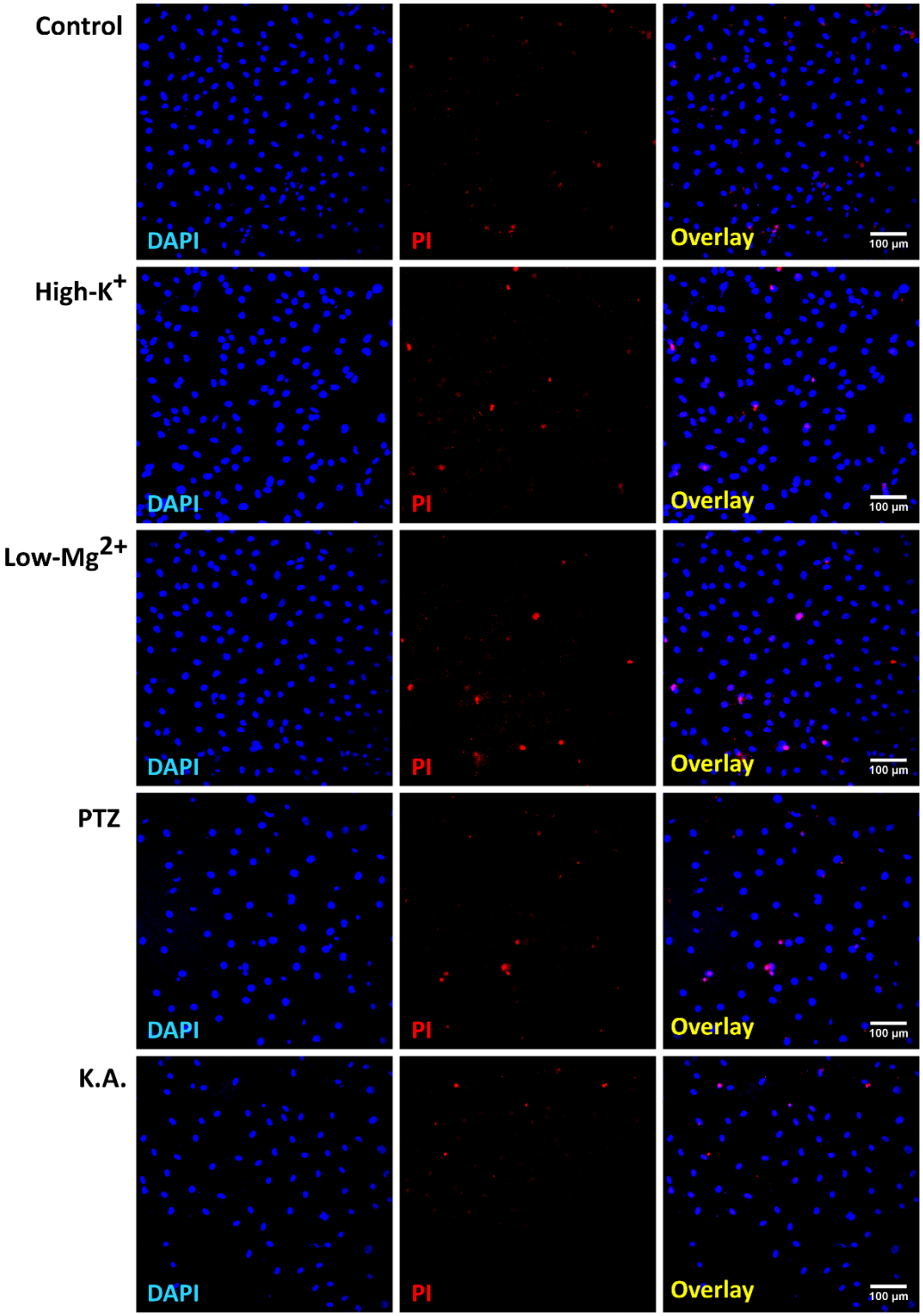

Figure 5.2 Representative confocal images of cell-death assay

DAPI staining (blue fluorescence) for all cell nuclei and PI staining (red fluorescence) for dead cells in control cultures and High-K^+, Low-Mg^{2+}, PTZ, and K.A. cell culture models. Only PI-stained nuclei that were confirmed by DAPI-stained cells in overlay images were counted. (Confocal images: 20X objective).

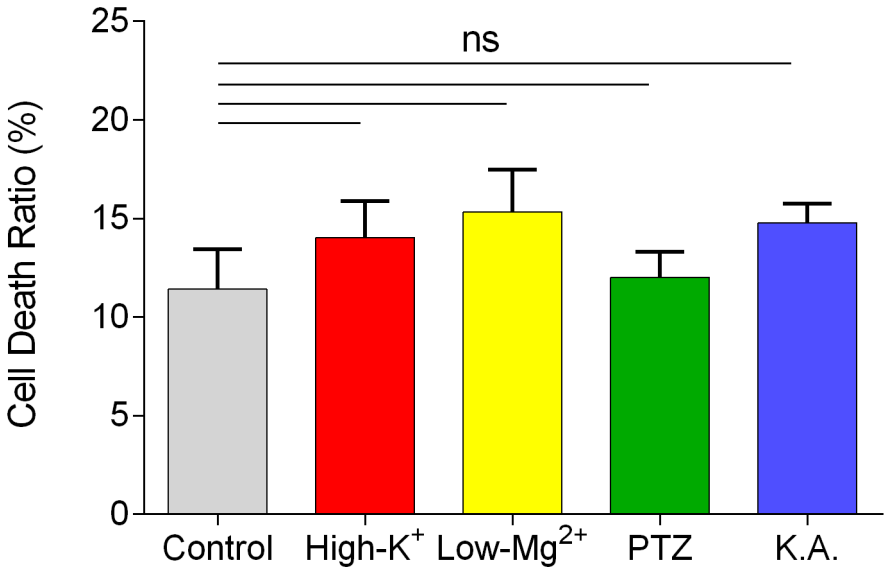

Figure 5.3 No difference of neuronal death ratio in untreated- and treated-groups

Quantification of cell-death analysis by the ratio of PI-positive cells compared to DAPI-positive cells for each cell culture model and the control group. (n = 6 in each group from five different preparations; ns = no significance, one-way ANOVA followed by Dunnett *post-hoc* test). Data are presented as mean ± SEM.

5.4.2 mRNA Expression in Different *In Vitro* Models for Epilepsy Study

All qRT-PCR datasets have been transformed to the logarithmic transformation of fold change (Log_2 FC) as is standard for statistical analysis of qRT-PCR (Ramon Goni et al., September 2009; Rieu and Powers, 2009). For clarity, the different expression level of mRNA coding for the gene of interest (GOI) for each cell culture model shown in Figure 5.4 - 5.5 is presented as the fold change (FC) with mean ± SEM.

5.4.2.1 REST, BDNF, HCN1, ICERII, CCL2 and KCNA1 are up-regulated in all models

REST/NRSF and BDNF mRNA expression exhibited a significant increase in all of the High-K^+, Low-Mg^{2+}, PTZ and K.A. cell culture models (REST: $F(2.985, 26.87) = 10.99$, $p < 0.0001$; BDNF: $F(4, 36) = 50.41$, $p < 0.001$; one-way ANOVA) (Figure 5.4A). In particular, there was a higher than 10-fold change in BDNF mRNA levels compared with the control group in the High-K^+ and Low-Mg^{2+} models. Moreover, the mRNA levels of CREM (ICERII), HCN1, KCNA1 and CCL2 were consistently up-regulated in all models with CREM (ICERII) and CCL2 significantly overexpressed in both High-K^+ and Low-Mg^{2+} models (ICERII: $F(4, 36) = 43.87$, $p < 0.0001$; CCL2: $F(4, 36) = 26.71$, $p < 0.0001$; one-way ANOVA) (Figure 5.4A and B). HCN1 mRNA was significantly increased in the High-K^+, Low-Mg^{2+} and PTZ models ($F(4, 36) = 23.26$, $p < 0.0001$; one-way ANOVA). In contrast, the increase in KCNA1 only reached significance in the Low-Mg^{2+} model (Figure 5.4A and B). Among these four cell culture models, the High-K^+ and low-Mg^{2+} models displayed the most similar pattern of mRNA regulation among the over-expressed genes.

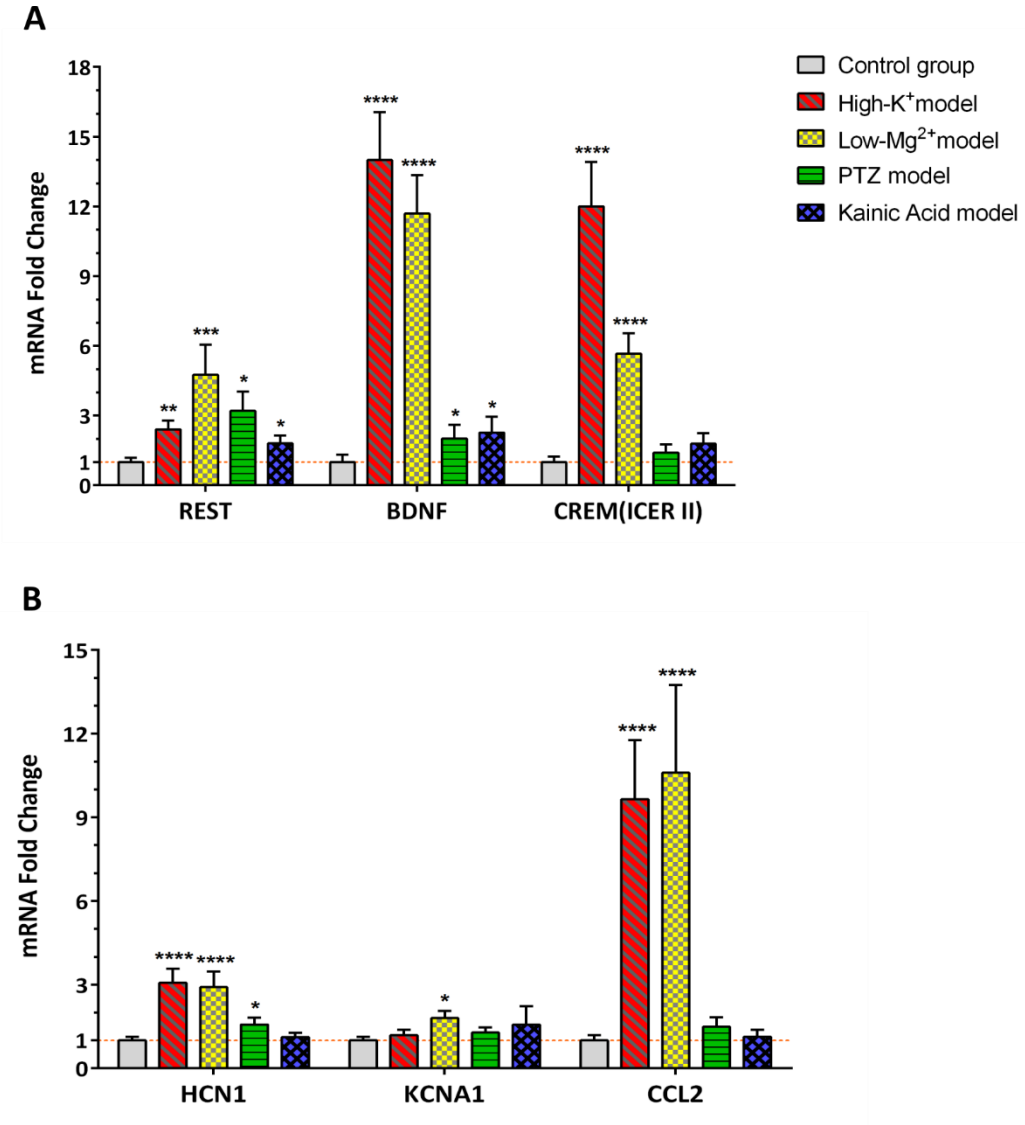

Figure 5.4 Overexpression of mRNA in all the experimental cell culture models

Relative quantification of mRNA transcript levels by comparative qRT-PCR analysis presented as "fold change" of mean ± SEM compared to control, thus the mRNA value in the control group is "1". (A) mRNA up-regulation in all of the models was seen for REST (High-K^+, Low-Mg^{2+}, PTZ, K.A. models: p = 0.0019, 0.0004, 0.023, 0.019, respectively), BDNF (p < 0.0001, < 0.0001, = 0.035, = 0.026, respectively), and CREM(ICERII) (High-K^+: p < 0.0001, Low-Mg^{2+}: p < 0.0001). (B) mRNA overexpression was present but less robust in all models for HCN1 (p < 0.0001, < 0.0001, = 0.033, ns, respectively), KCNA1 (Low-Mg^{2+}: p = 0.03), and CCL2 (High-K^+: p < 0.0001, Low-Mg^{2+}: p < 0.0001). (A, B) Among these up-regulated genes, REST/NRSF and BDNF exhibit the strongest changes in all experimental models, followed by HCN1.
(n = 10/group, matched measures one-way ANOVA with Dunnett *post-hoc* test versus control group, *p < 0.05, **p < 0.01, ***p < 0.001, ****p < 0.0001)

5.4.2.2 NRGN and ADK are down-regulated in most models

In contrast to the genes that were broadly increased in expression in these models, the changes of NRGN mRNA were consistently down-regulated in the four models and the decreases were significant in the High-K^+ and Low-Mg^{2+} models ($F(4,36) = 18.04$, $p < 0.0001$; one-way ANOVA) (Figure 5.5A). Apart from the K.A. model, the ADK mRNA expression also had a tendency of reduction in most models, but were not significantly altered (Figure 5.5A).

5.4.2.3 mTOR, GABRA5, HCN2, SNAP-25 and GFAP are variably regulated across models

Figure 5.5B outlines the mRNA expression of mTOR, GABRA5, HCN2, SNAP-25, and GFAP. These changes in these genes were highly variable across the four experimental models. The mRNA expression of mTOR exhibited significant up-regulation in the Low-Mg^{2+} and PTZ models and a small increase in the K.A. model, whereas there was a downward trend in the High-K^+ model ($F(4, 36) = 11.43$, $p < 0.0001$; one-way ANOVA). A noticeable decrease of GABRA5 mRNA and a distinct down-regulation of HCN2 in the High-K^+ model were seen, as well as a minimal decline of both genes in the K.A. model (GABRA5: $F(4, 36) = 19.24$, $p < 0.0001$; HCN2: $F(4, 36) = 7.508$, $p < 0.0002$; one-way ANOVA). However, GABRA5 and HCN2 showed increases in the Low-Mg^{2+} and PTZ models. There was a mild increase of SNAP-25 mRNA level in the High-K^+, Low-Mg^{2+}, and K.A. models but it was slightly reduced in the PTZ model ($F(4, 36) = 1.592$; $p < 0.197$; one-way ANOVA). The expression of GFAP mRNA increased in both the High-K^+ and PTZ models, but decreased in the Low-Mg^{2+} and K.A. models without statistical significance.

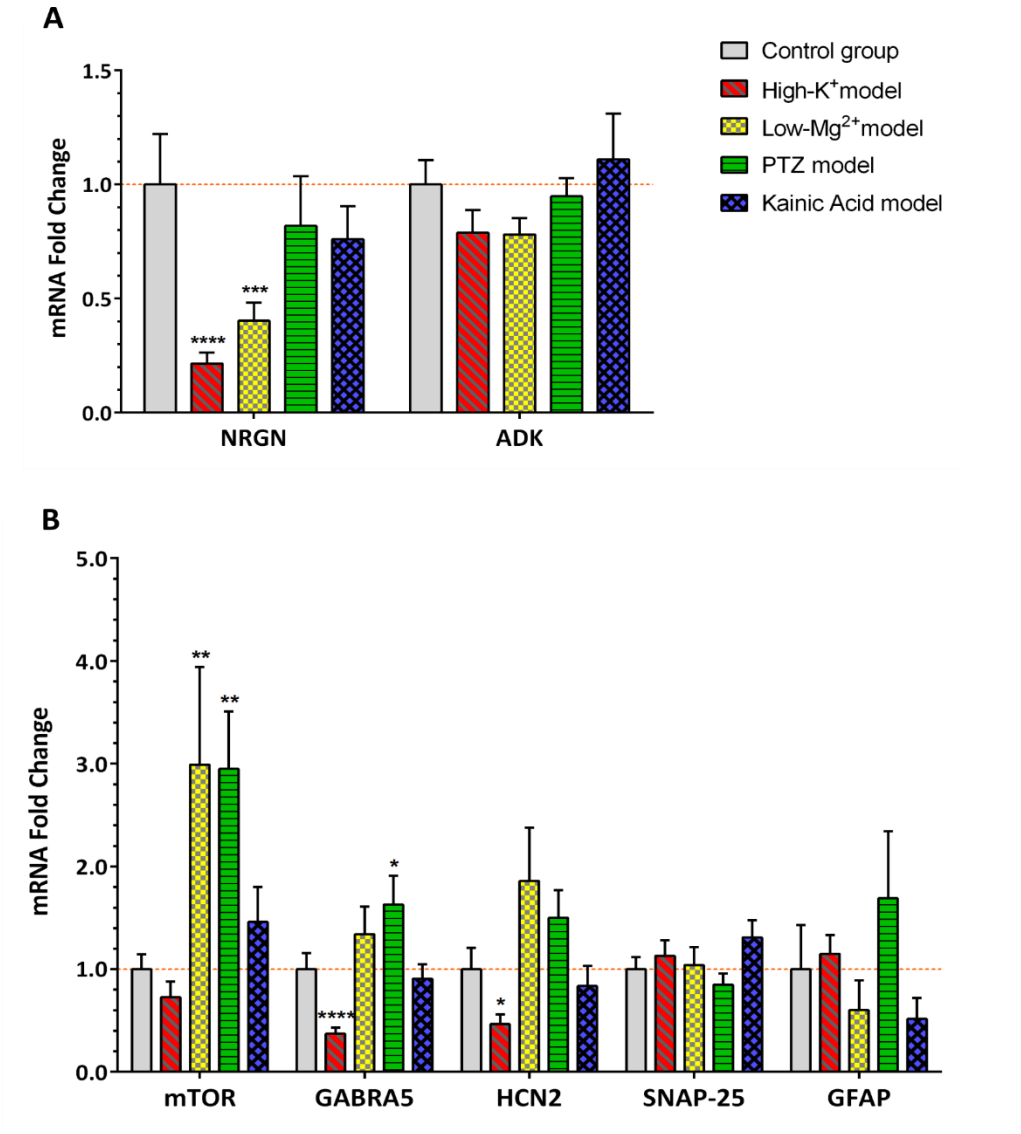

Figure 5.5 Relative quantification of mRNA expression in cell culture models of epilepsy study

(A) mRNA expression of NRGN and ADK. Down-regulation of NRGN was manifested in these experimental models and was statistically significant in the High-K^+ and Low-Mg^{++} models ($p < 0.0001$, and $p = 0.0008$, respectively). ADK mRNA also had downward changes in the High-K^+, Low-Mg^{++}, and PTZ models. (B) The mRNA quantity of mTOR, GABRA5, HCN2, SNAP-25 and GFAP showed inconsistent changes in these models of seizure like activity. In the Low-Mg^{2+} and PTZ models, the increase of mTOR mRNA revealed significance ($p = 0.005$, and $p = 0.0036$ respectively). In the High-K^+ model, there was profound down-regulation of GABRA5 ($p < 0.0001$) and HCN2 ($p = 0.026$).

(n = 10/ group, matched measures one-way ANOVA, Dunnett *post-hoc* test versus control group, *p < 0.05, **p < 0.01, ***p < 0.001, ****p < 0.0001). Data are presented as mean ± SEM.

5.5 Discussion

A few previous studies proposed that some of the gene expression changes during seizure, such as REST, might be attributed to neuronal death induced by proepileptic treatment such as K.A. or ischemia (Calderone et al., 2003; Spencer et al., 2006). However, no difference of cell viability was seen between control group and convulsant-treated groups in my data, therefore these results provide the evidence that neuronal death is not the major cause of the alterations of mRNA expression in my experimental cell culture models of seizure like activity.

Comparing these four models, High-K^+, Low-Mg^{2+}, PTZ and K.A., which elicit seizure-like activity through different mechanisms, the K.A. model showed the least similarity and consistency of the alteration of gene expression against the other four models. This may be due to the kainate receptors are mainly expressed in the hippocampus (Collingridge and Lester, 1989; Levesque and Avoli, 2013; Miller et al., 1990) with relatively less expression in neocortical neurons. Therefore, K.A. applied to the neocortical culture might not be sufficient to induce robust epileptiform activity or much higher dosage of K.A. might be needed to elicit robust seizure-like activity compared to hippocampal culture. On the other hand, both the High-K^+ and Low-Mg^{2+} models generally were the most similar in the changes of gene regulation among these models.

The similarities and discrepancies in gene expression changes across these different experimental models for epilepsy study may elucidate why some gene expression changes are seen in some studies but are not reproduced or are even contradictory in other studies. Furthermore, the genes which did display consistent changes in regulation across the different models might be important regulators or hallmarks of epileptogenesis, and may provide targets for further investigation to understand the mechanisms of epileptogenesis in human epilepsy.

Genes Significantly up-regulated in all models

In the present study, we observed that the mRNA expression of REST/NRSF and BDNF are significantly up-regulated in all of the cell culture models of epilepsy via different seizure-inducing mechanisms. REST/NRSF is a transcriptional repressor that is able to modify long-term, cell-specific gene repression through binding to a 23 bp DNA-binding sequence called neuron-restrictive silencer elements (NRSEs; also known as RE1 elements) (Schoenherr and Anderson, 1995). REST/NRSF is prominently expressed in non-neuronal cells with the function of suppressing the expression of many neuronal genes, and its levels are relative low in mature neuronal cells but it regulates the expression of neuronal genes coding for ion channels, neurotransmitter receptors, calcium-related molecules, phospho-enzymes and other transcription factors governing neuronal plasticity, function, network behaviour, differentiation, and neurogenesis within the brain (Aoki et al., 2012; Ballas et al., 2005; Chen et al., 1998; McClelland et al., 2014; Palm et al., 1998). More and more evidence supports that REST/NRSF is able to regulate a set of genes that crucially influences downstream gene expression and signalling pathways which may contribute to epileptogenesis (Goldberg and Coulter, 2013; Pozzi et al., 2013). Indeed, our data also suggest that there was no difference between *in vitro* models of REST/NRSF overexpression during epileptiform activity, but that the changes where highly conserved.

BDNF is one of the neurotrophins that not only regulates growth, survival and differentiation, but also activates rapid neuronal signalling through modulation of ion channel function, neuronal excitability, and synaptic plasticity via TrkB-mediated intracellular protein phosphorylation and cascades of secondary messengers, and it may have the ability to gate ion channels directly and rapidly while also potentially modifying the CNS structure and function in mature brain (Blum and Konnerth, 2005; Scharfman, 2005). In our data, we found that BDNF showed consistent over-expression among the models of seizure-like activity regardless of the method used for seizure induction and such up-regulation can be tremendously robust. Although there are some studies have indicated that BDNF can cause a decrease in GABAergic

transmission (Frerking et al., 1998a; Tanaka et al., 1997), an increase in glutamatergic transmission (Patterson et al., 1992), and rapid action at $Na_v1.9$ leading to neuronal depolarization (Kovalchuk et al., 2004) and some hypotheses about how BDNF up-regulation contributes to the development of epilepsy have been proposed (Binder et al., 2001), a definitive mechanism linking BDNF with epileptogenesis has not been demonstrated. Our data show BDNF is consistently upregulated, but cannot determine whether this is pro- or anti-epileptogenic.

Genes with variable up-regulation across models

Our data also showed the mRNA expression of HCN1, CREM/ICERII, CCL2, and KCNA1 have a consistent tendency for up-regulation in these models, however they are not all significantly increased for each model. HCN channel is a tetrameric complex which is assembled by different combinations of four different channel isoforms (HCN1-4) (Noam et al., 2011). HCN channels made by different homo-tetrameric or hetero-tetrameric complexes have different properties with unique activation and expression characteristics and function in the regulation of cellular excitability, network activity, as well as synaptic plasticity (Albertson et al., 2013; Nolan et al., 2004). Enhanced expression of HCN1 channels in the granule cells of the dentate gyrus from the resected human hippocampal tissue with mesial temporal lobe epilepsy has been reported (Bender et al., 2003). Many studies have reported alterations of HCN expression, particularly HCN1 and HCN2, during the epileptogenic process (Brewster et al., 2005; Jung et al., 2007), however, there are some conflicts among these reports about whether there is an increase or decrease in expression of HCN1 and HCN2 genes, and this may be consistent with the dysregulation of HCN channels having distinct temporal and spatial patterns in epilepsy (Noam et al., 2011). Also, the HCN1 and HCN2 revealed distinct regulation patterns in my experimental models with a significant increase of HCN1 but decrease of HCN2 in High-K^+ model which implies that different aetiologies of epilepsy might cause diverse expression of HCN2.

ICER is a transcription factor. It is one of the protein products from the CREM gene and functions as an important transcriptional regulator of neuronal plasticity and apoptosis through repressing CRE-mediated gene transcription and inhibiting the transcriptional activity of CREB (cAMP-responsive element binding protein) (Mioduszewska et al., 2003; Molina et al., 1993). Previous studies have shown ICER levels are elevated in epileptic animals (Fitzgerald et al., 1996; Konopka et al., 1998; Zhu et al., 2012). Moreover, it has been reported that null mice lacking ICER in CREM/ICER developed more severe epilepsy (Porter et al., 2008). Another study also showed that overexpression of ICER retarded epilepsy development in the electrical kindling animal model (Kojima et al., 2008). Both of these studies suggested increasing ICER during epileptogenesis may have a role in suppressing epilepsy. However, other studies also proposed that the overexpression of ICER during epileptogenic process is responsible for the decrease in $GABA_A$ α1 subunit expression leading to reduced synaptic inhibition (Brooks-Kayal et al., 2009). Although the role of ICER in epileptogenesis is still controversial, our data showing ICERII was consistently up-regulated in all models with particularly large changes in the High-K^+ and Low-Mg^{2+} models. Furthermore, ICERII also seemed to exhibit similar and synchronised regulation patterns with the BDNF and CCL2 which implied that there might have close interplay between these genes.

NRGN: Consistently down-regulation in all four models

In contrast to the group of genes above, mRNA expression of NRGN showed down-regulation across the different *in vitro* models of seizure-like activity. NRGN is the only gene with this pattern. NRGN is a neuron-specific postsynaptic protein and its major known function is to bind to the Ca^{2+}-free form of calmodulin (CaM), and CaM is an critical factor that can induce either long-term potentiation or long-term depression within the same spine by different pathways (Zhong and Gerges, 2012). NRGN is able to enhance postsynaptic sensitivity and synaptic strength via the interaction of NRGN-calmodulin (Zhong et al., 2009) and recent reports are focusing on its relevance to schizophrenia (Rose et al., 2012; Walton et al., 2013), and

Alzheimer's disease (Kvartsberg et al., 2014). The relation between NRGN and epilepsy is still unknown and our findings suggest its role may need further investigation.

Although it is not possible to determine which of these changes contribute to the initiation of epileptogenesis and which are compensatory phenomena, here we characterised and provided insights into how these genes are expressed across different mechanisms of seizure induction models. The regulation of gene expression during epileptogenesis is probably driven by transcriptional regulators (such as REST/NRSF and ICER) that bind to specific target genes and modify their expression then trigger one or more large-scale molecular signalling cascades and pathways (such as BDNF or NRGN-dependent pathways). Our snapshot of gene expression allows a comparison across models of epilepsy to ask which genes may play consistent roles independent of the aetiology of the disease. The aim is to use this information to inform future treatment strategies.

5.6 Summary

In this chapter we explored whether the seizure-like activity induced via different mechanisms in cell culture models will cause similar patterns of gene expression. We also aimed to identify genes which exhibit the same expression profile regardless of models. These observations could provide us the indication that some genes may be involved in diverse expression with different aetiologies of epilepsy, whereas a few genes which exhibit consistent changes in all models possibly could be the key molecular regulators for further study to understand the epileptogenesis in human epilepsy, and would be beneficial to epilepsy treatment.

Overall, most genes were differentially regulated across different models of seizure-like activity in our data. However, REST/NRSF, BDNF, HCN1, and NRGN all displayed relatively consistent expression characteristics across models. In addition, ICERII, CCL2 and mTOR had similar regulation tendencies in all models (except mTOR

in the High-K^+ model) which suggests they may also be important regulators in the majority of epilepsies.

Chapter 6 Gene Regulation in the Tetanus Toxin model of Focal Neocortical Epilepsy

6.1 Introduction

The development of epilepsy, either from genetic or acquired causes, is a continuous process that is regulated temporally and spatially by changes in multitudes of genes. The epilepsy disorder itself is not a static state. Despite the complexities of molecular regulation during epileptogenesis and the course of epilepsy disorders, some genes have been frequently shown to change and implicated to play a critical role in epilepsy. Among these genes, REST/NRSF and CREM are transcriptional factors which govern intrinsic homeostasis of neuronal circuits (Fitzgerald et al., 1996; McClelland et al., 2014; Pozzi et al., 2013), and mTOR is expressed in neurons and astrocytes as a key regulator of translational factors to control protein synthesis related to many functions (Chen et al., 2007; Tang et al., 2002; Vezzani, 2012). Their overexpression has been reported in some animal models of epilepsy or in human epileptic tissue (Wong, 2008). Moreover, dysregulation of ion channels including HCN, GABAergic receptors, and aberrant functions of glial cells have also been shown.

However, conflicting and divergent findings regarding these molecular alterations in epilepsy have been reported in experimental models of epilepsies and some clinical studies. These controversies are likely at least partly because gene expression is dynamically regulated during the development of epilepsy and the course of disease. Also, whether and which genes could be common master regulators during epileptogenesis remains unclear. Therefore, investigating the dynamic changes in mRNA expression will help us to better understand the molecular basis of epileptogenesis and epilepsy then further provide better insights into the mechanisms and possible conserved targets for epilepsy treatment, prevention or even, eventually a cure for epilepsy. Here we are interested in elucidating the temporally regulated patterns of these molecular profiles during epileptogenesis.

Hence three time points (acute, subacute, and chronic stages) according to the concept of time course of epileptogenic cascades (Rakhade and Jensen, 2009) were designed to investigate the temporal changes in gene expression in epilepsy.

At present, the animal models exploited in most epilepsy studies including the exploration of gene regulation are SE-induced epilepsy models, such as K.A. or pilocarpine models, which predominately model mTLE, or transgenic mouse models to study specific diseases, such as using mice with genetic modification in TSC to investigate the tuberous sclerosis complex and focal malformations of cortical development. However, whether these findings can be applied in other epilepsy models or human epileptic syndromes still remains uncertain. Furthermore, since about 62.2% of epilepsies are focal epilepsy and neocortical epilepsy is the second most common form of focal epilepsy (Tellez-Zenteno and Hernandez-Ronquillo, 2012), as well as are commonly resistant to current AEDs (Loscher et al., 2008), it is necessary to develop an optimal animal model of neocortical epilepsy for epilepsy research. While a model of visual cortical epilepsy using TeNT injection in mice has been generated, only ictal and interictal electrographic epileptiform discharges without behavioural seizures were displayed in this mouse model (Mainardi et al., 2012). To better map genetic changes and for the purpose of future translation applications in a syndrome which urgently needs new treatments, we developed a rat model of focal neocortical epilepsy by injection of TeNT into the visual cortex.

6.2 Aims

This chapter starts with the characterization of the anatomic properties, electrographic features, time course and temporal evolution of epilepsy after TeNT injection, and the behaviour manifestations associated with seizures in the TeNT model of visual cortical epilepsy in rats. The second aim is to use this focal neocortical *in vivo* model to investigate the dynamic changes of gene regulation during the epileptogenic process. We further hope to identify the potential master regulators of epileptogenesis by comparing our different experimental epilepsy models.

6.3 Methods

6.3.1 ECoG interpretation and Seizure event detection

Continuous 24h/7 day ECoG recording was carried out during the whole period of the experiment for each animal after surgery. The entire ECoG recording for each animal was interpreted manually by myself using the same criteria for detecting epileptic seizures, which are defined as an evolution of frequency and amplitude over time with a sudden, repetitive, rhythmic, evolving and stereotypic abnormal electrographic activity with high amplitude (>2 times of baseline) and a minimum duration of 10 seconds (Abend and Wusthoff, 2012; Fisher et al., 2014b; Pitkanen et al., 2005; Shah et al., 2012). As seizure duration within an individual animal might vary largely, median was used to represent seizure duration of each individual animal for further statistical analysis to avoid the influence of that the data might be skewed by a small number of extremely large or small values.

6.3.2 Behavioural classification of seizures

Top-down video footage time-locked to the ECoG trace was utilized to assess the seizure behaviours. A subset of seizures was randomly selected from animals with video-ECoG recordings for about 5 weeks by my colleague (A. Snowball) using a Python script. Then seizure types corresponding to human seizure semiology were evaluated and classified by myself according to the ILAE 2017 classification.

6.3.3 Brain tissue preparation from different time points

Both control and experimental (TeNT) animals were divided into three sets for three different categorized stages of experiment: (1) acute stage: 48-72 hours after first spontaneous seizure occurred; (2) subacute stage: about 2 weeks after first seizure; (3) chronic stage: 30 days after the initial spontaneous seizure (Figure 6.1).

Cortices from epileptic animals were harvested individually according to these three different time points and time matched cortices from control animals were prepared according to this schedule as well.

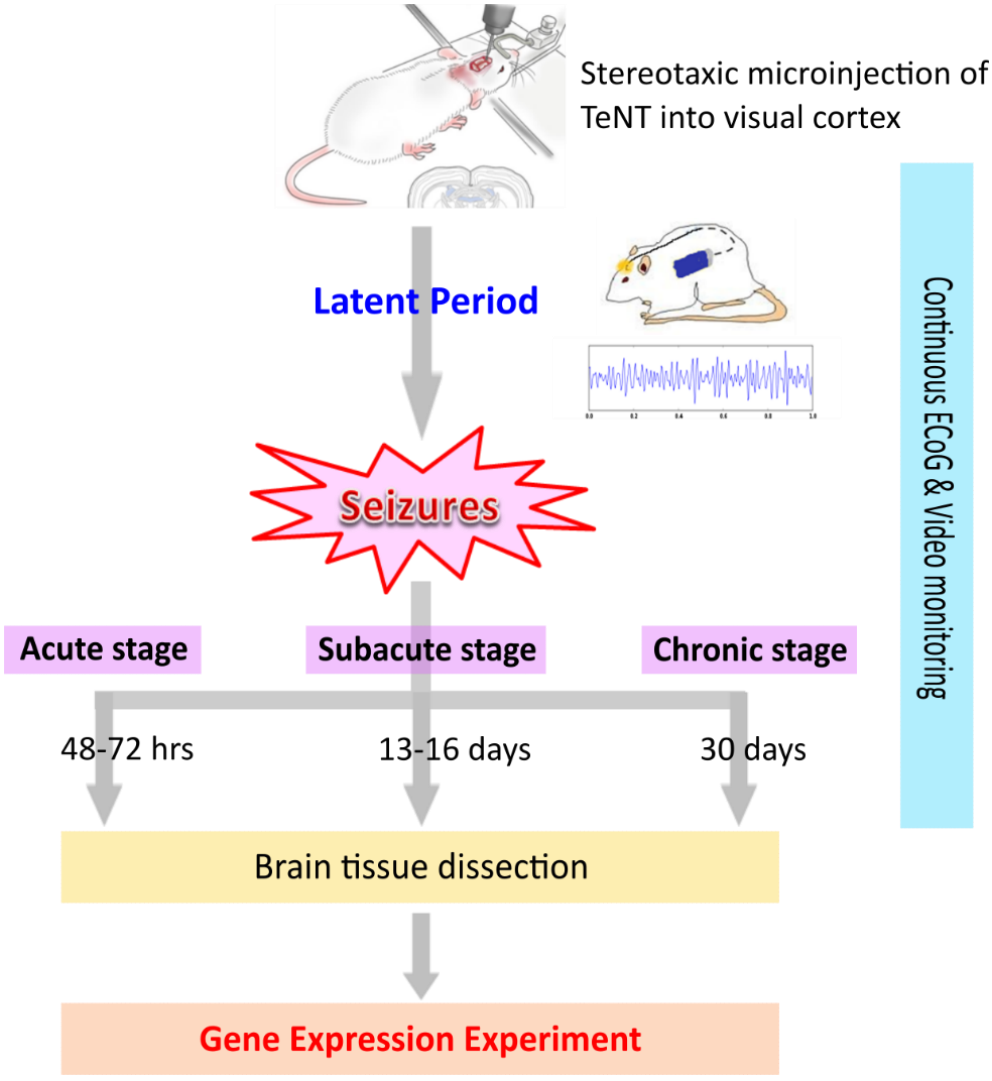

Figure 6.1 The time flow of the *in vivo* experiment.

6.4 Results

6.4.1 A single application of TeNT into the visual cortex produces a focal neocortical epilepsy model

Microinjection of a single dose TeNT into the visual cortex in rats induced chronic visual cortical epilepsy with frequent, discrete spontaneous seizures. From a total of 39 rats that received TeNT microinjection, 33 rats developed chronic spontaneous seizures a few days after TeNT administration (see below and Figure 6.2A for analysis), and thus the overall successful rate of TeNT elicited visual cortical epilepsy is approximately 84.6%. Most of the animals tolerated the application of TeNT and the seizures very well and were in good health, as well as behaved normally apart from seizures. There was no SUDEP (sudden unexpected death in epilepsy) or mortality because of seizures themselves or from the toxic effects of TeNT. Two animals (5%) were sacrificed due to more than 15% of body weight loss, and two animals were culled because of the headset detachment and one due to a defective transmitter. Some epileptiform spikes were seen in the 6 rats receiving the same surgical procedure and TeNT injection into the visual cortex, but these did not develop epileptic seizures. There was no evidence of behavioural changes in these 6 rats and they were all in good health. In addition, no epileptic seizures, epileptiform activity or behavioural abnormalities were found in the vehicle control animals which received the same surgical procedure but with 0.9% normal saline microinjection into the visual cortex.

Seizures emerged beginning approximately 5 days after the injection of TeNT, whilst this latent period could range from 3 to 8 days (Figure 6.2A). The seizure frequency gradually increased over the time course of the epilepsy establishment and reached a peak on the 3rd week following the onset of first spontaneous seizure, and seizure frequency reduced in most of the animals from the 4th to 5th week after seizure onset (Figure 6.2B, left panel). In terms of the cumulative seizure frequency, this reached a plateau around 20 days after seizure onset, and the total seizure

numbers among the individual animals was highly variable, and could range from fewer than a hundred seizures to several hundred of seizures over 5-6 weeks of recordings (Figure 6.2B right panel, C). Moreover, the seizure duration evolved over time with the progress of the epileptogenic process. The average of median seizure duration increased from under 50 seconds in the initial 48-72 hrs to a stable duration of around 90-120 seconds for the following days (Figure 6.2D).

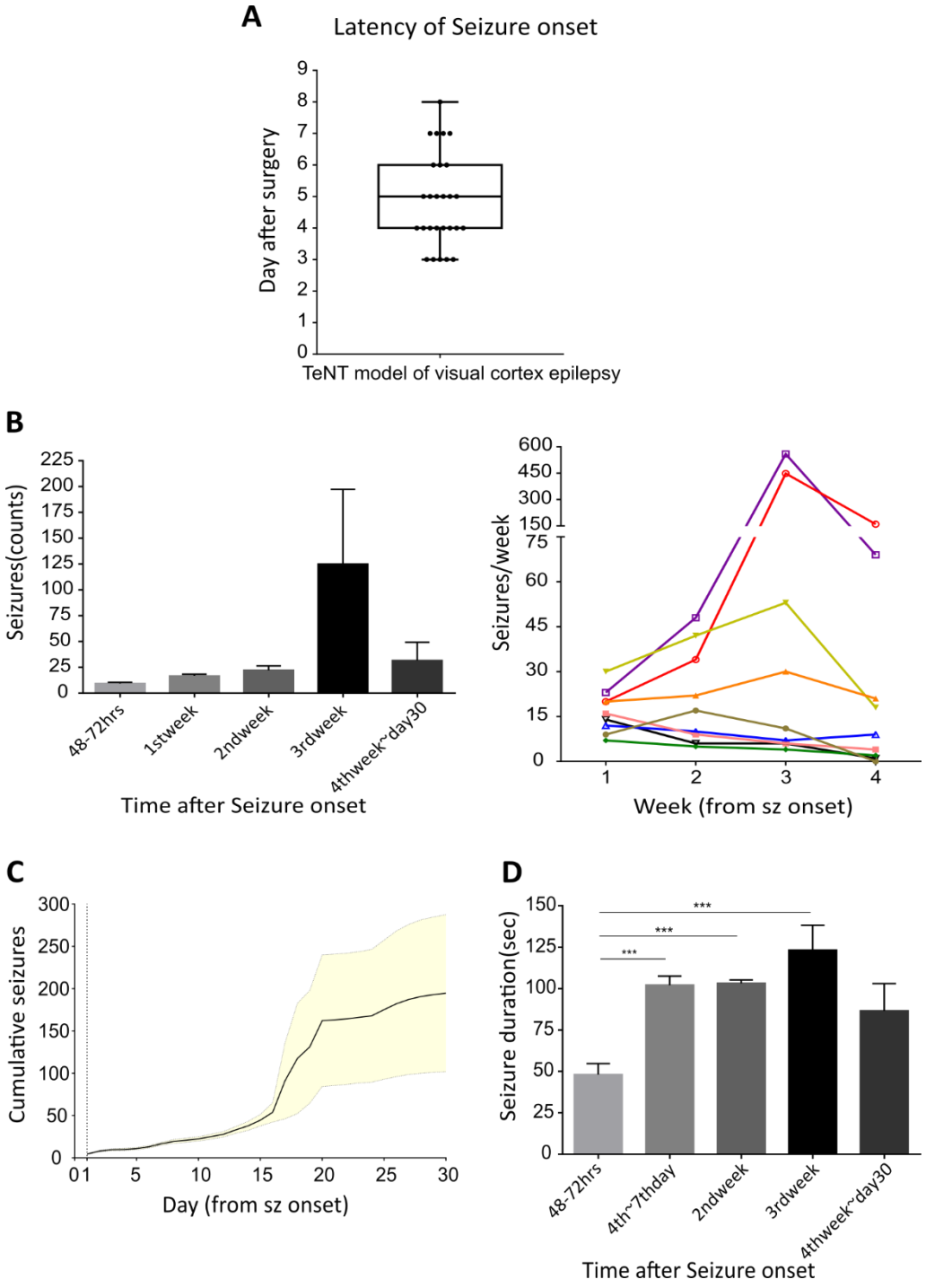

Figure 6.2 Characterization of the TeNT model of visual cortical epilepsy

(A) The median latency of seizure onset is 5 days and the latent period in the majority of animals was between 4 to 6 days (n = 27 animals). (B) left panel: Number of seizures at different time points after the beginning of spontaneous seizures showing an increasing seizure frequency over time to the peak at week 3, followed by a decline from week 4 (48-

72hrs: n = 27 animals; 1st-2nd week: n = 18 animals; 3rd week-30 days: n = 9 animals); right panel: Number of seizures per week for the 9 individual animals recorded for 5 weeks (used for the chronic stage RNA extraction) revealing the variability of seizure frequency in the TeNT model of visual cortical epilepsy. (C) Plot of cumulative seizures per day. (D) Average of median seizure duration at different time points throughout the whole recording period showing brief seizures at the first few days followed by a significant rise in the following days. (Kruskal-Wallis test followed by Dunn's correction, ***$p < 0.001$). Data are presented as mean ± SEM.

6.4.2 The TeNT model of epilepsy presented as Focal seizure with or without Secondary Generalisation

A total of 102 randomly selected seizures from 8 epileptic rats with continuous 24h/7 day video-ECoG recordings for 5 weeks were used to assess the correlated seizure behaviours (Figure 6.3). 45 seizures (44.1%) were non-motor focal seizures presenting as behavioural changes, including repetitive eye blinking, suddenly freezing or jumpy, or agitatedly and aggressively searching behaviour which could be due to visual hallucinations arising from the seizure focus. The 19 seizures (18.6%) that were classified as unilateral motor involvement manifested as contralateral limb twitching. Seizures propagating to bilateral motor symptoms were observed in a further 6 (5.9%) animals. Another 21 seizures (20.6%) evolved to generalised tonic-clonic seizures. Apart from these observable seizures, the associated behaviours of 11 seizures (10.8%) were uncertain or unobservable due to the animals staying out of sight within the environmental enrichment material or due to the transient interruption of video recordings.

Intermittent photic stimulation was employed in three Lister Hooded rats with robust seizures arising from TeNT visual cortical epilepsy to examine whether seizures or photoconvulsive (photoepileptiform) response can be provoked in this animal model of epilepsy. However, this manipulation was unable to trigger seizures or apparent corresponding epileptiform activity in TeNT model of visual cortical epilepsy.

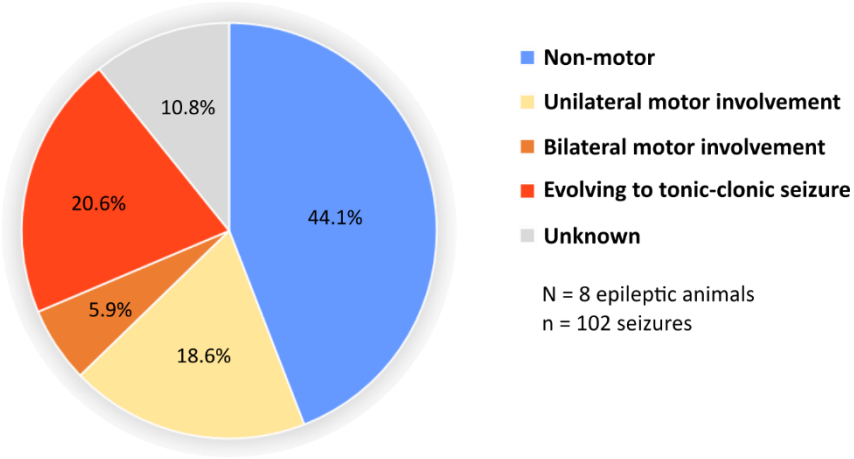

Figure 6.3 Semiology classification of seizures in TeNT model of visual cortical epilepsy in rats

The seizure manifestations of a randomly selected subset of electrographic seizures (n = 102 seizures) from 8 male Sprague Dawley rats. The majority of seizures are presented as focal seizure without secondary generalisation. The “unknown” means the behaviours were not visible because the animals were beneath the environmental material or interrupted video signals.

6.4.3 Electrographic features in the TeNT model of visual cortical epilepsy in rats

TeNT injection into rat visual cortex produced not only clear interictal epileptiform discharges but also typical discrete spontaneous ictal activity with behavioural correlates. The electrographic features of ictal epileptic discharges are depicted in Figure 6.4. The ictal epileptic activity usually started with low-amplitude fast activity for few seconds followed by the evolution of frequency and amplitude over time, containing spikes, sharp waves, polyspikes or polyspikes-and-wave. Most of the seizures lasted for around 1-2 mins. And the ECoG often displayed transient decrement of electrographic activity following the end of seizure.

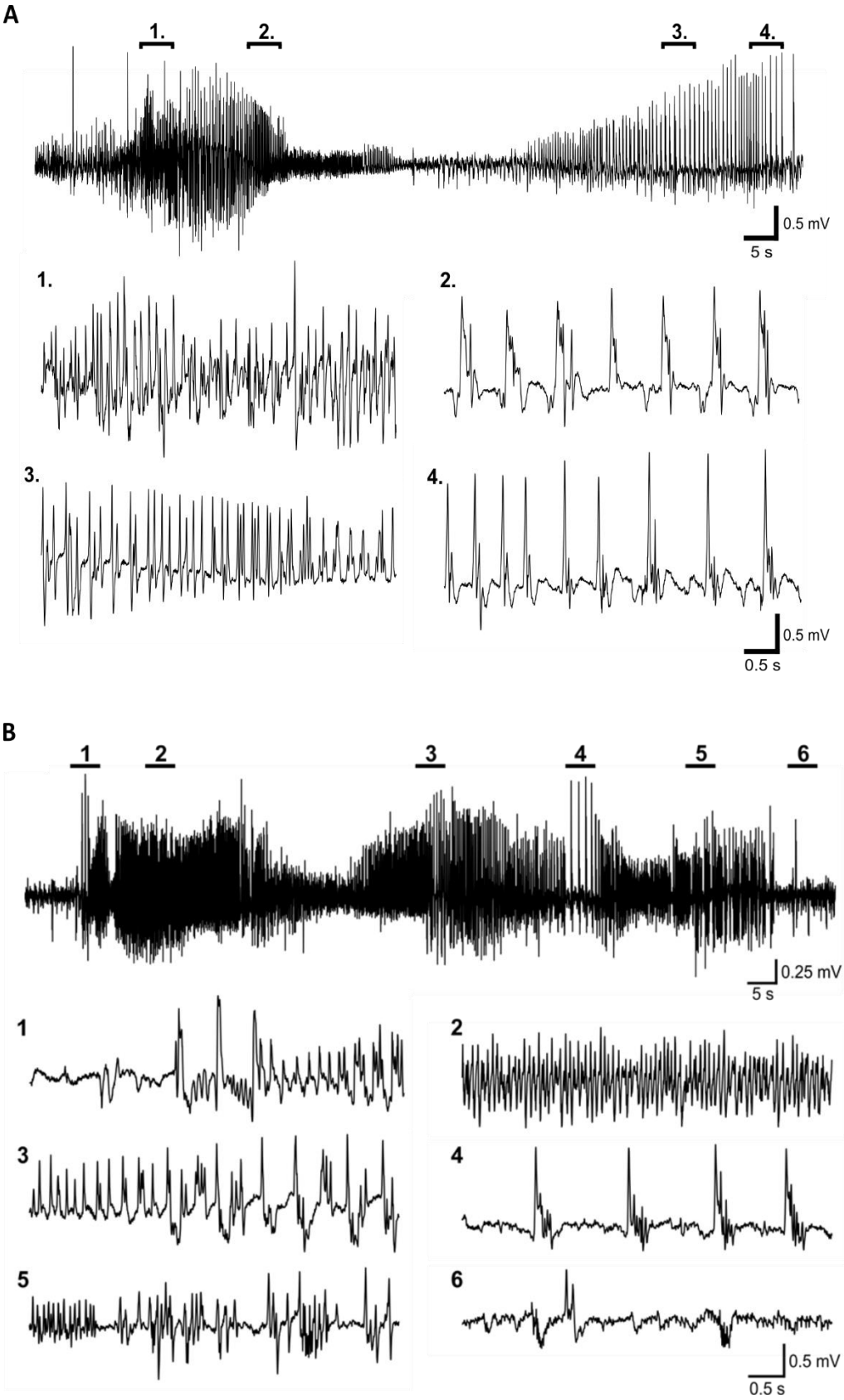

Figure 6.4 Representative ECoG features of ictal discharges in the epilepsy model of TeNT injection in rat visual cortex

(A, B) Two discrete seizures showing the ictal events typically last for around 100 seconds and start with fast activity evolving into high-amplitude and high-frequency waves with propagation then (A) the epileptic activity may end by a train of rhythmic high-amplitude sharp waves or polyspikes-and-wave, or (B) the electrographic activity gradually subsides at end of the seizure.

6.4.4 Seizures are prone to occur during sleep

To understand whether the physiologic circadian rhythm of day/night cycles would influence the occurrence of seizures, we analysed the distribution of seizure occurrence in light-on/light-off (7 a.m./7 p.m.) period from 9 rats with continuous ECoG recordings for 5 weeks. As there is considerable variability of seizure frequency between individual animals, this comparison was done by estimating the proportion of seizure occurrence between light and dark for each animal (Figure 6.5A). Throughout the long-term recordings, the occurrence of spontaneous seizures is significantly higher in light-on (sleeping state) than in light-off (activity/awake state) for the overall recording period (unpaired Student's t test, $p = 0.003$).

We further asked whether the difference in seizure occurrence between the sleeping state and activity/awake state are correlated to the epileptogenesis and the development of epilepsy. More detailed analysis was carried out (Figure 6.5B). No difference was found in the early phase of epilepsy development (paired Student's t test, $p = 0.639$), but the apparent difference of seizure occurrence in light/dark cycles emerged during the subacute phase and was sustained to the chronic period (paired Student's t test, $p = 0.035$).

Next, the seizure duration in light/dark cycles was examined to assess whether the sleeping/awake states would have an impact on seizure architecture (Figure 6.5C). However, no obvious difference was seen in these animals (Wilcoxon matched-pairs signed rank test, $p = 0.359$).

Consequently, the above phenomena indicate that day/night circadian cycles affect seizure activity by changing the seizure frequency, but not on the seizure duration. This influence is correlated to the epileptogenic process and becomes prominent only from the subacute phase of epilepsy establishment.

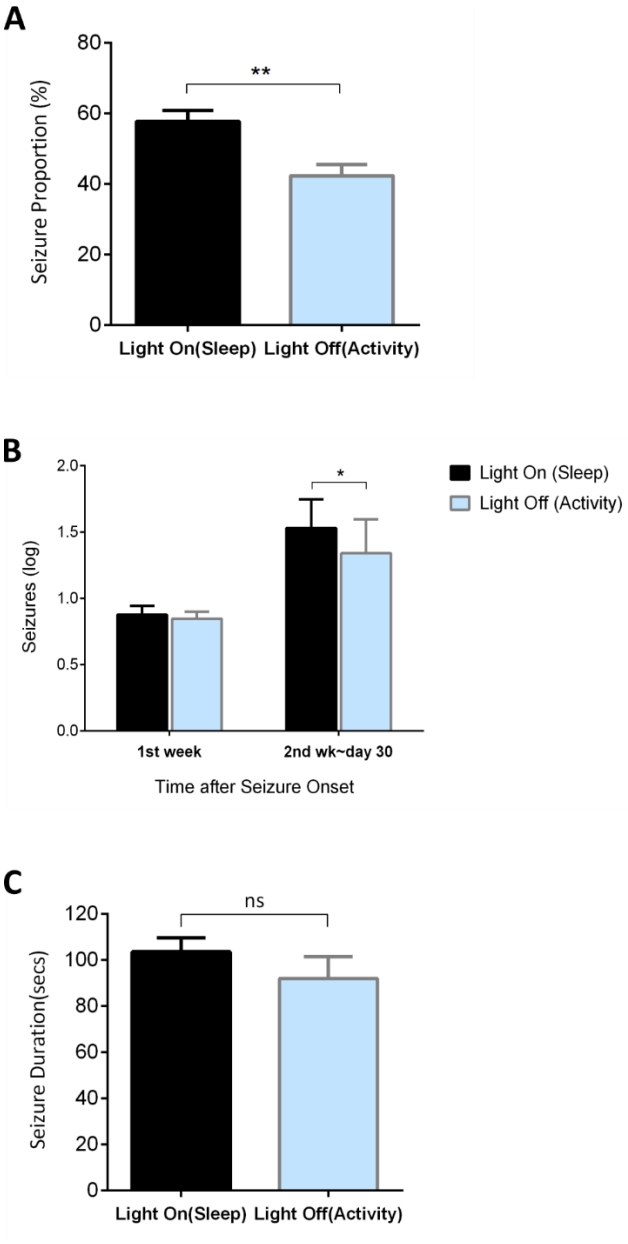

Figure 6.5 Seizure activity in light/dark cycles

Seizure activity in 12/12 hour light/dark cycle (light cycle 7 a.m. ~ 7 p.m.) in the TeNT model of visual cortical epilepsy in rats. (A) The proportion of seizure occurrence in individual animals during light-on and light-off over the whole recording time (5 weeks) showing around 60% of seizures occurred in light-on period (sleeping state), and about 40% of seizures in light-off (activity state) (n = 9 animals, unpaired t-test, **p < 0.01). (B) The occurrence of seizures during light/dark cycles revealed no difference in the 1st week after seizure onset, but displayed higher seizures in sleeping state from 2nd week and thereafter (n=9, paired t-test, *p < 0.05). (C) Average of median seizure duration (n = 9, Wilcoxon signed rank test, p > 0.05, ns = no significance). Data are presented as mean ± SEM.

6.4.5 The TeNT model of focal epilepsy does not rely on neuronal death

To evaluate whether the TeNT epilepsy model was triggered by toxin induced neuronal death, and to ensure the molecular changes we observed were not caused by cell death or glial proliferation due to the injection of TeNT, immunohistochemistry staining was performed in animals one week after microinjection of either TeNT or 0.9% normal saline (Figure 6.6). NeuN stained cell counting surrounding the site of injection was carried out as described in Section 3.2.9 and the neuron density was calculated. Figure 6.7 shows that there was no significant difference in the quantification of neurons between control and TeNT-treated epileptic animals (unpaired Student's t test, $p = 0.586$). This result demonstrates that TeNT does not lead to significant neuronal loss and the TeNT model of focal epilepsy does not rely on toxin induced cell death. As a result, the following study of molecular changes during epileptogenesis mainly results from the epileptogenic process itself instead of toxin related neurodegeneration.

Furthermore, the GFAP staining revealed that compared to the vehicle control group, no obvious increase in astrocyte proliferation was found in TeNT injected animals (Figure 6.6B). This indicates that there was no TeNT induced astrocytosis. Minor mechanical tissue damage due to local microinjection is inevitable, however, the injection related mechanical injury in both groups was identical. Hence, local damage would not interfere with assessing the consequences of comparative gene expression during epileptogenesis.

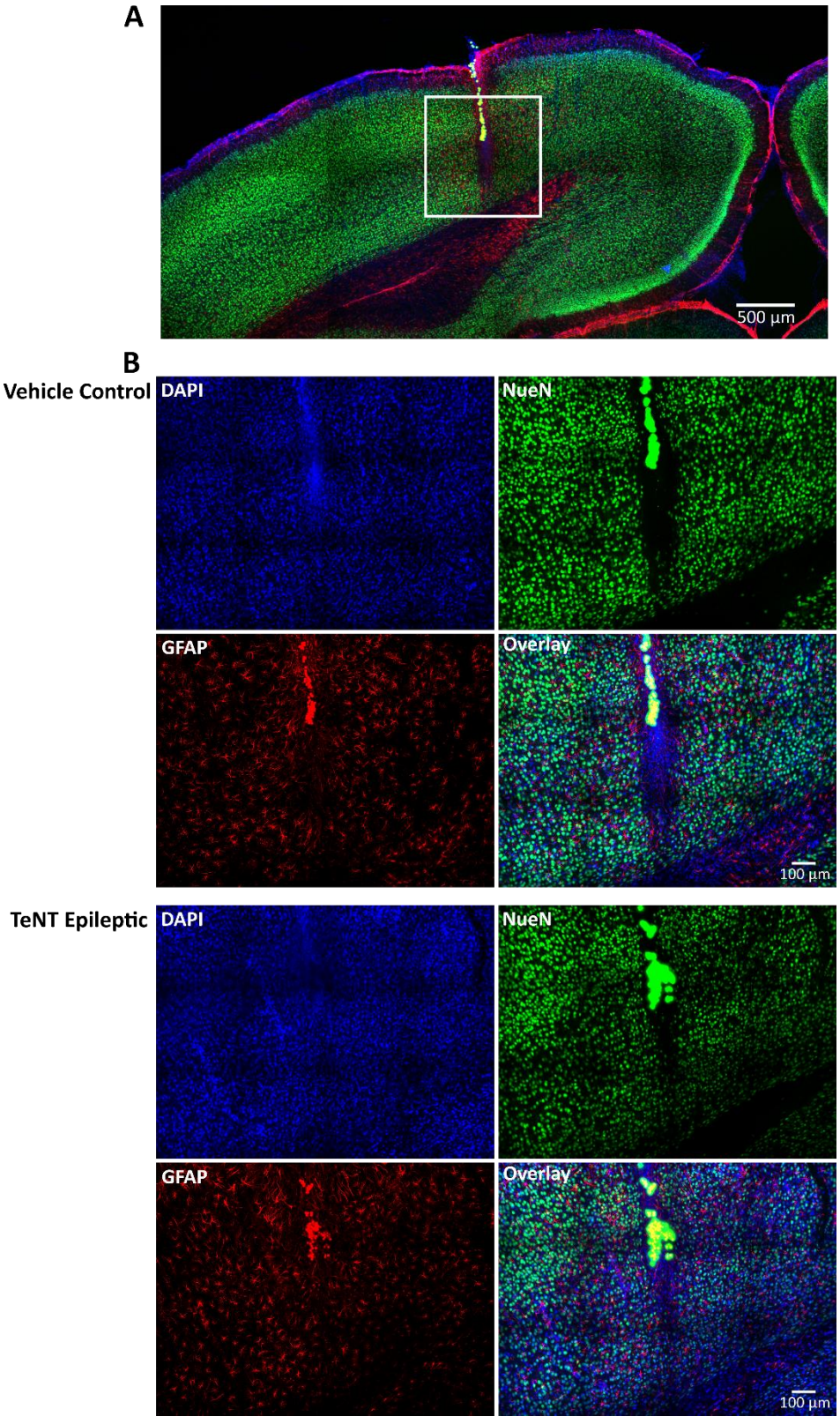

Figure 6.6 Representative immunohistochemistry of visual cortex injection

(A) A representative immunofluorescence image of a brain slice shows the injection targeting to layer V of primary visual cortex and the area (white square) selected for neuron counting.

(B) NeuN, a neuronal marker (green), neuronal cell counting around the site of injection with normal saline in vehicle control rats and the epileptogenic zone in TeNT epileptic rats. GFAP, an astrocyte marker (red), all displaying no apparent difference between control and TeNT epileptic animals. (Scale bar: 100 µm).

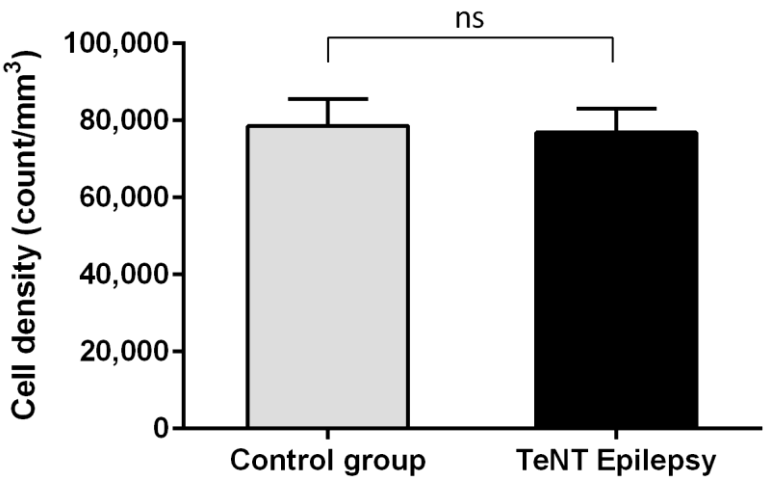

Figure 6.7 Volumetric cell count around the region of injection

Neurons surrounding the epileptogenic zone and the zone of normal saline injection were quantified. The neuron counting was carried while blinded to treatment. (n = 9 from 3 animals in each group; unpaired t-test, ns = not significant). Data presented as mean ± SEM.

6.4.6 Candidate Genes are differentially regulated during Epileptogenesis

To investigate the dynamically temporal regulation of gene expression during epileptogenesis for the TeNT model of visual cortical epilepsy in rats, mRNA expression in three different stages during the establishment of epilepsy was conducted. In the acute stage, the mRNA expression of GFAP, an astrocyte associated protein, showed significant up-regulation ($p = 0.046$, two-way ANOVA) (Figure 6.8A). Similarly, the mRNA levels of REST/NRSF, mTOR, CCL2, KCNA1, and NRGN were also increased in the acute phase but did not reach statistical significance (REST: $p = 0.187$; mTOR: $p = 0.628$; CCL2: $p = 0.949$; KCNA1: $p = 0.464$; NRGN: $p = 0.991$; two-way ANOVA) (Figure 6.8B-E). In contrast, there was apparent down-regulation of BDNF mRNA in the early period of epileptogenic process ($p = 0.035$, two-way ANOVA) (Figure 6.8B), whilst there were only subtle decreases of mRNA expression in ADK, SNAP-25, CREM/ICERII, GABRA5, HCN1 and HCN2 during the acute stage (ADK: $p = 0.240$; SNAP-25: $p = 0.562$; CREM/ICERII: $p = 0.050$; GABRA5: $p = 0.121$; HCN1: $p = 0.114$; HCN2: $p = 0.969$; two-way ANOVA) (Figure 6.8A-E).

During the subacute stage, significant overexpression of GFAP, SNAP-25, REST/NRSF, and mTOR were seen (GFAP: $p = 0.005$; SNAP-25: $p = 0.037$; REST: $p = 0.001$; mTOR: $p = 0.0003$; two-way ANOVA) (Figure 6.8A-C). There was a non-significant trend for a rise in mRNA expression in most of the remaining genes, aside from NRGN and CREM/ICERII mRNA, which show mild decreases (ADK: $p = 0.769$; BDNF: $p = 0.974$; GABRA5: $p = 0.658$; CCL2: $p = 0.825$; KCNA1: $p = 0.094$; HCN1: $p = 0.138$; HCN2: $p = 0.192$; NRGN: $p = 0.819$; CREM/ICERII: $p = 0.092$; two-way ANOVA) (Figure 6.8A-E).

By the chronic state, mRNA expression of CCL2 was strongly up-regulated ($p = 0.035$, two-way ANOVA), whereas the GABRA5 was significantly down-regulated ($p = 0.024$, two-way ANOVA) (Figure 6.8D). There was only a subtly increased tendency of GFAP, ADK, BDNF, REST/NRSF, and KCNA1 mRNA (GFAP: $p = 0.934$; ADK: $p = 0.99$; BDNF: $p = 0.780$; REST/NRSF: $p = 0.99$; KCNA1: $p = 0.959$; two-way ANOVA). However,

a small decline of mRNA level was shown in SNAP-25, NRGN, CREM/ICERII, mTOR, HCN1 and HCN2 (SNAP-25: $p = 0.130$; NRGN: $p = 0.420$; ICERII: $p = 0.310$; mTOR: $p = 0.279$; HCN1: $p = 0.085$; HCN2: $p = 0.055$; two-way ANOVA).

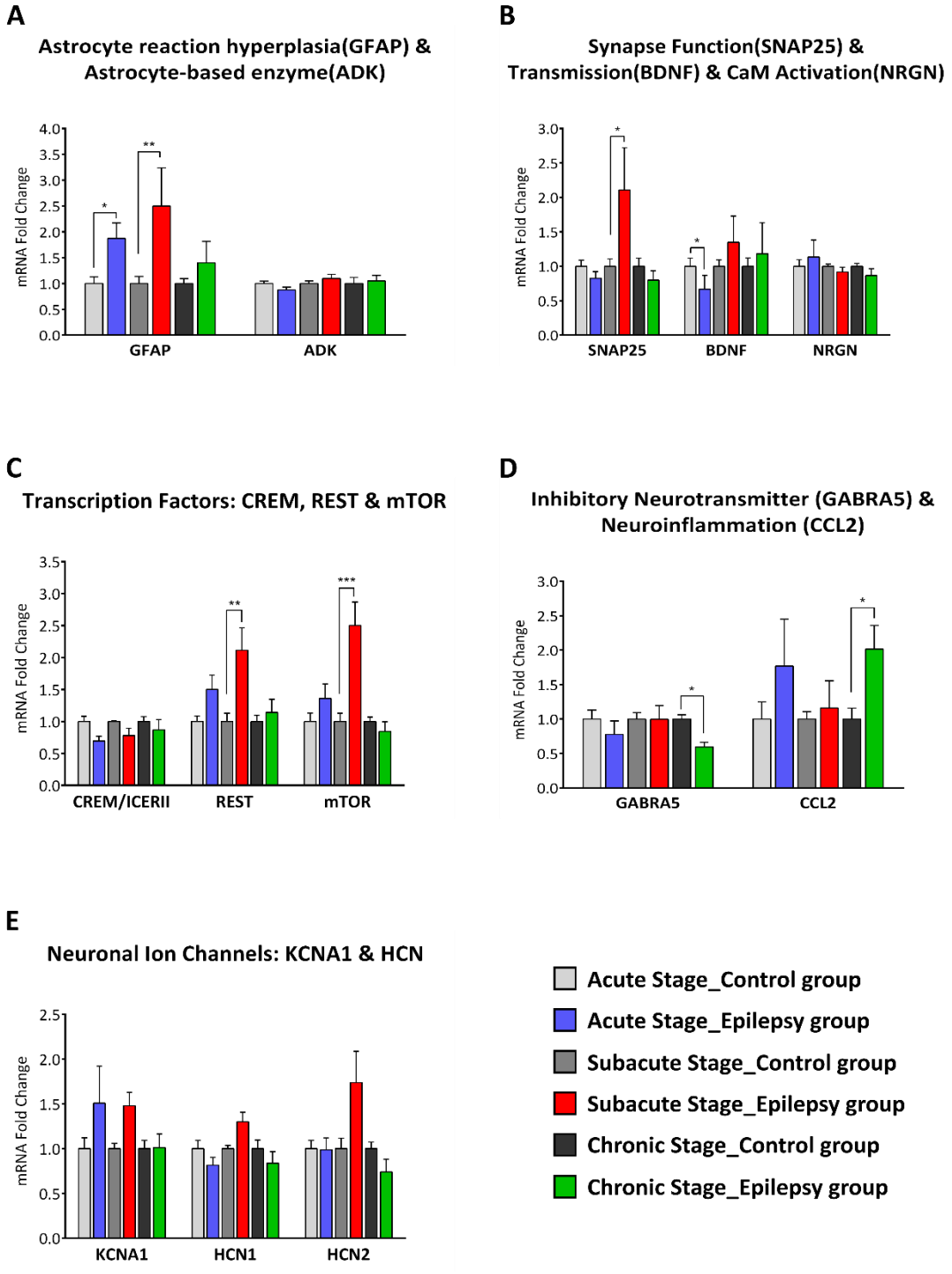

Figure 6.8 Relative mRNA expression in different stages of epileptogenesis

(A)-(E) These selected candidate genes have been linked to epileptogenesis in different crucial functional pathways or have been repeatedly shown to change in epilepsy. (A) GFAP is significantly up-regulated during both acute and subacute periods, whereas there is no clear mRNA fold difference compared with control in ADK, an astrocyte-specific enzyme, across the whole period of epilepsy. (B) BDNF is a neurotrophin gene showing significant

down-regulation in acute phase followed by a tendency of up-regulation. The SNARE gene, SNAP-25 has strong overexpression in subacute stage only. (C) CREM/ICERII and REST/NRSF are important transcriptional factors involved in neuronal gene regulation. The mRNA level of CREM/ICERII is mildly down-regulated, whilst REST/NRSF is up-regulated over the entire period of epileptogenic process and revealing a significant increase of REST/NRSF in subacute period. mTOR which not only contributes to gene transcription but also protein translation, displays remarkable overexpression in subacute stage. (D) CCL2, a chemokine gene, exhibits a rise over all stages and is significantly up-regulated in chronic stage only. In contrast, GABRA5 has obvious hypo-expression in chronic phase. (E) The neuronal ion channel genes, KCNA1 and HCN, all have a tendency of increased expression in subacute stage, but the changes are mild and variable during the development of epilepsy. (n = 9 in each group; matched measures two-way ANOVA followed by Sidak correction for multiple comparisons, *$p < 0.05$, **$p < 0.01$, ***$p < 0.001$). Data are shown as mean ± SEM.

Respecting to the patterns of change in mRNA expression across different time points of epileptogenesis, REST, mTOR, GFAP, SNAP-25, HCN1 and HCN2 have a similar trend of dynamic gene regulation during the epileptogenic process and the establishment of epilepsy (Figure 6.9A, B). Furthermore, mRNA expression of mTOR, SNAP-25 and HCN1 along the time progress of epilepsy development have significant difference (Acute vs. Subacute: mTOR, $p = 0.0023$; SNAP-25, $p = 0.0008$; HCN1, $p = 0.0003$; Subacute vs. Chronic: mTOR, $p < 0.0001$; SNAP-25, $p < 0.0001$; HCN1, $p = 0.0002$; two-way ANOVA). Also, REST, GFAP and HCN2 mRNA were differentially regulated between subacute and chronic periods (REST, $p = 0.0006$; GFAP, $p = 0.0103$; HCN2, $p = 0.0002$; two-way ANOVA). Figure 6.9C shows there was a rising tendency over time of mRNA regulation in ADK, BDNF, and CREM (Acute vs. Subacute: ADK, $p = 0.0277$; BDNF, $p = 0.0087$). However, KCNA1 and NRGN mRNA levels were going down over the whole period of epilepsy (Subacute vs. Chronic: KCNA1, $p = 0.0238$; two-way ANOVA) (Figure 6.9D). Interestingly, GABRA5 and CCL2 revealed opposite regulatory directions during epileptogenesis (Subacute vs. Chronic: CCL2, $p = 0.0028$; two-way ANOVA) (Figure 6.9E).

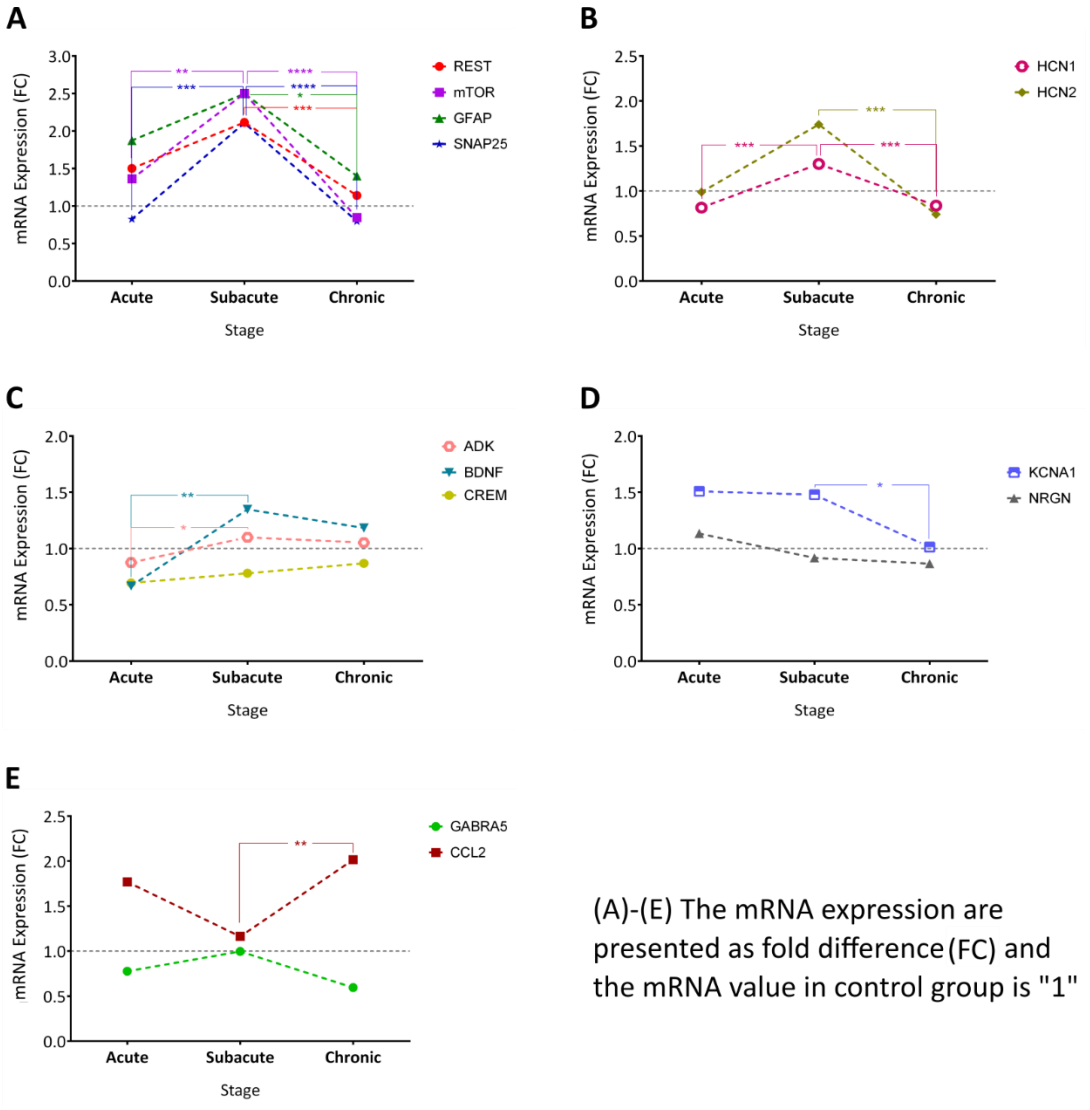

Figure 6.9 Trends of Dynamic gene regulation during epileptogenesis in the TeNT model of visual cortical epilepsy

(A)-(E) Trends comparing the patterns of gene regulation over time in different stages of the epileptogenic process. (n= 9 in each stages; matched measures two-way ANOVA, *post hoc* Tukey's test, *p < 0.05, **p < 0.01, ***p < 0.001, ****p < 0.0001). Data are shown as mean of mRNA fold change (FC).

6.4.7 No apparent correlation between Seizure activity and Gene expression levels

To explore whether the gene expression levels were correlated to seizure activity, correlation coefficient analysis was performed. In the acute stage, there were no significant correlations between mRNA expression levels and number of seizures in all of the candidate genes (Figure 6.10A). Likewise, neither positive nor negative correlations were found between mRNA fold change and seizure frequency (per week) in the last week of the subacute phase (Figure 6.10B). Apart from the REST/NRSF showing little significant positive correlation between the expression of mRNA and seizure activity (seizures/ last week) after the establishment of epilepsy ($r = 0.6891$, $p = 0.0469$, nonparametric Spearman correlation coefficient), no relationships between these two factors were shown in the remaining genes (Figure 6.10C). Moreover, no association was observed between seizure duration and mRNA levels of the genes in all stages. These overall data reflect that the molecular changes do not correlate to the seizure frequency and severity.

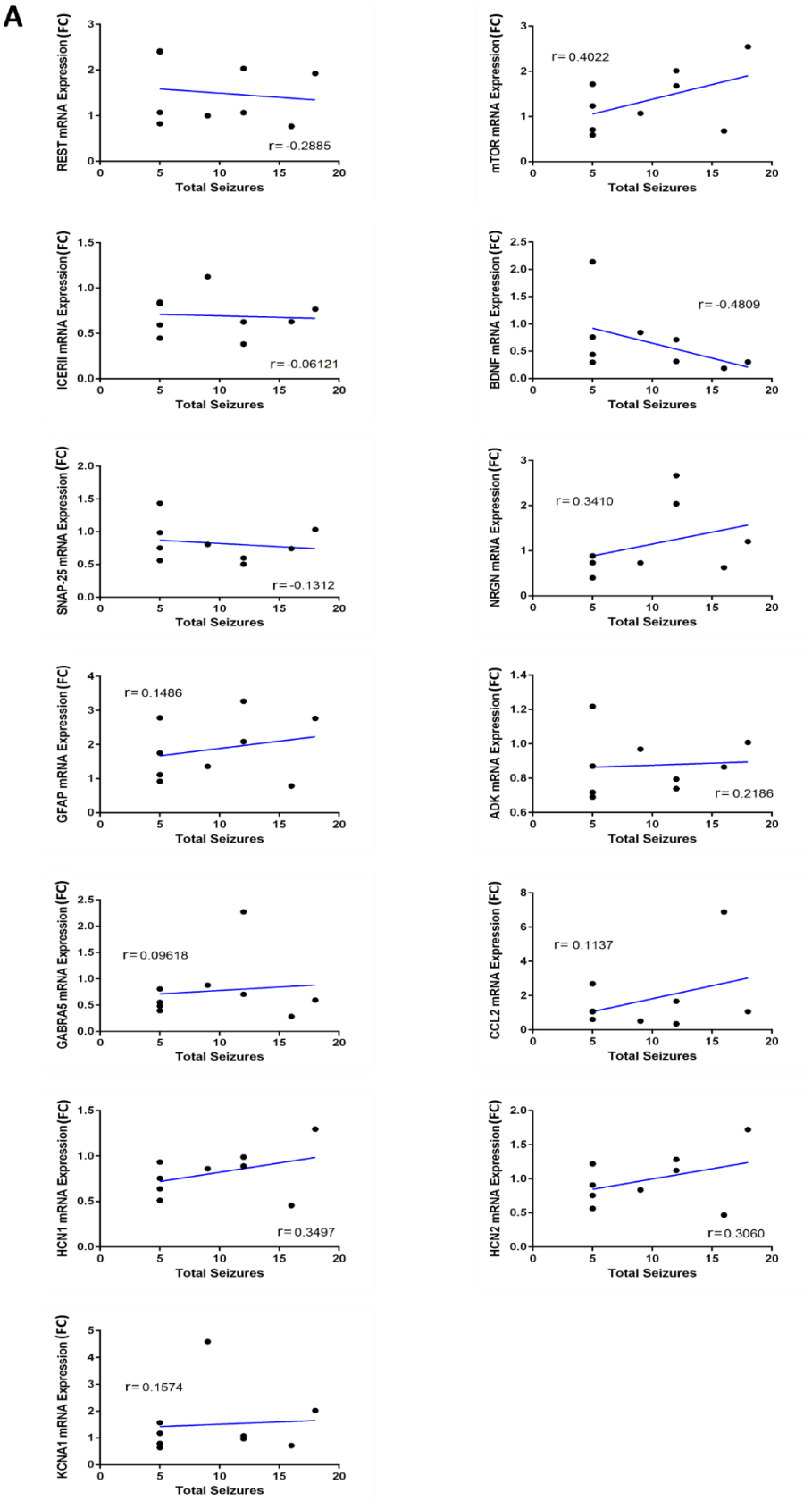

Figure 6.10 (A) Correlation between average of mRNA fold changes and total seizures during the acute stage. (n = 9; nonparametric Spearman correlation coefficient).

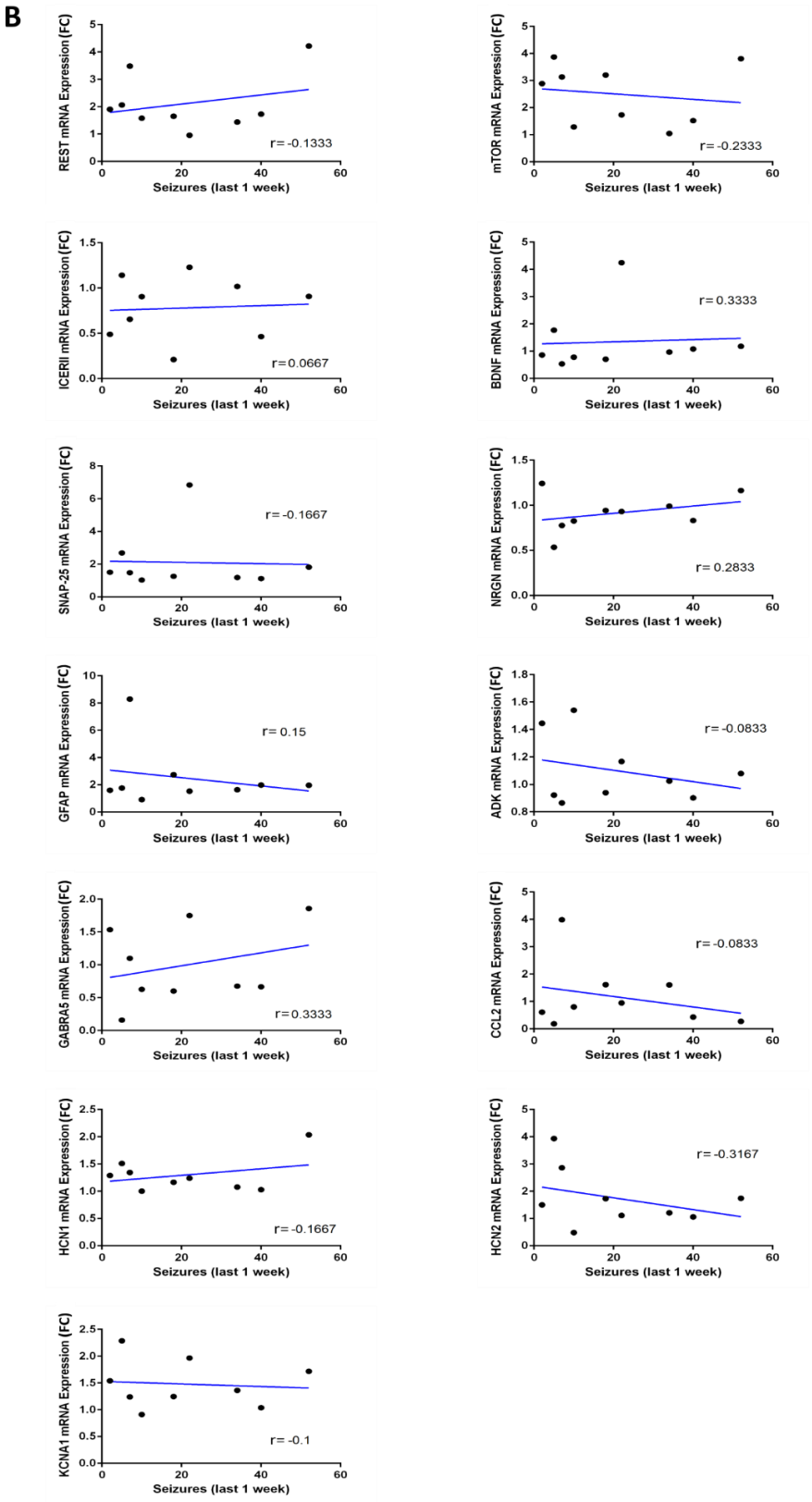

Figure 6.10 (B) Plot of mRNA expression levels versus the last week of seizure frequency in the subacute stage. (n = 9; nonparametric Spearman correlation coefficient).

C

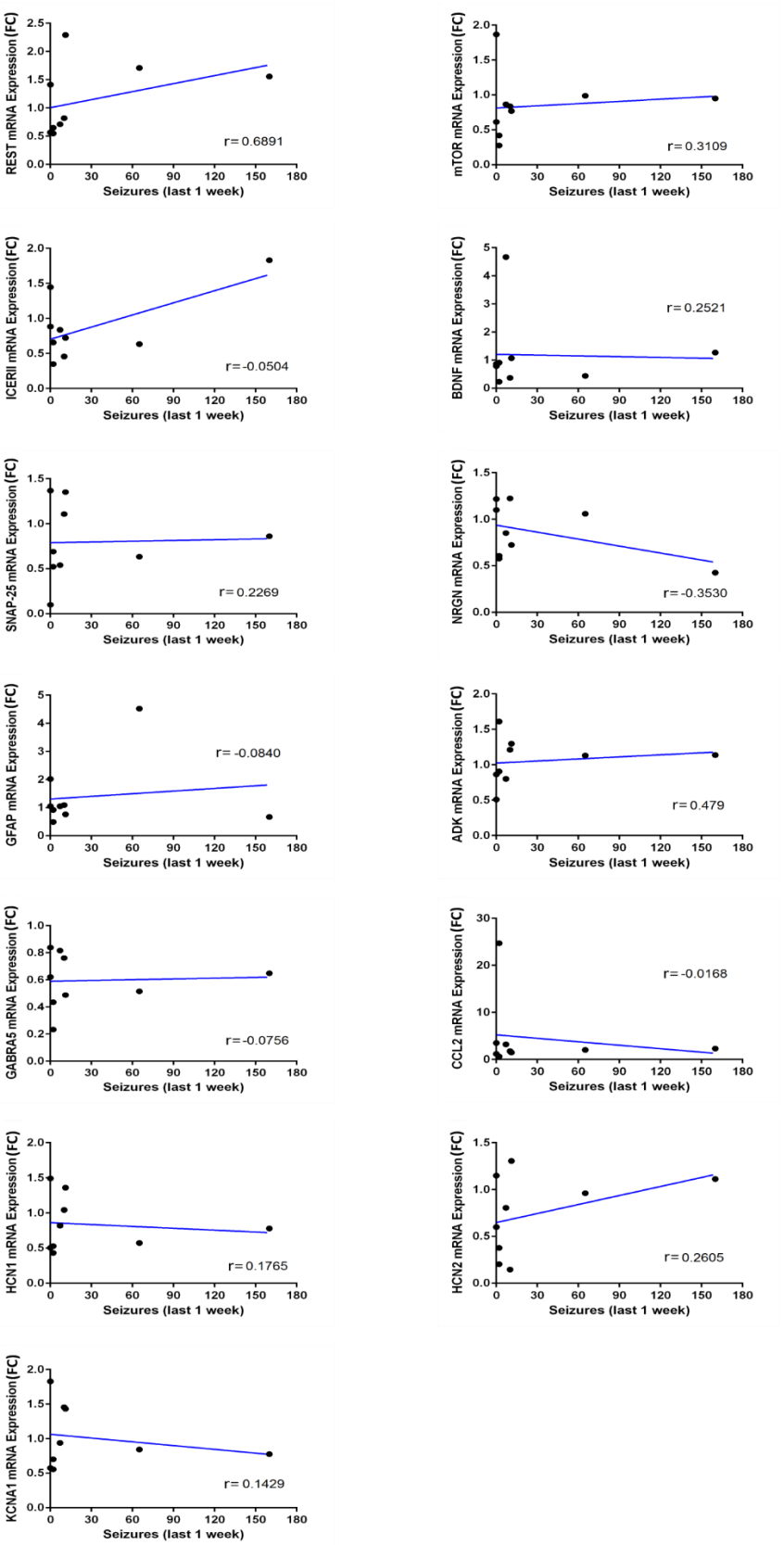

Figure 6.10 (C) The relationship of mRNA fold changes and seizure number in the last week of chronic period. (n = 9; nonparametric Spearman correlation coefficient).

6.5 Discussion

Mesial temporal lobe epilepsy following focal injection of TeNT into rat hippocampus has been well documented (Jefferys et al., 1995; Jiruska et al., 2010). In addition, focal motor cortical epilepsy induced by TeNT has been shown in rats with the major characterization of frequent brief bursts of high-frequency EEG activity, and rare longer events which may associate with behavioural seizures, but this model is relatively poorly tolerated, with a proportion of animals experiencing >15% weight loss or death following a severe seizure (Wykes et al., 2012). Mainardi et al. reported a mouse model using TeNT in the visual cortex, however, this produced electrographic epileptiform discharges, and no behavioural correlates were found in mice (Mainardi et al., 2012).

In our study, we have optimized the model in rats and demonstrated that a single dose application of TeNT into rat visual cortex produces a reliable model of focal neocortical epilepsy exhibiting both clear ictal electrographic epileptic discharges and associated behavioural seizures. There is a high induction rate of long-term recurrent spontaneous seizures with very low risk of morbidity/mortality and no SUDEP which indicates this is a well-tolerated and reproducible rat model of epilepsy. Previous studies have revealed that TeNT is cleared from the brain a few days after local administration (Mellanby, 1989), but the effect on disruption of Vesicle Associated Membrane Protein (VAMP) persists much longer, resulting in recurring spontaneous seizures over a long period (Ferecsko et al., 2015; Mainardi et al., 2012).

Unlike other commonly used animal models of epilepsy, e.g. K.A. or pilocarpine models, in which epilepsy is induced by initial SE accompanied extensive neuronal death (Reddy and Kuruba, 2013), the major advantages of TeNT model of focal epilepsy are the epileptogenesis is not triggered by SE and does not rely upon neuronal loss or major disruption of the tissue. As demonstrated in our animals, TeNT appears to be consistent with a non-lesional epilepsy model which indeed is supported by another detailed study of the TeNT model (Jiruska et al., 2010).

Moreover, the TeNT model has a consistent latent period prior to when the spontaneous seizures start to occur which is followed by progressively increasing seizure frequency and duration during the establishment of epilepsy, and finally reaches a plateau. This time course reflects that the epileptic activity and severity evolve during the epileptogenic process and suggests this animal model may reproduce the natural course of epileptogenesis in human conditions. Despite the limitation that the electrographic activity was only recorded from a recording electrode at the epileptogenic zone, seizures propagated and spread to other ipsilateral and/or contralateral brain regions could be observed from the seizure behaviours. All of above characteristics resemble the majority of human focal epilepsies and provide a model for studying human epileptogenesis and epilepsy disorders.

The seizures induced by TeNT injection into visual cortex exhibit markedly longer duration (usually 50-180 secs) than those induced in motor cortex (mostly lasting only a few seconds) (Wykes et al., 2012). The underlying mechanisms that resulted in the different consequences of TeNT application in motor and visual cortices are still not known, but perhaps may be due to different connectivity in the frontal and occipital cortices. A limitation of this model is that although robust seizures were observed in the TeNT model of visual cortical epilepsy, the seizure frequency could be highly variable among individual animals and gradually declined from week 4-5 of initial seizure onset, leaving it unclear whether chronic was fully established.

Some specific human epilepsy syndromes, encompassing generalized and focal epilepsy, have been recognized to have potential links with epileptic photosensitivity (the propensity to seizures induced by photic stimulation), including Jeavons syndrome (Eyelid Myoclonia with Absences), JME (juvenile myoclonic epilepsy), and idiopathic photosensitivity occipital lobe epilepsy etc. (Fisher et al., 2005a; Kasteleijn-Nolst Trenite et al., 2012). A strong genetically prone or genetically determined trait has been suggested in the “photosensitive epilepsy” (Stephani et al., 2004; Verrotti et al., 2004). Considering the poor vision of Sprague Dawley rats

(Prusky et al., 2002) which may influence detection and provocation of seizures by visual stimulation, we performed intermittent flickering light stimulation in Lister Hooded epileptic rats with the TeNT model of visual cortical epilepsy. However, none of these animals (total of 3 animals) manifested photic-induced seizures or displayed prominent ECoG changes in our pilot study. A possible explanation is the wide variability of prevalence and incidence of photosensitivity in "photosensitivity epilepsy", and with the comparison to generalized seizures, occipital focal seizures induced by photic stimulation are far less common (Panayiotopoulos, 2005). Another possibility is that the visually induced seizures may only present in certain genetic models rather than the acquired/symptomatic models of epilepsy used here.

Some evidence has suggested that seizures are susceptible to circadian variations and sleep, and vice versa, epilepsy influences sleep-wake pattern and circadian rhythms as well (Quigg, 2000). Here, a significantly higher seizure occurrence during light time (sleep period) was observed in our TeNT model of visual cortical epilepsy. This pattern was not distinct at the very beginning of seizure onset, but clearly appeared after the acute stage of epilepsy. This may indicate that there was lower seizure threshold in the sleep states and the epileptogenic process perhaps had an impact on the reciprocal influences between sleep-wake cycles and epilepsy. Higher activity of seizures and interictal epileptiform discharges during non-rapid eye movement (NREM) sleep has been shown in human epilepsies and some experimental animal models (Badawy et al., 2009b; Hofstra and de Weerd, 2009). Thalamocortical synchronization has been frequently invoked to account for this association (Badawy et al., 2009b; Timofeev et al., 2012). Circadian regulation at many different levels including CLOCK genes, molecular pathways, chemical and cellular alterations, as well as network oscillations etc. have been proposed to explain the relationships between epilepsy and circadian rhythm (Cho, 2012; Quigg, 2000). Further studies will be needed to explore the interactions between epilepsy and circadian variations, as well as their underlying mechanisms.

So far, the chronological changes of gene expression during the epileptogenic process have not been well-characterized. Yet, investigating the dynamic gene

regulation during the development of epilepsy could not only help us to understand the mechanisms of epileptogenesis, but also could provide us with a hypothesis of when may be the appropriate timing to modify potential master regulator molecules for the purpose of disease modification in the future. Herein, we focus on disclosing the molecular regulation in the temporal course of epilepsy. Indeed, our study revealed that these candidate genes are differentially regulated during the epileptogenesis and over the course of epilepsy. BDNF, a member of neurotrophic factors, is ubiquitous in central nervous system and acts diverse roles in development, synaptic plasticity, neurotransmission etc., and much literature has shown that various neurological diseases involving perturbed BNDF signalling (Binder, 2004; Scharfman, 2013). Increased BDNF mRNA has been discovered in many *in vitro* experiments and animal models of epilepsy, e.g. K.A., pilocarpine, PTZ, kindling, and electroconvulsive shock (Binder, 2009; Binder et al., 2001; Liang et al., 1998). The upregulation of BDNF is temporary after seizure onset and returns to control levels in some published reports (Chavko et al., 2002; Gall, 1993; Nawa et al., 1995). Whereas, Prince et al. reported the decreased expression of BDNF in the "undercut" cortical injury model of epilepsy (Li et al., 2011; Prince et al., 2009). Our data show BDNF mRNA was temporarily down-regulated in the acute phase (48-72 hrs after seizure onset) then returned to the control levels with a subtle tendency towards up-regulation, which is contrary to some studies. A possible explanation for this is that down-regulation of BDNF mRNA is very transient and may exist in region-specific changes, which may differ in epilepsy in focal neocortex and hippocampus. Moreover, many animal models induce epilepsy via triggering substantial structural destruction which may lead to different pathogenesis and expression of relevant genes for cell death and recovery. The role of BDNF in epilepsy regarding providing neuroprotection and restoring the connectivity in the disrupted area or contributing to an increase in neuronal excitability in turn facilitating epileptogenesis is possibly model dependent.

GFAP is a marker used for assessing the development of reactive astrocytosis/ astrogliosis (Clasadonte and Haydon, 2012). Astrocytes govern many key functions in the CNS including cell-cell communication, integrating excitatory and inhibitory

synaptic transmission, modulating neuronal and synaptic functions, glutamate regulation, BBB (such as vasculature tone), ion and water homeostasis, neuroinflammatory response, and so on (Binder and Steinhauser, 2006; Devinsky et al., 2013; Haydon, 2001; Seifert et al., 2006). Reactive astrocytosis in the hippocampus has been described in human epilepsy with hippocampal sclerosis and some animal models of mTLE (Cohen-Gadol et al., 2004; Shapiro et al., 2008). Transient increases of GFAP mRNA and protein in the early phase of electrically-induced and PTZ-induced seizures have been reported in literature (Torre et al., 1993). Interestingly, it has been shown that direct stimulation of astrocytes via photolysis of caged Ca^{2+} is sufficient to evoke paroxysmal depolarization shifts with hypersynchronous neuronal firing in acute seizure models (Tian et al., 2005). We have shown that there was no difference in the minor mechanical tissue disruption between normal saline and TeNT-injected animals, as well as no toxin induced astrogliosis in our animal model. Thus, the alteration of GFAP can be considered as astrocytosis in response to the epileptogenic process. Marked reactive overexpression of GFAP mRNA predominantly emerged in the acute and subacute stages of epilepsy development was demonstrated in our study. This evidence reflects that astrocytes probably play a crucial pathophysiological role during the epileptogenic process, but have relatively less influence after epilepsy has become established. In spite of this, our data are still unable to determine the causality between the reactive astrocyotsis and the development of epilepsy, and further work will be required.

SNAP-25 is a central component of the SNARE protein complex playing an essential role in synaptic vesicle exocytosis and neurotransmitter release through regulating synaptic vesicle docking and fusion. SNAP-25 dysfunction has been frequently linked to several human psychiatric diseases such as attention-deficit/hyperactivity disorder (ADHD), schizophrenia, and bipolar disorder (Antonucci et al., 2016). Furthermore, Rohena et al. reported SNAP-25 mutations in humans can lead to epilepsy (Rohena et al., 2013). In addition, an animal model of epilepsy in the SNAP-25 knock-in mouse has also been developed (Watanabe et al., 2015). Our data reveal that SNAP-25 exhibited considerable elevation only in the subacute period,

the time animals usually experienced the highest seizure frequency, during the process of epilepsy in our model. Therefore, whether the increase of SNAP-25 is a compensatory phenomenon which reflects the vigorous synaptic activity during the peak of seizure activity needs to be clarified.

Gene expression in neurons has sophisticated regulation through subsets of transcription factors which eventually give neurons individual functions, properties and phenotypes. REST/NRSF is one of the master transcription factors that modulates neuronal gene expression temporally and spatially during neurogenesis, neuronal differentiation, and epileptogenesis (Spencer et al., 2006). Indeed, our present study shows that REST/NRSF is pronouncedly up-regulated during the subacute phase of epilepsy maturation then returns to near the control levels in the late phase. An abundance of neuronal gene expression is dynamically regulated by the REST/NRSF-NRSE system including genes involving either neuronal hyperexcitability or neural circuit inhibition. Hence, REST/NRSF modulates the intrinsic homeostasis of neural circuits and deeply impacts the stabilization of neural network. Two hypotheses regarding the actions of REST/NRSF in epileptogenesis have been proposed. One suggests that REST/NRSF serves a protective effect by reducing neuronal excitability. For examples, Pozzi et al. reported upregulation of REST/NRST can reduce the expression of voltage-gated Na^+ channels leading to suppressed neuronal excitability and reducing the entire neuronal network firing activity (Pozzi et al., 2013), and a potential antiepileptic effect of REST via repressing BDNF expression has also been described (Garriga-Canut et al., 2006). Moreover, accelerated seizure susceptibility and progression was observed after conditional deletion of REST/NRSF in an electrical kindling model (Hu et al., 2011). However, another hypothesis has argued that the upregulation of REST/NRSF contributes to epileptogenesis. For instance, McClelland et al. showed that REST/NRST is responsible for HCN1 down-regulation and blocking REST/NRSF can significantly rescue HCN1 expression and function, and markedly reducing spontaneous seizure frequency in K.A. rats (McClelland et al., 2014; McClelland et al., 2011a). Although REST/NRSF has been strongly associated with epilepsy, its definite role in epileptogenesis remains controversial. A possible explanation is that there are different binding affinities for REST/NRSF to the NRSE-

containing genes which results in only a few NRSE-containing genes being selectively silenced/repressed by REST/NRSF in different conditions and in specific levels of REST/NRSF expression (McClelland et al., 2014).

In recent years, mTORopathies have been avidly investigated. mTOR plays an important role in regulating transcription, mRNA translation, mRNA turnover, protein stability and degradation, organization of cytoskeletal actin, autophagy, and immune response (Dello Russo et al., 2013; Inoki et al., 2005; Wong, 2008, 2010). Thus the mTOR signalling network widely controls cellular functions including cell growth, metabolism, synaptic plasticity, expression of various ion channels and neurotransmitter receptors etc. (Goldberg and Coulter, 2013). Accumulating evidence suggests that mTOR dysregulation is not only seen in patients with mTORopathies (e.g. TSC and focal cortical malformations), but also is importantly associated with many acquired epilepsies including infantile spasm, post-traumatic epilepsy, mTLE, and hypoxia-induced seizures etc. (Meng et al., 2013; Ryther and Wong, 2012; Sha et al., 2012). Thereby, aberrant mTOR signalling plays a pivotal role and may be a communal molecular alteration in the pathophysiology of a spectrum of epilepsy disorders. Biphasic activation of mTOR pathway immediately after SE (peak at 3-6 hrs) and a second distinct rise during 5-10 days after SE has been shown in the K.A. model of TLE (Zeng et al., 2009). In our current study, a striking overexpression of mTOR was shown in the subacute period (approximately 2 weeks after seizure onset) in the non-SE initiated and non-lesional neocortical model of epilepsy. It is not surprising that application of Rapamycin, an mTORC1 inhibitor, in TSC/PTEN genetic models is able to suppress seizures. In acquired epilepsy models, it has been reported that rapamycin attenuates seizure susceptibility in the model of acute hypoxia-induced neonatal seizures (Talos et al., 2012), and blocks epileptogenesis and reduces seizure frequency in the pilocarpine and K.A. rodent models of epilepsy (Huang et al., 2010; Zeng et al., 2009). However, some contradictory findings have emerged: administration of rapamycin only represses mossy fibre sprouting and does not abolish epileptogenesis or reduce seizures in either the pilocarpine model or the amygdala stimulation model (Buckmaster and Lew, 2011; Sliwa et al., 2012). Furthermore, clinical trials in patients with TSC and

experimental preclinical studies also showed paradoxical exacerbation of epilepsy with mTOR inhibition treatment (Krueger et al., 2010; Muncy et al., 2009; Zeng et al., 2010). Comprehensively understanding the precise temporal regulation of mTOR will be necessary to know when are the appropriate time points and proper circumstances to hit mTOR expression in epileptogenesis and disrupt the progress of epilepsy. Our data suggests that subacute phase rather than late phase of epilepsy development may be a critical time point.

Growing evidence supports that neuroinflammatory processes comprising inflammatory and immune responses play key roles in the pathogenesis of epilepsy. Among various inflammatory/immunological mediators, chemokines serve as chemo-attractants and have been implicated as contributors to a complex mechanism in the generation and exacerbation of epilepsy (Fabene et al., 2010; Vezzani et al., 2011). For example, clinical evidence shows that CCL2 (also known as chemokine monocyte chemotactic protein-1, MCP1) is overexpressed in epilepsy patients with focal cortical dysplasia (Iyer et al., 2010), tuberous sclerosis, and TLE (Andjelkovic and Pachter, 2000; Vezzani et al., 2011; Wu et al., 2008). Moreover, up-regulation of CCL2 in experimental models, such as pilocarpine (Foresti et al., 2009; Xu et al., 2009) and K.A. (Bozzi and Caleo, 2016) models, has been reported. Interestingly, we revealed a remarkable elevation of CCL2 in the chronic stage after epilepsy has been well established, and only mild or moderate rises in early and subacute phases of the epileptogenic cascade. This may indicate that immunological disruption, at least at the level of CCL2/CCR2 signalling, mainly impacts on the late phase of the epileptogenic process. However, this result still cannot exclude the potential pathophysiological role of other immunological and inflammatory mechanisms in the earlier phases of epileptogenesis.

GABA receptor-mediated neuronal inhibition is functionally classified as phasic and tonic inhibition (Glykys and Mody, 2006). Phasic (or Synaptic) inhibition refers to activation of GABA receptors located in synapses, whereas tonic (or extrasynaptic) inhibition indicates activation of GABA receptors localized extrasynaptically via ambient GABA (Bonin et al., 2013). In the TeNT model, the

expression of GABRA5 remained near control levels until the chronic stage and underwent a dramatic decline in the late phase. As the $GABA_A$ α5 subunit or δ subunit is responsible for tonic inhibition (Bonin et al., 2013), we hypothesize that the neuronal network attempts to maintain tonic inhibition during the epileptogenic process, but eventually becomes decompensated when epilepsy matures.

However, we still have to keep in mind that as the seizure frequency in the TeNT model of visual cortical epilepsy might gradually decline from week 4-5 of initial seizure onset, it is difficult to determine that whether the gene expressions in the chronic stage (late phase) of this animal model were mainly correlated to the full establishment of epilepsy or might be caused by the neural network recovery from the TeNT induced neural disruption. Hence, comparison of this set of gene expressions in the corresponding phase of established epilepsy in an alternative animal model of neocortical epilepsy will be helpful to clarify this issue.

6.6 Summary

The quantification of expression of different candidate genes revealed different regulatory behaviours during the process of epileptogenesis. In the acute stage, BDNF is distinctly down-regulated, whereas GFAP is markedly up-regulated. During the subacute stage, GFAP, SNAP-25, REST and mTOR are all significantly up-regulated. By the chronic state, CCL2 is strongly over-expressed and GABRA5 is dramatically down-regulated. Here, our study demonstrates that the candidate genes are regulated by a time-dependent manner, which depends on the time elapsed from the initial precipitating insults or disease start.

In this chapter, we show that, in the TeNT model of visual cortical epilepsy, GFAP, SNAP-25, REST and mTOR are all transiently up-regulated and BDNF is transiently down-regulated during epileptogenesis, while CCL2 is up-regulated later when epilepsy is established. Moreover, the down-expression of GABRA5 suggests that this GABAergic signalling may be down-regulated in the late stage of

epileptogenesis. Our work highlights how different candidate genes are differentially regulated during epileptogenesis, and how the regulation of genes changes as epileptogenesis progresses. Further work comparing this set of genes at similar time points in additional models may reveal how conserved (or not) gene regulation is during epileptogenesis.

Chapter 7 Intracerebral Kainic Acid model of Acute Seizures or Epilepsy

7.1 Introduction

Mesial temporal lobe epilepsy (mTLE) is the most common type of focal epilepsy in adult humans and approximate 60-70% of patients experience uncontrolled seizure despite appropriate therapy with AEDs (Cendes, 2005). Thus, investigating the seizure generation and the underlying mechanisms of mTLE is very important, and a vast majority of epilepsy research has focused on it. In addition, the insights gained from studying mTLE can also help us to understand or may be applied to other forms of epilepsy. K.A. and pilocarpine animal models of epilepsy are the most frequently used rodent models in epilepsy research. However, in contrast to pilocarpine model which also produces more extensive damage in neocortical areas, the lesions in the K.A. animal model are more restricted to hippocampus, amygdala, piriform cortex, entorhinal cortex, septum and medial thalamus (Kandratavicius et al., 2014; Reddy and Kuruba, 2013).

K.A. can be administered either systemically (intraperitoneally or subcutaneously) or intracerebrally to the desired brain region, but is mostly applied to limbic system, to generate the model of limbic epilepsy. The K.A. animal model, either systemic or local brain administration, represents a SE-induced epilepsy model and existing many electrophysiological similarities and remarkable histopathological correlates of hippocampal sclerosis in human mTLE, including neuronal death, astrogliosis, granule cell dispersion in dentate gyrus, aberrant mossy fibre sprouting etc. (Levesque and Avoli, 2013; Raedt et al., 2009). Consequently, this model has a broad utility for exploring the pathophysiology and mechanisms of human SE and mTLE. Even though K.A. model of epilepsy might generate robust and persistent spontaneous recurrent seizures, animals of different species, strains, age, genders and weight exhibit variable sensitivity, vulnerability and response to K.A. and this may lead to variable epilepsy profiles (Buckmaster, 2004; Levesque and Avoli, 2013).

For instance, juvenile rats (30 to 40 days old) are more susceptible to K.A. induced seizures than are adult rats (70-90 days old), but significantly less hippocampal damage is seen after K.A. treatment in immature brains (Hui Yin et al., 2013). Furthermore, K.A. can be applied with different permutations such as in a single high dose or in multiple low doses which may result in different successful induction rate of SE, behavioural seizure severity, mortality rate, and variable proportion of animals developing spontaneous recurrent seizures (Buckmaster, 2004; Tanaka et al., 1988). Therefore, prior to use in experiments, it is necessary to optimize the relevant conditions of the model.

7.2 Aims

We have used an optimized TeNT model of visual cortical epilepsy for our gene regulation and gene therapy studies. As the TeNT model we used is a model of focal neocortical epilepsy, we further attempted to develop an additional animal model. Ideally we would have identify an additional long-lasting model of focal neocortical epilepsy. Alternatively we could develop a model mimicking a different epilepsy syndrome through a different seizure-induced mechanism, that does not overlap the putative mechanism of TeNT-dependent epileptogenesis (i.e. suppression of GABAergic signalling). Hence, my additional objective is to validate and optimize an alternative animal model that can be applied to investigate how similar (or how different) gene regulation is at similar time points of epileptogenesis across different models of epilepsy syndromes. In addition, if sufficiently reproducible this model could allow testing epilepsy gene therapy in parallel.

The first aim here is to test whether K.A. local administration into neocortex can induce chronic spontaneous recurrent seizures. The second aim is to establish and optimize a limbic epilepsy model in rats with intra-amygdala K.A. injection to improve the consistency and decrease individual variability including generating a more consistent latent period and spontaneous recurrent seizures with sustained and reproducible frequency.

7.3 Methods

Following a recovery period of one week after surgery, rats received K.A. microinjection into the target brain area. Sequentially, continuous 24-hour/ 7 day video-telemetric ECoG recording was carried out to observe and record seizure activity. In addition, Racine score (Table 7.1) was applied to assess the behavioural seizure severity of SE. After this, we conducted continuous 24-hour/ 7 day video-telemetric ECoG recording for up to around 16-20 weeks in most of the animals.

7.3.1 Kainic acid injection into visual cortex

The rats were anaesthetised with isoflurane (3%) in 2 L/min O_2 in an anaesthetic chamber. Then the animals were placed in a stereotaxic frame with head-fixed and kept anaesthetic under 2% isoflurane in 2 L/min O_2. The K.A. was stereotaxically delivered via the injection cannula affixed above right visual cortex (see Section 3.2.3.2) using a 33-gauge needle with Hamilton syringe. Either 0.1 µg or 0.5 µg of K.A. in a total volume of 0.5 µl with the injection rate of 0.5 µl/min was administered into the layer V of right primary visual cortex (coordinates from Bregma: lateral, 3 mm; posterior, 7 mm; depth, 1mm below the pia), and the needle was removed immediately after injection.

7.3.2 Kainic acid injection into amygdala

Animals were head fixed in the stereotaxic frame under low dose anaesthesia and K.A. was stereotaxically injected into right basolateral amygdala nucleus at a depth of 7.8 mm below dura via the guide cannula (see Section 3.2.3.3) by inserting a 33-gauge needle with Hamilton syringe. Different dosages (0.1 µg, 0.2 µg, 0.3 µg, 0.4 µg, 0.5 µg, 0.8 µg, and two separate dosages of 0.5 µg) of K.A. in a total volume of 0.5 µl were applied, and the injection rate was 0.5 µl/min. Two non-seizure control

rats underwent the same surgical procedures but received the same volume of 0.9% saline injection at basolateral nucleus of amygdala.

The animals' behaviour and ECoG (or local field potential, LFP) were intensively monitored after administration of kainic acid. A subset of animals received diazepam (10-20 mg/kg; intraperitoneal) to terminate the seizures 1 hour after SE onset. The ECoG (or LFP) and animals were further monitored for up to 3 hours to ensure the cessation of status epilepticus. The video-telemetric ECoG surveillance was continued thereafter for long-term analysis of spontaneous seizures.

Table 7.1 Racine score: Behavioural scores of seizure activity during status epilepticus based on Racine stages (Racine, 1972)**.**

Stage	Seizure behaviour
1	Mouth and facial movements
2	Head nodding with more severe facial and mouth movements (wet dog shakes)
3	Forelimb clonus
4	Rearing and bilateral forelimb clonus
5	Rearing and falling, with loss of posture control, full motor seizure or wild jumpy

7.4 Results

7.4.1 Visual cortex K.A. injection only induces acute cluster seizures

In this pilot study, an adult male Lister Hooded rat received 0.1 μg K.A. at layer V of right visual cortex, and another one received 0.5 μg K.A. A Lister Hooded rat was used because there are some concerns about visual acuity in albino strains such as Sprague Dawley. In the rat with 0.5 μg of K.A. administration, first acute seizure onset at 1.5 hours following neocortical injection, and cluster seizures developed from 2.5 hours after K.A. administration and lasted for 2 hours (Figure 7.1). Sequentially, frequent intermittent inter-ictal epileptiform discharges without obvious seizure behaviours were observed, and this persisted for several hours (up to 4-5 hours) then gradually subsided. Most of the seizures had a duration around 60-120 s. However, the rat did not exhibit SE and no spontaneous recurrent seizures were detected under video-ECoG recordings for 3 months. In addition, no SE, acute seizures or spontaneous seizures were detected in the animal with 0.1 μg of K.A. administration.

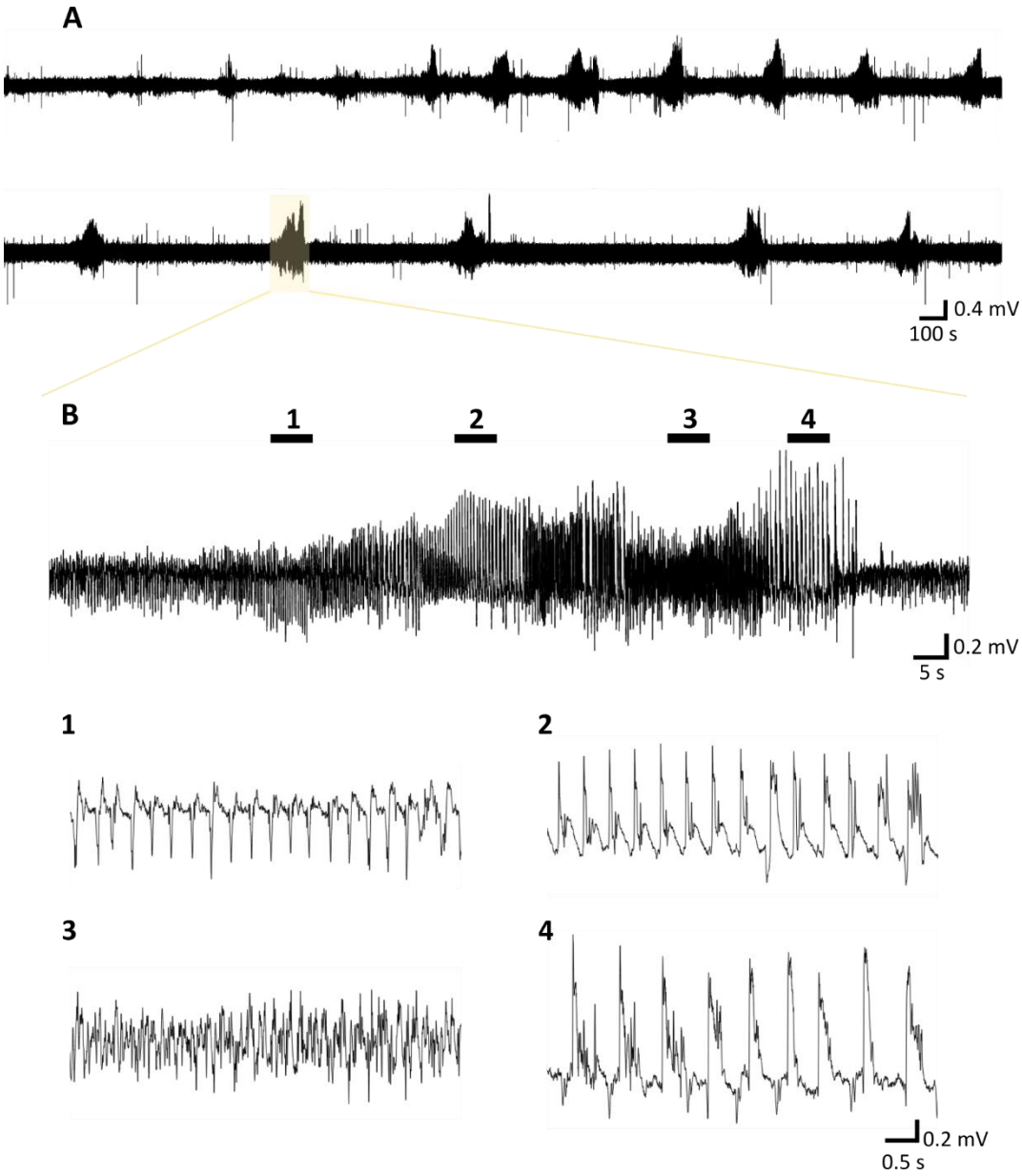

Figure 7.1 Acute cluster seizures after K.A. application in visual cortex

(A) The acute cluster seizures within two hours (one trace indicates one hour). The initial hour showing higher seizure frequency than the following hour.

(B) A representative seizure displaying its four major ECoG waveforms and the progression over time.

7.4.2 Intra-amygdala K.A. injection induces SE and Chronic limbic epilepsy

In this pilot experiment, the animal implanted with recording electrode in the right neocortex (coordinates: 4 mm lateral, 5.2 mm posterior) received 0.1 µg of K.A. in the ipsilateral amygdala. Electrographic seizures accompanied behavioural correlates (complex partial seizure-like behaviours) were shown at 10-15 minutes after injection followed by gradually increasing seizure frequency and intensity and then eventually achieved full-blown SE (Figure 7.2A). According to the seizure behaviours during SE, the rat predominately experienced complex partial status epilepticus with intermittently secondary GTCs and achieving the stage 5 of Racine score. The SE persisted for 3 hours followed by intermittent cluster seizures for a few hours then turn to frequent inter-ictal epileptiform activity for several hours.

After this, the animal entered a silent period of seizures and the first spontaneous seizure emerged 12 days following K.A. administration. A few spontaneous recurrent seizures were detected based on the cortical recording electrode (Figure 7.2B & Figure 7.3). However, the seizure frequency was likely much higher than the seizures we detected from the cortical recording electrode, as we noticed that the rat exhibited some prolonged bizarre behaviours resembling limbic seizures with associated surface ECoG background changes but not typical electrographic features of epileptic discharges.

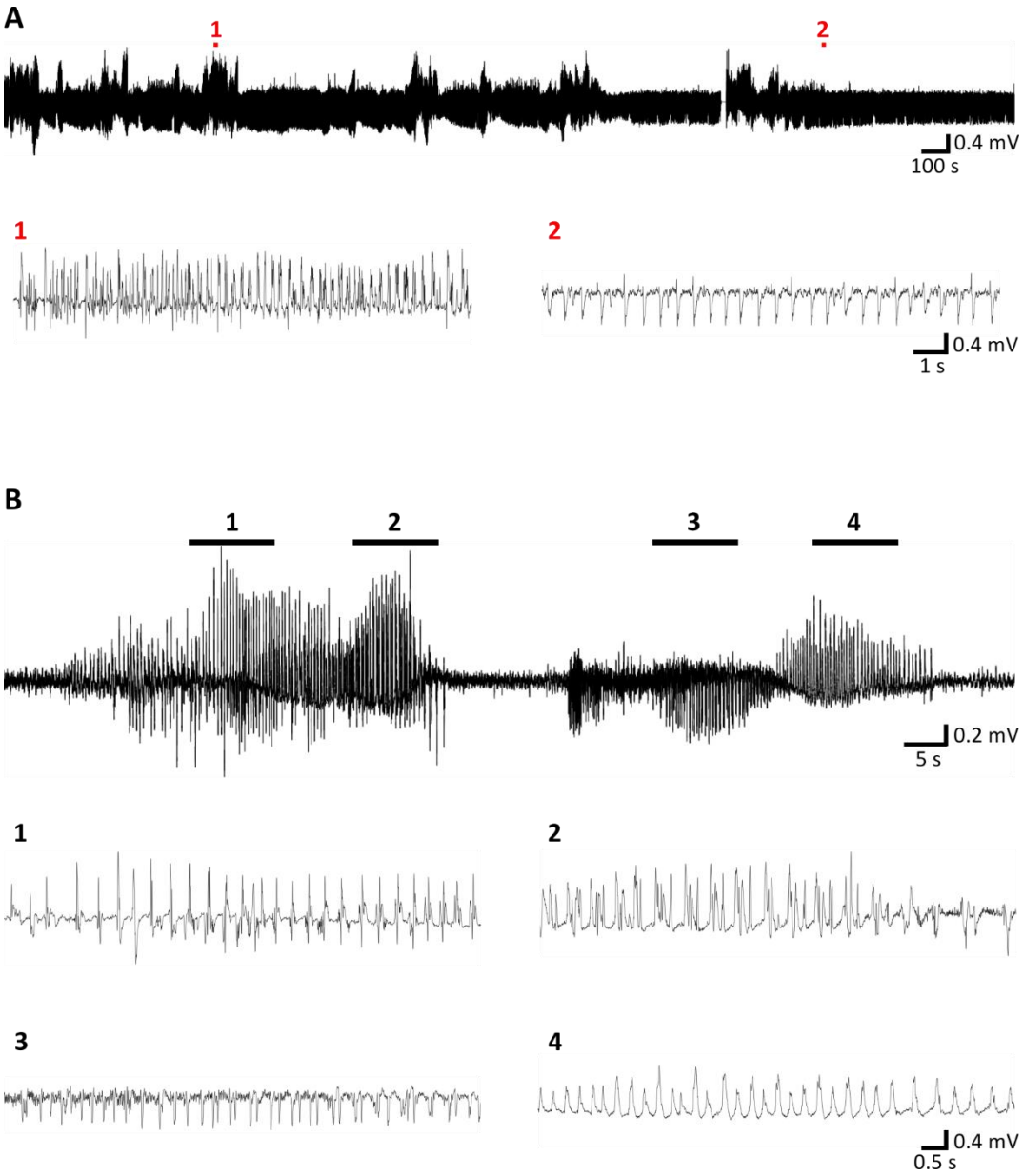

Figure 7.2 Electrographic characterization from the cortical electrode in the intra-amygdala K.A. model of epilepsy

(A) Representative hour of status epilepticus from an adult male Lister Hooded rat. The ECoG shows continuous epileptic activity.

(B) A representative seizure from the chronic spontaneous recurrent seizure showing its long duration and evolution over time.

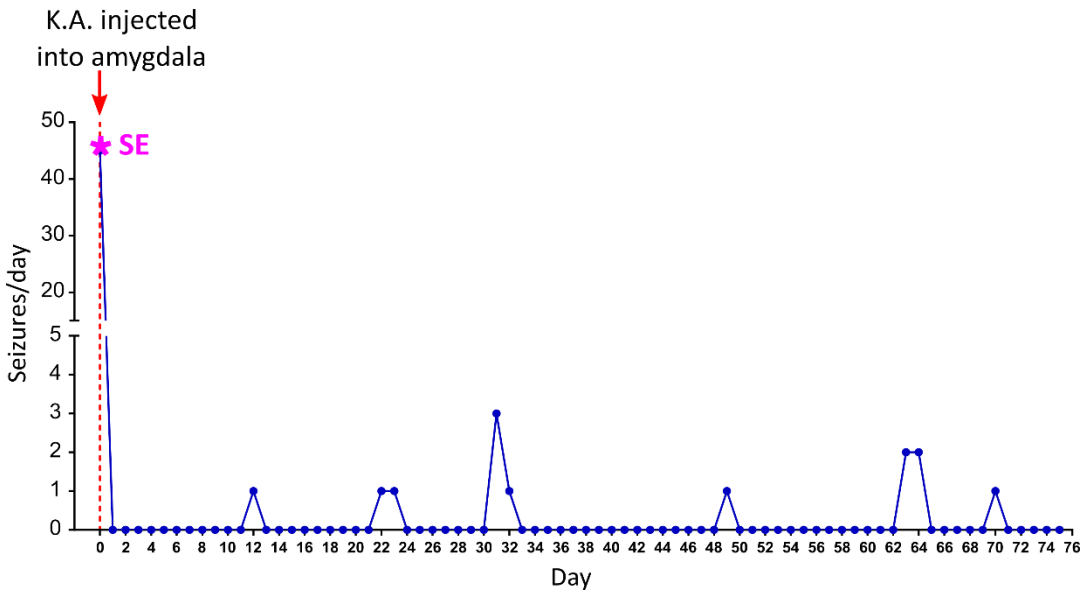

Figure 7.3 Seizure frequency for the rat of intra-amygdala K.A. model of epilepsy

The frequency of chronic spontaneous recurrent seizures detected with the cortical recording electrode.

7.4.3 Optimisation of the intra-amygdala K.A. model of Epilepsy in rats

As we noticed that the cortical surface recording electrode might not be able to detect some of the limbic seizures, and the frequency of spontaneous recurrent seizure might be underestimated in our pilot study. We next implanted depth recording electrode into the hippocampus (see Section 3.2.3.3) which enabled us to acquire the local field potential (LFP) from the limbic brain region. Moreover, in order to have the consistency of the animal strain in our studies, which had used Sprague Dawley rats, adult male Sprague Dawley rats were used for the optimisation of this animal model.

7.4.3.1 Verification of the location of implanted depth electrode and site of K.A. injection

The placement of the tip of the depth recording electrode was well targeted at the CA1 of right dorsal hippocampus (Figure 7.4A), and the administration of K.A. also precisely injected into the right basolateral amygdaloid nucleus (Figure 7.4B).

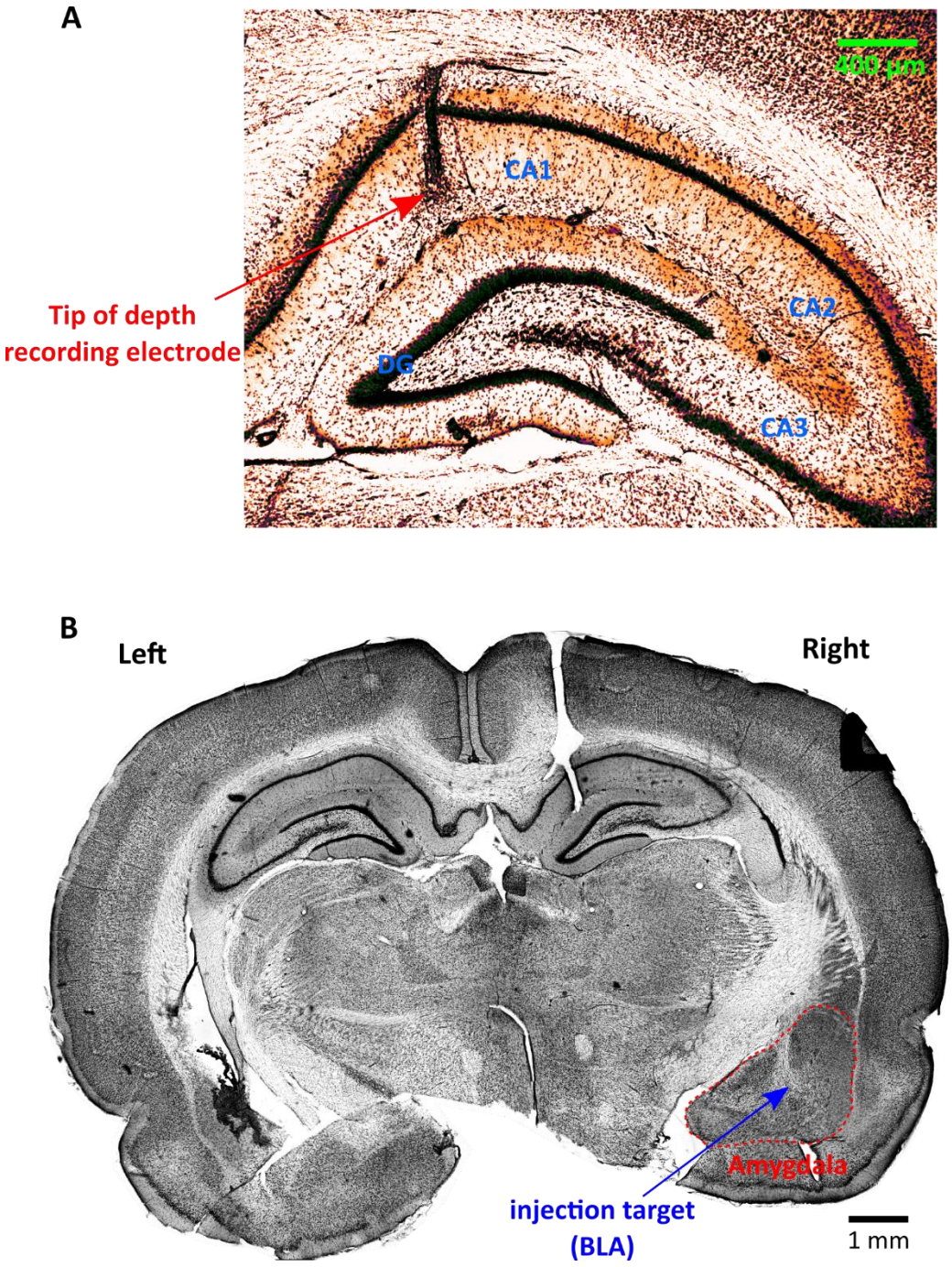

Figure 7.4 Histology verification of the location of depth electrode and K.A. injection

The cresyl violet staining of nissl bodies shows that (A) the tip of depth recording electrode was placed in the desired location of CA1. (B) K.A. was administered into the ipsilateral basolateral nucleus of amygdala. (BLA: basolateral anygdaliod nucleus)

7.4.3.2 Dose optimization & Characterization of SE and its LFP

As we found there was high variability of the latency from the intra-amygdala K.A. injection to the first spontaneous recurrent seizure, which range from approximately 2 weeks to more than 2 months, we tested different strategies of intra-amygdala K.A. application to optimize this animal model. Table 7.2 summarizes the strategies we applied and the delineation of the associated observations during SE. In total, 14 Sprague Dawley rats were used and the electrophysiological epileptic activity (Figure 7.5) started within 5-30 mins following the rats awoke from the anaesthesia and the acute behavioural seizures also displayed in all the animals with different dosage of K.A. administration. Two animals died during SE, one with a single dose of 0.8 µg K.A., and the other with a total dosage of 1 µg K.A. administered by an initial 0.5 µg of K.A., followed by a second dose of 0.5 µg K.A. an hour after the onset of acute seizures after the initial SE did not achieve the stage 5 on the Racine scale. In the animals that did not receive diazepam, the SE sustained up to 2-3 hours and could be followed by cluster seizures for several hours and frequent inter-ictal epileptiform activity for 1-2 days.

Table 7.2 Summary of the strategies applied on the optimization of intra-amygdala K.A. model of epilepsy in rats

Animal (#)	K.A. dosage (μg)	Time of acute seizure onset	SE & outcome	Diazepam
1	0.2	~ 30 mins	SE (+); survived	not applied
2	0.2	~ 10 mins	SE (+); survived	an hour after SE: total 20 mg/kg
3	0.2	~ 10 mins	SE (+); survived	an hour after SE: total 12 mg/kg
4	0.2	~ 15 mins	SE (+); survived	an hour after SE: total 20 mg/kg
5	0.2	~25 mins	SE (+); survived	1.5 hrs after SE: total 10 mg/kg
6	0.2	~15 mins	SE (+); survived	not applied
7	0.3	~10 mins	SE (+); survived	not applied
8	0.4	~10 mins	SE (+); survived	not applied
9	0.5	~ 5 mins	SE (+); survived	not applied
10	total: 1 (initial 0.5 μg & an hr after Sz onset: repeated 0.5 μg)	~ 20 mins	SE(+); died during SE	not applied
11	0.8	~ 5 mins	SE (+); survived	not applied
12	0.8	~10 mins	SE (+); survived	not applied
13	0.8	~ 10 mins	SE (+); survived	not applied
14	0.8	~ 5 mins	SE (+); died during SE	not applied

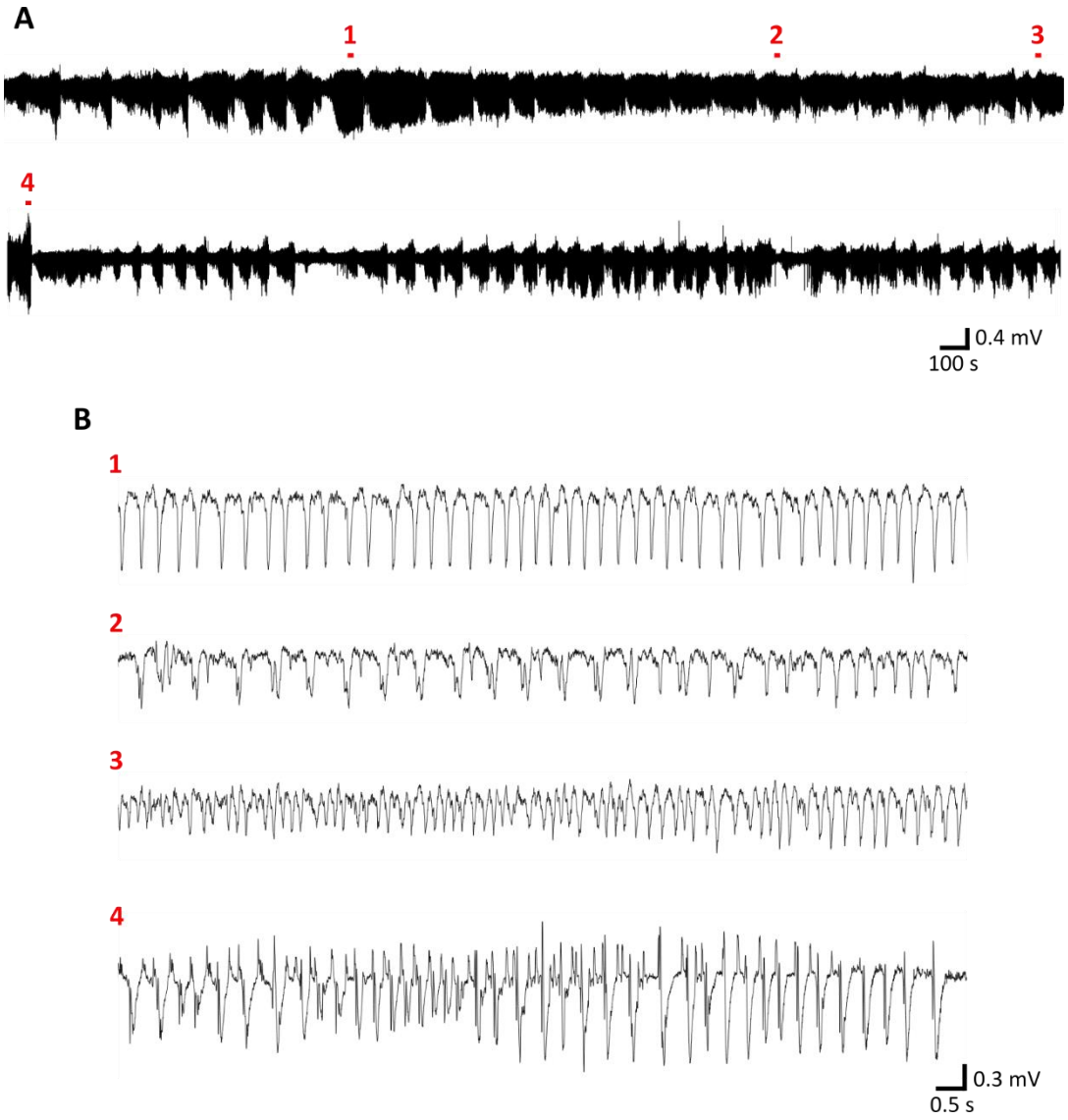

Figure 7.5 Characterization of local field potential (LFP) during SE

(A) Representative SE induced by intra-amygdala K.A. injection showing continuous epileptic activity and its evolution over time. (One trace indicates one hour).

(B) Four major electrographic features of LFP during SE from the animals implanted with depth recording electrode at CA1 area.

7.4.3.3 The Development of Chronic Epilepsy & Unilateral Hippocampal Atrophy

Spontaneous recurrent seizures have been observed in the animals, and the preliminary findings revealed that limbic epilepsy was induced by a low to moderate dose of intra-amygdala K.A. application in rats. However, the complete analysis of the long-term continuous video-telemetric ECoG is still ongoing.

The histopathological changes for these animals at the end of long-term video-telemetric ECoG monitoring (around 16-20 weeks following SE) showed apparent unilateral hippocampal atrophy on the ipsilateral side of K.A. injected amygdala (Figure 7.6). Moreover, compared to the contralateral part, CA3 neuronal loss and marked structural alteration of the injected amygdala were also exhibited.

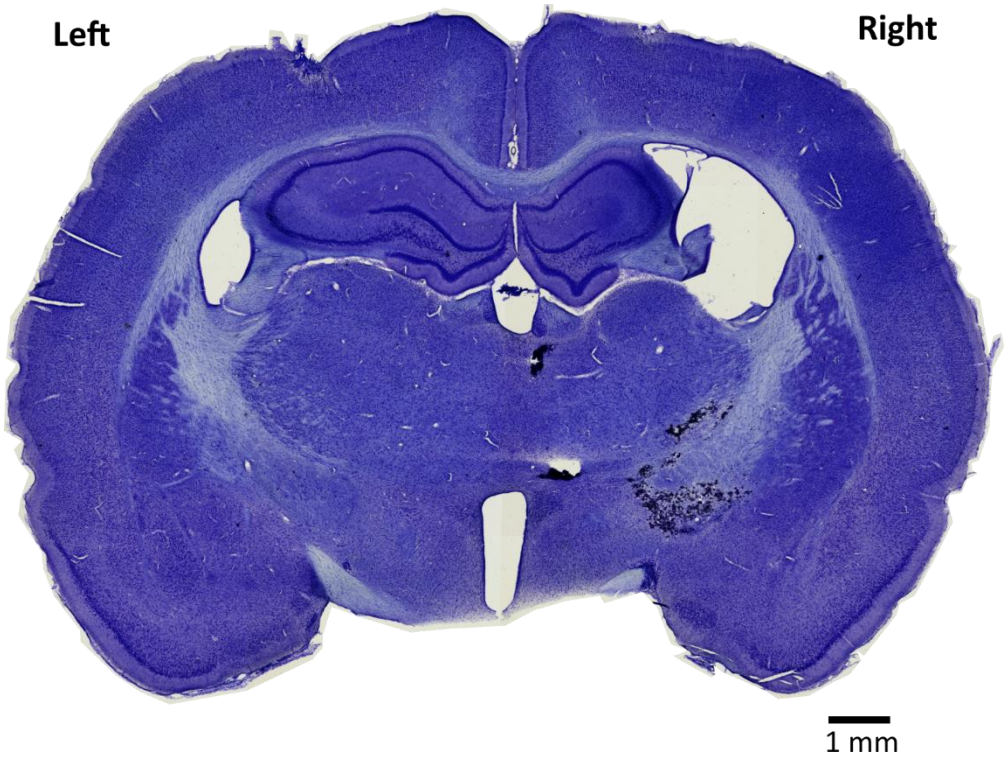

Figure 7.6 Unilateral hippocampal atrophy in the intra-amygdala K.A. model of epilepsy

This representative histology image (Nissl staining) was obtained from a tissue 19.5 weeks after SE from a rat receiving 0.2 µg of K.A. injection into right amygdala without diazepam showing significant right hippocampal atrophy and distinct tissue disorganization over right amygdala. The bright-field images of the brain slice were acquired using an Axio Imager A1 fluorescence microscope (Axiovision LE software) equipped with a 2.5x objective (Zeiss) and the image processing was performed using ImageJ software and the composite images were assembled using MosaicJ ImageJ plugin.

7.5 Discussion

In contrast to the TeNT model of visual cortical epilepsy, K.A. administration into visual cortex only produces acute cluster seizures with neither SE episodes nor subsequent chronic neocortical epilepsy. Furthermore, a higher dose of K.A. was required to elicit acute seizures in neocortex comparing to that needed in the intra-amygdala K.A. model, and this is possibly because of relatively few kainate receptors in neocortex compared with the levels expressed in hippocampus, amygdala and entorhinal cortex (Levesque and Avoli, 2013), as well as being ascribed to the neural network in hippocampus being much vulnerable to the convulsive stimulation with higher susceptibility to establish epilepsy circuitry.

It has been shown that a considerable fraction of behavioural spontaneous seizures in the intrahippocampal K.A. epilepsy model in rats are partial seizures without secondary generalization (Raedt et al., 2009). Given the failure to detect some limbic seizures using a cortical recording electrode in our pilot study, we strongly suggest applying depth recording electrodes in hippocampus for models of mTLE in rat. Even though there is highly reproducible rate of chronic spontaneous recurrent seizures, the major drawbacks of the K.A. model are a wide variation in latent period and spontaneous seizure frequency (Levesque and Avoli, 2013; Raedt et al., 2009). These shortcomings increase the difficulty in exploring the molecular mechanisms of epileptogenesis in the temporal basis, and developing further epileptogenic target-driven approaches. In addition, different strategies of K.A. administration could contribute to diverse profiles of limbic epilepsy including the mortality rate, SE and seizure severity, latent period and the probability of unprovoked seizures. According to our preliminary results, we suggest moderate dose of K.A. administered into amygdala may be an ideal strategy to generate a more consistent latent period and appropriate seizure frequency for the rat model of mTLE.

In my observation, compared with the rat model, the latency and spontaneous seizure frequency seems to be more consistent among individual animals and the epileptic seizures are predominately presented as secondary GTCs

in the intra-amygdala K.A. model in mice, which have employed by my colleagues in the Institute of Neurology and by the research group led by professor David Henshall (Mouri et al., 2008). However, the major behavioural manifestations of chronic spontaneous seizures in rats are minor motor or non-motor focal seizures with less propagation to secondary GTCs, and this might mimic the automatisms or some non-motor behaviours observed in human mTLE.

Furthermore, a considerable limitation of the K.A. model is that the direct excitotoxic effects of K.A. result in extensive neuronal damage and death that makes it difficult to distinguish the neuronal damage caused by direct effects of K.A. from SE, seizures and epileptogenesis, particularly in systemic and intra-hippocampal K.A. administration. Unlike the systemic K.A. model which produces bilateral hippocampal atrophy and profound, extensive neuronal loss in bilateral CA1 and CA3/CA4 regions (Ben-Ari et al., 1980b; Levesque and Avoli, 2013; Zhang et al., 2002), my experiments revealed that the rats receiving low to moderate dose of intra-amygdala K.A. microinjection without diazepam had principally unilateral hippocampal atrophy, and the hippocampus was relatively much better preserved in the animals receiving diazepam. Furthermore, a much more confined lesion with unilateral cell loss in CA3 and minor damage in ipsilateral CA1 was observed and this matches similar findings in other reports (Ben-Ari et al., 1979a; Ben-Ari et al., 1980a; Mouri et al., 2008). These histopathological signatures of the intra-amygdala K.A. model are more similar to human conditions as the hallmarks of human mTLE with hippocampal sclerosis is mainly unilateral and asymmetric hippocampal neuron loss.

Some extent of pathological lesions over the extra-hippocampal regions and cortices have been shown in the systemic K.A. model (Ben-Ari, 1985; Ben-Ari et al., 1979b), while Mouri et al. and Henshall et al. detected only restricted damage in the intra-amygdala K.A. model with minimal injury in ipsilateral cortical neurons (Mouri et al., 2008), and this further mimics human conditions since absent or only limited neuronal loss is exhibited in mTLE patients (Bothwell et al., 2001; Dawodu and Thom, 2005).

Our detailed video-telemetric ECoG data analysis for the intra-amygdala K.A. model of epilepsy in rat are still underway and more comprehensive results regarding the characterization of this rat model and potentially optimal K.A. dosage will rely on completion of this analysis.

7.6 Summary

In this chapter, we demonstrated that local application of K.A. in neocortex only generates acute cluster seizures without epilepsy. Moreover, the utility of depth recording electrodes placed in the hippocampus is better for electrophysiological monitoring in the animal models mimicking mTLE. Even if the intra-amygdala K.A. model is still a lesion-induced limbic epilepsy model, the direct excitotoxic effects of K.A. are restricted to the injected amygdala. Taken together the epilepsy phenotype and the signatures of the histopathological changes, suggest the intra-amygdala K.A. model in rats better resembles human mTLE comparing with the mouse model or the systemic K.A. model. An additional advantage of this model is that there is lower mortality and morbidity compared to the model of systemic K.A. administration. However, similar to other rat K.A. models, the current limitation of intra-amygdala K.A. model in rats lies with the high variability in latent period and the frequency of epileptic seizures.

Chapter 8 General Discussion

Genetic mutations in neuronal genes may change neuronal properties and result in epilepsy (Meisler MH, 2012; Oliva et al., 2012). Moreover, the neuronal phenotypes and behaviours are dynamically regulated by gene expression throughout life (Bale et al., 2010; Sweatt, 2013) and the mechanisms of epileptogenesis, derived by known or unknown epilepsy-provoking insults, are also associated with alterations of gene expression that affect neuronal function and network activity (McClelland et al., 2011b; Roopra et al., 2012). The molecular signalling basis of epileptogenesis remains unclear and the most important concept in studying the molecular markers and gene regulation of epileptogenesis is that the epileptogenesis is a serial, consecutive and progressive process with different stages. In addition, no single existing experimental epilepsy model can completely mimic human epilepsy. Experimental models trigger seizures or epilepsy through different mechanism providing an opportunity for searching for commonality downstream. The genes which have been reported to be related to epileptogenesis are often studied using only one experimental epilepsy model but whether such genetic and molecular changes are the same in different epilepsy models, and if this can represent or is consistent with the gene regulation during epileptogenesis in human epilepsy still needs to be determined. Therefore, it is important to explore whether there is a group of genes that are co-regulated, perhaps relying upon specific common properties and signalling pathways which can lead to epilepsy in different epilepsy models.

The principle focus of this thesis is to investigate the characterisation of gene regulation during epileptogenesis, and to explore the alteration of which key changes in gene expression may contribute to generate “epileptic neurons”. First, we demonstrated that mRNA expression is variably regulated in different mechanisms of *in vitro* seizure models, with the Low-Mg^{2+} model and the High-K^{+} model exhibiting the most similar profiles in gene regulation. Next, we followed the regulation of the candidate genes to show that during epileptogenesis they have highly differing

profiles during different stages of epileptogenic process in the *in vivo* model of neocortical epilepsy, and revealed mTOR, REST and CCL2 are master molecular regulators of epilepsy development, as well as astrocytes play important action during epileptogenesis.

Here, we will first discuss the characterisation of mRNA expression during epileptogenesis comparing *in vitro* models and the *in vivo* model. Then we will further discuss the possible impact of the gene regulation and their key molecular pathways during epileptogenesis progresses.

8.1 Comparison of the Characterisation of Gene expression between *in vitro* models & *in vivo* model of epilepsy

A variety of *in vitro* models have been broadly exploited in seizure and epilepsy research. However, which model exhibits the most similar characteristics to *in vivo* condition is not clear. Our work uncovered that among the four most commonly used neocortical culture models, High-K^+, Low-Mg^{2+}, K.A., and PTZ models, the mRNA expression profile in the Low-Mg^{2+} model showed highest similarity with the *in vivo* TeNT model of neocortical epilepsy, and was followed by the High-K^+ model.

Extracellular neuronal magnesium concentration regulates the excitability of NMDA receptors. It is intriguing that even if Low-Mg^{2+} evoked seizure-like activity primarily through the mechanism of activating NMDA receptors, whilst the TeNT model of epilepsy acts via interference with the GABAergic system, both of them result in similar changes in gene regulation. Moreover, while activation of NMDA receptors can lead to the reduction of GABAergic inhibition probably via increasing the $GABA_A$ receptor endocytosis (Blair et al., 2004; Stelzer et al., 1987), this is

insufficient to explain why mRNA expression in Low-Mg^{2+} model rather than PTZ model, which uses a $GABA_A$ receptor blocker, more resembles TeNT model *in vivo*.

One translational advantage of the Low-Mg^{2+} model, is that it could be a mimic of the clinical conditions of hypomagnesemia associated human epilepsy (Durlach, 1967). In addition, magnesium sulphate is the primary treatment in eclampsia, in which seizures occur in pregnant women complicated with severe hypertension and proteinuria (de Baaij et al., 2015). Our findings suggest that the Low-Mg^{2+} model is also a more ideal *in vitro* model for seizure and epilepsy research, at least in the respect of molecular gene expression, and support the hypothesis that there might exist some commonality in key gene regulators and molecular pathways during epileptogenesis among various epilepsy syndromes. Hence, to seek possible common master regulators and dissect their actions during epilepsy development to advance our understanding of the fundamental mechanisms of epilepsy disorders, and provide great impact on developing therapeutic strategies for treatment, cure and even prevention of epilepsies.

Another obstacle to the investigation of epileptogenesis is that it is difficult to set a series of similar time points for *in vitro* models (i.e. hours/days) that can be compatible with the time course of *in vivo* experiments (i.e. weeks/months). Nevertheless, our data suggest that the pattern of molecular regulation at 72 hours following convulsive agent application for the *in vitro* models corresponding to the subacute to chronic stages of *in vivo* conditions.

8.2 Gene regulation during epileptogenesis is a time-dependent manner

The dynamics of the epileptogenic process and the course of epilepsy disorders involve complicated factors, and the relationships of these factors are not yet well understood. Our data show that the pathological molecular changes of the candidate genes during the development of epilepsy do not correlate to the seizure

activity and severity. A probable explanation is that gene regulation during epileptogenesis is predominantly disease stage-dependent (or disease phase-dependent) instead of seizure activity-dependent. This consequence also implicates that specific crucial genes and molecular mechanisms are driven and operated in different stages of epileptogenesis and time course of epilepsy disorders. Further, this time-dependent manner of regulation can account for, at least in part, the inconsistency and discrepancy in some previous reports since different time points of epileptogenesis and time course of epilepsy were looked at.

However, this study cannot exclude the possibility that there may still have some correlation between a few of the candidate genes and seizure frequency/severity if the number of experimental samples was significantly increased.

8.3 Astrocytes participate in important roles during epileptogenesis

In recent decades, knowledge of astrocyte function has progressed rapidly. Astrocytes serve an important role in maintaining homeostasis of neural network through intimate involvement of diverse neuronal functions including modulation of synaptogenesis, synaptic function and plasticity; tuning the extracellular microenvironment via buffering the concentrations of ions (especially K^+), water and neurotransmitters; and regulating the BBB permeability (Devinsky et al., 2013). Moreover, astrocytes are also important for shepherding newborn dentate granule cells to their final destinations (Shapiro et al., 2005).

Growing evidence has shown acute seizures and epilepsy involve structural and functional changes in astrocytes (Binder and Steinhauser, 2006; Nimmerjahn and Bergles, 2015). Furthermore, a variety of membrane channels, neurotransmitter receptors, transporters, and molecular events expressed in astrocytes have been reported to be altered in epileptic brain tissue (Seifert et al., 2010; Seifert et al., 2006).

GFAP is the major intermediate filament protein and a key component of cytoskeleton in astrocytes. The evidence to date has shown that GFAP not only executes pivotal structural roles in astrocytes, but also is critically involved in a number of astrocytic functions during regeneration, synaptic plasticity and reactive gliosis…etc. (Middeldorp and Hol, 2011), therefore GFAP essentially can be a reliable marker reflecting the reactive response of astrocytes. Here, we looked at the chronological alterations of GFAP expression in the animal model of epilepsy, and demonstrated a striking overexpression of GFAP shown in acute and subacute phases of epileptogenesis. Recent studies have revealed there are different subpopulations of astrocytes expressing distinct GFAP isoforms, which likely contributes to the functional heterogeneity within the astrocyte populations (Martinian et al., 2009; Middeldorp and Hol, 2011).

Several potential mechanisms regarding dysregulation of the reactive astrocytes have been proposed to contribute to epileptogenesis: (1) decreased expression of Kir4.1 ion channels and dysfunction of AQP4 water channels, (2) disruption of gap junctions, (3) alterations of astroglial glutamate transporters (EAAT1, EAAT2), responsible for glutamate uptake, causing the impairment of glutamate clearance from the extracellular space by astrocytes, (4) excessive astrocyte-neuron chemical signalling contributing to dysregulation of gliotransmission and excessive gliotransmitter release by astrocytes, including glutamate, D-serine and ATP, (5) downregulation of glutamine synthetase resulting in reducing conversion of glutamate to glutamine, (6) upregulation of adenosine kinase accelerating metabolism of adenosine, a inhibitory molecule, (7) inducing microvasculature proliferation (angiogenesis) and affecting BBB permeability causing brain extravasation of serum albumin and leukocyte transmigration leading to serial reactions associated with increasing excitability and inflammation, (8) imbalance of proinflammatory, inflammatory and immune molecules (e.g. chemokines and cytokines) released by activated astrocytes decreasing seizure threshold and increasing excitotoxicity (Devinsky et al., 2013; Wetherington et al., 2008).

Indeed, our findings not only agree with, but also strengthen previous reports and the hypothesis that astrocytes play crucial roles in the genesis and progression of epilepsy. Our data further highlight that the astrocytic over-reaction predominantly occurs preceding the well-established epilepsy.

8.4 mTOR dysregulation is strikingly shown in the development of epilepsy

The homeostasis of a neural network is orchestrated via intricate spatial and temporal regulation of diverse molecular pathways resulting in alterations of synaptic strength (synaptic homeostasis) and neuronal firing properties (intrinsic homeostasis) (Turrigiano, 2011). mTOR kinase plays a major role in controlling initiation of mRNA translation which consequently regulates protein synthesis (Chen et al., 2007). In addition, mTOR also regulates a plethora of molecules and enzymes controlling a wide range of cellular functions such as gene transcription, mRNA turnover, protein stability, immune response and so on (Inoki et al., 2005; Lipton and Sahin, 2014). mTOR responds to multiple inputs such as growth factors, amino acids, glutamatergic transmission and the energy state of the cells and acts by regulating a variety of neuronal gene expression including expression of ion channels, neurotransmitter receptors, synaptic plasticity, morphological alterations (Bockaert and Marin, 2015; Goldberg and Coulter, 2013).

Although mTOR over-activation has been strongly linked to epileptogenesis and the pathological activation of the mTOR pathway contributes to the genesis and progression of epilepsy as has been described recently (Figure 8.1), the temporal regulation pattern of mTOR expression during epileptogenesis has not been completely explored. Our present study discloses that the dysregulation of mTOR signalling pathway is most prominent in the subacute stage of epileptogenesis, and consequently it may serve as a master signalling regulator that activates multiple downstream epileptogenic pathways and processes as epileptogenesis progresses.

mTORC1 can be inhibited by rapamycin, whereas mTORC2 is rapamycin-insensitive (Ryther and Wong, 2012). Tang et al. reported that disruption of mTOR translation signalling pathway by rapamycin inhibits BDNF-induced synaptic potentiation in hippocampal slices (Tang et al., 2002). In addition, it has also been proposed that BDNF is a putative upstream activator of mTOR (Talos et al., 2012). Previous studies have revealed that the translation of Kv1.1 mRNA is repressed by mTORC1 kinase activity. They showed that inhibition of mTORC1 kinase activity by rapamycin increased the surface expression of Kv1.1 voltage-gate potassium channel protein on dendrites without altering its axonal expression in hippocampal neurons (Raab-Graham et al., 2006). Sosanya et al. further demonstrated the mechanism of mTORC1 kinase-dependent translational regulation of Kv1.1 mRNA, and suggested the mTORC1 had a role as a molecular switch role for bidirectional changes in dendritic expression of Kv1.1. protein (Sosanya et al., 2013). More recently, several groups have suggested that mTOR overexpression in neurons and glial cells (especially astrocytes) regulates neuroinflammatory and immunologic responses contributing to the mechanisms of epilepsy development (Alyu and Dikmen, 2017; Russo et al., 2014).

There is only subtle upregulation of mTOR in the early stage of epileptogenesis but there is dramatic overexpression of mTOR in the later subacute stage of epileptogenic process in our data. Hence, we suggest that between the early to middle phase of subacute stage of epileptogenesis would potentially be the ideal timing to block the development of epilepsy through mTOR inhibition.

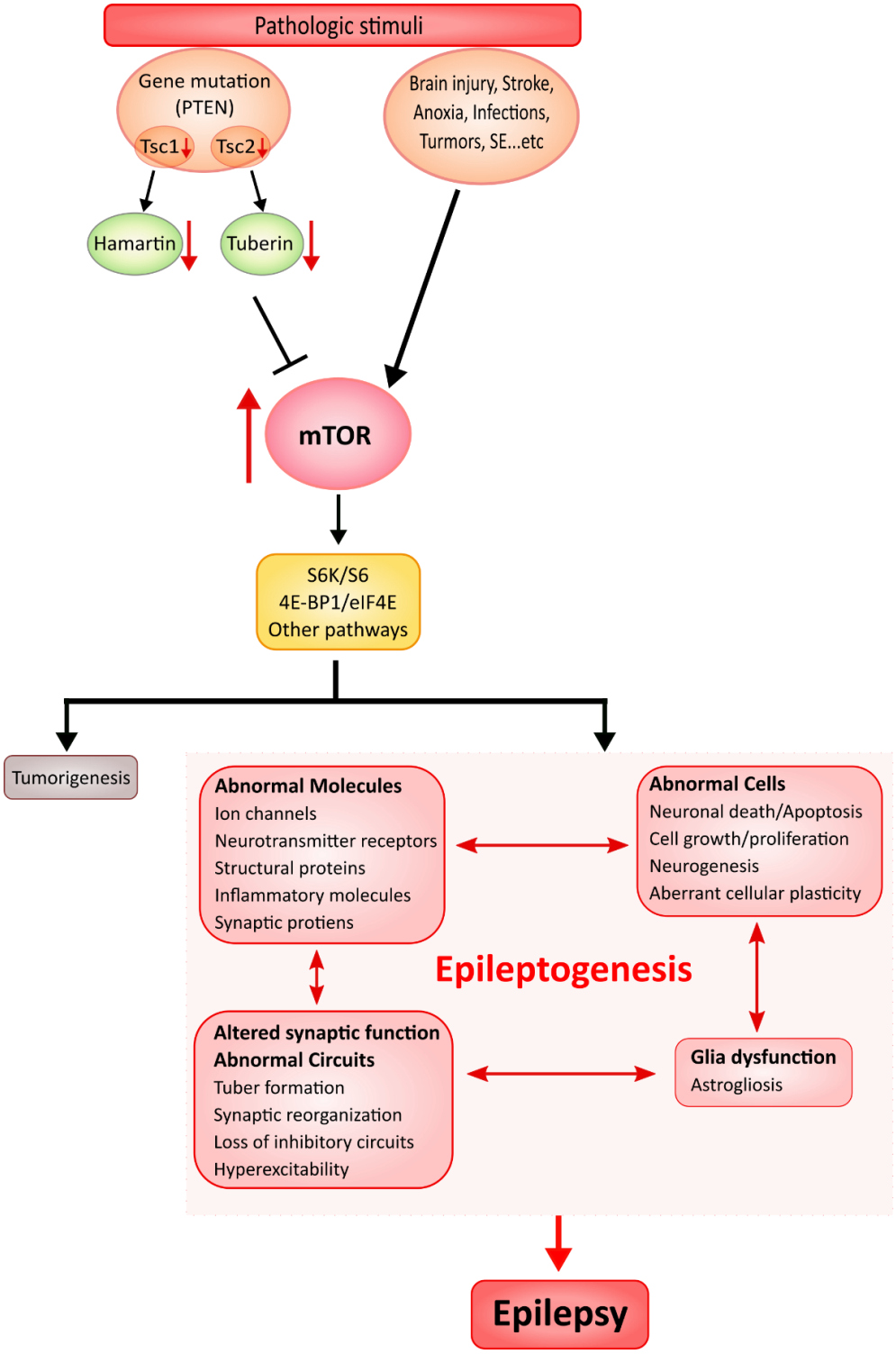

Figure 8.1 Pathophysiological mTOR signalling pathway in epilepsy development

Pathologic over activity of the mTOR pathway with overexpression of mTOR contributing to maladaptive activity of molecular signalling pathways and to cellular changes during epileptogenesis and ultimately leading to the development of epilepsy. Figure is based on (Meng et al., 2013; Vezzani, 2012).

8.5 REST/NRSF signalling pathway is significantly involved during Epileptogenesis

At present, hundreds of neuron-specific genes are known to be regulated by REST/NRSF and many of them code for channel proteins, neurotransmitters, and vesicular transports etc. REST/NRSF represses gene transcription via binding to various co-repressors (e.g. mSin3, CoRest) through both chromatin-dependent mechanisms, by recruitment of histone deacetylase (HDAC), and through chromatin-independent mechanisms (Goldberg and Coulter, 2013; Zhao et al., 2017). Significant up-regulation of REST/NRSF in seizures and epilepsy has been shown in many studies. However, the role of REST/NRSF in epilepsy development is still highly debated. Some studies show that REST/NRSF contributes to epileptogenesis and inhibition of REST/NRSF enables to reduce seizure frequency, whereas other groups argue that up-regulated REST/NRSF serves as a potential compensatory protective effect to inhibit neuronal hyperexcitability and restore the physiological homeostasis.

Reciprocal actions between REST/NRSF and some cytokines, noncoding RNAs (ncRNAs), such as long ncRNAs and microRNAs (epigenetic factors), as well as ubiquitin and REST4 (its own truncated isoform) have been found (Qureshi and Mehler, 2009; Zhao et al., 2017). REST/NRSF represses the expression and function of ncRNAs (e.g. miRNA124a, miRNA-9, miRNA132) which modify various post-transcriptional processes involving RNA processing, editing and trafficking (Conaco et al., 2006; Wu and Xie, 2006). On the other hand, REST/NRSF expression is also tightly regulated by ncRNAs suggesting there are bidirectional feedback loops (Rossbach, 2011). Intriguingly, a recent study revealed that raised expression of REST/NRSF lowers TSC2 (tuberin) levels in the pheochromocytoma neuronal cell line (Tomasoni et al., 2011), which implies there is interplay between REST and mTOR signalling pathways.

Our present study shows that REST/NRSF is up-regulated throughout the epileptogenic process, but is only significantly increased in the subacute stage. Furthermore, it has been demonstrated that the REST/NRSF targets genes modulated

by REST/NRSF in different extents and conditions because of the variable repeat number of RE-1 sequences located in the promotor regions contributing to variable REST/NRSF binding affinity (Bruce et al., 2009). As a result, different levels of REST/NRSF could result in distinct net changes of excitatory and inhibitory gene expression. Herein, we speculate that REST/NESF acts like a “double-edged sword” during the epilepsy formation and may exert either a dominantly pathologic role or a largely protective effect according to the variation of REST/NRSF expression during different stages of epileptogenic process, whereby REST/NRSF can mediate not only cell type-specific but also stage-specific gene expression and repression/activation during epileptogenesis. Given the complexity of REST/NRSF regulation and action, further work is required to clarify this speculation.

8.6 Chronic neuroinflammatory pathways in Epilepsy

Neuroinflammatory mechanisms have frequently been highlighted as one of the principle determinants in generation and exacerbation of epilepsy (Alyu and Dikmen, 2017; Marchi et al., 2014; Vezzani et al., 2011). Even if the development of epilepsy is likely to involve both acute and chronic inflammatory mechanisms, so far, most studies focus on acute neuroinflammation and seizure-related immune response. Several key inflammatory and immune mediators including cytokines and chemokines produced by glial cells and/or neurons are activated during epileptogenic process. Among numerous inflammatory processes, IL-1β/Toll-like receptor signalling and CCL2/CCR2 signalling pathways have been most frequently emphasized.

Our data indicate that CCL2 signalling is mainly involved in the chronic neuroinflammatory pathway during the epileptogenesis cascade. Similarly, Xu et al. reported induced expression of CCL2 (also known as MCP-1) in hippocampal reactive astrocytes and blood vessels at late time point (2 months) after pilocarpine induced SE (Xu et al., 2009). Growing evidence shows that upregulation of CCL2 is potentially related to changes in BBB permeability (Yao and Tsirka, 2014), as well as to direct

leukocyte trafficking and recruitment during epileptogenic process (Fabene et al., 2010). Furthermore, other potential actions of CCL2 in the mechanisms of epilepsy have been described, such as directly increasing neuronal excitability by altering Ca^{2+} signalling or by enhancing excitatory post synaptic currents, and CCL2 might induce other inflammatory mediators (e.g. IL-1β) which consequently promote seizures (Bozzi and Caleo, 2016).

Since both CCL2 and mTOR overexpression have also been shown in human TSC, focal cortical dysplasia II, mTLE and in many animal models of epilepsy, it would be valuable to explore whether and the interaction between mTOR and CCL2 signalling pathways, as this may provide important perspective for further uncovering the molecular mechanisms of epileptogenesis.

8.7 Conclusions & Perspectives

Genes are selectively and differentially regulated at different stages of the epileptogenic process. Gene expression in the time course of epileptogenesis and their net spatiotemporal alterations critically determine the underlying molecular and cellular mechanisms of epilepsy. Among the commonly used *in vitro* models, gene regulation in Low-Mg^{2+} model is most similar to our *in vivo* model of epilepsy. Our work highlights that mTOR, and REST signalling pathways, as well as GFAP act pivotal roles as epileptogenesis progresses, particularly in early and middle phases. Moreover, CCL2 related chronic neuroinflammation is a key regulator during the late stage in the epileptogenic process. Further, the changes of gene regulation during epileptogenesis occur in a time-dependent (disease-phase dependent) manner rather than seizure activity-dependent.

This study also provides a suggestion for when could be the best time points to target the different regulators to block the progression of epilepsy disorders. However, further investigations are required to determine the interplay and the

causal relationships among these master genes and their functional pathways during the process of epilepsy development.

8.8 Future Directions

Exploring and identifying the dynamic alterations of gene expression and the molecular mechanisms of epilepsy is crucial for developing “anti-epileptic” and “anti-epileptogenesis” therapy for the disease-modifying treatments of epilepsy disorders. In this thesis, we have characterised the dynamic gene regulation during epileptogenesis and determined several potential master regulators. In the following work, it would be important to dissect what are the genuine roles of these markers in epileptogenic process, which of the gene changes is causal or consequential, and how these functional changes contribute to epileptogenesis and which are compensatory phenomena. As targeting these potential master regulators, particularly REST and mTOR, during the progress of epilepsy is like a “double-edged sword” with both pro- and anti-epileptic effects, the roles of these regulatory changes need to be very precisely understood prior to manipulating their spatiotemporal expression in epilepsy. Thus, in addition to the temporal regulation, characterising the gene regulation in different cell subtypes (the spatial alterations), as well as their reciprocal actions and the interplay of these pivotal signalling pathways with the associated upstream modulators and target downstream mediators will provide a foundation to determine how to manipulate these key regulators. Furthermore, due to the dynamics of mRNA expression and translation of these changes may not completely reflect the expression of functional protein, it is also essential to elucidate that whether the protein expression profile is similar to the dynamic mRNA expression.

Although there is still a lack of optimal experimental models that can faithfully reflect the chronic disorders of human epilepsy syndromes, it is still valuable to develop *in vivo* models of epilepsy to improve our understanding of the mechanisms of the disease and to identify novel therapeutic strategies. I am continuing to analyse the EEG and seizure manifestations for the rat intra-amygdala K.A. model of epilepsy and will try to establish the optimal protocol to better apply for investigating the mechanisms of epilepsy, and serve as a suitable preclinical model in epilepsy research, particularly for epilepsy gene therapy.

Bibliography

Abend, N.S., and Wusthoff, C.J. (2012). Neonatal Seizures and Status Epilepticus. J Clin Neurophysiol *29*, 441-448.

Albertson, A.J., Williams, S.B., and Hablitz, J.J. (2013). Regulation of epileptiform discharges in rat neocortex by HCN channels. Journal of neurophysiology *110*, 1733-1743.

Albus, U., and Habermann, E. (1983). Tetanus toxin inhibits the evoked outflow of an inhibitory (GABA) and an excitatory (D-aspartate) amino acid from particulate brain cortex. Toxicon : official journal of the International Society on Toxinology *21*, 97-110.

Alyu, F., and Dikmen, M. (2017). Inflammatory aspects of epileptogenesis: contribution of molecular inflammatory mechanisms. Acta Neuropsychiatr *29*, 1-16.

Anderson, W.W., Lewis, D.V., Swartzwelder, H.S., and Wilson, W.A. (1986). Magnesium-free medium activates seizure-like events in the rat hippocampal slice. Brain Res *398*, 215-219.

Andjelkovic, A.V., and Pachter, J.S. (2000). Characterization of binding sites for chemokines MCP-1 and MIP-1alpha on human brain microvessels. Journal of neurochemistry *75*, 1898-1906.

Antonucci, F., Corradini, I., Fossati, G., Tomasoni, R., Menna, E., and Matteoli, M. (2016). SNAP-25, a Known Presynaptic Protein with Emerging Postsynaptic Functions. Front Synaptic Neurosci *8*, 7.

Aoki, H., Hara, A., Era, T., Kunisada, T., and Yamada, Y. (2012). Genetic ablation of Rest leads to in vitro-specific derepression of neuronal genes during neurogenesis. Development *139*, 667-677.

Avanzini, G. (1995). Animal models relevant to human epilepsies. Italian journal of neurological sciences *16*, 5-8.

Avanzini, G., and Franceschetti, S. (2003). Cellular biology of epileptogenesis. The Lancet Neurology *2*, 33-42.

Bacci, A., Huguenard, J.R., and Prince, D.A. (2003). Functional autaptic neurotransmission in fast-spiking interneurons: a novel form of feedback inhibition in the neocortex. The Journal of neuroscience : the official journal of the Society for Neuroscience *23*, 859-866.

Badawy, R.A., Harvey, A.S., and Macdonell, R.A. (2009a). Cortical hyperexcitability and epileptogenesis: understanding the mechanisms of epilepsy - part 1. J Clin Neurosci *16*, 355-365.

Badawy, R.A., Harvey, A.S., and Macdonell, R.A. (2009b). Cortical hyperexcitability and epileptogenesis: Understanding the mechanisms of epilepsy - part 2. J Clin Neurosci *16*, 485-500.

Bagdy, G., Kecskemeti, V., Riba, P., and Jakus, R. (2007). Serotonin and epilepsy. Journal of neurochemistry *100*, 857-873.

Bale, T.L., Baram, T.Z., Brown, A.S., Goldstein, J.M., Insel, T.R., McCarthy, M.M., Nemeroff, C.B., Reyes, T.M., Simerly, R.B., Susser, E.S.*, et al.* (2010). Early life programming and neurodevelopmental disorders. Biological psychiatry *68*, 314-319.

Balestrino, M., Aitken, P.G., and Somjen, G.G. (1986). The effects of moderate changes of extracellular K+ and Ca2+ on synaptic and neural function in the CA1 region of the hippocampal slice. Brain Res *377*, 229-239.

Ballas, N., Grunseich, C., Lu, D.D., Speh, J.C., and Mandel, G. (2005). REST and its corepressors mediate plasticity of neuronal gene chromatin throughout neurogenesis. Cell *121*, 645-657.

Banerjee, P.N., Filippi, D., and Allen Hauser, W. (2009). The descriptive epidemiology of epilepsy-a review. Epilepsy research *85*, 31-45.

Barnard, E. (2001). The molecular architecture if $GABA_A$ receptors. In:Mohler H, ed. Pharmacology of GABA and glycine neurotransmission. Handbook of Experimental Pharmacology 150 Berline: Springer, 94-100.

Baruscotti, M., Bottelli, G., Milanesi, R., DiFrancesco, J.C., and DiFrancesco, D. (2010). HCN-related channelopathies. Pflugers Archiv : European journal of physiology *460*, 405-415.

Bates-Withers, C., Sah, R., and Clapham, D.E. (2011). TRPM7, the Mg(2+) inhibited channel and kinase. Advances in experimental medicine and biology *704*, 173-183.

Ben-Ari, Y. (1985). Limbic seizure and brain damage produced by kainic acid: mechanisms and relevance to human temporal lobe epilepsy. Neuroscience *14*, 375-403.

Ben-Ari, Y., and Cossart, R. (2000). Kainate, a double agent that generates seizures: two decades of progress. Trends in neurosciences *23*, 580-587.

Ben-Ari, Y., Lagowska, J., Tremblay, E., and Le Gal La Salle, G. (1979a). A new model of focal status epilepticus: intra-amygdaloid application of kainic acid elicits repetitive secondarily generalized convulsive seizures. Brain Res *163*, 176-179.

Ben-Ari, Y., Tremblay, E., Berger, M., and Nitecka, L. (1984). Kainic acid seizure syndrome and binding sites in developing rats. Brain Res *316*, 284-288.

Ben-Ari, Y., Tremblay, E., and Ottersen, O.P. (1979b). [Primary and secondary cerebral lesions produced by kainic acid injections in the rat]. Comptes rendus des seances de l'Academie des sciences Serie D, Sciences naturelles *288*, 991-994.

Ben-Ari, Y., Tremblay, E., and Ottersen, O.P. (1980a). Injections of kainic acid into the amygdaloid complex of the rat: an electrographic, clinical and histological study in relation to the pathology of epilepsy. Neuroscience *5*, 515-528.

Ben-Ari, Y., Tremblay, E., Ottersen, O.P., and Meldrum, B.S. (1980b). The role of epileptic activity in hippocampal and "remote" cerebral lesions induced by kainic acid. Brain Res *191*, 79-97.

Ben-Ari, Y., Tremblay, E., Riche, D., Ghilini, G., and Naquet, R. (1981). Electrographic, clinical and pathological alterations following systemic administration of kainic acid, bicuculline or pentetrazole: metabolic mapping using the deoxyglucose method with special reference to the pathology of epilepsy. Neuroscience *6*, 1361-1391.

Bender, R.A., Soleymani, S.V., Brewster, A.L., Nguyen, S.T., Beck, H., Mathern, G.W., and Baram, T.Z. (2003). Enhanced expression of a specific hyperpolarization-activated cyclic nucleotide-gated cation channel (HCN) in surviving dentate gyrus granule cells of human and experimental epileptic hippocampus. The Journal of neuroscience : the official journal of the Society for Neuroscience *23*, 6826-6836.

Benini, R., Roth, R., Khoja, Z., Avoli, M., and Wintermark, P. (2016). Does angiogenesis play a role in the establishment of mesial temporal lobe epilepsy? International journal of developmental neuroscience : the official journal of the International Society for Developmental Neuroscience *49*, 31-36.

Benn, C.L., Fox, H., and Bates, G.P. (2008). Optimisation of region-specific reference gene selection and relative gene expression analysis methods for pre-clinical trials of Huntington's disease. Mol Neurodegener *3*, 17.

Berg, A.T., Berkovic, S.F., Brodie, M.J., Buchhalter, J., Cross, J.H., van Emde Boas, W., Engel, J., French, J., Glauser, T.A., Mathern, G.W.*, et al.* (2010). Revised terminology and concepts for organization of seizures and epilepsies: report of the ILAE Commission on Classification and Terminology, 2005-2009. Epilepsia *51*, 676-685.

Bernard, C. (2012). Alternations in synaptic function in epilepsy. In Jasper's Basic Mechanisms of the Epilepsies, J.L. Noebels, M. Avoli, M.A. Rogawski, R.W. Olsen, and A.V. Delgado-Escueta, eds.

Bialer, M., and White, H.S. (2010). Key factors in the discovery and development of new antiepileptic drugs. Nat Rev Drug Discov *9*, 68-82.

Binder, D.K. (2004). The role of BDNF in epilepsy and other diseases of the mature nervous system. Advances in experimental medicine and biology *548*, 34-56.

Binder, D.K. (2009). Role of BDNF in Animal Models of Epilepsy. Encyclopedia of Basic Epilepsy Research, Vols 1-3, 936-941.

Binder, D.K., Croll, S.D., Gall, C.M., and Scharfman, H.E. (2001). BDNF and epilepsy: too much of a good thing? Trends in neurosciences *24*, 47-53.

Binder, D.K., and Steinhauser, C. (2006). Functional changes in astroglial cells in epilepsy. Glia *54*, 358-368.

Blair, R.E., Sombati, S., Lawrence, D.C., McCay, B.D., and DeLorenzo, R.J. (2004). Epileptogenesis causes acute and chronic increases in GABAA receptor endocytosis that contributes to the induction and maintenance of seizures in the hippocampal culture model of acquired epilepsy. The Journal of pharmacology and experimental therapeutics *310*, 871-880.

Blum, R., and Konnerth, A. (2005). Neurotrophin-mediated rapid signaling in the central nervous system: mechanisms and functions. Physiology *20*, 70-78.

Bockaert, J., and Marin, P. (2015). mTOR in Brain Physiology and Pathologies. Physiological reviews *95*, 1157-1187.

Boison, D. (2008). The adenosine kinase hypothesis of epileptogenesis. Progress in neurobiology *84*, 249-262.

Bonin, R.P., Zurek, A.A., Yu, J., Bayliss, D.A., and Orser, B.A. (2013). Hyperpolarization-activated current (In) is reduced in hippocampal neurons from Gabra5-/- mice. PloS one *8*, e58679.

Borges, K., Gearing, M., McDermott, D.L., Smith, A.B., Almonte, A.G., Wainer, B.H., and Dingledine, R. (2003). Neuronal and glial pathological changes during epileptogenesis in the mouse pilocarpine model. Exp Neurol *182*, 21-34.

Bothwell, S., Meredith, G.E., Phillips, J., Staunton, H., Doherty, C., Grigorenko, E., Glazier, S., Deadwyler, S.A., O'Donovan, C.A., and Farrell, M. (2001). Neuronal hypertrophy in the neocortex of patients with temporal lobe epilepsy. The Journal of neuroscience : the official journal of the Society for Neuroscience *21*, 4789-4800.

Bourne, J.N., and Harris, K.M. (2008). Balancing structure and function at hippocampal dendritic spines. Annu Rev Neurosci *31*, 47-67.

Bozzi, Y., and Borrelli, E. (2013). The role of dopamine signaling in epileptogenesis. Front Cell Neurosci *7*, 157.

Bozzi, Y., and Caleo, M. (2016). Epilepsy, Seizures, and Inflammation: Role of the C-C Motif Ligand 2 Chemokine. DNA Cell Biol *35*, 257-260.

Bozzi, Y., Dunleavy, M., and Henshall, D.C. (2011). Cell signaling underlying epileptic behavior. Front Behav Neurosci *5*, 45.

Brandt, C., Potschka, H., Loscher, W., and Ebert, U. (2003). N-methyl-D-aspartate receptor blockade after status epilepticus protects against limbic brain damage but not against epilepsy in the kainate model of temporal lobe epilepsy. Neuroscience *118*, 727-740.

Brener, K., Amitai, Y., Jefferys, J.G., and Gutnick, M.J. (1991). Chronic epileptic foci in neocortex: in vivo and in vitro effects of tetanus toxin. The European journal of neuroscience *3*, 47-54.

Brewster, A.L., Bernard, J.A., Gall, C.M., and Baram, T.Z. (2005). Formation of heteromeric hyperpolarization-activated cyclic nucleotide-gated (HCN) channels in the hippocampus is regulated by developmental seizures. Neurobiology of disease *19*, 200-207.

Brill, J., and Huguenard, J.R. (2010). Enhanced infragranular and supragranular synaptic input onto layer 5 pyramidal neurons in a rat model of cortical dysplasia. Cereb Cortex *20*, 2926-2938.

Brima, T., Otahal, J., and Mares, P. (2013). Increased susceptibility to pentetrazol-induced seizures in developing rats after cortical photothrombotic ischemic stroke at P7. Brain Res *1507*, 146-153.

Brooks-Kayal, A.R., Raol, Y.H., and Russek, S.J. (2009). Alteration of epileptogenesis genes. Neurotherapeutics : the journal of the American Society for Experimental NeuroTherapeutics *6*, 312-318.

Brooks-Kayal, A.R., Shumate, M.D., Jin, H., Rikhter, T.Y., and Coulter, D.A. (1998). Selective changes in single cell GABA(A) receptor subunit expression and function in temporal lobe epilepsy. Nature medicine *4*, 1166-1172.

Brooks, V.B., and Asanuma, H. (1962). Action of tetanus toxin in the cerebral cortex. Science *137*, 674-676.

Bruce, A.W., Lopez-Contreras, A.J., Flicek, P., Down, T.A., Dhami, P., Dillon, S.C., Koch, C.M., Langford, C.F., Dunham, I., Andrews, R.M.*, et al.* (2009). Functional diversity for REST (NRSF) is defined by in vivo binding affinity hierarchies at the DNA sequence level. Genome research *19*, 994-1005.

Buckmaster, P.S. (2004). Laboratory animal models of temporal lobe epilepsy. Comparative medicine *54*, 473-485.

Buckmaster, P.S., and Lew, F.H. (2011). Rapamycin suppresses mossy fiber sprouting but not seizure frequency in a mouse model of temporal lobe epilepsy. The Journal of neuroscience : the official journal of the Society for Neuroscience *31*, 2337-2347.

Burnashev, N., Schoepfer, R., Monyer, H., Ruppersberg, J.P., Gunther, W., Seeburg, P.H., and Sakmann, B. (1992). Control by asparagine residues of calcium permeability and magnesium blockade in the NMDA receptor. Science *257*, 1415-1419.

Bustin, S.A., Benes, V., Garson, J.A., Hellemans, J., Huggett, J., Kubista, M., Mueller, R., Nolan, T., Pfaffl, M.W., Shipley, G.L*., et al.* (2009). The MIQE guidelines: minimum information for publication of quantitative real-time PCR experiments. Clin Chem *55*, 611-622.

Calderone, A., Jover, T., Noh, K.M., Tanaka, H., Yokota, H., Lin, Y., Grooms, S.Y., Regis, R., Bennett, M.V., and Zukin, R.S. (2003). Ischemic insults derepress the gene silencer REST in neurons destined to die. The Journal of neuroscience : the official journal of the Society for Neuroscience *23*, 2112-2121.

Caputi, A., Melzer, S., Michael, M., and Monyer, H. (2013). The long and short of GABAergic neurons. Current opinion in neurobiology *23*, 179-186.

Casillas-Espinosa, P.M., Powell, K.L., and O'Brien, T.J. (2012). Regulators of synaptic transmission: roles in the pathogenesis and treatment of epilepsy. Epilepsia *53 Suppl 9*, 41-58.

Cavalheiro, E.A., Riche, D.A., and Le Gal La Salle, G. (1982). Long-term effects of intrahippocampal kainic acid injection in rats: a method for inducing spontaneous recurrent seizures. Electroencephalography and clinical neurophysiology *53*, 581-589.

Cendes, F. (2005). Mesial temporal lobe epilepsy syndrome: an updated overview. Journal of Epilepsy and Clinical Neurophysiology *11*, 141-144.

Chang, P., Hashemi, K.S., and Walker, M.C. (2011). A novel telemetry system for recording EEG in small animals. Journal of neuroscience methods *201*, 106-115.

Chavko, M., Nadi, N.S., and Keyser, D.O. (2002). Activation of BDNF mRNA and protein after seizures in hyperbaric oxygen: implications for sensitization to seizures in re-exposures. Neurochemical research *27*, 1649-1653.

Chen, J.W., and Wasterlain, C.G. (2006). Status epilepticus: pathophysiology and management in adults. The Lancet Neurology *5*, 246-256.

Chen, K., Aradi, I., Thon, N., Eghbal-Ahmadi, M., Baram, T.Z., and Soltesz, I. (2001). Persistently modified h-channels after complex febrile seizures convert the seizure-induced enhancement of inhibition to hyperexcitability. Nature medicine *7*, 331-337.

Chen, S., Atkins, C.M., Liu, C.L., Alonso, O.F., Dietrich, W.D., and Hu, B.R. (2007). Alterations in mammalian target of rapamycin signaling pathways after traumatic brain injury. Journal of cerebral blood flow and metabolism : official journal of the International Society of Cerebral Blood Flow and Metabolism *27*, 939-949.

Chen, Z.F., Paquette, A.J., and Anderson, D.J. (1998). NRSF/REST is required in vivo for repression of multiple neuronal target genes during embryogenesis. Nature genetics *20*, 136-142.

Cho, C.H. (2012). Molecular mechanism of circadian rhythmicity of seizures in temporal lobe epilepsy. Front Cell Neurosci *6*, 55.

Clasadonte, J., and Haydon, P.G. (2012). Astrocytes and Epilepsy. In Jasper's Basic Mechanisms of the Epilepsies, J.L. Noebels, M. Avoli, M.A. Rogawski, R.W. Olsen, and A.V. Delgado-Escueta, eds. (Bethesda (MD)).

Cohen-Gadol, A.A., Pan, J.W., Kim, J.H., Spencer, D.D., and Hetherington, H.H. (2004). Mesial temporal lobe epilepsy: a proton magnetic resonance spectroscopy study and a histopathological analysis. J Neurosurg *101*, 613-620.

Collingridge, G.L., and Lester, R.A. (1989). Excitatory amino acid receptors in the vertebrate central nervous system. Pharmacological reviews *41*, 143-210.

Collingridge, G.L., and McLennan, H. (1981). The effect of kainic acid on excitatory synaptic activity in the rat hippocampal slice preparation. Neuroscience letters *27*, 31-36.

Conaco, C., Otto, S., Han, J.J., and Mandel, G. (2006). Reciprocal actions of REST and a microRNA promote neuronal identity. Proceedings of the National Academy of Sciences of the United States of America *103*, 2422-2427.

Cook, N.L., Vink, R., Donkin, J.J., and van den Heuvel, C. (2009). Validation of reference genes for normalization of real-time quantitative RT-PCR data in traumatic brain injury. Journal of neuroscience research *87*, 34-41.

Cossart, R., Dinocourt, C., Hirsch, J.C., Merchan-Perez, A., De Felipe, J., Ben-Ari, Y., Esclapez, M., and Bernard, C. (2001). Dendritic but not somatic GABAergic inhibition is decreased in experimental epilepsy. Nature neuroscience *4*, 52-62.

Cossart, R., Esclapez, M., Hirsch, J.C., Bernard, C., and Ben-Ari, Y. (1998). GluR5 kainate receptor activation in interneurons increases tonic inhibition of pyramidal cells. Nature neuroscience *1*, 470-478.

Cox, J.H., Seri, S., and Cavanna, A.E. (2014). Clinical utility of implantable neurostimulation devices as adjunctive treatment of uncontrolled seizures. Neuropsychiatric disease and treatment *10*, 2191-2200.

Da Silva, F.H., Gorter, J.A., and Wadman, W.J. (2012). Epilepsy as a dynamic disease of neuronal networks. Handbook of clinical neurology *107*, 35-62.

Dawodu, S., and Thom, M. (2005). Quantitative neuropathology of the entorhinal cortex region in patients with hippocampal sclerosis and temporal lobe epilepsy. Epilepsia *46*, 23-30.

de Baaij, J.H., Hoenderop, J.G., and Bindels, R.J. (2015). Magnesium in man: implications for health and disease. Physiological reviews *95*, 1-46.

De Deyn, P.P., D'Hooge, R., Marescau, B., and Pei, Y.Q. (1992). Chemical models of epilepsy with some reference to their applicability in the development of anticonvulsants. Epilepsy research *12*, 87-110.

de Vries, E.E., van den Munckhof, B., Braun, K.P., van Royen-Kerkhof, A., de Jager, W., and Jansen, F.E. (2016). Inflammatory mediators in human epilepsy: A systematic review and meta-analysis. Neuroscience and biobehavioral reviews *63*, 177-190.

Debanne, D., Guerineau, N.C., Gahwiler, B.H., and Thompson, S.M. (1995). Physiology and pharmacology of unitary synaptic connections between pairs of cells in areas CA3 and CA1 of rat hippocampal slice cultures. Journal of neurophysiology *73*, 1282-1294.

Decollogne, S., Tomas, A., Lecerf, C., Adamowicz, E., and Seman, M. (1997). NMDA receptor complex blockade by oral administration of magnesium: comparison with MK-801. Pharmacology, biochemistry, and behavior *58*, 261-268.

Deitch J.S., and Fischer, I. (1999). The neuron in tissue culture. In Hippocampus. Chichester ; New York : John Wiley, pp. 531-539.

Dello Russo, C., Lisi, L., Feinstein, D.L., and Navarra, P. (2013). mTOR kinase, a key player in the regulation of glial functions: relevance for the therapy of multiple sclerosis. Glia *61*, 301-311.

DeLorenzo, R.J. (2006). Epidemiology and clinical presentation of status epilepticus. Advances in neurology *97*, 199-215.

DeLorenzo, R.J., Pal, S., and Sombati, S. (1998). Prolonged activation of the N-methyl-D-aspartate receptor-Ca2+ transduction pathway causes spontaneous recurrent epileptiform discharges in hippocampal neurons in culture. Proceedings of the National Academy of Sciences of the United States of America *95*, 14482-14487.

DeLorenzo, R.J., Sun, D.A., Blair, R.E., and Sombati, S. (2007). An in vitro model of stroke-induced epilepsy: elucidation of the roles of glutamate and calcium in the induction and maintenance of stroke-induced epileptogenesis. International review of neurobiology *81*, 59-84.

Devinsky, O., Vezzani, A., Najjar, S., De Lanerolle, N.C., and Rogawski, M.A. (2013). Glia and epilepsy: excitability and inflammation. Trends in neurosciences *36*, 174-184.

Di Maio, R. (2014). Neuronal mechanisms of epileptogenesis. Front Cell Neurosci *8*, 29.

Dichter, M.A. (1978). Rat cortical neurons in cell culture: culture methods, cell morphology, electrophysiology, and synapse formation. Brain Res *149*, 279-293.

Dreier, J.P., Zhang, C.L., and Heinemann, U. (1998). Phenytoin, phenobarbital, and midazolam fail to stop status epilepticus-like activity induced by low magnesium in

rat entorhinal slices, but can prevent its development. Acta neurologica Scandinavica *98*, 154-160.

Dube, C., Richichi, C., Bender, R.A., Chung, G., Litt, B., and Baram, T.Z. (2006). Temporal lobe epilepsy after experimental prolonged febrile seizures: prospective analysis. Brain : a journal of neurology *129*, 911-922.

Duggan, M.J., and Stephenson, F.A. (1990). Biochemical evidence for the existence of gamma-aminobutyrateA receptor iso-oligomers. The Journal of biological chemistry *265*, 3831-3835.

Durlach, J. (1967). [Apropos of a case of the "epileptic" form of latent tetany due to a magnesium deficiency]. Revue neurologique *117*, 189-196.

Dyhrfjeld-Johnsen, J., Morgan, R.J., Foldy, C., and Soltesz, I. (2008). Upregulated H-current in hyperexcitable CA1 dendrites after febrile seizures. Front Cell Neurosci *2*, 2.

Elger, C.E., and Schmidt, D. (2008). Modern management of epilepsy: a practical approach. Epilepsy & behavior : E&B *12*, 501-539.

Empson, R.M., Amitai, Y., Jefferys, J.G., and Gutnick, M.J. (1993). Injection of tetanus toxin into the neocortex elicits persistent epileptiform activity but only transient impairment of GABA release. Neuroscience *57*, 235-239.

Engel, J., Jr. (1992). Experimental animal models of epilepsy: classification and relevance to human epileptic phenomena. Epilepsy research Supplement *8*, 9-20.

Engel, J., Jr. (2011). The etiologic classification of epilepsy. Epilepsia *52*, 1195-1197; discussion 1205-1199.

Engel, J., Jr., and International League Against, E. (2001). A proposed diagnostic scheme for people with epileptic seizures and with epilepsy: report of the ILAE Task Force on Classification and Terminology. Epilepsia *42*, 796-803.

Engel, J., Jr., and Pedley, T.A. (1997). Epilepsy: Aa comphrensive Textbook

Vol vol 1, 2, and 3 (Philadephia: Lippincott-Raven).

Engel, J.J. (2009). Model Characterization in Relationship to Human Disorders, Vol 2 (Elsevier Ltd).

Fabene, P.F., Bramanti, P., and Constantin, G. (2010). The emerging role for chemokines in epilepsy. J Neuroimmunol *224*, 22-27.

Fabene, P.F., Laudanna, C., and Constantin, G. (2013). Leukocyte trafficking mechanisms in epilepsy. Mol Immunol *55*, 100-104.

Fabene, P.F., Navarro Mora, G., Martinello, M., Rossi, B., Merigo, F., Ottoboni, L., Bach, S., Angiari, S., Benati, D., Chakir, A.*, et al.* (2008). A role for leukocyte-endothelial adhesion mechanisms in epilepsy. Nature medicine *14*, 1377-1383.

Farrar, J.J., Yen, L.M., Cook, T., Fairweather, N., Binh, N., Parry, J., and Parry, C.M. (2000). Tetanus. Journal of neurology, neurosurgery, and psychiatry *69*, 292-301.

Ferecsko, A.S., Jiruska, P., Foss, L., Powell, A.D., Chang, W.C., Sik, A., and Jefferys, J.G. (2015). Structural and functional substrates of tetanus toxin in an animal model of temporal lobe epilepsy. Brain Struct Funct *220*, 1013-1029.

Finnerty, G.T., and Jefferys, J.G. (2000). 9-16 Hz oscillation precedes secondary generalization of seizures in the rat tetanus toxin model of epilepsy. Journal of neurophysiology *83*, 2217-2226.

Finnerty, G.T., and Jefferys, J.G. (2002). Investigation of the neuronal aggregate generating seizures in the rat tetanus toxin model of epilepsy. Journal of neurophysiology *88*, 2919-2927.

Fisher, R.S. (1989). Animal models of the epilepsies. Brain research Brain research reviews *14*, 245-278.

Fisher, R.S. (2012). Therapeutic devices for epilepsy. Annals of neurology *71*, 157-168.

Fisher, R.S., Acevedo, C., Arzimanoglou, A., Bogacz, A., Cross, J.H., Elger, C.E., Engel, J., Jr., Forsgren, L., French, J.A., Glynn, M.*, et al.* (2014a). ILAE official report: a practical clinical definition of epilepsy. Epilepsia *55*, 475-482.

Fisher, R.S., and Alger, B.E. (1984). Electrophysiological mechanisms of kainic acid-induced epileptiform activity in the rat hippocampal slice. The Journal of neuroscience : the official journal of the Society for Neuroscience *4*, 1312-1323.

Fisher, R.S., Cross, J.H., D'Souza, C., French, J.A., Haut, S.R., Higurashi, N., Hirsch, E., Jansen, F.E., Lagae, L., Moshe, S.L.*, et al.* (2017a). Instruction manual for the ILAE 2017 operational classification of seizure types. Epilepsia.

Fisher, R.S., Cross, J.H., French, J.A., Higurashi, N., Hirsch, E., Jansen, F.E., Lagae, L., Moshe, S.L., Peltola, J., Roulet Perez, E.*, et al.* (2017b). Operational classification of seizure types by the International League Against Epilepsy: Position Paper of the ILAE Commission for Classification and Terminology. Epilepsia.

Fisher, R.S., Harding, G., Erba, G., Barkley, G.L., Wilkins, A., and Epilepsy Foundation of America Working, G. (2005a). Photic- and pattern-induced seizures: a review for the Epilepsy Foundation of America Working Group. Epilepsia *46*, 1426-1441.

Fisher, R.S., Scharfman, H.E., and Decurtis, M. (2014b). How Can We Identify Ictal and Interictal Abnormal Activity? Issues in Clinical Epileptology: A View from the Bench *813*, 3-23.

Fisher, R.S., van Emde Boas, W., Blume, W., Elger, C., Genton, P., Lee, P., and Engel, J., Jr. (2005b). Epileptic seizures and epilepsy: definitions proposed by the International League Against Epilepsy (ILAE) and the International Bureau for Epilepsy (IBE). Epilepsia *46*, 470-472.

Fitzgerald, L.R., Vaidya, V.A., Terwilliger, R.Z., and Duman, R.S. (1996). Electroconvulsive seizure increases the expression of CREM (cyclic AMP response element modulator) and ICER (inducible cyclic AMP early repressor) in rat brain. Journal of neurochemistry *66*, 429-432.

Fleige, S., and Pfaffl, M.W. (2006). RNA integrity and the effect on the real-time qRT-PCR performance. Mol Aspects Med *27*, 126-139.

Foresti, M.L., Arisi, G.M., Katki, K., Montanez, A., Sanchez, R.M., and Shapiro, L.A. (2009). Chemokine CCL2 and its receptor CCR2 are increased in the hippocampus following pilocarpine-induced status epilepticus. J Neuroinflammation *6*, 40.

Frerking, M., Malenka, R.C., and Nicoll, R.A. (1998a). Brain-derived neurotrophic factor (BDNF) modulates inhibitory, but not excitatory, transmission in the CA1 region of the hippocampus. Journal of neurophysiology *80*, 3383-3386.

Frerking, M., Malenka, R.C., and Nicoll, R.A. (1998b). Synaptic activation of kainate receptors on hippocampal interneurons. Nature neuroscience *1*, 479-486.

Friedman, A., Kaufer, D., and Heinemann, U. (2009). Blood-brain barrier breakdown-inducing astrocytic transformation: novel targets for the prevention of epilepsy. Epilepsy research *85*, 142-149.

Fujikawa, D.G. (1996). The temporal evolution of neuronal damage from pilocarpine-induced status epilepticus. Brain Res *725*, 11-22.

Fujikawa, D.G. (2005). Prolonged seizures and cellular injury: understanding the connection. Epilepsy & behavior : E&B *7 Suppl 3*, S3-11.

G. Fritsch, and Hitzig, E. (1870). Ueber die elektrische Erregbarkeit des Grosshirns. *Archiv fur Anatomie, Physiologie und Wissenschaftliche Medicin 37*, 300-332.

Gabernet, L., Jadhav, S.P., Feldman, D.E., Carandini, M., and Scanziani, M. (2005). Somatosensory integration controlled by dynamic thalamocortical feed-forward inhibition. Neuron *48*, 315-327.

Galanopoulou, A.S., Buckmaster, P.S., Staley, K.J., Moshe, S.L., Perucca, E., Engel, J., Jr., Loscher, W., Noebels, J.L., Pitkanen, A., Stables, J.*, et al.* (2012a). Identification of new epilepsy treatments: issues in preclinical methodology. Epilepsia *53*, 571-582.

Galanopoulou, A.S., Gorter, J.A., and Cepeda, C. (2012b). Finding a better drug for epilepsy: the mTOR pathway as an antiepileptogenic target. Epilepsia *53*, 1119-1130.

Gall, C.M. (1993). Seizure-induced changes in neurotrophin expression: implications for epilepsy. Exp Neurol *124*, 150-166.

Galvan, M., Grafe, P., and ten Bruggencate, G. (1982). Convulsant actions of 4-aminopyridine on the guinea-pig olfactory cortex slice. Brain Res *241*, 75-86.

Garcia Garcia, M.E., Garcia Morales, I., and Matias Guiu, J. (2010). [Experimental models in epilepsy]. Neurologia *25*, 181-188.

Garriga-Canut, M., Schoenike, B., Qazi, R., Bergendahl, K., Daley, T.J., Pfender, R.M., Morrison, J.F., Ockuly, J., Stafstrom, C., Sutula, T.*, et al.* (2006). 2-Deoxy-D-glucose reduces epilepsy progression by NRSF-CtBP-dependent metabolic regulation of chromatin structure. Nature neuroscience *9*, 1382-1387.

Gautier, N.M., and Glasscock, E. (2015). Spontaneous seizures in Kcna1-null mice lacking voltage-gated Kv1.1 channels activate Fos expression in select limbic circuits. Journal of neurochemistry *135*, 157-164.

Gibbs, J.W., 3rd, Sombati, S., DeLorenzo, R.J., and Coulter, D.A. (1997). Physiological and pharmacological alterations in postsynaptic GABA(A) receptor function in a hippocampal culture model of chronic spontaneous seizures. Journal of neurophysiology *77*, 2139-2152.

Giorgi, F.S., Malhotra, S., Hasson, H., Veliskova, J., Rosenbaum, D.M., and Moshe, S.L. (2005). Effects of status epilepticus early in life on susceptibility to ischemic injury in adulthood. Epilepsia *46*, 490-498.

Glykys, J., and Mody, I. (2006). Hippocampal network hyperactivity after selective reduction of tonic inhibition in GABA A receptor alpha5 subunit-deficient mice. Journal of neurophysiology *95*, 2796-2807.

Goldberg, E.M., and Coulter, D.A. (2013). Mechanisms of epileptogenesis: a convergence on neural circuit dysfunction. Nature reviews Neuroscience *14*, 337-349.

Gonzalez, M.I., Cruz Del Angel, Y., and Brooks-Kayal, A. (2013). Down-regulation of gephyrin and GABAA receptor subunits during epileptogenesis in the CA1 region of hippocampus. Epilepsia *54*, 616-624.

Goodkin, H.R., Joshi, S., Kozhemyakin, M., and Kapur, J. (2007). Impact of receptor changes on treatment of status epilepticus. Epilepsia *48 Suppl 8*, 14-15.

Gradinaru, V., Mogri, M., Thompson, K.R., Henderson, J.M., and Deisseroth, K. (2009). Optical deconstruction of parkinsonian neural circuitry. Science *324*, 354-359.

Graves, T.D. (2006). Ion channels and epilepsy. QJM : monthly journal of the Association of Physicians *99*, 201-217.

Guenin, S., Mauriat, M., Pelloux, J., Van Wuytswinkel, O., Bellini, C., and Gutierrez, L. (2009). Normalization of qRT-PCR data: the necessity of adopting a systematic, experimental conditions-specific, validation of references. J Exp Bot *60*, 487-493.

Gurbanova, A.A., Aker, R.G., Sirvanci, S., Demiralp, T., and Onat, F.Y. (2008). Intra-amygdaloid injection of kainic acid in rats with genetic absence epilepsy: the relationship of typical absence epilepsy and temporal lobe epilepsy. The Journal of neuroscience : the official journal of the Society for Neuroscience *28*, 7828-7836.

Hagemann, G., Hoeller, M., Bruehl, C., Lutzenburg, M., and Witte, O.W. (1999). Effects of tetanus toxin on functional inhibition after injection in separate cortical areas in rat. Brain Res *818*, 127-134.

Hauser, W.A., Annegers, J.F., and Kurland, L.T. (1991). Prevalence of epilepsy in Rochester, Minnesota: 1940-1980. Epilepsia *32*, 429-445.

Hauser, W.A., J.F., A., and W.A., R. (1996). Descriptive epidemiology of epilepsy: contributions of population-based studies from Rochester, Minnesota. Mayo Clinic Proceedings *7*, 576-586.

Hawkins, C.A., and Mellanby, J.H. (1987). Limbic epilepsy induced by tetanus toxin: a longitudinal electroencephalographic study. Epilepsia *28*, 431-444.

Hayashi, T. (1952). A physiological study of epileptic seizures following cortical stimulation in animals and its application to human clinics. The Japanese journal of physiology *3*, 46-64.

Haydon, P.G. (2001). GLIA: listening and talking to the synapse. Nature reviews Neuroscience *2*, 185-193.

Hellier, J.L., and Dudek, F.E. (2005). Chemoconvulsant model of chronic spontaneous seizures. Current protocols in neuroscience / editorial board, Jacqueline N Crawley [et al] *Chapter 9*, Unit 9 19.

Henshall, D.C., and Meldrum, B.S. (2012). Cell death and survival mechanisms after single and repeated brief seizures. In Jasper's Basic Mechanisms of the Epilepsies, J.L. Noebels, M. Avoli, M.A. Rogawski, R.W. Olsen, and A.V. Delgado-Escueta, eds. (Bethesda (MD)).

Henshall, D.C., and Murphy, B.M. (2008). Modulators of neuronal cell death in epilepsy. Curr Opin Pharmacol *8*, 75-81.

Henshall, D.C., Sinclair, J., and Simon, R.P. (2000). Spatio-temporal profile of DNA fragmentation and its relationship to patterns of epileptiform activity following focally evoked limbic seizures. Brain Res *858*, 290-302.

Hofstra, W.A., and de Weerd, A.W. (2009). The circadian rhythm and its interaction with human epilepsy: a review of literature. Sleep Med Rev *13*, 413-420.

Hu, X.L., Cheng, X., Cai, L., Tan, G.H., Xu, L., Feng, X.Y., Lu, T.J., Xiong, H., Fei, J., and Xiong, Z.Q. (2011). Conditional deletion of NRSF in forebrain neurons accelerates epileptogenesis in the kindling model. Cereb Cortex *21*, 2158-2165.

Huang, X., Zhang, H., Yang, J., Wu, J., McMahon, J., Lin, Y., Cao, Z., Gruenthal, M., and Huang, Y. (2010). Pharmacological inhibition of the mammalian target of rapamycin pathway suppresses acquired epilepsy. Neurobiology of disease *40*, 193-199.

Huettner, J.E. (2003). Kainate receptors and synaptic transmission. Progress in neurobiology *70*, 387-407.

Hui Yin, Y., Ahmad, N., and Makmor-Bakry, M. (2013). Pathogenesis of epilepsy: challenges in animal models. Iranian journal of basic medical sciences *16*, 1119-1132.

ILAE (1989). Proposal for revised classification of epilepsies and epileptic syndromes. Commission on Classification and Terminology of the International League Against Epilepsy. Epilepsia *30*, 389-399.

Inoki, K., Corradetti, M.N., and Guan, K.L. (2005). Dysregulation of the TSC-mTOR pathway in human disease. Nature genetics *37*, 19-24.

Ivens, S., Kaufer, D., Flores, L.P., Bechmann, I., Zumsteg, D., Tomkins, O., Seiffert, E., Heinemann, U., and Friedman, A. (2007). TGF-beta receptor-mediated albumin uptake into astrocytes is involved in neocortical epileptogenesis. Brain : a journal of neurology *130*, 535-547.

Iyer, A., Zurolo, E., Spliet, W.G., van Rijen, P.C., Baayen, J.C., Gorter, J.A., and Aronica, E. (2010). Evaluation of the innate and adaptive immunity in type I and type II focal cortical dysplasias. Epilepsia *51*, 1763-1773.

Jabs, R., Seifert, G., and Steinhauser, C. (2008). Astrocytic function and its alteration in the epileptic brain. Epilepsia *49 Suppl 2*, 3-12.

Jefferys, J.G., Borck, C., and Mellanby, J. (1995). Chronic focal epilepsy induced by intracerebral tetanus toxin. Italian journal of neurological sciences *16*, 27-32.

Jefferys, J.G., and Haas, H.L. (1982). Synchronized bursting of CA1 hippocampal pyramidal cells in the absence of synaptic transmission. Nature *300*, 448-450.

Jensen, M.S., and Yaari, Y. (1988). The relationship between interictal and ictal paroxysms in an in vitro model of focal hippocampal epilepsy. Annals of neurology *24*, 591-598.

Jessberger, S., Zhao, C., Toni, N., Clemenson, G.D., Jr., Li, Y., and Gage, F.H. (2007). Seizure-associated, aberrant neurogenesis in adult rats characterized with retrovirus-

mediated cell labeling. The Journal of neuroscience : the official journal of the Society for Neuroscience *27*, 9400-9407.

Jimbo, Y., and Robinson, H.P. (2000). Propagation of spontaneous synchronized activity in cortical slice cultures recorded by planar electrode arrays. Bioelectrochemistry *51*, 107-115.

Jin, X., Prince, D.A., and Huguenard, J.R. (2006). Enhanced excitatory synaptic connectivity in layer v pyramidal neurons of chronically injured epileptogenic neocortex in rats. The Journal of neuroscience : the official journal of the Society for Neuroscience *26*, 4891-4900.

Jiruska, P., Finnerty, G.T., Powell, A.D., Lofti, N., Cmejla, R., and Jefferys, J.G. (2010). Epileptic high-frequency network activity in a model of non-lesional temporal lobe epilepsy. Brain : a journal of neurology *133*, 1380-1390.

Jung, S., Jones, T.D., Lugo, J.N., Jr., Sheerin, A.H., Miller, J.W., D'Ambrosio, R., Anderson, A.E., and Poolos, N.P. (2007). Progressive dendritic HCN channelopathy during epileptogenesis in the rat pilocarpine model of epilepsy. The Journal of neuroscience : the official journal of the Society for Neuroscience *27*, 13012-13021.

Jurgen Wenzel, H., Born, D.E., Dubach, M.F., Gunderson, V.M., Maravilla, K.R., Robbins, C.A., Szot, P., Zierath, D., and Schwartzkroin, P.A. (2000). Morphological plasticity in an infant monkey model of temporal lobe epilepsy. Epilepsia *41 Suppl 6*, S70-75.

Kadam, S.D., White, A.M., Staley, K.J., and Dudek, F.E. (2010). Continuous electroencephalographic monitoring with radio-telemetry in a rat model of perinatal hypoxia-ischemia reveals progressive post-stroke epilepsy. The Journal of neuroscience : the official journal of the Society for Neuroscience *30*, 404-415.

Kaech, S., and Banker, G. (2006). Culturing hippocampal neurons. Nature protocols *1*, 2406-2415.

Kandratavicius, L., Balista, P.A., Lopes-Aguiar, C., Ruggiero, R.N., Umeoka, E.H., Garcia-Cairasco, N., Bueno-Junior, L.S., and Leite, J.P. (2014). Animal models of epilepsy: use and limitations. Neuropsychiatric disease and treatment *10*, 1693-1705.

Karceski, S., Morrell, M.J., and Carpenter, D. (2005). Treatment of epilepsy in adults: expert opinion, 2005. Epilepsy & behavior : E&B *7 Suppl 1*, S1-64; quiz S65-67.

Kasteleijn-Nolst Trenite, D., Rubboli, G., Hirsch, E., Martins da Silva, A., Seri, S., Wilkins, A., Parra, J., Covanis, A., Elia, M., Capovilla, G*., et al.* (2012). Methodology of photic stimulation revisited: updated European algorithm for visual stimulation in the EEG laboratory. Epilepsia *53*, 16-24.

Kojima, N., Borlikova, G., Sakamoto, T., Yamada, K., Ikeda, T., Itohara, S., Niki, H., and Endo, S. (2008). Inducible cAMP early repressor acts as a negative regulator for

kindling epileptogenesis and long-term fear memory. The Journal of neuroscience : the official journal of the Society for Neuroscience *28*, 6459-6472.

Konopka, D., Szklarczyk, A.W., Filipkowski, R.K., Trauzold, A., Nowicka, D., Hetman, M., and Kaczmarek, L. (1998). Plasticity- and neurodegeneration-linked cyclic-AMP responsive element modulator/inducible cyclic-AMP early repressor messenger RNA expression in the rat brain. Neuroscience *86*, 499-510.

Kossoff, E.H., and Hartman, A.L. (2012). Ketogenic diets: new advances for metabolism-based therapies. Current opinion in neurology *25*, 173-178.

Kovalchuk, Y., Holthoff, K., and Konnerth, A. (2004). Neurotrophin action on a rapid timescale. Current opinion in neurobiology *14*, 558-563.

Krueger, D.A., Care, M.M., Holland, K., Agricola, K., Tudor, C., Mangeshkar, P., Wilson, K.A., Byars, A., Sahmoud, T., and Franz, D.N. (2010). Everolimus for subependymal giant-cell astrocytomas in tuberous sclerosis. The New England journal of medicine *363*, 1801-1811.

Kvartsberg, H., Duits, F.H., Ingelsson, M., Andreasen, N., Ohrfelt, A., Andersson, K., Brinkmalm, G., Lannfelt, L., Minthon, L., Hansson, O.*, et al.* (2014). Cerebrospinal fluid levels of the synaptic protein neurogranin correlates with cognitive decline in prodromal Alzheimer's disease. Alzheimer's & dementia : the journal of the Alzheimer's Association.

Kwan, P., Arzimanoglou, A., Berg, A.T., Brodie, M.J., Allen Hauser, W., Mathern, G., Moshe, S.L., Perucca, E., Wiebe, S., and French, J. (2010). Definition of drug resistant epilepsy: consensus proposal by the ad hoc Task Force of the ILAE Commission on Therapeutic Strategies. Epilepsia *51*, 1069-1077.

Kwan, P., and Brodie, M.J. (2000). Early identification of refractory epilepsy. The New England journal of medicine *342*, 314-319.

Kwan, P., and Brodie, M.J. (2004). Drug treatment of epilepsy: when does it fail and how to optimize its use? CNS spectrums *9*, 110-119.

Lange, C., Storkebaum, E., de Almodovar, C.R., Dewerchin, M., and Carmeliet, P. (2016). Vascular endothelial growth factor: a neurovascular target in neurological diseases. Nature reviews Neurology *12*, 439-454.

Laplante, M., and Sabatini, D.M. (2009). mTOR signaling at a glance. Journal of cell science *122*, 3589-3594.

Leal, G., Comprido, D., and Duarte, C.B. (2014). BDNF-induced local protein synthesis and synaptic plasticity. Neuropharmacology *76 Pt C*, 639-656.

Lee, P.R., and Kossoff, E.H. (2011). Dietary treatments for epilepsy: management guidelines for the general practitioner. Epilepsy & behavior : E&B *21*, 115-121.

Lenth, R.V. (2007). Statistical power calculations. Journal of animal science *85*, E24-E29.

Leppik, I.E. (1992). Intractable epilepsy in adults. Epilepsy research Supplement *5*, 7-11.

Lerche, H., Shah, M., Beck, H., Noebels, J., Johnston, D., and Vincent, A. (2013). Ion channels in genetic and acquired forms of epilepsy. The Journal of physiology *591*, 753-764.

Levesque, M., and Avoli, M. (2013). The kainic acid model of temporal lobe epilepsy. Neuroscience and biobehavioral reviews *37*, 2887-2899.

Li, H., McDonald, W., Parada, I., Faria, L., Graber, K., Takahashi, D.K., Ma, Y., and Prince, D. (2011). Targets for preventing epilepsy following cortical injury. Neuroscience letters *497*, 172-176.

Liang, F., Le, L.D., and Jones, E.G. (1998). Reciprocal up- and down-regulation of BDNF mRNA in tetanus toxin-induced epileptic focus and inhibitory surround in cerebral cortex. Cereb Cortex *8*, 481-491.

Lipton, J.O., and Sahin, M. (2014). The neurology of mTOR. Neuron *84*, 275-291.

Loscher, W. (2011). Critical review of current animal models of seizures and epilepsy used in the discovery and development of new antiepileptic drugs. Seizure *20*, 359-368.

Loscher, W., and Brandt, C. (2010). Prevention or modification of epileptogenesis after brain insults: experimental approaches and translational research. Pharmacological reviews *62*, 668-700.

Loscher, W., Gernert, M., and Heinemann, U. (2008). Cell and gene therapies in epilepsy--promising avenues or blind alleys? Trends in neurosciences *31*, 62-73.

Loscher, W., Klitgaard, H., Twyman, R.E., and Schmidt, D. (2013). New avenues for anti-epileptic drug discovery and development. Nat Rev Drug Discov *12*, 757-776.

Lothman, E.W., Collins, R.C., and Ferrendelli, J.A. (1981). Kainic acid-induced limbic seizures: electrophysiologic studies. Neurology *31*, 806-812.

Louis, E.D., Williamson, P.D., and Darcey, T.M. (1990). Chronic focal epilepsy induced by microinjection of tetanus toxin into the cat motor cortex. Electroencephalography and clinical neurophysiology *75*, 548-557.

Louvel, J., and Heinemann, U. (1981). [Mode of action of pentetrazole at the cellular level (author's transl)]. Revue d'electroencephalographie et de neurophysiologie clinique *11*, 335-339.

Lowenstein, D.H., and Alldredge, B.K. (1998). Status epilepticus. The New England journal of medicine *338*, 970-976.

Lowenstein, D.H., Bleck, T., and Macdonald, R.L. (1999). It's time to revise the definition of status epilepticus. Epilepsia *40*, 120-122.

Lukasiuk, K., Dabrowski, M., Adach, A., and Pitkanen, A. (2006). Epileptogenesis-related genes revisited. Progress in brain research *158*, 223-241.

Lutas, A., and Yellen, G. (2013). The ketogenic diet: metabolic influences on brain excitability and epilepsy. Trends in neurosciences *36*, 32-40.

Ma, S., Abou-Khalil, B., Blair, M.A., Sutcliffe, J.S., Haines, J.L., and Hedera, P. (2006). Mutations in GABRA1, GABRA5, GABRG2 and GABRD receptor genes are not a major factor in the pathogenesis of familial focal epilepsy preceded by febrile seizures. Neuroscience letters *394*, 74-78.

Macdonald, R.L., Saxena, N.C., and Angelotti, T.P. (1996). Functional expression of recombinant GABAA receptor channels in L929 fibroblasts. Epilepsy research Supplement *12*, 177-185.

Madeja, M., Stocker, M., Musshoff, U., Pongs, O., and Speckmann, E.J. (1994). Potassium currents in epilepsy: effects of the epileptogenic agent pentylenetetrazol on a cloned potassium channel. Brain Res *656*, 287-294.

Magiorkinis, E., Diamantis, A., Sidiropoulou, K., and Panteliadis, C. (2014). Highights in the history of epilepsy: the last 200 years. Epilepsy Res Treat *2014*, 582039.

Magiorkinis, E., Sidiropoulou, K., and Diamantis, A. (2010). Hallmarks in the history of epilepsy: epilepsy in antiquity. Epilepsy & behavior : E&B *17*, 103-108.

Mainardi, M., Pietrasanta, M., Vannini, E., Rossetto, O., and Caleo, M. (2012). Tetanus neurotoxin-induced epilepsy in mouse visual cortex. Epilepsia *53*, e132-136.

Marchi, N., Granata, T., and Janigro, D. (2014). Inflammatory pathways of seizure disorders. Trends in neurosciences *37*, 55-65.

Martinian, L., Boer, K., Middeldorp, J., Hol, E.M., Sisodiya, S.M., Squier, W., Aronica, E., and Thom, M. (2009). Expression patterns of glial fibrillary acidic protein (GFAP)-delta in epilepsy-associated lesional pathologies. Neuropathology and applied neurobiology *35*, 394-405.

Mazarati, A., Lundstrom, L., Sollenberg, U., Shin, D., Langel, U., and Sankar, R. (2006). Regulation of kindling epileptogenesis by hippocampal galanin type 1 and type 2 receptors: The effects of subtype-selective agonists and the role of G-protein-mediated signaling. The Journal of pharmacology and experimental therapeutics *318*, 700-708.

Mazarati, A.M. (2004). Galanin and galanin receptors in epilepsy. Neuropeptides *38*, 331-343.

Mazarati, A.M., Wasterlain, C.G., Sankar, R., and Shin, D. (1998). Self-sustaining status epilepticus after brief electrical stimulation of the perforant path. Brain Res *801*, 251-253.

Mazzuferi, M., Kumar, G., van Eyll, J., Danis, B., Foerch, P., and Kaminski, R.M. (2013). Nrf2 defense pathway: Experimental evidence for its protective role in epilepsy. Annals of neurology *74*, 560-568.

McClelland, S., Brennan, G.P., Dube, C., Rajpara, S., Iyer, S., Richichi, C., Bernard, C., and Baram, T.Z. (2014). The transcription factor NRSF contributes to epileptogenesis by selective repression of a subset of target genes. eLife *3*, e01267.

McClelland, S., Flynn, C., Dube, C., Richichi, C., Zha, Q., Ghestem, A., Esclapez, M., Bernard, C., and Baram, T.Z. (2011a). Neuron-restrictive silencer factor-mediated hyperpolarization-activated cyclic nucleotide gated channelopathy in experimental temporal lobe epilepsy. Annals of neurology *70*, 454-464.

McClelland, S., Korosi, A., Cope, J., Ivy, A., and Baram, T.Z. (2011b). Emerging roles of epigenetic mechanisms in the enduring effects of early-life stress and experience on learning and memory. Neurobiology of learning and memory *96*, 79-88.

McKernan, R.M., Quirk, K., Prince, R., Cox, P.A., Gillard, N.P., Ragan, C.I., and Whiting, P. (1991). GABAA receptor subtypes immunopurified from rat brain with alpha subunit-specific antibodies have unique pharmacological properties. Neuron *7*, 667-676.

McNamara, J.O., Huang, Y.Z., and Leonard, A.S. (2006). Molecular signaling mechanisms underlying epileptogenesis. Science's STKE : signal transduction knowledge environment *2006*, re12.

Meisler MH, O.B.J. (2012). Gene interactions and modifiers in epilepsy.

Meldrum, B.S. (1999). The revised operational definition of generalised tonic-clonic (TC) status epilepticus in adults. Epilepsia *40*, 123-124.

Meldrum, B.S., and Rogawski, M.A. (2007). Molecular targets for antiepileptic drug development. Neurotherapeutics : the journal of the American Society for Experimental NeuroTherapeutics *4*, 18-61.

Meldrum, B.S., Vigouroux, R.A., and Brierley, J.B. (1973). Systemic factors and epileptic brain damage. Prolonged seizures in paralyzed, artificially ventilated baboons. Archives of neurology *29*, 82-87.

Mellanby, J., George, G., Robinson, A., and Thompson, P. (1977). Epileptiform syndrome in rats produced by injecting tetanus toxin into the hippocampus. Journal of neurology, neurosurgery, and psychiatry *40*, 404-414.

Mellanby, J.H. (1989). Elimination of 125I from rat brain after injection of small doses of 125I-labelled tetanus toxin into the hippocampus. Neurosci Lett *36*, S55.

Meng, X.F., Yu, J.T., Song, J.H., Chi, S., and Tan, L. (2013). Role of the mTOR signaling pathway in epilepsy. J Neurol Sci *332*, 4-15.

Middeldorp, J., and Hol, E.M. (2011). GFAP in health and disease. Progress in neurobiology *93*, 421-443.

Miles, R., and Wong, R.K. (1986). Excitatory synaptic interactions between CA3 neurones in the guinea-pig hippocampus. The Journal of physiology *373*, 397-418.

Miller, L.P., Johnson, A.E., Gelhard, R.E., and Insel, T.R. (1990). The ontogeny of excitatory amino acid receptors in the rat forebrain--II. Kainic acid receptors. Neuroscience *35*, 45-51.

Millikan, D., Rice, B., and Silbergleit, R. (2009). Emergency treatment of status epilepticus: current thinking. Emergency medicine clinics of North America *27*, 101-113, ix.

Ming, G.L., and Song, H. (2011). Adult neurogenesis in the mammalian brain: significant answers and significant questions. Neuron *70*, 687-702.

Mioduszewska, B., Jaworski, J., and Kaczmarek, L. (2003). Inducible cAMP early repressor (ICER) in the nervous system--a transcriptional regulator of neuronal plasticity and programmed cell death. Journal of neurochemistry *87*, 1313-1320.

Mody, I., Lambert, J.D., and Heinemann, U. (1987). Low extracellular magnesium induces epileptiform activity and spreading depression in rat hippocampal slices. Journal of neurophysiology *57*, 869-888.

Molina, C.A., Foulkes, N.S., Lalli, E., and Sassone-Corsi, P. (1993). Inducibility and negative autoregulation of CREM: an alternative promoter directs the expression of ICER, an early response repressor. Cell *75*, 875-886.

Montecucco, C., and Schiavo, G. (1993). Tetanus and botulism neurotoxins: a new group of zinc proteases. Trends in biochemical sciences *18*, 324-327.

Morgan, R.J., and Soltesz, I. (2008). Nonrandom connectivity of the epileptic dentate gyrus predicts a major role for neuronal hubs in seizures. Proceedings of the National Academy of Sciences of the United States of America *105*, 6179-6184.

Mori, H., Masaki, H., Yamakura, T., and Mishina, M. (1992). Identification by mutagenesis of a Mg(2+)-block site of the NMDA receptor channel. Nature *358*, 673-675.

Morin-Brureau, M., Rigau, V., and Lerner-Natoli, M. (2012). Why and how to target angiogenesis in focal epilepsies. Epilepsia *53*, 64-68.

Morioka, N., Abe, H., Araki, R., Matsumoto, N., Zhang, F.F., Nakamura, Y., Hisaoka-Nakashima, K., and Nakata, Y. (2014). A beta1/2 adrenergic receptor-sensitive intracellular signaling pathway modulates CCL2 production in cultured spinal astrocytes. J Cell Physiol *229*, 323-332.

Mouri, G., Jimenez-Mateos, E., Engel, T., Dunleavy, M., Hatazaki, S., Paucard, A., Matsushima, S., Taki, W., and Henshall, D.C. (2008). Unilateral hippocampal CA3-predominant damage and short latency epileptogenesis after intra-amygdala microinjection of kainic acid in mice. Brain Res *1213*, 140-151.

Muncy, J., Butler, I.J., and Koenig, M.K. (2009). Rapamycin reduces seizure frequency in tuberous sclerosis complex. J Child Neurol *24*, 477.

Nadler, J.V. (1981). Minireview. Kainic acid as a tool for the study of temporal lobe epilepsy. Life sciences *29*, 2031-2042.

Nawa, H., Carnahan, J., and Gall, C. (1995). BDNF protein measured by a novel enzyme immunoassay in normal brain and after seizure: partial disagreement with mRNA levels. The European journal of neuroscience *7*, 1527-1535.

Nelissen, K., Smeets, K., Mulder, M., Hendriks, J.J.A., and Ameloot, M. (2010). Selection of reference genes for gene expression studies in rat oligodendrocytes using quantitative real time PCR. Journal of neuroscience methods *187*, 78-83.

Neobels, J. (1999). Single-gene models of epilepsy. Jasper's basic mechanisms of the epilepsies, 3rd ed Advances in Neurology Philadelphia: Lippincott-Raven *In: Delgado A, Wilson W, Olsen R, Porter R, editors*, 227-238.

Nilsen, K.E., Walker, M.C., and Cock, H.R. (2005). Characterization of the tetanus toxin model of refractory focal neocortical epilepsy in the rat. Epilepsia *46*, 179-187.

Nimmerjahn, A., and Bergles, D.E. (2015). Large-scale recording of astrocyte activity. Current opinion in neurobiology *32*, 95-106.

Noam, Y., Bernard, C., and Baram, T.Z. (2011). Towards an integrated view of HCN channel role in epilepsy. Current opinion in neurobiology *21*, 873-879.

Noe, F., Pool, A.H., Nissinen, J., Gobbi, M., Bland, R., Rizzi, M., Balducci, C., Ferraguti, F., Sperk, G., During, M.J.*, et al.* (2008). Neuropeptide Y gene therapy decreases chronic spontaneous seizures in a rat model of temporal lobe epilepsy. Brain : a journal of neurology *131*, 1506-1515.

Noebels, J. (2011). A perfect storm: Converging paths of epilepsy and Alzheimer's dementia intersect in the hippocampal formation. Epilepsia *52 Suppl 1*, 39-46.

Nolan, M.F., Malleret, G., Dudman, J.T., Buhl, D.L., Santoro, B., Gibbs, E., Vronskaya, S., Buzsaki, G., Siegelbaum, S.A., Kandel, E.R., *et al.* (2004). A behavioral role for dendritic integration: HCN1 channels constrain spatial memory and plasticity at inputs to distal dendrites of CA1 pyramidal neurons. Cell *119*, 719-732.

Oliva, M., Berkovic, S.F., and Petrou, S. (2012). Sodium channels and the neurobiology of epilepsy. Epilepsia *53*, 1849-1859.

Olney, J.W., Rhee, V., and Ho, O.L. (1974). Kainic acid: a powerful neurotoxic analogue of glutamate. Brain Res *77*, 507-512.

Olsen, R.W. (1981). The GABA postsynaptic membrane receptor-ionophore complex. Site of action of convulsant and anticonvulsant drugs. Molecular and cellular biochemistry *39*, 261-279.

Otto, S.J., McCorkle, S.R., Hover, J., Conaco, C., Han, J.J., Impey, S., Yochum, G.S., Dunn, J.J., Goodman, R.H., and Mandel, G. (2007). A new binding motif for the transcriptional repressor REST uncovers large gene networks devoted to neuronal functions. The Journal of neuroscience : the official journal of the Society for Neuroscience *27*, 6729-6739.

Pal, S., Sun, D., Limbrick, D., Rafiq, A., and DeLorenzo, R.J. (2001). Epileptogenesis induces long-term alterations in intracellular calcium release and sequestration mechanisms in the hippocampal neuronal culture model of epilepsy. Cell calcium *30*, 285-296.

Palm, K., Belluardo, N., Metsis, M., and Timmusk, T. (1998). Neuronal expression of zinc finger transcription factor REST/NRSF/XBR gene. The Journal of neuroscience : the official journal of the Society for Neuroscience *18*, 1280-1296.

Palmada, M., and Centelles, J.J. (1998). Excitatory amino acid neurotransmission. Pathways for metabolism, storage and reuptake of glutamate in brain. Frontiers in bioscience : a journal and virtual library *3*, d701-718.

Palop, J.J., Chin, J., Roberson, E.D., Wang, J., Thwin, M.T., Bien-Ly, N., Yoo, J., Ho, K.O., Yu, G.Q., Kreitzer, A., *et al.* (2007). Aberrant excitatory neuronal activity and compensatory remodeling of inhibitory hippocampal circuits in mouse models of Alzheimer's disease. Neuron *55*, 697-711.

Panayiotopoulos, C.P. (2005). In The Epilepsies: Seizures, Syndromes and Management (Oxfordshire (UK)).

Parent, J.M., and Kron, M.M. (2012). Neurogenesis and Epilepsy. In Jasper's Basic Mechanisms of the Epilepsies, J.L. Noebels, M. Avoli, M.A. Rogawski, R.W. Olsen, and A.V. Delgado-Escueta, eds. (Bethesda (MD)).

Patterson, S.L., Grover, L.M., Schwartzkroin, P.A., and Bothwell, M. (1992). Neurotrophin expression in rat hippocampal slices: a stimulus paradigm inducing LTP in CA1 evokes increases in BDNF and NT-3 mRNAs. Neuron *9*, 1081-1088.

Paxinos, G., and Watson, C. (1998). The Rat Brain in Stereotaxic Coordinations, 4th edn. Academic Press, Sydney.

Paz, J.T., Bryant, A.S., Peng, K., Fenno, L., Yizhar, O., Frankel, W.N., Deisseroth, K., and Huguenard, J.R. (2011). A new mode of corticothalamic transmission revealed in the Gria4(-/-) model of absence epilepsy. Nature neuroscience *14*, 1167-1173.

Paz, J.T., Chavez, M., Saillet, S., Deniau, J.M., and Charpier, S. (2007). Activity of ventral medial thalamic neurons during absence seizures and modulation of cortical paroxysms by the nigrothalamic pathway. The Journal of neuroscience : the official journal of the Society for Neuroscience *27*, 929-941.

Paz, J.T., and Huguenard, J.R. (2015). Microcircuits and their interactions in epilepsy: is the focus out of focus? Nature neuroscience *18*, 351-359.

Peirson, S.N., and Butler, J.N. (2007). RNA extraction from mammalian tissues. Methods Mol Biol *362*, 315-327.

Perreault, P., and Avoli, M. (1989). Effects of low concentrations of 4-aminopyridine on CA1 pyramidal cells of the hippocampus. Journal of neurophysiology *61*, 953-970.

Perucca, E., and Tomson, T. (2011). The pharmacological treatment of epilepsy in adults. The Lancet Neurology *10*, 446-456.

Pfeiffer, M., Draguhn, A., Meierkord, H., and Heinemann, U. (1996). Effects of gamma-aminobutyric acid (GABA) agonists and GABA uptake inhibitors on pharmacosensitive and pharmacoresistant epileptiform activity in vitro. British journal of pharmacology *119*, 569-577.

Pitkanen, A., Kharatishvili, I., Karhunen, H., Lukasiuk, K., Immonen, R., Nairismagi, J., Grohn, O., and Nissinen, J. (2007). Epileptogenesis in experimental models. Epilepsia *48 Suppl 2*, 13-20.

Pitkanen, A., Kharatishvili, I., Narkilahti, S., Lukasiuk, K., and Nissinen, J. (2005). Administration of diazepam during status epilepticus reduces development and severity of epilepsy in rat. Epilepsy research *63*, 27-42.

Pitkanen, A., and Lukasiuk, K. (2009). Molecular and cellular basis of epileptogenesis in symptomatic epilepsy. Epilepsy & behavior : E&B *14 Suppl 1*, 16-25.

Pitkanen, A., and Lukasiuk, K. (2011). Mechanisms of epileptogenesis and potential treatment targets. The Lancet Neurology *10*, 173-186.

Pitkanen, A., Schwartzkroin, P.A., and Moshe, S.L. (2006). Models of Seizures and Epilepsy. Elsevier Academic Press.

Pitkanen, A., and Sutula, T.P. (2002). Is epilepsy a progressive disorder? Prospects for new therapeutic approaches in temporal-lobe epilepsy. The Lancet Neurology *1*, 173-181.

Poolos, N.P., and Johnston, D. (2012). Dendritic ion channelopathy in acquired epilepsy. Epilepsia *53 Suppl 9*, 32-40.

Poolos, N.P., Mauk, M.D., and Kocsis, J.D. (1987). Activity-evoked increases in extracellular potassium modulate presynaptic excitability in the CA1 region of the hippocampus. Journal of neurophysiology *58*, 404-416.

Porter, B.E., Lund, I.V., Varodayan, F.P., Wallace, R.W., and Blendy, J.A. (2008). The role of transcription factors cyclic-AMP responsive element modulator (CREM) and inducible cyclic-AMP early repressor (ICER) in epileptogenesis. Neuroscience *152*, 829-836.

Potter, S.M., and DeMarse, T.B. (2001). A new approach to neural cell culture for long-term studies. Journal of neuroscience methods *110*, 17-24.

Pozzi, D., Lignani, G., Ferrea, E., Contestabile, A., Paonessa, F., D'Alessandro, R., Lippiello, P., Boido, D., Fassio, A., Meldolesi, J.*, et al.* (2013). REST/NRSF-mediated intrinsic homeostasis protects neuronal networks from hyperexcitability. The EMBO journal *32*, 2994-3007.

Prince, D.A., Jacobs, K.M., Salin, P.A., Hoffman, S., and Parada, I. (1997). Chronic focal neocortical epileptogenesis: does disinhibition play a role? Canadian journal of physiology and pharmacology *75*, 500-507.

Prince, D.A., Parada, I., Scalise, K., Graber, K., Jin, X., and Shen, F. (2009). Epilepsy following cortical injury: cellular and molecular mechanisms as targets for potential prophylaxis. Epilepsia *50 Suppl 2*, 30-40.

Prusky, G.T., Harker, K.T., Douglas, R.M., and Whishaw, I.Q. (2002). Variation in visual acuity within pigmented, and between pigmented and albino rat strains. Behavioural brain research *136*, 339-348.

Qi, J., Wang, Y., Jiang, M., Warren, P., and Chen, G. (2006a). Cyclothiazide induces robust epileptiform activity in rat hippocampal neurons both in vitro and in vivo. The Journal of physiology *571*, 605-618.

Qi, J.S., Yao, J., Fang, C., Luscher, B., and Chen, G. (2006b). Downregulation of tonic GABA currents following epileptogenic stimulation of rat hippocampal cultures. The Journal of physiology *577*, 579-590.

Qu, H., Eloqayli, H., and Sonnewald, U. (2005). Pentylenetetrazole affects metabolism of astrocytes in culture. Journal of neuroscience research *79*, 48-54.

Quigg, M. (2000). Circadian rhythms: interactions with seizures and epilepsy. Epilepsy research *42*, 43-55.

Qureshi, I.A., and Mehler, M.F. (2009). Regulation of non-coding RNA networks in the nervous system--what's the REST of the story? Neuroscience letters *466*, 73-80.

Raab-Graham, K.F., Haddick, P.C., Jan, Y.N., and Jan, L.Y. (2006). Activity- and mTOR-dependent suppression of Kv1.1 channel mRNA translation in dendrites. Science *314*, 144-148.

Racine, R.J. (1972). Modification of seizure activity by electrical stimulation. II. Motor seizure. Electroencephalography and clinical neurophysiology *32*, 281-294.

Raedt, R., Van Dycke, A., Van Melkebeke, D., De Smedt, T., Claeys, P., Wyckhuys, T., Vonck, K., Wadman, W., and Boon, P. (2009). Seizures in the intrahippocampal kainic acid epilepsy model: characterization using long-term video-EEG monitoring in the rat. Acta neurologica Scandinavica *119*, 293-303.

Rafiq, A., DeLorenzo, R.J., and Coulter, D.A. (1993). Generation and propagation of epileptiform discharges in a combined entorhinal cortex/hippocampal slice. Journal of neurophysiology *70*, 1962-1974.

Rakhade, S.N., and Jensen, F.E. (2009). Epileptogenesis in the immature brain: emerging mechanisms. Nature reviews Neurology *5*, 380-391.

Ramon Goni, Patricia Garcia, and Foissac, S. (September 2009). The qPCR data statistical analysis. Integromics White Paper, 1-9.

Rasmussen, T., Olszewski, J., and Lloydsmith, D. (1958). Focal Seizures Due to Chronic Localized Encephalitis. Neurology *8*, 435-445.

Reddy, D.S., and Kuruba, R. (2013). Experimental models of status epilepticus and neuronal injury for evaluation of therapeutic interventions. International journal of molecular sciences *14*, 18284-18318.

Richichi, C., Brewster, A.L., Bender, R.A., Simeone, T.A., Zha, Q., Yin, H.Z., Weiss, J.H., and Baram, T.Z. (2008). Mechanisms of seizure-induced 'transcriptional channelopathy' of hyperpolarization-activated cyclic nucleotide gated (HCN) channels. Neurobiology of disease *29*, 297-305.

Rieu, I., and Powers, S.J. (2009). Real-time quantitative RT-PCR: design, calculations, and statistics. The Plant cell *21*, 1031-1033.

Rigau, V., Morin, M., Rousset, M.C., de Bock, F., Lebrun, A., Coubes, P., Picot, M.C., Baldy-Moulinier, M., Bockaert, J., Crespel, A.*, et al.* (2007). Angiogenesis is associated with blood-brain barrier permeability in temporal lobe epilepsy. Brain : a journal of neurology *130*, 1942-1956.

Robinson, J.H., and Deadwyler, S.A. (1981). Kainic acid produces depolarization of CA3 pyramidal cells in the vitro hippocampal slice. Brain Res *221*, 117-127.

Rogawski, M.A., and Loscher, W. (2004). The neurobiology of antiepileptic drugs. Nature reviews Neuroscience *5*, 553-564.

Rohena, L., Neidich, J., Truitt Cho, M., Gonzalez, K.D., Tang, S., Devinsky, O., and Chung, W.K. (2013). Mutation in SNAP25 as a novel genetic cause of epilepsy and intellectual disability. Rare Dis *1*, e26314.

Roopra, A., Dingledine, R., and Hsieh, J. (2012). Epigenetics and epilepsy. Epilepsia *53 Suppl 9*, 2-10.

Roopra, A., Huang, Y., and Dingledine, R. (2001). Neurological disease: listening to gene silencers. Molecular interventions *1*, 219-228.

Rose, E.J., Morris, D.W., Fahey, C., Robertson, I.H., Greene, C., O'Doherty, J., Newell, F.N., Garavan, H., McGrath, J., Bokde, A.*, et al.* (2012). The effect of the neurogranin schizophrenia risk variant rs12807809 on brain structure and function. Twin research and human genetics : the official journal of the International Society for Twin Studies *15*, 296-303.

Rossbach, M. (2011). Non-Coding RNAs in Neural Networks, REST-Assured. Front Genet *2*, 8.

Rossignol, E., Kruglikov, I., van den Maagdenberg, A.M., Rudy, B., and Fishell, G. (2013). CaV 2.1 ablation in cortical interneurons selectively impairs fast-spiking basket cells and causes generalized seizures. Annals of neurology *74*, 209-222.

Roux E, B.A. (1898). Tétanos cérébral et immunité contre le tétanos. Ann Inst Pasteur *4*, 225-239.

Rozen, S., and Skaletsky, H. (2000). Primer3 on the WWW for general users and for biologist programmers. Methods Mol Biol *132*, 365-386.

Russo, E., Andreozzi, F., Iuliano, R., Dattilo, V., Procopio, T., Fiume, G., Mimmi, S., Perrotti, N., Citraro, R., Sesti, G.*, et al.* (2014). Early molecular and behavioral response to lipopolysaccharide in the WAG/Rij rat model of absence epilepsy and depressive-like behavior, involves interplay between AMPK, AKT/mTOR pathways and neuroinflammatory cytokine release. Brain Behav Immun *42*, 157-168.

Ryther, R.C., and Wong, M. (2012). Mammalian target of rapamycin (mTOR) inhibition: potential for antiseizure, antiepileptogenic, and epileptostatic therapy. Curr Neurol Neurosci Rep *12*, 410-418.

Sah, N., and Sikdar, S.K. (2013). Transition in subicular burst firing neurons from epileptiform activity to suppressed state by feedforward inhibition. The European journal of neuroscience *38*, 2542-2556.

Sarkisian, M.R. (2001). Overview of the Current Animal Models for Human Seizure and Epileptic Disorders. Epilepsy & behavior : E&B *2*, 201-216.

Sasaki, S., Huda, K., Inoue, T., Miyata, M., and Imoto, K. (2006). Impaired feedforward inhibition of the thalamocortical projection in epileptic Ca2+ channel mutant mice, tottering. The Journal of neuroscience : the official journal of the Society for Neuroscience *26*, 3056-3065.

Scharfman, H.E. (2005). Brain-derived neurotrophic factor and epilepsy--a missing link? Epilepsy currents / American Epilepsy Society *5*, 83-88.

Scharfman, H.E. (2013). Cutting through the complexity: the role of brain-derived neurotrophic factor in post-traumatic epilepsy (Commentary on Gill et al.). The European journal of neuroscience *38*, 3552-3553.

Scheffer, I.E., Berkovic, S., Capovilla, G., Connolly, M.B., French, J., Guilhoto, L., Hirsch, E., Jain, S., Mathern, G.W., Moshe, S.L*., et al.* (2017). ILAE classification of the epilepsies: Position paper of the ILAE Commission for Classification and Terminology. Epilepsia.

Schiavo, G., Benfenati, F., Poulain, B., Rossetto, O., Polverino de Laureto, P., DasGupta, B.R., and Montecucco, C. (1992a). Tetanus and botulinum-B neurotoxins block neurotransmitter release by proteolytic cleavage of synaptobrevin. Nature *359*, 832-835.

Schiavo, G., Matteoli, M., and Montecucco, C. (2000). Neurotoxins affecting neuroexocytosis. Physiological reviews *80*, 717-766.

Schiavo, G., Poulain, B., Rossetto, O., Benfenati, F., Tauc, L., and Montecucco, C. (1992b). Tetanus toxin is a zinc protein and its inhibition of neurotransmitter release and protease activity depend on zinc. The EMBO journal *11*, 3577-3583.

Schmittgen, T.D., and Livak, K.J. (2008). Analyzing real-time PCR data by the comparative C(T) method. Nature protocols *3*, 1101-1108.

Schoenherr, C.J., and Anderson, D.J. (1995). The neuron-restrictive silencer factor (NRSF): a coordinate repressor of multiple neuron-specific genes. Science *267*, 1360-1363.

Schwartzkroin, P.A., and Prince, D.A. (1978). Cellular and field potential properties of epileptogenic hippocampal slices. Brain Res *147*, 117-130.

Schwob, J.E., Fuller, T., Price, J.L., and Olney, J.W. (1980). Widespread patterns of neuronal damage following systemic or intracerebral injections of kainic acid: a histological study. Neuroscience *5*, 991-1014.

Seifert, G., Carmignoto, G., and Steinhauser, C. (2010). Astrocyte dysfunction in epilepsy. Brain research reviews *63*, 212-221.

Seifert, G., Schilling, K., and Steinhauser, C. (2006). Astrocyte dysfunction in neurological disorders: a molecular perspective. Nature reviews Neuroscience *7*, 194-206.

Sha, L.Z., Xing, X.L., Zhang, D., Yao, Y., Dou, W.C., Jin, L.R., Wu, L.W., and Xu, Q. (2012). Mapping the spatio-temporal pattern of the mammalian target of rapamycin (mTOR) activation in temporal lobe epilepsy. PloS one *7*, e39152.

Shah, D.K., Boylan, G.B., and Rennie, J.M. (2012). Monitoring of seizures in the newborn. Arch Dis Child-Fetal *97*, F65-F69.

Shah, M.M. (2014). Cortical HCN channels: function, trafficking and plasticity. The Journal of physiology *592*, 2711-2719.

Shah, M.M., Anderson, A.E., Leung, V., Lin, X., and Johnston, D. (2004). Seizure-induced plasticity of h channels in entorhinal cortical layer III pyramidal neurons. Neuron *44*, 495-508.

Shapiro, L.A., Korn, M.J., Shan, Z., and Ribak, C.E. (2005). GFAP-expressing radial glia-like cell bodies are involved in a one-to-one relationship with doublecortin-immunolabeled newborn neurons in the adult dentate gyrus. Brain Res *1040*, 81-91.

Shapiro, L.A., Wang, L., and Ribak, C.E. (2008). Rapid astrocyte and microglial activation following pilocarpine-induced seizures in rats. Epilepsia *49 Suppl 2*, 33-41.

Sharma, A.K., Reams, R.Y., Jordan, W.H., Miller, M.A., Thacker, H.L., and Snyder, P.W. (2007). Mesial temporal lobe epilepsy: pathogenesis, induced rodent models and lesions. Toxicologic pathology *35*, 984-999.

Shin, M.C., Nonaka, K., Wakita, M., Yamaga, T., Torii, Y., Harakawa, T., Ginnaga, A., Ito, Y., and Akaike, N. (2012). Effects of tetanus toxin on spontaneous and evoked transmitter release at inhibitory and excitatory synapses in the rat SDCN neurons. Toxicon : official journal of the International Society on Toxinology *59*, 385-392.

Shinozaki, H., and Konishi, S. (1970). Actions of several anthelmintics and insecticides on rat cortical neurones. Brain Res *24*, 368-371.

Shorvon, S., and Ferlisi, M. (2011). The treatment of super-refractory status epilepticus: a critical review of available therapies and a clinical treatment protocol. Brain : a journal of neurology *134*, 2802-2818.

Sliwa, A., Plucinska, G., Bednarczyk, J., and Lukasiuk, K. (2012). Post-treatment with rapamycin does not prevent epileptogenesis in the amygdala stimulation model of temporal lobe epilepsy. Neuroscience letters *509*, 105-109.

Sohal, V.S., Keist, R., Rudolph, U., and Huguenard, J.R. (2003). Dynamic GABA(A) receptor subtype-specific modulation of the synchrony and duration of thalamic

oscillations. The Journal of neuroscience : the official journal of the Society for Neuroscience *23*, 3649-3657.

Sohal, V.S., Pangratz-Fuehrer, S., Rudolph, U., and Huguenard, J.R. (2006). Intrinsic and synaptic dynamics interact to generate emergent patterns of rhythmic bursting in thalamocortical neurons. The Journal of neuroscience : the official journal of the Society for Neuroscience *26*, 4247-4255.

Sombati, S., and Delorenzo, R.J. (1995). Recurrent spontaneous seizure activity in hippocampal neuronal networks in culture. Journal of neurophysiology *73*, 1706-1711.

Sosanya, N.M., Huang, P.P., Cacheaux, L.P., Chen, C.J., Nguyen, K., Perrone-Bizzozero, N.I., and Raab-Graham, K.F. (2013). Degradation of high affinity HuD targets releases Kv1.1 mRNA from miR-129 repression by mTORC1. The Journal of cell biology *202*, 53-69.

Spencer, E.M., Chandler, K.E., Haddley, K., Howard, M.R., Hughes, D., Belyaev, N.D., Coulson, J.M., Stewart, J.P., Buckley, N.J., Kipar, A.*, et al.* (2006). Regulation and role of REST and REST4 variants in modulation of gene expression in in vivo and in vitro in epilepsy models. Neurobiology of disease *24*, 41-52.

Sperk, G., Lassmann, H., Baran, H., Seitelberger, F., and Hornykiewicz, O. (1985). Kainic acid-induced seizures: dose-relationship of behavioural, neurochemical and histopathological changes. Brain Res *338*, 289-295.

Stables, J.P., Bertram, E., Dudek, F.E., Holmes, G., Mathern, G., Pitkanen, A., and White, H.S. (2003). Therapy discovery for pharmacoresistant epilepsy and for disease-modifying therapeutics: summary of the NIH/NINDS/AES models II workshop. Epilepsia *44*, 1472-1478.

Stables, J.P., Bertram, E.H., White, H.S., Coulter, D.A., Dichter, M.A., Jacobs, M.P., Loscher, W., Lowenstein, D.H., Moshe, S.L., Noebels, J.L.*, et al.* (2002). Models for epilepsy and epileptogenesis: report from the NIH workshop, Bethesda, Maryland. Epilepsia *43*, 1410-1420.

Stasheff, S.F., Bragdon, A.C., and Wilson, W.A. (1985). Induction of epileptiform activity in hippocampal slices by trains of electrical stimuli. Brain Res *344*, 296-302.

Stelzer, A., Slater, N.T., and ten Bruggencate, G. (1987). Activation of NMDA receptors blocks GABAergic inhibition in an in vitro model of epilepsy. Nature *326*, 698-701.

Stephani, U., Tauer, U., Koeleman, B., Pinto, D., Neubauer, B.A., and Lindhout, D. (2004). Genetics of photosensitivity (photoparoxysmal response): a review. Epilepsia *45 Suppl 1*, 19-23.

Storvik, M., Linden, A.M., Kontkanen, O., Lakso, M., Castren, E., and Wong, G. (2000). Induction of cAMP response element modulator (CREM) and inducible cAMP early repressor (ICER) expression in rat brain by uncompetitive N-methyl-D-aspartate receptor antagonists. The Journal of pharmacology and experimental therapeutics *294*, 52-60.

Sun, D.A., Sombati, S., and DeLorenzo, R.J. (2001). Glutamate injury-induced epileptogenesis in hippocampal neurons: an in vitro model of stroke-induced "epilepsy". Stroke; a journal of cerebral circulation *32*, 2344-2350.

Swann, J.W., and Brady, R.J. (1984). Penicillin-induced epileptogenesis in immature rat CA3 hippocampal pyramidal cells. Brain Res *314*, 243-254.

Sweatt, J.D. (2013). The emerging field of neuroepigenetics. Neuron *80*, 624-632.

Takei, H., Wilfong, A., Yoshor, D., Armstrong, D.L., and Bhattacharjee, M.B. (2007). Evidence of increased cell proliferation in the hippocampus in children with Ammon's horn sclerosis. Pathol Int *57*, 76-81.

Talos, D.M., Sun, H., Zhou, X., Fitzgerald, E.C., Jackson, M.C., Klein, P.M., Lan, V.J., Joseph, A., and Jensen, F.E. (2012). The interaction between early life epilepsy and autistic-like behavioral consequences: a role for the mammalian target of rapamycin (mTOR) pathway. PloS one *7*, e35885.

Tanaka, S., Kondo, S., Tanaka, T., and Yonemasu, Y. (1988). Long-term observation of rats after unilateral intra-amygdaloid injection of kainic acid. Brain Res *463*, 163-167.

Tanaka, T., Saito, H., and Matsuki, N. (1997). Inhibition of GABAA synaptic responses by brain-derived neurotrophic factor (BDNF) in rat hippocampus. The Journal of neuroscience : the official journal of the Society for Neuroscience *17*, 2959-2966.

Tang, S.J., Reis, G., Kang, H., Gingras, A.C., Sonenberg, N., and Schuman, E.M. (2002). A rapamycin-sensitive signaling pathway contributes to long-term synaptic plasticity in the hippocampus. Proceedings of the National Academy of Sciences of the United States of America *99*, 467-472.

Taylor, C.P., and Dudek, F.E. (1982). Synchronous neural afterdischarges in rat hippocampal slices without active chemical synapses. Science *218*, 810-812.

Tellez-Zenteno, J.F., and Hernandez-Ronquillo, L. (2012). A review of the epidemiology of temporal lobe epilepsy. Epilepsy Res Treat *2012*, 630853.

Tian, G.F., Azmi, H., Takano, T., Xu, Q., Peng, W., Lin, J., Oberheim, N., Lou, N., Wang, X., Zielke, H.R.*, et al.* (2005). An astrocytic basis of epilepsy. Nature medicine *11*, 973-981.

Timofeev, I., Bazhenov, M., Seigneur, J., and Sejnowski, T. (2012). Neuronal Synchronization and Thalamocortical Rhythms in Sleep, Wake and Epilepsy. In

Jasper's Basic Mechanisms of the Epilepsies, J.L. Noebels, M. Avoli, M.A. Rogawski, R.W. Olsen, and A.V. Delgado-Escueta, eds. (Bethesda (MD)).

Timpe, L.C., and Jan, L.Y. (1987). Gene dosage and complementation analysis of the Shaker locus in Drosophila. The Journal of neuroscience : the official journal of the Society for Neuroscience *7*, 1307-1317.

Tomasoni, R., Negrini, S., Fiordaliso, S., Klajn, A., Tkatch, T., Mondino, A., Meldolesi, J., and D'Alessandro, R. (2011). A signaling loop of REST, TSC2 and beta-catenin governs proliferation and function of PC12 neural cells. Journal of cell science *124*, 3174-3186.

Torre, E.R., Lothman, E., and Steward, O. (1993). Glial response to neuronal activity: GFAP-mRNA and protein levels are transiently increased in the hippocampus after seizures. Brain Res *631*, 256-264.

Traynelis, S.F., and Dingledine, R. (1988). Potassium-induced spontaneous electrographic seizures in the rat hippocampal slice. Journal of neurophysiology *59*, 259-276.

Trinka, E., Cock, H., Hesdorffer, D., Rossetti, A.O., Scheffer, I.E., Shinnar, S., Shorvon, S., and Lowenstein, D.H. (2015). A definition and classification of status epilepticus--Report of the ILAE Task Force on Classification of Status Epilepticus. Epilepsia *56*, 1515-1523.

Trzeciakiewicz, A., Opolski, A., and Mazur, A. (2005). [TRPM7: a protein responsible for magnesium homeostasis in a cell]. Postepy Hig Med Dosw (Online) *59*, 496-502.

Turrigiano, G. (2011). Too many cooks? Intrinsic and synaptic homeostatic mechanisms in cortical circuit refinement. Annu Rev Neurosci *34*, 89-103.

van Vliet, E.A., Aronica, E., and Gorter, J.A. (2015). Blood-brain barrier dysfunction, seizures and epilepsy. Semin Cell Dev Biol *38*, 26-34.

van Vliet, E.A., da Costa Araujo, S., Redeker, S., van Schaik, R., Aronica, E., and Gorter, J.A. (2007). Blood-brain barrier leakage may lead to progression of temporal lobe epilepsy. Brain : a journal of neurology *130*, 521-534.

Vandesompele, J., De Preter, K., Pattyn, F., Poppe, B., Van Roy, N., De Paepe, A., and Speleman, F. (2002). Accurate normalization of real-time quantitative RT-PCR data by geometric averaging of multiple internal control genes. Genome Biol *3*, RESEARCH0034.

Vernadakis, A., and Woodbury, D.M. (1969). The developing animal as a model. Epilepsia *10*, 163-178.

Verrotti, A., Trotta, D., Salladini, C., di Corcia, G., and Chiarelli, F. (2004). Photosensitivity and epilepsy. J Child Neurol *19*, 571-578.

Vezzani, A. (2012). Before epilepsy unfolds: finding the epileptogenesis switch. Nature medicine *18*, 1626-1627.

Vezzani, A., French, J., Bartfai, T., and Baram, T.Z. (2011). The role of inflammation in epilepsy. Nature reviews Neurology *7*, 31-40.

Vezzani, A., Friedman, A., and Dingledine, R.J. (2013). The role of inflammation in epileptogenesis. Neuropharmacology *69*, 16-24.

Vezzani, A., Sperk, G., and Colmers, W.F. (1999). Neuropeptide Y: emerging evidence for a functional role in seizure modulation. Trends in neurosciences *22*, 25-30.

Vreugdenhil, M., Hack, S.P., Draguhn, A., and Jefferys, J.G. (2002). Tetanus toxin induces long-term changes in excitation and inhibition in the rat hippocampal CA1 area. Neuroscience *114*, 983-994.

Walton, E., Geisler, D., Hass, J., Liu, J., Turner, J., Yendiki, A., Smolka, M.N., Ho, B.C., Manoach, D.S., Gollub, R.L*., et al.* (2013). The impact of genome-wide supported schizophrenia risk variants in the neurogranin gene on brain structure and function. PloS one *8*, e76815.

Wasterlain, C.G. (1974). Mortality and morbidity from serial seizures. An experimental study. Epilepsia *15*, 155-176.

Watanabe, S., Yamamori, S., Otsuka, S., Saito, M., Suzuki, E., Kataoka, M., Miyaoka, H., and Takahashi, M. (2015). Epileptogenesis and epileptic maturation in phosphorylation site-specific SNAP-25 mutant mice. Epilepsy research *115*, 30-44.

Wetherington, J., Serrano, G., and Dingledine, R. (2008). Astrocytes in the epileptic brain. Neuron *58*, 168-178.

Wheless, J.W., Clarke, D.F., Arzimanoglou, A., and Carpenter, D. (2007). Treatment of pediatric epilepsy: European expert opinion, 2007. Epileptic disorders : international epilepsy journal with videotape *9*, 353-412.

WHO (2017). Epilepsy. WHO fact sheets.

Wierschke, S., Lehmann, T.N., Dehnicke, C., Horn, P., Nitsch, R., and Deisz, R.A. (2010). Hyperpolarization-activated cation currents in human epileptogenic neocortex. Epilepsia *51*, 404-414.

Williams, P.A., White, A.M., Clark, S., Ferraro, D.J., Swiercz, W., Staley, K.J., and Dudek, F.E. (2009). Development of spontaneous recurrent seizures after kainate-induced status epilepticus. The Journal of neuroscience : the official journal of the Society for Neuroscience *29*, 2103-2112.

Winer, J., Jung, C.K., Shackel, I., and Williams, P.M. (1999). Development and validation of real-time quantitative reverse transcriptase-polymerase chain reaction

for monitoring gene expression in cardiac myocytes in vitro. Analytical biochemistry *270*, 41-49.

Wolfart, J., and Laker, D. (2015). Homeostasis or channelopathy? Acquired cell type-specific ion channel changes in temporal lobe epilepsy and their antiepileptic potential. Front Physiol *6*, 168.

Wong, M. (2008). Mechanisms of epileptogenesis in tuberous sclerosis complex and related malformations of cortical development with abnormal glioneuronal proliferation. Epilepsia *49*, 8-21.

Wong, M. (2010). Mammalian target of rapamycin (mTOR) inhibition as a potential antiepileptogenic therapy: From tuberous sclerosis to common acquired epilepsies. Epilepsia *51*, 27-36.

Wong, M., and Crino, P.B. (2012). mTOR and Epileptogenesis in Developmental Brain Malformations. In Jasper's Basic Mechanisms of the Epilepsies, J.L. Noebels, M. Avoli, M.A. Rogawski, R.W. Olsen, and A.V. Delgado-Escueta, eds. (Bethesda (MD)).

Wu, J., and Xie, X. (2006). Comparative sequence analysis reveals an intricate network among REST, CREB and miRNA in mediating neuronal gene expression. Genome Biol *7*, R85.

Wu, Y., Wang, X., Mo, X., Xi, Z., Xiao, F., Li, J., Zhu, X., Luan, G., Wang, Y., Li, Y.*, et al.* (2008). Expression of monocyte chemoattractant protein-1 in brain tissue of patients with intractable epilepsy. Clin Neuropathol *27*, 55-63.

Wykes, R.C., Heeroma, J.H., Mantoan, L., Zheng, K., MacDonald, D.C., Deisseroth, K., Hashemi, K.S., Walker, M.C., Schorge, S., and Kullmann, D.M. (2012). Optogenetic and potassium channel gene therapy in a rodent model of focal neocortical epilepsy. Science translational medicine *4*, 161ra152.

Wykes, R.C., Lee, M., Duffy, S.M., Yang, W., Seward, E.P., and Bradding, P. (2007). Functional transient receptor potential melastatin 7 channels are critical for human mast cell survival. J Immunol *179*, 4045-4052.

Xu, D., Miller, S.D., and Koh, S. (2013). Immune mechanisms in epileptogenesis. Front Cell Neurosci *7*, 195.

Xu, J.H., Long, L., Tang, Y.C., Zhang, J.T., Hut, H.T., and Tang, F.R. (2009). CCR3, CCR2A and macrophage inflammatory protein (MIP)-1a, monocyte chemotactic protein-1 (MCP-1) in the mouse hippocampus during and after pilocarpine-induced status epilepticus (PISE). Neuropathology and applied neurobiology *35*, 496-514.

Yao, Y., and Tsirka, S.E. (2014). Monocyte chemoattractant protein-1 and the blood-brain barrier. Cellular and molecular life sciences : CMLS *71*, 683-697.

Zaczek, R., Nelson, M., and Coyle, J.T. (1981). Kainic acid neurotoxicity and seizures. Neuropharmacology *20*, 183-189.

Zeng, L.H., McDaniel, S., Rensing, N.R., and Wong, M. (2010). Regulation of cell death and epileptogenesis by the mammalian target of rapamycin (mTOR): a double-edged sword? Cell cycle *9*, 2281-2285.

Zeng, L.H., Rensing, N.R., and Wong, M. (2009). The mammalian target of rapamycin signaling pathway mediates epileptogenesis in a model of temporal lobe epilepsy. The Journal of neuroscience : the official journal of the Society for Neuroscience *29*, 6964-6972.

Zhang, C.L., Dreier, J.P., and Heinemann, U. (1995). Paroxysmal epileptiform discharges in temporal lobe slices after prolonged exposure to low magnesium are resistant to clinically used anticonvulsants. Epilepsy research *20*, 105-111.

Zhang, L., Liu, S., Zhang, L., You, H., Huang, R., Sun, L., He, P., Chen, S., Zhang, H., and Xie, P. (2014). Real-time qPCR identifies suitable reference genes for Borna disease virus-infected rat cortical neurons. International journal of molecular sciences *15*, 21825-21839.

Zhang, X., Cui, S.S., Wallace, A.E., Hannesson, D.K., Schmued, L.C., Saucier, D.M., Honer, W.G., and Corcoran, M.E. (2002). Relations between brain pathology and temporal lobe epilepsy. The Journal of neuroscience : the official journal of the Society for Neuroscience *22*, 6052-6061.

Zhao, C., Deng, W., and Gage, F.H. (2008). Mechanisms and functional implications of adult neurogenesis. Cell *132*, 645-660.

Zhao, Y., Zhu, M., Yu, Y., Qiu, L., Zhang, Y., He, L., and Zhang, J. (2017). Brain REST/NRSF Is Not Only a Silent Repressor but Also an Active Protector. Molecular neurobiology *54*, 541-550.

Zhong, L., Cherry, T., Bies, C.E., Florence, M.A., and Gerges, N.Z. (2009). Neurogranin enhances synaptic strength through its interaction with calmodulin. The EMBO journal *28*, 3027-3039.

Zhong, L., and Gerges, N.Z. (2012). Neurogranin targets calmodulin and lowers the threshold for the induction of long-term potentiation. PloS one *7*, e41275.

Zhu, X., Han, X., Blendy, J.A., and Porter, B.E. (2012). Decreased CREB levels suppress epilepsy. Neurobiology of disease *45*, 253-263.